UNIVERSITAT
POLITÈCNICA
DE VALÈNCIA

Centre de Biomaterials
i Enginyeria Tissular
Universitat
Politècnica de València

PRINCIPE FELIPE
CENTRO DE INVESTIGACION

Laboratorio de
Polímeros Terapéuticos

DEVELOPMENT OF CONTROLLED DRUG DELIVERY SYSTEMS OF POLYMERIC NANOMEDICINES ASSOCIATED TO SCAFFOLDS FOR TISSUE REGENERATION

GABRIELA DE JESUS RODRIGUEZ ESCALONA

Doctoral Thesis UPV/2016

Thesis Directors:

Manuel Monleón Pradas, UPV

María J. Vicent Docón, CIPF

Dr Manuel Monleón Pradas, Ph.D, Professor of Universitat Politècnica de Valencia, UPV and Dr. María J. Vicent Docón, Ph.D. and Head of Laboratorio de Polímeros Terapéuticos at the Centro de Investigación Príncipe Felipe, CBIT (Valencia, Spain)

CERTIFY, that the work

"DEVELOPMENT OF CONTROLLED DRUG DELIVERY SYSTEMS OF POLYMERIC NANOMEDICINES ASSOCIATED TO SCAFFOLDS FOR TISSUE REGENERATION"

(Desarrollo de un sistema de liberación controlada de fármacos basado en nanomedicinas asociadas a scaffolds para la regeneración de tejidos)

has been developed by Gabriela de Jesús Rodríguez Escalona under their supervision in both, the CBIT-UPV and CIPF as a thesis project to obtain a Ph.D degree from the Universitat Politècnica de Valencia.

INDEX

ABSTRACT

Nowadays, one of the biggest concerns that permanently keep the attention of main important sectors of human society is health. Modern medical science is compromised with not only providing good adequate treatments but also effective specific solutions for each type of disease or human pathology.

In this direction, innovative approaches like tissue engineering or regenerative medicine, controlled drug delivery systems and nanomedicines emerge to bring alternatives to situations hard to solve with conventional treatment and strategies, including the replacement of damaged or diseases tissues and/or organs.

Specifically, this research is mainly aimed to design a combined system for controlled, stable and localized release of therapeutic agents that are able to exert their effect selectively on the area that warrants treatment.

This construct will have enough versatility to be adapted to almost any kind of treatment, from cancer to tissue regeneration, always that the key requirement of the treatment was the need to provide the treatment of localized, stable and controlled manner.

With the purposes of making easier the understanding as well as the design of the system, I was decided, for the proof of concept, to use

drugs and materials with known activity applied on tissue regeneration and for the treatment of chronic wounds.

The system in question consists of three main elements:

1) The first element is the **polymer conjugates of therapeutic agents**, which contribute to increasing the selectivity of the therapeutic action of the drug, as well as improved stability, bioavailability and biocompatibility thereof. If the drug is hydrophobic, conjugation contributes to increase its solubility in water, and in the case of proteins used as therapeutic agents, the combination helps reduce the body's immune response, increasing the chance of successful of the treatment.

2) The second element are the biodegradable **polymeric microparticles,** which in this case act like encapsulation agents for polymeric conjugate , thus allowing to have a second control point in the release kinetics of the therapeutic agents . Simultaneously, the microparticles also play a role in modifying the texture of the final construct, ascribing mechanical and physicochemical properties that help to improve some biological properties of the final material, such as the affinity, adhesion and cell proliferation.

3) The third element consists of a **nanoporous membrane** made of a biodegradable polymer by electrospinning, which constitute the unifier element of the whole system. This membrane provides manageability to the construct and is itself the last point of control in the release kinetics of the therapeutic agent or agents. Besides,

it must be biocompatible and stable at ambient conditions, since this probably is going to be exposed to the environment while protecting the wound, in the case of this kind of application.

These three elements, which themselves are complex systems separately, are systematically combined to achieve a synergistic relationship between them so that each one power the qualities of the other two.

The resulting construct was characterized and it demonstrated to have characteristic properties that can be used as a control parameter during manufacture of this new material. Also, preliminary biological studies developed "in vitro" indicated that the proposed system may be a good candidate for deeper studies as alternative treatment for chronic wounds and other pathologies that require localized administration for long periods of time.

RESUMEN

Actualmente, una de las mayores preocupaciones que permanentemente laman la atención de los principales sectores de la sociedad humana es la salud. La ciencia médica moderna está comprometida no solo con suministrar tratamientos adecuados, sino más bien ofrecer soluciones efectivas y específicas para cada tipo de enfermedad o patología humana.

En este sentido, estrategias innovadoras como la ingeniería de tejidos o la medicina regenerativa, los sistemas de liberación controlada de fármacos y las nanomedicinas, surgen como buenas alternativas para abordar situaciones difíciles de resolver aplicando los tratamientos y estrategias terapéuticas convencionales, como es el caso cuando se hace necesario reemplazar tejidos o incluso órganos dañados por algún traumatismo o enfermedad.

Concretamente, el presente trabajo de investigación tiene por objetivo principal diseñar un sistema combinado para la liberación controlada, estable y localizada de agentes terapéuticos que sean capaces de ejercer su efecto de forma selectiva sobre la zona que amerita el tratamiento.

Este constructo tendrá la versatilidad suficiente como para poder adaptarse a casi cualquier tipo de tratamiento, desde el cáncer hasta la regeneración de tejido, siempre que el requisito clave del

tratamiento sea la necesidad de suministrar el tratamiento de manera localizada, estable y controlada.

Para efectos de facilitar la compresión y el diseño del sistema se escogió para la prueba de concepto materiales y fármacos asociados a la regeneración de tejidos, como tratamiento para casos de heridas crónicas.

El sistema en cuestión está constituido por tres elementos principales:

1) El primer elemento son los **conjugados poliméricos** de agentes terapéuticos que contribuirán a aumentar la selectividad de la acción terapéutica del fármaco, así como también a mejora la estabilidad, biodisponibilidad y biocompatibilidad de los mismos. En caso de que el fármaco sea hidrofóbico, la conjugación contribuye a aumentar su solubilidad en agua, y en el caso de usar proteínas como agentes terapéuticos, la conjugación contribuye a disminuir la respuesta inmunológica del cuerpo incrementando las posibilidad de éxito del tratamiento.

2) El segundo elemento son **micropartículas poliméricas biodegradables**, que en este caso actúan con agentes de encapsulación para los conjugados poliméricos, permitiendo así contar con un segundo punto de control en la cinética de liberación de los agentes terapéuticos. Simultáneamente, las micropartículas también cumplen un papel de modificador de la textura del constructo final, adjudicándole propiedades mecánica y fisicoquímicas que contribuyen a mejorar las propiedades

biológicas del material final, como son la afinidad, la adhesión y la proliferación celular.

3) El tercer elemento consiste en una **membrana polimérica biodegradable nanoporosa** hecha por electrospinning, que constituyen el elemento unificados del sistema, aporta manejabilidad al constructo y es en sí mismo el último punto de control en la cinética de liberación del agente terapéutico. Este último debe ser biocompatible y estable en condiciones ambientales, puesto que probablemente este expuesto al ambiente mientras protege la herida, en el caso concreto de este tipo de aplicación.

Estos tres elementos, que en sí mismos constituyen sistemas complejos por separado, se han combinado sistemáticamente para alcanzar una relación sinérgica entre ellos de manera que cada uno potencia las cualidades de los otros dos.

El constructo resultante se caracterizó demostrando tener propiedades características que se pueden utilizar como parámetro de control durante la fabricación del mismo. Así mismo estudios in vitro del sistema desarrollado señalan que puede ser un buen candidato para el tratamiento de heridas crónicas entre otras patologías que requieran tratamientos localizados.

RESUM

Actualment, una de les majors preocupacions que permanentment llepen l'atenció dels principals sectors de la societat humana és la salut. La ciència mèdica moderna està compromesa no solament amb subministrar tractaments adequats, sinó més aviat oferir solucions efectives i específiques per a cada tipus de malaltia o patologia humana.

En aquest sentit, estratègies innovadores com l'enginyeria de teixits o la medicina regenerativa, els sistemes d'alliberament controlat de fàrmacs i les nanomedicines, sorgeixen com a bones alternatives per a abordar situacions difícils de resoldre aplicant els tractaments i estratègies terapèutiques convencionals, com és el cas quan es fa necessari reemplaçar teixits o fins i tot òrgans danyats per algun traumatisme o malaltia.

Concretament, el present treball de recerca té per objectiu principal dissenyar un sistema combinat per a l'alliberament controlat, estable i localitzada d'agents terapèutics que seguen capaços d'exercir el seu efecte de forma selectiva sobre la zona que amirita el tractament. Aquest constructe tindrà la versatilitat suficient com per a poder adaptar-se a quasi qualsevol tipus de tractament, des del càncer fins a la regeneració de teixit, sempre que el requisit clau del tractament sega la necessitat de subministrar el tractament de manera localitzada, estable i controlada.

Per a efectes de facilitar la compressió i el disseny del sistema es va escollir per a la prova de concepte materials i fàrmacs associats a la regeneració de teixits, com a tractament per a casos de ferides cròniques.

El sistema en qüestió està constituït per tres elements principals:

1) El primer element són els conjugats polimèrics d'agents terapèutics que contribuiran a augmentar la selectivitat de l'acció terapèutica del fàrmac, així com també a millora l'estabilitat, biodisponibilitat i biocompatibilitat dels mateixos. En cas que el fàrmac sega hidrofòbic, la conjugació contribueix a augmentar la seua solubilitat en aigua, i en el cas d'usar proteïnes com a agents terapèutics, la conjugació contribueix a disminuir la resposta immunològica del cos incrementant les possibilitat d'èxit del tractament.

2) El segon element són microparticles polimèriques biodegradables, que en aquest cas actuen amb agents d'encapsulació per als conjugats polimèrics, permetent així comptar amb un segon punt de control en la cinètica d'alliberament de l'agent terapèutics. Simultàniament, les microparticles també compleixen un paper de texturitzant del constructe final, adjudicant-li propietats mecànica i fisicoquímiques que contribueixen a millorar la propietats biològiques del material final, com són l'afinitat, l'adhesió i la proliferació cel·lular.

3) El tercer element consisteix en una membrana polimèrica biodegradable nanoporosa feta per electrospinning, que constitueixen el element unificats del sistema, aporta manejabilitat al constructe i és en si mateix el ultimi punt de control en la cinètica d'alliberament de l'agent terapèutic. Aquest últim ha de ser biocompatible i estable en condicions ambientals, ja que probablement aquest exposat a l'ambient mentre protegeix la ferida, en el cas concret d'aquest tipus d'aplicació.

Aquests tres elements que en si mateixos constitueixen sistemes complexos per separat, s'han combinat sistemàticament per a aconseguir una relació sinergètica entre ells de manera que cadascun potencia les qualitats dels altres dos.

El constructe resultant es va caracteritzar demostrant tenir propietats característiques que es poden utilitzar com a paràmetre de control durant la fabricació del mateix. Així mateix estudis in vitro del sistema desenvolupat assenyalen que pot ser un bon candidat per al tractament de ferides cròniques entre altres patologies que requeriren tractaments localitzats.

1 INTRODUCTION

Nowadays, one of the biggest concerns that permanently keeps the attention of main important sectors of human society is health. Modern medical science is compromised with not only providing good adequate treatments but also effective specific solutions for each type of disease or human pathology.

In this direction, innovative approaches like tissue engineering or regenerative medicine, controlled drug delivery systems and nanomedicines emerge to bring alternatives to situations hard to solve with conventional treatment and strategies, including the replacement of damaged or diseases tissues and/or organs.

Taking into account the vast range of application of these biotechnologies and provided that it is difficult to circumvent a desired disease target with a single technology, it is natural that they have been combined in order to develop better strategies to improve the treatments of this kind of pathologies with special needs.

In the recent literature, overwhelming examples of biomaterials for tissue repair/engineering have been reported. The review article from Stevens' group in the well-known journal *Nature Materials* included a list of commercial tissue engineering products and biomaterials at various stages of development for the treatment of vast amount of diseases and injuries, including applications for burns, legs ulcers, diabetic foot ulcers, wounds, spinal function, bone injury, dental bone,

bone defects, heart valves replacement, nerve injuries, diabetes mellitus, among others[1]. The remarkable idea is that all these pathologies could be treated applying technologies based on tissue engineering.

Furthermore, in some cases, when tissues have an innate capacity to regenerate, like skin and bones, cells can be stimulated to form new tissue under the adequate conditions, just using biomaterial-based approaches, taking profit of the own body as a 'bioreactor'[1]. Nevertheless, this strategy is not always applicable, since there are other tissues which need more complex matrixes to stimulate their growth, maybe from stem cells. In those cases, having controlled delivery systems for the bioactive agents that are responsible to promote tissue regeneration could be crucial.

On the other hand, the successful clinical application of nanomedicines such as polymer–protein conjugates (PEGylated enzymes and cytokines) and the promising results arising from clinical trials with polymer-bound chemotherapy have established the potential of Polymer Therapeutics (PT) as anticancer therapy [2–4]. Furthermore, these examples have also provided a firm foundation for a more sophisticated second-generation of constructs whose main research lines included the use of controlled architectures properly characterized, the application of polymer–based drug combinations and the direction towards new molecular targets, including regenerative medicine, and tissue repair [5–8].

Until now these two approaches for drug delivery have provided important information about mechanism for tissue regeneration and they represent interesting and viable alternatives as future therapies in this field. Unfortunately, the effect of the combination of both technologies has not been deeply studied yet. With that in mind, the aim of this project is to design intelligent composite system for tissue regeneration through the combination of biomaterial science and nanoconjugate synthesis, in order to have a structure with double control on drug release kinetics, and with the possibility to be used on different clinical applications, such as implants in damage tissue.

The proposed strategy in this work will offer a wide range of advantages over other systems. In the concrete case of protein therapy, it allows to overcome most of the limitations of this field since the use of nanosystems makes possible to keep protein or growth factors protected during circulation before being released from their scaffolds holding their activity with higher stability[9]. Moreover, by the application of these technologies, body residence time of the delivered protein/growth factor is dramatically increased, what in consequence, increases the therapeutic value[10]. In the case of the delivery of small drugs, this approach will increase the sustained and controlled release through a system with dual mechanism of control, the conjugate and the scaffold, what allows a specific local delivery of the drug, holding the therapeutic dose during the desired time lapse of application required[11–14].

Nevertheless, most of these nanosystems are design for systemic administration, limiting their range of application to pathologies that could be treated this way and making more difficult their use when local administration for local treatment is required. This kind of limitations could be overcome combining polymer therapeutics with an appropriate scaffolds made with innovative techniques in order to obtain a construct which was an optimum approach to be used as topic or surgical implants able to promote tissue regeneration but with a double function, provide support for cellular growth, as usually id done with scaffold of biomaterials[15–22], while supplied locally bioactive agents with specific therapeutic activity to improve local treatment, all at the same time with the same system.

Likewise, this approach could be implemented in therapies thought to improve the wound healing and promote tissue repair or even tissue regeneration, which could be treated in a better way modulating the drugs release kinetics to prolong the therapeutic effect of one dose that could be administered locally in the affected area. The expected result would be: increasing the efficiency of the treatment, reducing the time recovery of patients, and in consequence improving their live quality, that is the real goal of all and every one therapeutic strategy.

Having all these ideas in mind, the present research was conceived with the aim to develop a novel biomedical device designed for controlled and localized delivery of nanomedicines to promote tissue regeneration.

As mentioned, our approach is based on the development of a novel biomedical device that consists on a hybrid system composed by three main elements:

- **Polymer conjugates (PC):** These nanomedicines (polymers conjugated to drugs or proteins) improve the stability, solubility, bio-compatibility and bio-availability of therapeutic agents such as hydrophobic drugs or biomacromolecules (for example, proteins) which are fundamental for the treatment of the desired pathology[8,23–25]. Besides, polymer conjugates by themselves constitute the first point of control in the release kinetics of the therapeutic agent.

- **Biodegradable polymeric micro-particles (MPs):** This component accomplishes the function of vehicles for polymer conjugates, which will be encapsulated inside the micro-particles representing the second point of control in the release kinetics. MPs are also responsible of modifications in mechanical, surface, physico-chemical and biological properties of the final device[26,27].

- **Biodegradable polymeric membranes:** It is the element that unifies all components, making possible the handling of the final device. Loaded MPs will be effectively immobilized in the matrix of these membranes.

These three elements, which are complex systems by themselves, are supposed to be combined systematically and in the proper way in order to obtain a synergetic effect among them. The resulting single

structure will hold with particular physico-chemical, mechanical and biological properties, characteristics of a new biomaterial.
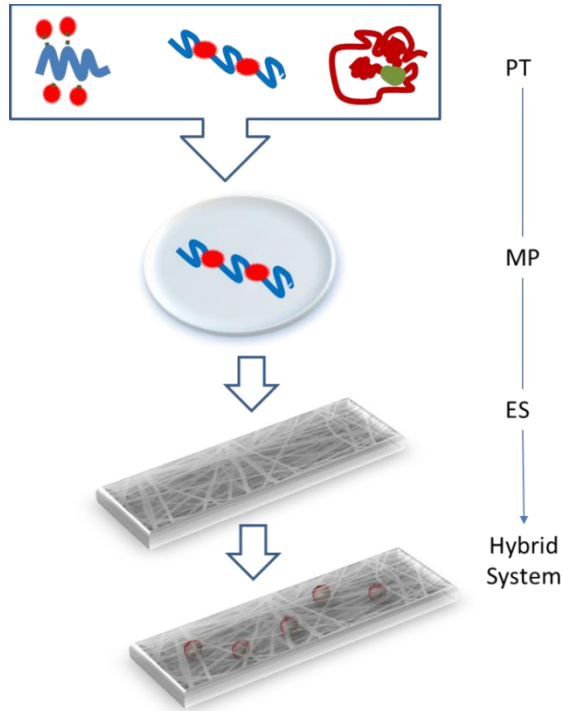
Figure 1.1 Diagram of composite system approach

As a proof of concept, the composite system proposed in this research could be used as model for different bioapplications. Wound healing was chosen as example to simplify its evaluation.

In order to complete the device three compounds were selected as model molecules of therapeutic agents:

- Curcumin (is a fluorescent hydrophobic small molecule drug, a natural polyphenolic compound, extracted from Curcuma longa, with various therapeutic properties, such as anti-inflammatory, anti-oxidant, antiviral, antibacterial and antitumor activity, able to promote hepatoprotection, as well as early-epithelialization, improved neovascularization and migratory activity of various cells into the wound bed, among others biological functions [28–31])
- Trypsin (protein with proteolytic enzymatic activity frequently used as model protein for evaluation of controlled drug delivery systems[32–34])

In the following paragraphs each element is going to be described to provide a better understanding of the whole system.

1.1   Regenerative Medicine

The idea of being able to augment or repair parts of our body dates to antiquity, when natural materials such as wood were used in an attempt to structurally replace tissues lost due to disease or trauma[35]. This concern has continued evolving until today to become one of the main areas of study of modern science.

Tissue engineering (TE), also called regenerative medicine is defined by the US National Institutes of Health as "the process of creating living, functional tissues to repair or replace tissue or organ function lost due to age, disease, damage, or congenital defects"[36.] Currently, it is an interdisciplinary field involving knowledge from medicine, biology, engineering and material science fields.[37–40]

Tao Jiang et al.,[38] defined "Regenerative Engendering" as the convergence of advanced materials science, nanotechnology, stem cell science, and developmental biology and state that this field represent the next multidisciplinary paradigm to engineer complex tissues. There is not any doubt that repair and regeneration of human tissues and organs using biomaterials, cells, and/or growth factors represents nowadays a great challenge for tissue engineers and surgeons.

As it was suggested at the beginning of this section, the TE concept was born from the need to find out alternative approaches to cover 1) the lack of organs for transplantation, 2) create tissue/organs analogs as substitutes to make the organs functional, 3) replace or restore a

damaged tissue or organ and 4) significantly improve the quality of life of millions of patients[41] .

First steps through biomaterial science and technology where taken at 1950's, and big progress have been seen since then. Three overlapping generations of biomaterials for surgical implants have evolved over time: from inert (with minimal tissue interaction, 1950's), to bioactive (with incorporated biologically interactive components to elicit a controlled reaction in the tissues, 1980's) and, finally, to biointeractive, integrative and resorbable (~2000>), able to regenerate functional tissue. This third generation involved the seeding of cells onto a scaffold, the *in vitro* culturing and finally the implantation into the body as prosthesis when matured. With engineered surfaces and bulk architectures tailored to specific applications, ''third generation'' biomaterials are intended to stimulate highly precise reactions with proteins and cells at the molecular level. Such materials provide the scientific foundation for molecular design of scaffolds that could be seeded with cells *in vitro* for subsequent implantation or specifically attract endogenous functional cells *in vivo*. The key concept is that a scaffold can contain specific chemical and structural information that controls tissue formation, in a manner analogous to cell–cell communication and patterning during embryological development. The natural tissue regeneration processes take place, blood vessels infiltrate the structure and the scaffold eventually degrades leading the newly formed tissue in place[42].

Even though to date the aim is still the same, we continue looking for the appropriate combination to be able to replace or facilitate the regrowth of damage or diseased tissue. The big difference is that now we possess more information about the importance of hierarchical tissue architecture and signaling pathway with bioactive molecules, influence of materials with nanotopographic features to promote the interaction between growth factors and their receptors and other important biological details specifics for each kind of tissue, organ or disease.

During the last years regenerative medicine has incorporated the advances in nanotechnology to strengthen its achievements.

A very instructive review written by Koel Chaudhury et al. [43]described several recent advances in nanomaterials use in this discipline, which have been trial *in vitro* and/or *in vivo* models. They explain that the advantages that nanotechnology offers to regenerative medicine lie in the fact that it can influence and even alter cellular behavior, which ultimately enhances the function of tissue or organs. These works, carried out between 2009 and 2014, were designed for applications in organ systems where considerable research is ongoing, encompassing bone, cartilage, peripheral nervous system, central nervous system, as well as myocardial tissue, dental, hepatic, ocular and skin regeneration. The newer and rational approaches include the combination of the traditional methods in nanotechnology: 1) nanoparticles; 2) scaffolds with nanofibers; 3) scaffolds with

nanotopographic modification; 4) drug/gene delivery; and 5) extracellular matrix (ECM) patterning[43].

Thus, the future of tissue engineering is closely related to the search of radical approaches which took advantage of emerging strategies such as the incorporation of nanomedicines and nanotechnology to well-known biomaterials such as scaffolds with nanofibers and micro-particulate systems, in order to be able to design a proof of concept of a novel platform to promote tissue repair/regeneration. As already stated, the aim of this project deals with that, focusing on applications related to prevent post-surgical undesired cell adhesion and wound healing as starting point. However, our expectancies are that this platform could be implemented in a broad range of tissue regenerative applications.

1.1.1 Wound Healing.

Skin is the largest organ in mammals. It forms a unique and flexible interface between our internal milieu and the external environment and possesses sensory, thermoregulatory, metabolic, and immunological functions. It is flexible enough to resist permanent distortion from movement and thin enough to allow the perception of stimuli. It also provides mechanical support to inner organs and plays a critical role in the synthesis of vitamin D. Besides, it is the more prone to mechanical injuries and infection, because it is directly exposed to potentially harmful microbial, thermal, mechanical and chemical influences[43,44].

Wound healing is a natural process that takes place spontaneously in healthy tissues after injury. There are two different mechanisms that cells an tissues can initiate after suffering practically any insult that causes tissue destruction: 1) Tissue regeneration and 2) Tissue repair.

Tissue regeneration refers to the proliferation of cells and tissues to replace lost structures, and complete recovery of tissue functionality. Actually, this mechanism rarely happens in mammals, but it also truth that tissues with high proliferative capacity, such as the hematopoietic system, the epithelia of the skin and gastrointestinal tract, are able to renew by themselves continuously after injury as long as the stem cells of these tissues are not destroyed. *Tissue repair*, on the other hand, consist on the formation of a scar by deposition of collagen and a compensatory tissue with some loss of the original functionality.[40]

Natural (acute) wound healing of skin or any soft tissue proceeds through several largely overlapping phases that involve: 1) hemostasis, 2) inflammatory response and associated cellular migration, 4) proliferation, 5) matrix deposition, and 6) tissue remodeling. [45]

If the wound healing cascade is negatively affected at any time, by interruption or deregulation of one or more phases of the wound-healing process, it might be slowed down or the wound can become chronic (non-healing) [45]. When the affected area of skin is too large and therefore cannot be successfully treated with conventional techniques, dramatic situations including patient death might take place[39].

Bryan K. Sun and co-workers have recently published in a review about the advances in skin grafting and treatment of cutaneous wounds, which explains than the skin, as the body's external epithelium, sustains and repairs injuries throughout a lifetime and therefore the ability of the skin to repair itself after injury is vital to human survival. The authors emphasized that there are a wide variety of factors that influence skin wounding and the speed and quality of healing which affect its vital role. Particularly warning is that several of such factors include a number of medications and common diseases, including age, infection, diabetes/vascular disease, and cancer, as well as smoking, alcohol and recreation drugs, can negatively affect the healing process in ways that are currently poorly understood. All previously said underscores the broad relevance of cutaneous wound healing issues to medicine, public health, and the global burden of disease[46]

Reinforcing this trend, in December 2014, Science Translational Medicine[45], also published a review about the state of art entitle "Wound repair and regeneration: Mechanisms, signaling, and translation" written by Sabine A. Eming and co-workers, whom introduced the article pointing out that traumatic injury is a leading cause of mortality in Europe and United States of America, in addition to the millions of surgical wounds created annually in the course of routine medical care.

Both articles emphasized that worldwide population should be aware of the number of patients suffering from chronic wounds. Moreover,

impaired healing conditions is reaching epidemic proportions and is expected to become even more burdensome in both human health and economic terms.[36,47,48]

In addition to acute wounds, the modern society way of life has promoted the prevalence of diabetes, obesity, and vascular disease in an aging population, and in consequence a steady rise in chronic skin wounds such as pressure ulcers and diabetic foot ulcers, which now affect more than 1% of all people during their lifetime. For instance, chronic skin wounds affect >6 million people at the US, what is translated in a cost of >$25 billion per year[46].

Advances in regenerative medicine have made possible the replacement of traditional wound dressing by more sophisticated devices. This is a very good incentive to continue investing in research, developing and innovation.

1.1.2   Biodegradable Polymeric Micro-particles for controlled delivery and tissue repair/regeneration

This section of the introduction is dedicated to remind why microparticulate systems are still valid alternatives as controlled drug delivery strategies for localized applications. There is always a controversy in the classification of nano and microparticles regarding sizes. Thus, it is worthy to point out that for this work, microparticles will be considered as those between 1–1000 μm and nanoparticles if they are between (1–1000 nm) [44]

Since 1987 to date, more than a hundred of research works have been published with the word "microparticles" and "delivery systems" in the title, according to a search made in PubMed in October 2015, using those key words. In this time is possible to observe how particulate drug delivery systems evolved from being scientific curiosities to become in an area with very active research interest, to clinical applications, as notice Dr. Kohane on his review about "Microparticles and Nanoparticles for Drug Delivery" published in 2007[49]. In this work, he explained that one of the most useful features of this kind of systems is that they are not only easy to inject, both, into tissue or intravenously, but also they are easily adapted to other milieus, for inhalation as a dry powder, or topically in an appropriate vehicle. This versatility lies on the fact that they can be injected or deposited directly at the site of action, providing a high local drug level over an extended period, while minimizing system toxicity. They can also be used as depot systems, injected at a convenient site (e.g. subcutaneously) with the intent of slowly releasing the drug for effect throughout the body. Particles themselves can also be distributed inclusive systemically but sent to specific desired sites at which to release their drugs, using active or passive targeting methods[49]

Micro and nanoparticles have properties that can make them more or less useful for any one of those types of applications. And one of the critical aspects that must be taken in account for designing the particles for a specific application is the size, together with the nature of polymeric material of what are going to be made of. Specifically, for

particles obtained by single and double emulsion methods, size have a direct relation with drug payload and, in the other hand, the polymer hardness will define the release kinetics mechanism and rate, as well as the "burst release" [49].

Single emulsion method involves the dispersion of an aqueous solution of the hydrophilic therapeutic agent (drug, protein, or any other compound) in an organic solution containing the polymer, leading to the formation of the primary water in oil (W/O) emulsion.

The double emulsion method involves the formation of a secondary oil in water (O/W) emulsion by dispersing, using continuous mechanical agitation, the primary W/O emulsion in an aqueous medium containing stabilizers such as poly(vinyl alcohol) (PVA) or poly(ethylene glycol) (PEG). Microspheres are produced by the evaporation of the organic solvent from the emulsion droplets. The microspheres are then collected either by centrifuging or filtration, washed and lyophilized to obtain the free flowing and dried microspheres. Revers systems are also possible, with w/o/w double emulsion. In any case, loaded microparticles can be formed either through chemical cross-linking or by solvent extraction[50].

According to Zeliha Gul Degim[44] the most common polymers for the preparation of microparticulate system for skin wound healing and drug delivery could be classify in the following manner. The most popular synthetic polymers used to synthesized microparticles are poly(lactic acid) (PLA) and poly(lactic glycolic acid) (PLGA), while the

natural polymers more used from de family of protein-based polymer are albumin and gelatin, from polysaccharide hyaluronic acid is a very well-known and commonly used. Among positively charged natural polymers the most frequently used are chitosan and trimethyl chitosan. Of course, there are several modified natural polymers that include starches, gums, fats, and waxes which have also been used in many different types of preparations for dermal and transdermal delivery with successful results.

Overall, the most commonly preferred polymers in wound healing are biodegradable and biocompatible polymers because of their surface properties, such as hydrophilicity, lubricity, smoothness, permeability, and degradability, and their biocompatibility with tissues and blood.

Some examples of application of microparticulate systems to tissue engineering field will be described.

Lee and colleagues[51] (2002) studied a laminin-modified infection-preventing collagen membrane containing silver sulfadiazine– hyaluronan microparticles. They prepared hyaluronan-based microparticles containing silver sulfadiazine (AgSD) incorporated into the two collagen layers (AgSD content 50mg/cm^2). They were able to demonstrate that the laminin-coated AgSD-medicated collagen membrane exhibited a higher wound size reduction and vessel proliferation and lower inflammation than the polyurethane control, suggesting that the laminin AgSD-medicated collagen membrane substantially improves dermal wound healing.

Haigang G. and Zhilian Y.[52] (2012) developed a controlled release strategy based on biodegradable microparticles for neurodegenerative disease therapy. MPs were made of Poly(lactide-co-glycolide) (PLGA; lactic acid/glycolic acid = 75/25) and loaded with a neurotrophic factor named Nerve growth factor (NGF). This protein has shown to improve the learning and memory ability as well as the survival of basal forebrain cholinergic neurons in aged or fimbria-fornix injured animals. Nevertheless, neurotrophic factors (NTFs) are large molecular proteins that do not really cross the blood-brain-barrier (BBB) and have short biologic half-life. Therefore, to improve their therapeutic efficacy and patient compliance, local and controlled delivery of NTFs directly to the desired brain area are preferred. The *in vivo* efficacy of these MPs was evaluated in a rat model of AD (Alzheimer's disease). Researchers affirm that compared to other existing approaches, the strategy based on biodegradable microparticles has demonstrated several advantages such as: 1) easier administration to the targeted area of brain, avoiding open operation and damage to surrounding tissue, 2) preservation of drug activity during encapsulation and storage. 3) localized, controlled released profile for a desire period, resulting in enhanced therapeutic effect while minimizing side effects, and 4) better safety profiles compared with gene therapy.

Feng S. and colleagues[53] (2015) carried on a study with mizolastine-loaded microparticles made of PLGA-mPEG, to evaluated the feasibility of use of this system as therapy for atopic dermatitis-like lesions in animal models. Microparticles were prepared using the oil-in-water

(O/W) emulsification-solvent evaporation method yielding a total drug loading of 4.2wt% (percentage in weight). Atopic dermatitis was induced to inner and outer sides of right ears in BALB/c mice model by repeated topical application of dinitrofluorobenzene. They applied two kinds of treatments and compared the effects on different groups of mice. Those mice which received daily mizolastine injection treatment showed almost complete recovery after 8 days as well as mice which receive one-dose treatment of mizolastine microparticles suspension by tail vein injection after the same time. Inflammatory cells infiltration into the ears and the plasma level of immunoglobulin E (IgE) were also suppressed by mizolastine microparticles according to the histopathology analysis. In conclusion, the researches affirm that these results suggested that the drug-loaded microparticulate systems proposed by them could be a proper candidate for the treatment of skin diseases.

Wang X. and co-workers[54] (2015) published their advances with a double wall microparticulate system made of poly(l-lactic acid) and poly(glycolic acid), designed to improves diabetic wound healing through redox modulation of wound microenvironment, through the early controlled release of peroxisome proliferator-activated receptor β/δ agonist GW501516. Microparticles are loaded with GW501516 (GW) as a wound healing drug, which is a peroxisome proliferation activated receptor PPARβ/δ agonist. This group based their work on the fact that diabetic wounds are imbued with an early excessive and protracted reactive oxygen species (ROS) production and previous

studies which support that PPARβ/δ is a valuable pharmacologic wound-healing target. Therefore they decided to synthesize double-layer encapsulated GW microparticles (PLLA:PLGA:GW). The study of different drug release profiles showed to have a significant influence on the therapeutic efficacy of GW and consequently in the diabetic wound closure.

Summarizing, in tissue engineering, drugs are classically adsorbed to the surface or encapsulated within the core of microspheres. Drug release from the microsphere matrix usually features a burst release associated with smaller quantities of drug attached to the surface of the microsphere, followed by a sustained release, which is associated with degradation of the polymer and release of encapsulated drug. *In vitro* trials are used to give promising results but when they are delivered *in vivo*, microspheres are sometimes susceptible to being cleared out of the animal and/or migrating away from the defect/implantation site. To maintain local treatment, microspheres are often combined with scaffolds or hydrogels in composite delivery systems[55]

Polymer scaffolds can also be manufactured from loaded microspheres with any therapeutic agent. Scaffold fabrication from microspheres could range from fusing of microparticles to form scaffolds. Nevertheless, a clear disadvantage associated to this kind of systems is the incompatibility of their mechanical properties with those required for the desire application. For this reason, composite

systems have been proposed as alternative to be able to take profit of all benefits of microparticulate system plus some improvement in biomechanical characteristics.

1.2 Nanotechnology for Controlled Drug Delivery Systems and Tissue Engineering

In the human body there are some tissues that contain cells capable of initiating regeneration or repair after injury. However, this ability varies between different cell types and depends on the nature of the injury or insult as reported by Sokolsky et al. For instance, there are tissues in constant renewing such as the skin, bone marrow and intestinal mucosa, which are capable of showing complete regrowth. Nevertheless, this ability highly depends on different factors including the size and the cause of the injury as well as the age of the individual. On the other hand, there are other types of tissues like heart muscle and nerves that lack of mechanisms for regeneration in adults. In these cases, stem cell biology offers the potential to grow tissue by following a developmental pathway that can be supported on a controlled drug delivery system[50].

In this context, scaffolds are very important components of many tissue engineering strategies as they provide an architectural structure in which extracellular matrix, cell-cell and growth factor interactions are combined to generate regenerative niches. Because of this, the materials used in their synthesis must be not only safe but also

suitable for the specific tissue that is desire to repair/regenerate. In general, a proper scaffold designed for clinical application should accomplish the following characteristics: [50]

1)   Possess mechanical properties matching those of the tissue at the implantation site and/or sufficient to shield cells from damaging compressive or tensile force without inhibiting appropriate biomechanical cues.

2)   Acceptable biocompatibility and toxicity profiles.

3)   Mimic the native extracellular matrix (ECM), and endogenous substances that surround the cells, into tissues and provide signals that aid cellular development and morphogenesis.

4)   Possess Interface adherence: defined as how cells or proteins attach on the scaffold surface. The scaffold should support cell adhesion and proliferation, facilitating cell-cell contact and cell migration.

5)   Appropriate Degradation rate: biodegradable scaffold should be bio-adsorbed at pre-determined time period, whereas the space initially occupied by the scaffold should be replaced by newly grown tissue.

Likewise, specific scaffolds designed with the additional purpose to work as drug delivery platforms should also address the following criteria[50]:

1)   High drug loading capacity: defined as the amount of bioactive agent that can be carried by the scaffold.

44

2)   Extended drug distribution: the bioactive agent needs to be dispersed homogeneously throughout the scaffold or in discrete areas if the spatial patterning of release is pretended to occur.

3)   Low binding affinity. The binding affinity is defined as how tightly the bioactive agent interacts or binds to the scaffold; this binding affinity must be sufficiently low to allow release.

4)   Controlled drug release kinetics. Kinetics of drug release needs to be controlled to allow the appropriate dose of bioactive agent required to reach the cells over a given period of time.

5)   Sufficient stability: the stability of the therapeutic agents when incorporated within the scaffold at physiological temperature must be enough in order to maintain their structure and activity over a prolong period of time.

Those requirements were taken in account to design the proof of concept of our system.

At this respect, Electrospinning (ES) is one of the most widely studied techniques used to construct biomaterials for their use as scaffolds to be cultivated with cells, and it has also been demonstrated to have given the most promising results in terms of tissue engineering applications. The interest about this technique has significantly increased after 2000[56], since it makes possible to obtain scaffolds with nanoscale architecture made of fibers from few nanometers to micrometers in diameter, high porosity and large surface areas, which

can mimic the extracellular matrix structure in terms of the chemistry and dimensions.[57]

1.2.1 Biodegradable Polymeric Membranes obtain by Electrospinning as scaffolds for tissue regeneration

Electrospinning (ES) could be defined as the deliberate application of the phenomenon of electrostatic spraying which occurs when electrical forces at the polymer solution overcome the surface tension, forming a polymer solution jet. The jet produces a fiber with diameters in the micron to nanoscale range (usually below 50 nm) as the solvent evaporates. [50]

The main components of an ES device are: 1) a syringe provided with a nozzle, 2) a pump, 3) a counter electrode (generally a metal plate), and 4) a source of electrical field. Briefly, the solution to be electro-spun, is applied to the system via the syringe's nozzle and is pulsed by the pump. It is then subjected to a difference in an electrical voltage present between the nozzle and the counter electrode. This electrical voltage generated by the source causes a cone-shaped deformation of the drop of the polymer solution. The solvent in the solution evaporates on its way to the counter electrode and, at the end of the process, solid continuous filaments are yielded. Gravitational forces do not interfere in the process because the acceleration of the fiber formation is up to 600 m/s^2, which is close to two orders of magnitude greater than the acceleration of gravitational forces and this fact

makes possible to form fibers of a wide range of arrangements including from top-down or bottom-up.[56]

Although the electrospinning process can be considered a simple method, there are several variables (multitude of molecular, processing and technical parameters) which must be taken in account to obtain fibers and mats with the desire characteristics. This includes: 1) environmental parameters, such as solution temperature, humidity and air velocity in the ES chamber; 2) solution properties, such as elasticity, viscosity, conductivity and surface tension; and 3) governing variables, such as distance between the tip and counter electrode, electrical potential, flow rate, molecular weight of the selected polymers, geometry of the collector, among others [57]

The choice of the right parameters is critical in order to be able to fabricate large and complex 3D structures to allow the cells to fill the structure in a 3D manner.

As deeper the knowledge about the parameters and polymer behavior are, more variation of the traditional process are proposed. The most recent modifications are related to coaxial ES (two components feed through different coaxial capillary channels) to obtain polymer core–shell fibers, hollow polymer core–shell fibers, hollow fibers containing polymer and/or ceramics and for the immobilization of functional objects or molecules. This methodology is very useful for drug and/or protein delivery, for the encapsulation of cells, bacteria, viruses, growth factors and others [15,56]

As stated before, fibers constructed by ES have the capability of closely mimicking the structure of the native environment of the cells. Nevertheless, the polymers that are commonly used to construct the scaffolds do not possess any specific groups for selective interactions with the cells. Therefore, the incorporation of biomolecules into the electrospun fibers could lead to a biofunctional scaffold, which would determine the efficiency of these fibers in regenerating biological functional tissues[16]. Due to the importance of this strategy, scientists around the world have been studying biomolecules to be incorporated, as well as ways of improving the efficiency of the incorporation of these agents.[56]

There are overwhelming examples that reveal the extraordinary potential and versatility of this technology in regenerative medicine, and also in combination with others micro and nano-technological devices. Selected relevant examples are summarized in this section to complete a global idea of its power.

Guorui Jin and colleagues[18,58] investigated the potential of human bone marrow (BM)-derived Mesenchymal Stem Cells (MSC) for epidermal cell differentiation *in vitro* on electrospun collagen/poly(L-lactic acid)–co-poly(3-caprolactone) (Coll/PLACL) nanofibrous scaffolds. The authors found out evidences that suggested their potential application in skin regeneration without regional differentiation. Subsequent studies about the effect of encapsulated multiple epidermal induction factors (EIF) into this kind of mat over

the epidermal differentiation potential of adipose-derived stem cells (ADSCs) was evaluated. The researchers observed that after 15 days of cell culture, the proliferation of ADSCs on EIF encapsulated core-shell nanofibers was promoted, demonstrated that the EIF encapsulated core-shell nanofibers might serve as a promising tissue engineered graft for skin regeneration.

Byung-Moo Min and co-workers[20] fabricated by ES silk fibroin (SF) nanofiber nonwovens for cell culture of normal human keratinocytes and fibroblasts. They found evidences in the cell activity assessment pointing out that the electrospun SF nanofibers were able to promote cell adhesion and spreading of type I collagen, because they provided a high level of surface area for cells to attach, provided their three-dimensional feature and their high surface area-to-volume ratio.

Vatankhah and colleagues[59] used electrospun cellulose acetate/gelatin membranes to study their potential as effective simulator of the structure and composition of native skin and their performance as a scaffold for either skin tissue engineering or as a wound dressing was evaluated. Their results demonstrated that electrospun Ac/Gel scaffolds are able to mimic both the morphological and structural features of normal skin and can be used either as a tissue-engineered scaffold or wound dressing just modulating their compositional ratios.

As Curcumin was chosen as model drug for this research some of the works related with electrospun system loaded with this compound are reviewed in the following lines.

Brahatheeswaran and co-worker[56,60] used zein protein (a class of prolamine protein found in corn) to form fibers for the delivery of curcumin, which was only mixed with the ES solution. The hydrolysis studies showed a burst release of the drug in the first hours, followed by a slight delivery. *In vitro* assays of zein–curcumin fibrous scaffold did not shown to induce any cytotoxic effects in the mouse fibroblast system.

Thi Thu Trang Mai and colleagues[61] published their finding with a nanofiber Cur-loaded poly(lactic) acid constructed by electrospinning. They reported that they were able to obtain PLA nanofiber mats with a total drug loading of 5wt% and fibers with mean diameter between 200 to 300 nm. Drug release kinetic was investigated in phosphate buffer saline (PBS) containing ethanol and after 24 h, 50% of the curcumin was released from curcumin-loaded PLA fibers.

Gyuldzhan Yakub and co-workers[62] also studied Curcumin-loaded poly(l-lactide-*co*-D,l-lactide) electrospun fibers and analyzed their antioxidant, anticoagulant, and antibacterial properties. PEG was added in the mixture to also develop other mats with the purpose of comparing the effect of the polymeric matrix over curcumin biological activity. They found that the polymer matrix composition had an impact on the capacity of curcumin to exhibit its antibacterial activity: coPLA/Curc displayed a stronger antibacterial effect than the coPLA/PEG/Curc mats. The fibrous materials obtained were suitable for wound dressing applications.

Gandhimathi C. and colleagues[63] studied biocomposite nanofibrous strategies for the controlled release of biomolecules for skin tissue regeneration. In this case, the study was performed to gain some insights into the applications of poly(l-lactic acid)-*co*-poly-(ε-caprolactone) (PLACL)/silk fibroin (SF)/vitamin E (VE)/curcumin nanofibrous scaffolds and to assess their potential as substrates for the culture of human dermal fibroblasts for skin tissue engineering. The electrospun nanofiber diameter obtained was between 198±4 nm and 332±13 nm for PLACL, PLACL/SF, PLACL/SF/VE, and PLACL/SF/VE/Curcumin nanofibrous scaffolds. The *in vitro* assays showed that the fibroblast proliferation, cell morphology, F-actin, 5-chloromethylfluoresein diacetate (CMFDA) dye expression, and secretion of collagen were significantly increased in PLACL/SF/VE/Curcumin when compared to PLACL nanofibrous scaffolds. Therefore, they concluded that due the accessibility of human dermal fibroblasts cultured on PLACL/SF/VE/Cur nanofibrous scaffolds, such systems are proved to be a potential scaffold for skin tissue regeneration. Their application is envisage in cell adhesion and proliferation to collagen secretion; and help support the sustained, localized delivery of biomolecules to the site of interest; so as to accelerate wound healing in skin tissue regeneration.

ES technique is so versatile than it can be successfully adapted to elaborate 3D-scaffolds for the healing and repair of diseased musculoskeletal tissues, that is a very complex matrix rely on many signaling pathways, involving numerous growth factors and their

receptors. One of the great challenges in this field, according to Tao Jiang et al, is to mimic closely the hierarchical architecture and properties of the extracellular matrices (ECM) of the native tissues [38]

However, not always cell adhesion is a property desirable in some application. This is the case of the work published by Arnal-Pastor[64] and colleagues. They accomplished to elaborate electrospun adherent–antiadherent bilayered membranes based on cross-linked hyaluronic acid for advanced tissue engineering applications where was sought to transplant cells on a tissue surface and keep them protected from the environment. To be more specific, the concept was to obtain a patch to prevent post-surgical adherences, which are a major issue in many surgeries. *In vitro* assays with L929 cell line of mouse fibroblasts shows very promising results. Their materials resulted to be not cytotoxic. Furthermore, the PLLA nanofiber face was cell friendly and promotes cell attachment and spreading therefore it could be used as a cell supply vehicle, while the HA face hindered cell adhesion and thus might prevent undesired adherences. Co-axial electrospinning technique was used in this case.

Likewise, during the last years several studies have been published that supports the fact that electrospun fibers can be associated with angiogenic and/or vasculogenic factors, epidermal factors and molecules with anti-inflammatory and antimicrobial properties to favor and enhance skin regeneration[19,21,38,58,59,65–69]

Taking into account the wide range of opportunities, we decided to explore the possibilities of composites material which combine ES with encapsulation of therapeutic agents directly into de fibers or inside a vehicle such as microparticles to promote tissue regeneration/repair.

The next section summarizes some relevant examples of composite systems that include electrospun mats as main component.

1.2.2 Composite Polymeric scaffolds with Nanofibrous architecture

Donald C. Aduba[70] and co-workers reported to have fabricated electrospun dendrimer-containing nanocomposite fibers with the purpose to obtain a functionalized system for drug delivery. In their design, the authors took profit of the possibility to chemically functionalize the surface groups of dendrimers to form a cross-linked network following electrospinning to further enhance structural stability and mechanical properties of the dendrimer-based fibrous mats. Although further studies must be done in order to assess their applicability, these systems represent a potential platform for drug delivery and tissue engineering applications.

Hongxu Qi et al.[71] published in 2006 their advances with the encapsulation of drug reservoirs in fibers by emulsion electrospinning and made preliminary release assessment. This work in particular was used as methodological reference for the present research. In this paper, they prepared composite fibers via electrospinning from either W/O or O/W emulsion and proved this technique to be an effective

method for microencapsulation. As a practical application, Ca-alginate microspheres, loaded with bovine serum albumin (BSA) as a model protein, were prepared in a reverse emulsion and then incorporated into poly (l-lactic acid) (PLLA) fibers by electrospinning. In *the in vitro* release test, BSA, which was released from composite fibers, achieved prolonged release profiles and lower burst release rates than those from naked Ca-alginate microspheres. They conclude that in comparison with other well-established techniques to prepare microcapsules, such as solvent evaporation and spray-drying techniques, emulsion electrospinning offers some advantages and opens the gate to try with other emulsion systems to fabricate new types of functional structures.

McCullen and co-workers[72], in 2007, were able to fabricate electrospun nanocomposites scaffolds by encapsulating multi-walled carbon nanotubes (MWNT) in poly (lactic acid) (PLA) nanofibers and studied their biocompatibility with adipose derived human mesenchymal stem cells. They observed that cells were able to proliferate until 14 days after been seeded. Furthermore, the authors arrived to the conclusion that, with the addition of MWNT to electrospun PLA fibers they are able to reduce the fiber diameter, increase the conductivity of the scaffold, and potentially provide a functional composite for tissue engineering.

Ionescu and co-workers [73] in 2010 designed a fabrication technique to entrap drug-delivering microspheres within nanofibrous scaffolds to

obtain an anisotropic nanofiber/microsphere composite with controlled release of biomolecules to promote musculoskeletal tissue regeneration. Their results showed that microspheres ranging from 10 ~ 20 microns in diameter could be electrospun in a dose-dependent manner to form nanofibrous composites. In this case, the release profiles of the composite structures were similar to free microspheres, with an initial burst release followed by a sustained release of the model molecules over 4 weeks. Furthermore, multiple model molecules were released from a single scaffold composite, demonstrating the capacity for multi-factor controlled release ideal for complex growth factor delivery from these structures. Precisely this last characteristic, the multi-facto delivery capability, through an alternative way to use microspheres for drug delivery without disrupting the scaffold mechanical properties were the main contribution of this work.

Jiqing Xu and co-workers in 2011 published their proposal for controlled dual release of hydrophobic and hydrophilic drugs from electrospun poly (l-lactic acid) fiber mats loaded with chitosan microspheres (CH-MPs). At difference of Hongxu Qi et al work, microparticles loaded with BSA (hydrophilic model drug) were previously made by spray drying, benzoin (hydrophobic model drug) was dissolved directly in PLLA solution and CH-MPs were suspended into this solution. Poly(vinylpirrolidone) (PVP) was added into PLLA solution to tune drug release behaviors. Their results showed that they were able to obtain a dual drug delivery system with sustain and

different rate of release for each component (BSA was released faster than Benzoin) and the released of both drugs could be adjusted by changing the ratio of PLLA/PVP.

Bhaarath and co-workers [74] published their findings with an electrospinning of curcumin loaded chitosan/poly (lactic acid) nanofilm and the evaluation of its medicinal characteristics in 2013. According to their results the better healing efficiency can be attributed to the presence of curcumin and chitosan. The optimal conditions to fabricate the nanofilm are: chitosan/PLA, 5.5% (w/v); curcumin, 11% (w/v); applied voltage, 20 kV. The maximum release rate was achieved between 120 and 360 min, when deposit over polyester and bamboo. The *in vitro* cytotoxicity test conducted on L-929 fibroblast showed no toxicity from the curcumin loaded chitosan/PLA nanofilm. *In vivo* wound healing studies on excision and incision wounds created on rat model showed significant reduction of wound area when compared to untreated group of rat. Finally, they concluded that these results suggested that the curcumin loaded chitosan/PLA nanofilm based bioactive wound healing material could be developed for wound management.

1.2.3   Polymer therapeutics

Polymers therapeutics are nanosized composite constructs that covalently combine a bioactive agent with a hydrosoluble polymer. They are considered the first nano-sized (5-100 nm) polymer-based medicines. Their definition involves rationally designed

macromolecular drugs and encompasses polymeric drugs (polymeric molecules that are biologically active in their own right); polymer-drug conjugates; polymer-protein conjugates; polymeric micelles to which drug is covalently bound, and multi-component polyplexes being developed as non-viral vectors for gene delivery. From the industrial standpoint, these nanosized medicines are more like considered 'new chemical entities' rather than conventional 'drug delivery systems or formulations' which simply entrap, solubilize or control drug release without resorting to chemical conjugation. [9]

Polymer therapeutics (PT) can be underlined as one of the most successful first generation of nanomedicines, with 15 products in routine clinical use. Furthermore, 2 of them are within the US Top 10 selling drugs, the polymeric drug glatiramer acetate for the treatment of multiple sclerosis (Copaxone®, Teva Pharm; $3.7 billion), and the polymer conjugate polyethylene glycol (PEG)-filgrastim for the treatment of neutropenia (Neulasta®, Amgen; $3.6 billion).[18]
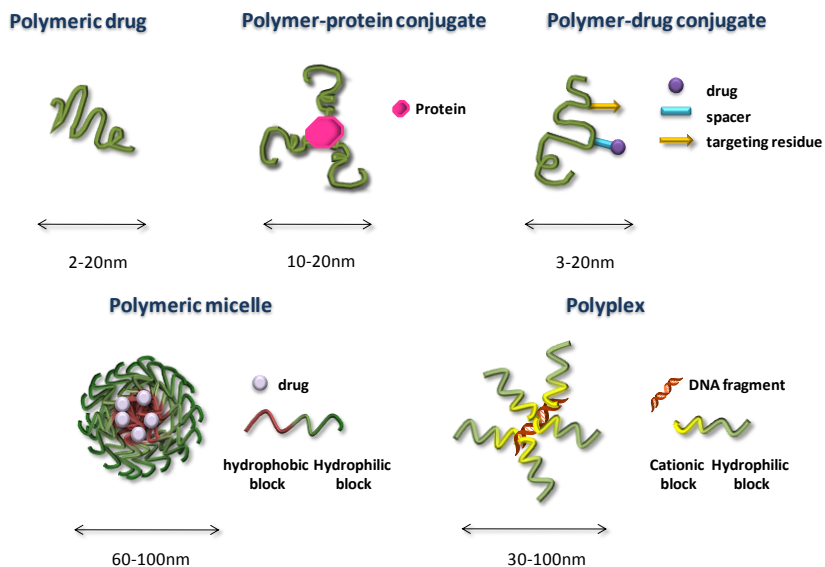
Figure 1.2 Schematic representation of the Polymer Therapeutics family. Redrawn from Duncan.[19]

Since the 1940s synthetic polymers have been explored as therapeutics with a dramatic increase in publications over the years. [3] **PT** are already well-established in the clinics for several treatments as single agents or as elements of combination, in particular for cancer therapy. The first generation of marketed PT are in Table 1 and those in clinical development are represented in Table 2.[4]

Table 1-1 First generation marketed polymer therapeutics. Adapted and updated from refs.[14, 40]

Product name	Technology	Indication	Route	Information source
Polymer-protein conjugates				
Zinostatin stimalmer®	Styrene maleic anhydride neocarzinostatin (SMANCS)	Cancer-hepatocellular carcinoma	Local via hepatic artery infusion	Yamanouchi[a] Japan
Oncaspar®	PEG-asparaginase	Cancer-acute Lymphocytic leukemia (ALL)	i.v./i.m.	Enzon[a]
Peg-intron®	PEG-Interferon alpha 2b	Hepatitis C	s.c.	Schering-Plough[a]
Pegasys®	PEG-Interferon alpha 2a	Hepatitis C	s.c.	Roche[a]
Neulasta™	PEG-hrGCSF	Chemotherapy-induced neutropenia	s.c.	Amgen[a]
Adagen®	PEG-adenosine deaminase	Severe combined immune deficiency syndrome	i.m.	Enzon[a]
Somavert®	PEG-HGH antagonist	Acromegalia	s.c.	Pfizer[a]
Mircera®	PEG-EPO (polyethylene glycol-epoetin beta)	Treatment of anemia associated with chronic kidney disease	i.v./ s.c.	Roche[a]
Cimzia (certolizumab pegol)	PEG-anti-TNF Fab	Rheumatoid arthritis Crohn's disease	s.c.	UCB[a]

Product name	Technology	Indication	Route	Information source
Krystexxa^{TM} pegloticase	PEG-uricase	Chronic gout	i.v.	Savient Pharmaceuticals
Polymer-aptamer conjugate				
Macugen®	PEG-aptamer (apatanib)	AMD	Intravitreous	OSI-Eyetech[a]
Polymer-drug conjugate				
Movantik^{TM}/Moventig® (NKTR-118)	PEG-naxolol	Opiod-induced constipation	Oral	AstraZeneca/ Daiichi Sankyo Co, Ltd.
Polymeric drugs				
Copaxone®	Glu, Ala, Tyr copolymer	Multiple sclerosis	s.c.	Teva[a]
Renagel®	Phosphate binding polymer	End stage renal failure	Oral	Genzyme (Daiichi Co, Ltd. Licensed)[a]
Welchol®	Cholesterol binding polymer	Type 2 diabetes	Oral	Genzyme

*Ala: Alanine, ALL: Acute lymphoblastic leukemia, AMD: Age-related Macular Degeneration, EPO: Epoetin beta; Fab: Fragment antigen-binding, HGH: Human Growth Hormone, hrGCSF: human recombinant Granulocyte-Colony Stimulating Factor, i.m.: intramuscular, i.v.: intravenous, s.c.: subcutaneous, Tyr: Tyrosine, TNF: Tumor Necrosis Factor.

Table 1-2 Examples of polymer therapeutics in clinical development. Adapted and updated from refs[14, 40]

Product name	Technology	Indication	Route	Stage	Information source
Polymer-protein conjugates					
ADI-PEG 20	PEG-arginine deaminase	Cancer-hepatocellular carcinoma, melanoma	i.v.	Phase III	Polaris Group
Hemospan® MP40X	PEG-hemoglobin	Delivery of O_2 in post-surgery and trauma patients	i.v.	Phase III	Sangart
CDP 791	PEG-anti VEGFR-2-Fab	Cancer-NSCLC	i.v.	Phase II	UCB Pharma
Polymer-aptamer conjugate					
ARC1779	PEG-anti-platelet-binding function of von Eillebrand Factor	Thrombotic microangiopathies	i.v.	Phase II	Archemix
E10030	PEG-anti-PDGF aptamer combination with Lucentis ®	AMD	Local intravitreal	Phase III	Ophthotech
Polymeric drugs					
AMG 223	Phosphate binding polymer	Hyperphosphatemia in CKD patients on hemodialysis	Oral	Phase II	Amgen
VivaGel®	Lysine-based dendrimer	microbiocide	Topical	Phase III	Starpharma

Product name	Technology	Indication	Route	Stage	Information source
Polymeric Drug-Conjugates					
CT-2103; Xyotax; Opaxio	Poly-glutamic acid (PGA)-paclitaxel	Cancer-NSCLC, ovarian, various other cancers and combinations	i.v.	Phase III	Cell Therapeutics Inc
Prolindac®	HPMA-copolymer-DACH platinate	Cancer-melanoma, ovarian	i.v.	Phase III	Access Pharmaceuticals
FCE 28068 (PK1)	HPMA-copolymer-DOX	Breast, lung and colon cancer	i.v.	Phase II	Pfizer
FCE 28069 (PK2)	HPMA-copolymer-DOX	Hepatocellular carcinoma	i.v.	Phase I/II	Pfizer
PEG-SN38	Multiarm PEG-camptothecan	Cancer-various	i.v.	Phase II/III	Enzon Inc
CRLX101	CD-PEG-camptothecin	Cancer-various	i.v.	Phase I/II	Cerulean Pharma
CRLX301	CD-PEG-Docetaxel	Solid tumors	i.v.	Phase I	Cerulean Pharma
DEP^{TM} Docetaxel	Dendrimer-Docetaxel	Solid tumors	i.v.	Phase I	Starpharma/AstraZeneca
NKTR-181	PEG-naloxone	Chronic pain	Oral	Phase III	Nektar
NKTR-171	PEG-Na$^+$ channel blocker	Neuropathic pain	Oral	Phase I	Nektar
NKTR-102	PEG-irinotecan	Cancer-various	i.v.	Phase II/III	Nektar
XMT-1001 (Fleximer® based)	Polyacetal-camptothecin	Cancer-various	i.v.	Phase I/II	Mersana
XMT-1107	Polyacetal-fumagillin	Solid tumors	i.v.	Phase I	Mersana/Teva

Product name	Technology	Indication	Route	Stage	Information source
Micelles					
SP1049C Biotransport™	Pluronic® formulation of DOX	Cancer-upper GI, NSCLC colorectal	i.v.	Phase III	Supratek Pharma Inc
NK 105 (Nanocarrier® technology)	Paclitaxel block copolymer micelle	Breast cancer	i.v.	Phase III	Nippon Kayaku Co
NC-6004, Nanoplatin™	Cisplatin block copolymer micelle	Cancer-various	i.v.	Phase I/II	NanoCarrier Co./ Orient Neuropharma
NC-4016 (Nanocarrier® technology)	Oxaliplatin block copolymer micelle	Solid Tumors	i.v.	Phase I	NanoCarrier Co
NC-6300 (K-912)	Epirubicin bock copolymer micelle	Solid Tumors	i.v.	Phase I	NanoCarrier Co./Kowa

*CD: Cyclodextrin, CKD: Chronic Kidney Disease, DACH: 1,2-diaminocyclohexane, GI: Gastro-Intestinal, NSCLC: Non-Small Cell Lung Cancer, PDGF: Platelet Derived Growth Factor, VEGF: Vascular Endothelial Growth Factor.

Clinical proof of concept for Polymer Therapeutics has been already achieved, however, many challenges and opportunities still lay ahead providing scope to develop this platform technology further. Through clinical use of polymer–protein conjugates (Table 1.1), and clinical development of polymer–anticancer drug conjugates (Table 1.2), PT is already well established as a new therapeutic class not only for cancer treatment,[36-38] but is also expanding its use to treat diseases other than cancer (i.e. PEG–interferon alpha conjugate known as Pegasys® or Peg-intron® can be used to cure hepatitis). Besides, many recent studies using polymer-drug conjugates have embraced a broad number of pathologies, including tissue regeneration.[39]

Lessons learned from the development of the first generation of polymer conjugates have facilitated the development of an improved second generation of PT. These improvements encompass the optimization of polymerization techniques and linking chemistry, as well as data gained in efficacy profiles, clinical toxicities and side effects. Current efforts are directed towards practical and cost-effective designs for specific targets with defined routes of administrations and dosage in order to reach personalize medicine as the ultimate goal. Towards this aim, four major research lines are now being explored including: : (1) the synthesis of novel biodegradable polymeric carriers with defined architectures; (2) the implementation of innovative physico-chemical characterization methods; (3) the use of polymer-based combination therapy to enhance treatment specificity and efficacy always looking for drug synergism and (4) their application in diseases other than cancer with an important focus on

pathologies related to the aging population and infectious diseases.[24,8].

All these strategies are summarized in Figure1. 3
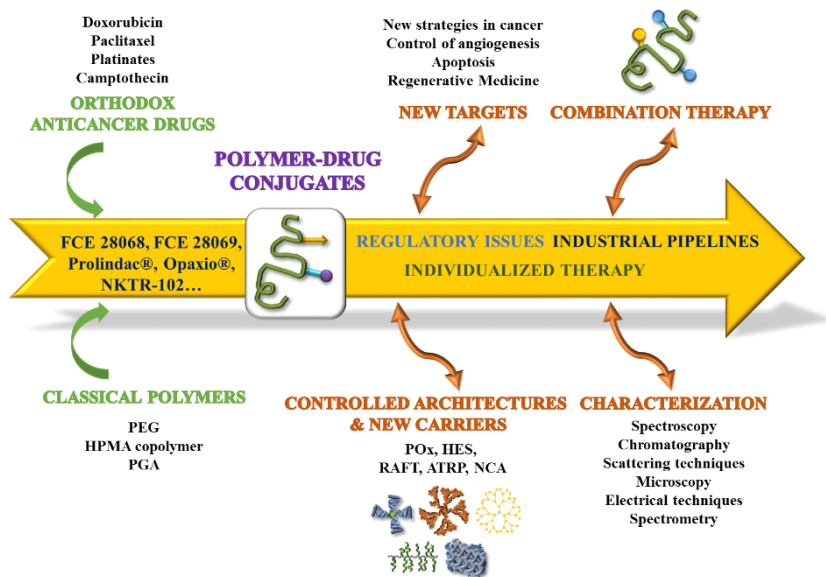
Figure 1.3. **Current research lines in PT field: novel molecular targets in cancer as well as other disease, polymer-based combination therapy, new architectures and polymeric systems, and an exhaustive physico-chemical characterization essential to clinical translation following regulatory indications. Redrawn from ref[24]**

Although many early products to market were developed to treat infectious diseases and cancer, i.e. life-threatening diseases, as already mentioned, there has been a continuing move towards PT directed against new molecular targets, and a wider range of therapeutic indications; especially those diseases of the ageing population that affect quality of life[3]. In particular application to tissue regeneration are one the most exciting and promising areas. In this respect, the transfer to market of Cimzia as a treatment for rheumatoid arthritis

and Crohn's disease, and Macugen for age-related macular degeneration have been important landmarks for PT being developed as treatments for chronic diseases that impact of quality of life.[3]

Progress continues with two polymer therapeutics being featured in the US Top 10 selling drugs list for 2013 Neulasta® and Copaxone®, and more products are arriving to market as innovator (new) products (e.g. Lymphoseek® (Tilmanocept), a mannonsylated dextran-based sentinel lymph node imaging agent for melanoma and breast cancer patients, and also into clinical trial as 'follow-on' (generic) products (e.g. PEG-G-CSF (DA-3031) [6]

1.2.3.1   Polymer Conjugates.

Polymer conjugates are water-soluble, composite constructs designed for systemic administration and fall into two main categories, polymer-protein conjugates and polymer-drug conjugates. Polymer conjugation to proteins reduces immunogenicity, prolongs plasma half-life and enhances protein stability. Polymer-drug conjugation promotes tumor targeting by the enhanced permeability and retention (EPR) effect and, at the cellular level following endocytic capture allows lysosomotropic drug delivery.

The original idea of covalently conjugating a low molecular weight drug to a hydrophilic polymer carrier to increase its therapeutic effect was proposed by Helmut Ringsdorf in 1975. Ringsdorf model consisted of four different components: a polymeric carrier, a drug, a biodegradable linker and a targeting group. A lot of studies were done

in collaboration with Ruth Duncan an Jindrich Kopecek that resulted in the clinical evaluation of HPMA copolymer-doxorubicin (DOX)(FCE28068, PK1) in 1994, which represented the first synthetic polymer-anticancer drug conjugate to be tested in humans[5,75]. At the same time Maeda and colleagues were carrying out studies on SMANCS (Zinostatin stimalamer®; a polymer (styrene-co-maleic anhydride (SMA))-anticancer protein (neocarzinostatin; NCS) conjugate, highlighted for the first time the tendency of macromolecules to passively accumulate in the tumor tissue. This effect is now well-described and is due to two contributing factors, (i) the hyperpermeability of tumor vasculature which allows selective extravasation of macromolecules into the tumor, (ii) the lack of an effective lymphatic drainage which provides increased retention of macromolecules in the tumor. This effect was described by Maeda who coined the phrase "enhanced permeability and retention effect" (EPR) and it is possibly the most important factor for macromolecular targeting to solid tumors[25]. For applications in cancer and inflamed areas (such as wound healing) polymer-drug conjugation promotes passive tumor targeting by the enhanced permeability retention (EPR) effect and allows for lysosomotropic drug delivery following endocytic capture.

Both polymer-drug and polymer-protein conjugates are tailor-made using a basic tripartite structure and they content a water-soluble polymer, a linker and a bioactive agent. It has become clear that the molecular mass and physico-chemical properties of the polymer are frequently the most important drivers governing biodistribution,

elimination and metabolism of the conjugate as a whole. The water-soluble polymeric carrier must be non-toxic, non-immunogenic and suitable for repeated administration. Poly(ethylene glycol) (PEG), poly(N-(2-hydroxypropylmetacrylamide)) p(HPMA) copolymers and poly(glutamic acid) (PGA) are the most widely tested in a clinical setting. Of these polymers, only PGA is biodegradable; consequently, the molecular masses of PEG and HPMA copolymers have been limited to <40KDa to ensure the eventual renal elimination. In the case of non-degradable polymers, the polymer-drug or protein linker is an important design feature [2]

- **Polymer-Drug Conjugates**

The concept of targetable polymer-drug conjugate was develop starting from the De Duve realization that the endocytic pathway might be useful for "lysosomotropic drug delivery" and the vision of Ringsdorf for the idealized polymer chemistry for drug conjugation. Drug conjugation to a water-soluble polymer platform restricts cellular uptake to the endocytic pathway and hence, allows tumor specific targeting of low-molecular-mass chemotherapeutic agents in addition to limiting the access of the conjugate to the normal site of toxicity. Use of a water-soluble polymers as a platform also helps to solubilized hydrophobic drugs, making a more convenient formulation to administer intravenously. The ideal polymer-drug linker is stable during transport to the tumor, but able to release drug at an optimum rate on arrival; because many of the drugs being transported exert their effects through an intracellular pharmacological receptor, it is essential that drug release actually occurs. Adequate drug carrying

capacity, in relation to the potency of the agent being carried, is essential, as is the ability to target the tumor by an active (receptor-ligand) or a passive (pathophysiological) mechanism: both of these are important design features [2]

There are several strategies to design intelligent systems able to response according to the environment where delivery is desired to be accomplished. In this research we are going to focus on systems with pH-sensitive polymers[25]

There are two main approaches: 1) nanocarriers composed of pH-sensitive polymers or 2) nanocarriers containing pH-sensitive linkers

Most of the work on pH-sensitive nanocarriers is based on the first approach, with polymers which alter their properties upon changes in the pH of the medium. These alterations occur either through hydrolytic degradation or through changes in the physicochemical properties, resulting in the disassembly of the carrier and thus the release of their cargo.

The pioneering work on polymeric systems comprising pH-sensitive polymers was done by Ulbrich and co-workers[76], with the synthesis and characterization of biodegradable polymeric prodrugs based on salicylic acid (the active component of aspirin) linked to poly(anhydride-ester). This prodrug was found to be stable under acidic conditions (pH 3), but released salicylic acid slowly at normal physiological pH (pH 7.4) and more quickly in basic conditions (pH 10), owing to the hydrolytic degradation of the polymer backbone. Potential applications for systems like this are the treatment of

gastrointestinal disease, where release in the basic environment of the lower intestine is necessary.

In the same line, **_POLYACETALS_** achieved through the reaction between vinyl ether and alcohols were first described by Heller *et al*. (1980)[77]. These systems can be hydrolyzed under mildly acidic conditions (pH 6.5), but are stable at physiological pH (7.4) as shown by Tomlinson *et al* in 2002[78]. Later in 2003 they also demonstrated a prolonged blood half-life and enhanced tumor accumulation for aminopendant polyacetal (APEG)–doxorubicin (DOX) conjugates when compared to the clinical conjugate *N*-(2-hydroxypropyl) methacrylamide (HPMA) copolymer–DOX, as well as lower liver and spleen uptake. *In vitro* cytotoxicity analysis confirmed that the serinol-succinoyl-DOX released during degradation remained active. *In vivo* studies were also performed in B16F10 melanoma-bearing mice[79]. A further step was reported by Vicent et al. in 2004[80] when the non-steroidal oestrogen diethylstilbestrol (DES) was incorporated within the polyacetal main chain. The first pH-responsive polymeric (tert-DES) drug adequate for lysosomotropic delivery was achieved in this way. These conjugates rapidly released DES at acidic pH (65% in 96h at pH 5.5) but were stable at neutral environment (4% in 96h at pH 7.4). Furthermore, the second generation of DES-polyacetals[12,81] with more controlled solution conformation has recently been described by Giménez *et al* in 2012 [81].

Following similar strategies, Tang and co-workers reported in 2010 the synthesis and characterization of similar systems based on curcumin-polyacetals[82], which were shown to be highly cytotoxic *in vitro* against

ovarian and breast cancer cell lines (SKOV-3, OVCAR-3 and MCF-7) and *in vivo*, with remarkable antitumor activity in a SKOV-3 ovarian cancer model in mice.

Recently, England et al. (2012) [12] confirmed the versatility of these carriers by reporting the first family of nanomedicine (polyacetal–stilbene conjugates) modulators of hypoxia inducible factor-1 (HIF-1), a key transcription factor involved in key cell processes.

The second strategy, based on nanocarriers containing pH-sensitive linkers often applied in the design of pH-sensitive nanoconstructs is the responsiveness of the polymer–drug linker. Hydrazone (HYD) ($R_1R_2C=NNH_2$) is one of the best known within this family, mostly via pioneering work from Ulbrich's group. In their studies the behavior of HYD-linked DOX to HPMA copolymer has been exhaustively described, with important therapeutic efficacy *in vivo* upon injection in tumor-bearing mice.[76,83–85]

Another pH-sensitive linker used for the preparation of smart nanocarriers for drug delivery is the cis-aconitic spacer. Choi *et al*., in 1999, conjugated DOX to HPMA through this spacer and observed increased release in acidic pH, resulting in significant cytotoxicity upon incubation with human ovarian carcinoma cells.

Interestingly, in a subsequent paper, Ulbrich *et al* (2003) compared HPMA–DOX conjugates containing DOX bound either through HYD or through a cis-aconitic spacer. A slower release from the cis-aconitic conjugates was observed at pH 5 as compared to the HYD ones, as well as a lower cytotoxicity *in vitro*. Consequently, the aconityl conjugates

did not show any therapeutic effect *in vivo*, indicating that drug release from the conjugate occurred but was not sufficient to result in therapeutic efficacy.

- **Polymer-Protein Conjugates**

David Abuchowski[86] and colleagues in 1970s carried out pioneering researches and developed the concept of polyethylene glycol (PEG)-protein conjugation (PEGylation).

The continuing entry of PEGylated proteins into the routine clinical use has been responsible for a paradigm shift in the acceptance of polymer based macromolecular medicines. This technique is used to increase protein solubility and stability, and reduce protein immunogenicity; moreover, polymer conjugation prolongs plasma half-life through prevention of renal elimination and avoidance of receptor-mediated protein uptake by cells of the reticuloendothelial system (RES)[25].

Consequently, polymer-conjugated therapeutics requires less frequent dosing, which is a great benefit to the patient. For an optimized synthesis of a polymer-protein conjugate, a semi-telechelic polymer (one with a single reactive group at one terminal end) is required to avoid protein cross-linking during conjugation; the linker used must be carefully chosen to ensure that the linking chemistry will not generate toxicity or immunogenicity. Appropriate stability characteristics and reproducible site specific protein modification are also required[2,25].

Linear and branched PEGs of different molecular masses can be used but this is very important because it has a great impact on their

pharmacokinetics. PEGylation could reduce the protein bioactivity but degradable PEG-protein linkage can be used to maximize the protein bioactivity[25].

Another important findings in this field has been reported by Hardwicke et al. (2008)[87], who designed Dextrin-rhEGF conjugates as bioresponsive nanomedicines for wound repair. These systems have very interesting application in impaired dermal wound healing like venous leg ulcers, diabetic foot ulcers and pressure sores. It is known that growth factors act in concert to promote wound repair, but their topical application rarely leads to a significant clinical improvement of chronic wounds due to premature inactivation in wound environment. The aim of this study was to synthesize a polymer–growth factor conjugate and investigate whether the novel concept called Polymer-masking-UnMasking-Protein Therapy (PUMPT) might be used to generate bioresponsive PT as nanomedicines able to promote tissue repair. The biodegradable polysaccharide dextrin, and recombinant human epidermal growth factor (rhEGF) were chosen here as models. It was expected that dextrin-rhEGF conjugate has the potential to treat acute and chronic wounds, most simply by topical administration or alternatively, via intravenous (i.v.) administration, to localize the rhEGF using enhanced vascular permeability at sites of inflammation (EPR effect).

Succinoylated dextrin ($\sim$85,000g/mol; $\sim$19mol% succinoylation), and rhEGF were chosen as a first model combination. The conjugate synthesized contained $\sim$16%wt rhEGF and <1% free protein. It exhibited increased stability towards proteolytic degradation by

trypsin and the clinically relevant enzyme neutrophil elastase. The dextrin component was degraded upon addition of α-amylase leading to sustained release of free rhEGF over time (52.7% release after 168h). When biological activity was assessed (±α-amylase) in proliferation assays using epidermoid carcinoma (HEp2) cells and HaCaT keratinocytes, as anticipated, polymer conjugation reduced rhEGF bioactivity (p=0.0035). However, exposure to physiological concentrations of α-amylase triggered dextrin degradation and this led to protein unmasking with restoration of bioactivity to the level seen for unmodified rhEGF. Indeed, prolongation of HEp2 proliferation was observed over 8days. The inability of dextrin, succinoylated dextrin or α-amylase alone to induce proliferative effects, and the ability of α-amylase-exposed dextrin–rhEGF to induce phosphorylation of the epidermal growth factor receptor (EGFR) in HEp2 cells confirmed a mechanism of action by stimulation of classical signal transduction pathways.

These observations suggested that this dextrin–rhEGF, and other dextrin-growth factor conjugates have potential for further development as bioresponsive nanomedicines for tissue repair[87]

Polymer conjugates in tissue regeneration

One of the first approaches in using polymer conjugates to promote tissue repair was published by Shaunak et al.(2004). They synthesized polyvalent dendrimer glucosamine conjugates to prevent scar tissue formation. Dendrimers are hyperbranched synthetic macromolecules that can be made using controlled sequential processes to give them

defined structural and molecular weight characteristics. The authors conjugated anionic polyamidoamine generation of 3.5 (PAMAM) dendrimer (Dendritech) with the aminosaccharides D(+)glucosamine and D(+)glucosamine-6-sulfate to obtain water-soluble conjugates with immuno-modulatory and antiangiogenic properties respectively. *In vitro* studies showed dendrimer glucosamine inhibited Toll-like receptor 4-mediated lipopolysaccharide induced synthesis of pro-inflammatory chemokines and cytokines from human dendritic cells and macrophages but allowed upregulation of the costimulatory molecules CD25, CD80, CD83 and CD86. Dendrimer glucosamine 6-sulfate blocked fibroblast growth factor-2 mediated endothelial cell proliferation and neoangiogenesis in human Matrigel and placental angiogenesis assays. Both conjugates were used in combination in a validated and clinically relevant rabbit model for scar tissue formation after glaucoma filtration surgery and they notice combination increased the long-term success of the surgery from 30% to 80% (p=0.029). Finally they concluded that dendrimers tailored to have specific immune-modulatory and antiangiogenic properties can be designed and used synergistically to prevent scar tissue formation.

Vicent M. and Perez-Payá (2006) developed the first antiapoptotic polymer conjugate nanomedicine that has been demonstrated to have therapeutic potential as a targeted drug delivery system that offers great capabilities as an inhibitor of apoptosis or programmed cell death. Apoptosis is a key cellular mechanism involved in a broad range of physiological processes. Deregulated apoptosis is associated with several human pathologies, such as cancer, ischemic injuries, and

neurological disorders. The aim of this study was to design, synthesize, and characterize a polymer conjugate that, by carrying a novel apoptotic protease activating factor 1 (Apaf-1) inhibitor (peptoid), would rescue cells from inappropriate apoptosis. Poly-L-glutamic acid (PGA) was chosen as a polymeric carrier because it can be readily degraded by lysosomal enzymes, it is stable in plasma, it contains functional groups for drug attachment and has excellent pharmacological properties. The rational of this study was based on the fact that to accomplish the full therapeutic potential of a bioactive agent, it is crucial that it is delivered to the disease area. It is known that PT can ensure the efficient release of the bioactive agent to the required intracellular compartment within and specific period of time. Therefore they conjugate the peptoid they had previously developed, a new structural class of Apaf-1 ligands (peptoid 1) as apoptosome inhibitor, with PGA to increase its therapeutic potential. They actually observed that this macromolecule PGA-peptoid 1 clearly enhance the antiapoptotic activity of peptoid 1 and diminish it cytotoxicity in different cell models.

Another important finding in this field has been reported by Hardwicke et al.[87], who designed Dextrin-rhEGF conjugates as bioresponsive nanomedicines for wound repair. These systems were previously described in section of polymer-protein conjugates.

One of the most recent approaches in this field was published by Conejos et al. in 2014 [88]. They proposed a novel specific nanoconjugate for the treatment of amyloidosis, and in particular familiar amyloidotic polyneuropathy. Their rational design started from an active

biomolecule of peptidic nature (RAGE peptide) that recognizes the TTR prefibrillar aggregates responsible to promote cell death in FAP patients. The clinical progress of this promising inhibitor was masked by the well-known limitations of peptides, such as low solubility, low stability and possible immunogenicity. PEGylation through various linking strategies was successfully accomplished here as a solution for the named drawbacks, using a systematic approach to maintain peptide activity and receptor binding specificity. The data relating to TTR binding affinity, conjugate linker stability and the conjugate size distribution in solution of PEG–RAGE peptide conjugates indicated that the conjugates containing amide linkers have the greatest potential for further development as FAP inhibitors. Moreover, this novel conjugate has promising possibilities as a FAP therapeutic to be used alone in the early stages of the disease or as part of rationally designed combination therapy. Preliminary *in vivo* studies (biodistribution) demonstrated the enhanced plasma stability of the peptide upon conjugation, showing no specific accumulation in any organ and renal excretion[88].

Conejos et al. (2015),[13] also proposed a novel library of PGA-doxycycline (DOXY) conjugates that were rationally designed to treat an inherited rare amyloidosis, FAP, with no current pharmacological clinical treatment available in particular for advanced disease stages. Screening their activity as fibril disrupters, PGA-CONH-DOXY conjugates bearing non-biodegradable polymer-drug linkers, showed the best response within all conjugates synthesized and parent drugs, promoting a greater activity at equal doxy equivalents. This fact confirmed that drug release was unnecessary to induce TTR fibril

disruption. PGA-X-DOXY conjugates were not hemolytic and were stable after plasma incubation, which confirmed their suitability for i.v. administration. With the selected candidate, biodistribution experiments were performed through optical imaging and Positron emission tomography (PET) techniques. Studies agreed on a clear renal elimination of the conjugate and a non-specific accumulation in any organ, establishing the suitability of the carrier for the purposed objective. A deeper understanding on organ toxicity through histological analysis disclosed a typical morphology structure without toxic evidences, corroborating the safety of the conjugate. Future directions will encompass *in vivo* evaluation in old FAP model, the possible development of combination therapies as well as the possible application in other amyloid-related diseases where doxycycline has evidenced its potential[13].

As can be notice either drug delivery systems based on nanofiber scaffolds as well as the polymers therapeutics controlled release systems are very promising for novel therapeutic strategies, this is the reason why in the present work they are combined to increase their efficiency for a local application, exploring the potential of composite systems in tissue regeneration.

2 OBJECTIVES

2.1 General Objective

The general objective of this thesis is based on the design and development of intelligent composite system for tissue regeneration through the combination of biomaterial science and nanoconjugate synthesis, in order to have a well-defined biodegradable and biocompatible system with dual mechanism of control on drug release kinetics, and with the possibility to be used on different clinical applications, such as implants in damaged tissue. This overall goal can be broken down into different individual specific objectives as highlighted in the following epigraphs.

2.1 Specific Objectives

- Design and development of novel biodegradable polymeric carriers based on the versatile pH-sensitive polyacetals with improved properties (good solubility, reduced polydispersity, higher loading capacity) as potential carriers to be used in the synthesis of polymer conjugates in combination with biodegradable polymeric scaffold.
- Design, synthesis and characterization of polymer-drug conjugates of model drugs and/or polymer-proteins conjugates with model proteins as prototypes, both with a specific biological activity to promote cellular proliferation and tissue regeneration *in vitro*.

- Design, synthesis and characterization of controlled and well-defined reproducible Microparticles of biocompatible and biodegradable materials such as hyaluronic acid, to serve as polymeric scaffolds to encapsulate the polymer conjugates selected from previous objectives.

- Design and construction of a biocompatible device based on poly-L-lactic acid in order to develop highly versatile patches as ultimate platform to incorporate the microparticles bearing polymer conjugates. This system will allow us to modulate drug release kinetics in applications that require localized supplied of medicines to promote tissue regeneration.

- Systematic *in vitro* studies of drug release kinetics at different pHs of polymer conjugates alone, after their inclusion within the scaffolds, and compared with the same system but loaded with free drug without previous conjugation.

- *In vitro* and *in vivo* evaluation of the systems, including cytotoxicity and proliferation studies in selected representative cell lines
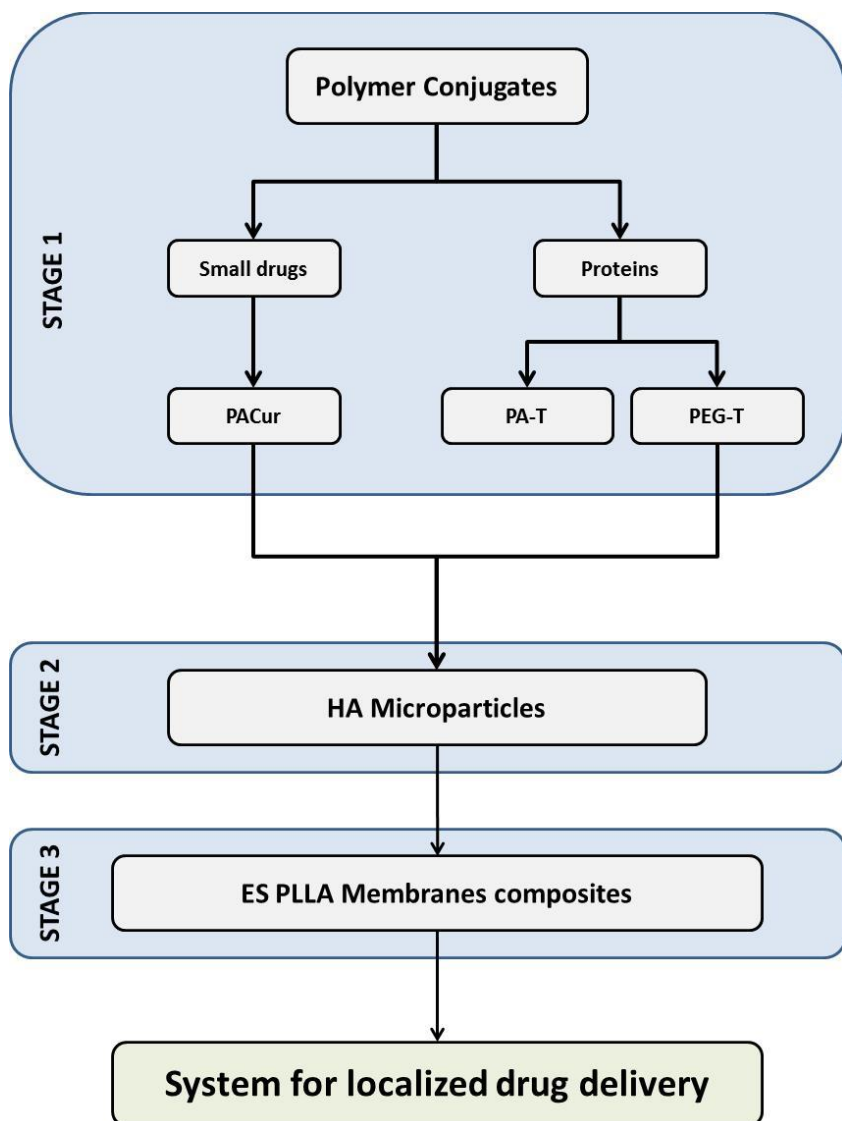
Figure 2.1. General flow diagram of research objective

3 MATERIALS   AND   EXPERIMENTAL TECHNIQUES

3.1 Materials

3.1.1 Polymers

3.1.1.1 *Poly(ethylene glycol) (PEG):*

Chemical   named   as   alpha-Hydro-omega-hydroxypoly(oxy-1,2-ethanediyl) is a polyether compound with many applications from industrial manufacturing to medicine. It is soluble in water, methanol, ethanol, acetonitrile, benzene, and dichloromethane, and is insoluble in diethyl ether and hexane. It is coupled to hydrophobic molecules to produce non-ionic surfactants[89].

Specifically in medical applications, PEG is frequently used as an excipient in many pharmaceutical products, was approved by the FDA for been used as the basis of laxatives, and the most relevant for this research porpoise, several PEGylated-proteins nanomedicine have been also approved for clinical regular use in treatment of different diseases as for example PEG-interferon alpha, which is used to treat hepatitis C, as it was previously described in the introduction section about Polymer Therapeutics.

For this research platelets of PEG with average molecular weight M_n 4000, were used as supplied from Sigma-Aldrich (Dorset, UK), as one of the monomers in the synthesis of poly(acetals).
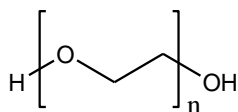
Figure 3.1. PEG$_{4000}$ Chemical Structure

Functionalized PEG were used in order to synthesize two families of PEGylated-trypsin conjugates.

3.1.1.2   α-methoxy-ω-carboxylic acid poly (ethylene glycol) (MeO-PEG-COOH),

First family, with MeO-PEG-COOH of different molecular weights: 1) M_W=20000Da with Mw/Mn=1.08; 2) Mw=11153Da, with Mw/Mn=1.08, and 3) Mw=1892Da with Mw/Mn=1.00. These products were used as supplied by IRIS Biotech GmbH (Germany).
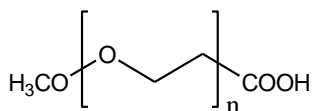
Figure 3.2. MeO-PEG-COOH Chemical Estructure

3.1.1.3   α-methoxy-ω-hydroxyl poly (ethylene glycol) (MeO-PEG-OH),

Second family with MeO-PEG-OH of different molecular weights: 1) M_W=20000Da with Mw/Mn=1.08; 2) Mw=11153Da, with

Mw/Mn=1.08, and 3) Mw=1892Da with Mw/Mn=1.00, These products were used as supplied by IRIS Biotech GmbH (Germany).
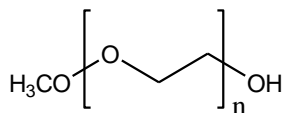
Figure 3.3.. MeO-PEG-OH Chemical Estructure

3.1.1.4   *Poly(L-lactic) acid (PLLA),*

PLA or poly-lactide was discovered in 1932 by Carothers (at DuPont). In comparison to other biopolymers, the production of PLA has numerous advantages including: (a) production of the lactide monomer from lactic acid, which is produced by fermentation of a renewable agricultural source corn; (b) fixation of significant quantities of carbon dioxide via corn (maize) production by the corn plant; (c) significant energy savings; (d) the ability to recycle back to lactic acid by hydrolysis or alcoholysis; (e) the capability of producing composite paper-plastic packaging that is compostable; (f) reduction of landfill volumes; (g) improvement of the agricultural economy; and (h) the all-important ability to tailor physical properties through material modifications[90]. Briefly, PLA is based on agricultural (crop growing), biological (fermentation), and chemical (polymerization) sciences and technologies.

It is classified as generally recognized as safe (GRAS) by the United State Food and Drug Administration (FDA) and is safe for all food packaging applications (Conn and others 1995; FDA 2002).[91]

Likewise, in the field of regenerative medicine, different devices made of PLA have been thoroughly study with very promising results. For all this reasons it was decided to use PLA as bulk material to prepared thin microporous membranes through the technique of electrospinning.

PLA used for this research was supplied by Ingeo™ Lactides, Natureworks, is a commercial amorphous PLA, specific for injection mold grade and having a 96:4 L:D ratio content and MW 66000g/mol.
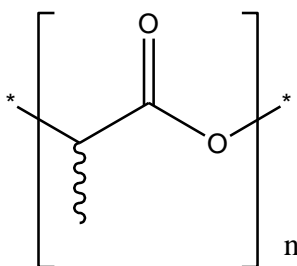
Figure 3.4. Poly(L-lactic) acid (PLLA) Chemical Structure

3.1.1.5 *Hyaluronic acid sodium salt (HA):*

HA is a linear polysaccharide composed of alternating d-glucuronic acid (GlcUA) and N-acetyl-d-glucosamine (GlcNAc) units. This anionic, non-sulfated glycosaminoglycan is the major component of the ECM. It is widely distributed in connective, epithelial and neural tissue[92]. Hyaluronan, as is also known, due to its ionic nature, interacts with a number of cell surface receptors, such as CD44, RHAMM (receptor for HAmediated motility) and ICAM-1 (intercellular adhesion molecule 1) and contributes to tissue hydrodynamics, cell proliferation and migration. Due to its high biocompatibility and low immunogenicity,

HA is gaining popularity as a biomaterial for tissue engineering and tissue regeneration[93].

For this research HA was used as row material to obtain micro-particles cross-linked with di-vynyl-sulfone, which were loaded with drugs, proteins and the respective polymeric conjugates, in order to study the release kinetic of each system afterward.   Hyaluronic acid sodium salt from Streptococcus equi (HA, Poly(β-glucuronic acid-[1→3]-β-N-acetylglucosamine-[1→4]), alternating) supplied by Sigma-Aldrich, with average Mw 1.63×10^6 Da.
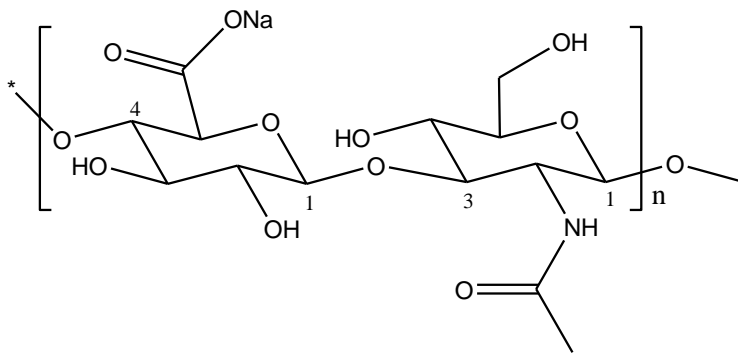
Figure 3.5. Chemical Structure of hyaluronic acid (HA).

3.1.1 Model Drugs

Curcumin (Cur)

This hydrophobic small drug is a natural polyphenolic compound, extracted from Curcuma longa, with proof anti-oxidant, anti-inflammatory, antiviral, antimicrobial and anticancer activity[28–31]

Curcumin ≥95% (HPLC) powder, was supplied by sigma-aldrich.
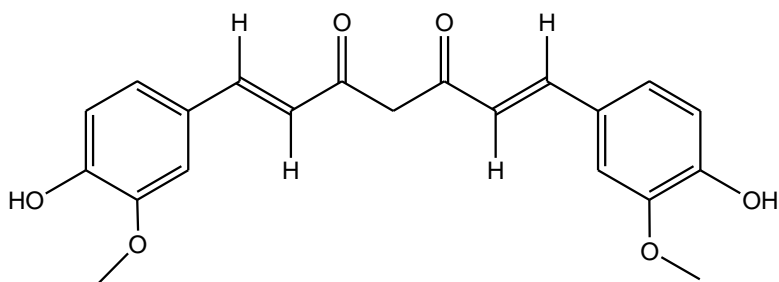
Figure 3.6. Chemical structure of curcumin

3.1.2 Model Protein

Trypsin

It is protein with proteolytic enzymatic activity frequently used as model protein for evaluation of controlled drug delivery systems[32–34]

In this work it was used Trypsin from porcine pancreas, Type IX-S, presented as a lyophilized powder, of 13,000-20,000 BAEE units/mg protein. Protein was supplied by Sigma-Aldrich
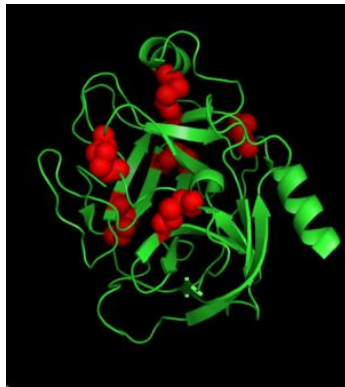
Porcine Trypsin [Green: Backbone, Red: Disulfide bonds]

http://prince.openwetware.org/FASP.html

Figure 3.7. Virtual Model of trypsin

3.1.3   Chemical reactive and solvents.

Tri(ethylene glycol) divinyl ether (TEGDVE), poly(ethylene glycol) (PEG) Mw 4000Da, p-toluenesulfonic acid monohydrate (p-TSA), 2-amino-1,3-propanediol (Serinol), 9-Fluorenylmethyloxycarbonyl chloride (Fmoc-Cl), succinic anhydride, , Dioctyl sulfosuccinate sodium salt, 98% (AOT), Divinylsulfon 97% (DVS), 4-(Dimethylamino)pyridine (DMAP) purum ≥98.0%, N,N-Diisopropylethylamine (DIEA) reagent plus, 1,4-dithio-dl-threitol (DTT), bromophenol blue ACS reagent, ammonium persulfate (APS) for electrophoresis, Nα-benzoyl-D,L-arginine-p-nitroanilide hydrochloride (L-BAPNA), Bradford solution, 2-mercaptoethanol, 2,4,6-trinitrobenzene sulfonic acid (TNBS), N-hydroxysuccinimide 98% (NHS) and N-hydroxysulfosuccinimide sodium salt (sulfo-NHS) ≥98.5% were used as supplied from Sigma-Aldrich (Dorset, UK). Diisopropilcarbodiimide (DIC), 1-ethyl-3-(3dimethylaminopropyl) carbodiimide hydrochloride (EDAC), 1-hydroxybenzotrialzole monohydrate 99.7% (HOBT), were supplied by IRIS Biotech GmbH (Germany)., Triethylamine was from Fluka Chemika (Masserschmittstr, D).

AppliChem(Germany) supplied 2,2'-dihydroxy-(2,2'-bi-indan)-1,1',3,3'-tetrone (Hydrindantin dihydrate). Ninhydrin GR for analysis was from MERCK (Germany). Tris(hydroxymethyl)aminomethane (Tris base) and sucrose were from Roche Biotest. Glycine (Gly), sodium dodecyl sufate (SDS), N,N,N,N'-tetramethylethylendiamine (TEMED), were from VWR (Germany). A 40% solution of acrylamide/bis(acrylamide) (ratio 29:1, 3.3%C) Acrylamid: N,N'-methylenbisacrylamid

electrophoresis purity reagent from Bio-Rad Laboratories (United States of America).

Solvents: 2,2,4-Trimethylpentane (isooctane) CHROMASOLV[®], for HPLC, ≥99%, 1-heptanol 98% (1-HP) was used as supplied from Sigma-Aldrich (Dorset, UK)., Tetrahydrofuran (THF) anhydrous (before use, THF was distilled from a sodium-benzophenone solution.), N,N-dimethylformamide (DMF) were from Fluka Chemika (Masserschmittstr, D). Dichloromethane (CH_2Cl_2) synthesis grade with approx. 50ppm of amylene, Ethanol (EtOH) absolute GR for analysis, Methanol (MeOH) HPLC grade and acetonitrile (AcCN) HPLC grade were from Scharlau (Spain).), n-hexane analytic grade were from VWR (Germany) The solvents used to obtain ^{1}H RMN and ^{13}C RMN spectra were chloroform-d 99.8 atom %D ($CDCl_3$), deuterium oxide 99.8 atom %D (D_2O) from Carlo Erba Réactifs-SDS (France), and Dimethyl sulfoxide-D6 99.8% from MERCK (U.K.).

Resins for liquid chromatography Sephadex LH-20 and Sephadex G-10 and pre-packet PD-10 columns were from GE healthcare (U.K.).

3.2   Experimental Techniques

3.2.1   NMR Spectroscopy: ^{1}H and ^{13}C.

Professor Joseph P. Hornak from Rochester Institute of Technology, explain on his book "The Basis of NMR" that Nuclear magnetic resonance, or NMR, is a phenomenon which occurs when the nuclei of certain atoms are immersed in a static magnetic field and exposed to a second oscillating magnetic field.   Nuclear magnetic resonance spectroscopy is the use of the NMR phenomenon to study physical, chemical, and biological properties of matter. As a consequence, NMR spectroscopy finds applications in several areas of science. NMR spectroscopy is routinely used by chemists to study chemical structure using simple one-dimensional techniques. Two-dimensional techniques are used to determine the structure of more complicated molecules[94].

In this experimental work, this technique was applied to corroborate the structures of polytacetals synthetized, their purity and effective drug loading after conjugation reaction.

Nuclear Magnetic Resonance analyses were performed using a BRUKER ADVANCE AC-300 (300 MHz) spectrometer in Centro de Investigación Príncipe Felipe in Valencia and NMR data were processed using the program Topspin 1.3 (Bruker GmbH, Karlsruhe, Germany). The chemical shifts of the nucleus are reported as **s** (singlet), **d** (doublet), **t** (triplet), **q** (quartet) or **m** (multiplet) and expressed by δ (ppm) taking as an intern reference the tetramethylsilane signal (TMS) 0.00 ppm, and the intermediate signal

in the quintuplet (49.86 ppm) in the carbon spectra. The J-coupling constants are expressed in hertzs (Hz). Besides ^{1}H and ^{13}C NMR experiments, two-dimensional NMR experiments were done also to including Correlation spectroscopy (COSY), and Diffusion-ordered spectroscopy (DOSY) to remove spectral overlap, facilitates spectral assignment, and obtain information related to number of different species present in a sample, available from resonance intensities and the diffusion coefficient of the polymers obtained.

3.2.2   UV Spectrophotometer.

UV spectroscopy technique was used to determine total drug loading in polymer-protein and polymer-drug conjugates, dissolving the compounds in PBS 1X pH 7.4 to prepare solutions of 1 to 3 mg/mL in polymer, depending on the absorbance on each case.

The calibration curve was built using a solution of de drug/protein that it was pretend to conjugate dissolved in the same solution than the polymer.

Hydrophobic drug was previously dissolve in ethanol and then diluted in PBS 1X pH 7.4.

Measurements were done with an UV-Vis double-beam spectrophotometer with single monochromator to cover a spectral wavelength range from 190 to 2700 nm. Equipment model was Jasco UV-670. Samples were analyzed in quartz cuvettes with a light path 1mm.

3.2.3   Gel Permeation Chromatography (GPC).

GPC, is an important analytical tool used to evaluate polydispersity (PDI) and molecular weight (Mw) characteristics of natural or synthetic polymers and proteins. Unlike HPLC, GPC relies, under ideal conditions, on a pure physical separation, where theoretically no chemical interactions of the sample with the GPC column (stationary phase) should be observed[95,96].   To be more precise, GPC separates molecules upon their size in solution, which is directly proportional to their hydrodynamic volume (Vh).

Calibration was accomplished with well-defined poly(ethylene glycol)/Polyethylen oxide (PEG) standards (GPC calibrating kit, supplied by MERCK) in order to be able to use them as reference to stablish a relative comparison with the polymers synthesized as part of this research, making possible to applied GPC technique to determine molecular weights of polymeric conjugates as well as following their degradation profile in solution at different pH (7.4, 6.5, 5.5) with time.

Gel permeation chromatograms were obtained in DMF/THF and Phosphate buffer solution (1X, pH 7.4) using two Waters Styragel 7.8x300mm Columns (HR3 and HR4) for DMF and two TSK-Gel Columns (G2500 and 3000) for samples in PBS and a Viscotek TDA 302 triple detector Array with refractive index (RI), Small Angle Light Scattering, Right Angle Light Scaterin, viscosimeter and a model 2501 UV as detector. OmniSec v.4.1 software was used to calculate the polydispersity (Mw/Mn) and molecular weight (Mw) characteristics.

Mobile phase preparation.

Aqueous mobil phase.   First, a 10X PBS solution was prepared by dissolving the compound mentioned below in the amounts specified in the table X in 1 L de-ionized, double distiled water.   Then, 1L of PBS 1X pH 7.4 solution was prepared by dilution, using a 1L volumetric flask and a graduated cylinder to be accurate. Following this protocol the final solution should be pH 7.4, and it was corroborated with a pH-meter. This way the variability of composition, ionic strength or pH in the mobile phase was prevent. The solution was then filtered through a nylon membrane filter (0.2 µm) and sonicated for 30min before use.

Organic mobil phase. THF (2.5 L bottle), of HPLC grade already stabilized with BHT (250 ppm) by the supplier was used as organic mobile phase. The solvent was used without further preparation because system was equipped with a degasser.

Sample preparations and running conditions

For the GPC measurements, samples were prepared with a known concentration (6mg/ml, 2 mL) dissolved in the previously prepared mobile phase (THF or PBS). Prior injection, the samples were filtered through single-use syringe filters with 0.2 µm nylon membrane. Then 100 µL of samples were loaded into the loop by the automatic sampler system, and running for 35min or 60min, at 30 °C with a 1mL/min flow rate.

3.2.4 Reverse Phase High performance liquid chromatography (RP-HPLC)

To determined free drug amount in polymer-drug conjugates, samples of 3mg/mg dissolved in ACN were analyzed using RP-HPLC technique. Calibration curve was built using solutions of different concentrations of the model drug dissolved in ACN.

Analyses were performed with a Shimadzu analytical HPLC system using 717plus auto-sampler and a LIChroCART®, Cat.1.50943 LIChrospher® 100, RP-18 (125 x 4 mm, 5 µm) column (Lot. L 56118817 No. 721869) purchased from Waters Ltd. (UK).   Buscar datos de HPLC del -1 y de CBIT

3.2.5 Fast Protein Liquid Chromatography (FPLC)

This instrument was an AKTA PURIFIER from Amersham Biosciences (now GE Healthcare) it has a dual-pump system (P900) with a Monitor pH/C-900 for On-line measurement of pH and conductivity. The machine is provided with an online UV detector (UV-900) which can be set for a maximum of three wavelengths covering a range from the far UV region (214nm) to the visible range (700nm). System includes an injector (INV-907) and a fraction collector (FRAC-900). It is handled with software Unicorn 4.11. In this case it was used a column HiPrep Sephacryl S300 XK26/60 and a column Superdex 200; both were purchased from GE Healthcare Bio-Sciences.

3.2.6   Circular Dicroism (CD) Spectrophotometer

This instrument was a Jasco J-1100, wavelength range 180 – 600 nm, sample were measure with microsampling quartz cuvettes.

All these equipments are located at Centro de Investigación Príncipe Felipe (Spain).

3.2.7   Differential Scanning Calorimetry (DSC)

Measurements were done with a METTLER-TOLEDO DSC model 823e (Mettler-Toledo Inc., Columbus, OH, USA) to determine thermal properties of different materials. Samples were accurately weighted in standard 30μL aluminum pans and pierced. Scanners were undergone precooling samples from room temperature to -30ºC at 10ºC/min, then analyses were programed to follow three cycles: heating-cooling-heating, since -30ºC to 300ºC and back.   Row data was processed with the software that is provided with the equipment (MettlerSTARe software) to determine values of glass transition (t_g) and heat capacity (ΔC_p).

3.2.8   Thermo Gravimetric Analysis (TGA)

The equipment used was a METTLER-TOLEDO model TGA/SDTA 851 operated through the software provide with the device STARexx. Samples were weighted in platinum crucibles and scanned from 30ºC to 800ªC at 10ºC/min under N_2 flow of 20mL/min.

3.2.9 Particle Size Analyzer

The instrument used for measuring particles average size was Malvern instrument, model Mastersizer 2000, Laser light scattering, based on Mie and Fraunhofer scattering analytical methodology. Data acquisition rate was 1 kHz; Optic system is composed by a Red light source (Max. 4mW He-Ne, 632.8nm), a Blue light source (Max. 0.3mW LED, 470nm), and Reverse Fourier (convergent beam) Lens arrangement. Particle size range measurement is 0.02 - 2000 μm, depending on sample and sample preparation, with accuracy better than 1% (polydisperse standard) and reproducibility better than 1% variation (polydisperse standard). Data Analysis was accomplished with Malvern Software Mastersizer 2000 v.5.60.

3.2.10 Contact angle measurements.

Materials surface wettability was estimated with a equipment Dataphysics OCA (DataPhysics Instruments GmbH, Filderstadt, Germany), measuring the contact angle between the material surface and a distilled water drop. Final values are the average from at list 10 measures by each sample.

3.2.11 Mechanical Tensile test.

The stretching assay of electrospun mats were performed in a stress-strain machine model Microtest SCM3000 95 (Microtest SA, Madrid, Spain). Samples were cut as rectangles of 0.5 x 1.5 cm^2 approximately. Stress rate was 0.2mm/min until fracture. Row data was process and plotted as stress (σ)-strain (ε), in order to calculate the elastic moduli

from the slope of the linear region of the curves. Final value is the average of at least 5 measures.

3.2.12   Scanning Electron Microscopy (SEM).

Equipment JEOL model JSM-6300 (JEOL Ltd., Tokyo, Japan) was used with samples previously sputter-coated with gold under vacuum. Analyses were carried out at 15kV of acceleration voltage and 15mm of distance working.

3.2.13   Optical Microscopy.

NIKON Eclipse microscope, model E6000, with objectives x20, x50 and x100 was used to analyzed samples placed over glass microscope slides.

3.2.14   Ultra-thin nanofibers microporous membranes made by Electrospinning.

Home-made electrospinning equipment, composed for a syringe pump from New Era Pump, Inc. and a high voltage source power Glassman High Voltage, Inc., model PS/FC30P04, input 220V, output +30kV, 4.0mA. All these equipments are located at Universidad Politècnica de Valencia (Spain).

3.2.15   Synthesis of Micro-particles by reverse phase Emulsion technique

Stirrer model IKA T-25-ULTRA TURRAX was used to prepared w/o emulsions. To obtain the micro-particles it was used a stirrer OST 20 basic digital IKA Yellow [line].

4. SYNTHESIS AND CHARACTERIZATION OF POLYMER PROTEIN CONJUGATES USING TRYPSIN AS MODEL PROTEIN.

4.1. Introduction

As stated in chapter 2, one of the objectives of this work was the encapsulation of polymer protein conjugates into microparticles and finally into membranes of PLLA fibers in order to provide a proteic nature drug with a greater stability in plasma once release from the scaffold enhancing in such manner its possible therapeutic output.

Looking at the polymeric carriers well-known for protein conjugation, polyethyleneglycol (PEG) appears as the most relevant as described in the introduction chapter, however, this carrier is non-biodegradable and even though has already demonstrated clinical safety, biodegradable polymers could offer benefits mainly if a chronic life-threating disease is considered as target. For this reason the two different strategies for protein conjugation were taken into account in this work, using trypsin as model protein: a) Protein PEGylation[32,97,98], as example of system with non-biodegradable polymer carriers and b) Protein conjugation with PEG-polyacetals[79,99], as example of a pH-responsive polymeric carrier.

The field of Polymer-Protein conjugates is experiencing an exponential growth in its use for the daily treatments applied in the clinic. However, there are still some important challenges to face regarding its formulations and clinical use. Before they reach their targets in the

body, these proteins can be degraded by the blood proteases or in the liver, suffer a fast renal excretion or generate an immunogenic response. Other drawbacks arise from their chemical nature, e.g., poor water solubility in some cases, lack of proper target specificity within the body, or low internalization kinetics[24].

Polymer-protein conjugates (also polymer-aptamer) have been introduced in the market in order to overcome these problems. Most of these nanomedicines are conjugates of poly(ethylene)glycol (PEG). Thus, Oncaspar® and Neulasta™ are already approved for cancer chemotherapy, PEG-Intron® and Pegasys® for Hepatitis C treatment, Cimzia® for Rheumatoid arthritis and Crohn's disease, Mircera® for the treatment of the anemia, Somvert® in the case of Acromegalia and Adagen® for the severe combined immune deficiency syndrome[10]. Nevertheless this first generation of conjugates shows still some weaknesses. The use of PEG in therapies where a chronic administration is required is limited due to its lack of biodegradability, which enables the risk of accumulation in the body during the treatment.[98,100] Therefore there is a need of developing a smarter second generation of polymer-protein conjugates.

The replacement of PEG by a biodegradable polymer in such compounds gives rise to a recently reported approach in Polymer Therapeutics. The so called polymer-masking-unmasking-protein therapy (PUMPT), first described by Duncan et al[87,99], provides a versatile strategy with potential to enable the protection of proteins normally inactivated while traveling to their therapeutic target and/or to allow controlled release with time of active proteins at the target

site promoted by the polymer degradation. Depending on the pharmacological target, the degradation must take place either extracellularly (as in the case of the growth factor, cytokines or antibody against membrane receptors) or after being internalized by endocytosis (e.g, with cytosolic enzyme delivery, in this case endosomolytic polymers are required or lysosomal replacement therapy).

Two different families of PUMPT has been described, namely these which use dextrin (DEX as partner polymer) and the ones with hyaluronic acid (HA). DEX-trypsin was originally chosen as a prove-of-concept model to illustrate PUMPT. Masking growth factors with DEX has also been successfully achieved and applied to inhibition of melanin production in B16F10 cells. Another prominent example is the case of DEX - rhEGF conjugated, which has proved its effectivity in vitro, as well as ex vivo and in vivo wound healing experiments with remarkable results. Fergusson et al[101,102] has enlarged the window of applicability of PUMPT by implementing a DEX-phospholipase conjugate, namely DEX-PLA2, in Polymer enzyme liposome therapy (PELT). The release of a non-soluble drug encapsulated in a liposome is controlled by the unmasking of the co-administered PUMPT conjugate.

HA-Trypsin and HA-EGF have been described as HA conjugate models in an attempt of combining PUMPT-guided delivery control with the inherent properties of this polymer, including tissue regeneration and wound healing[103].

Very recently in the group, Poly-L-glutamic acid (PGA)has been also explored as alternative carrier for PUMPT[104]. PGA is biodegradable(by lysosomal enzyme cathepsin B), multivalent, non-immunogenic, non-toxic polymer[105], and some PGA-drug conjugates have already reached the clinic, in fact one of the most advanced polymer-drug conjugates is Opaxio® in advanced phase III clinical trials, which was recently granted as an orphan drug for the treatment of glioblastoma when combined with radiotherapy[6,10] By rationally re-designing the PUMPT concept, PGA conjugates with anticancer enzymes can have high potential for the treatment of cancer, as they can accumulate in tumor tissues through the EPR effect[106]. In addition, due to the cellular uptake of PGA conjugates by endocytosis, PGA-based PUMPT conjugates can also have great potential for enzyme replacement therapy in lysosomal storage diseases, a family of diseases caused by deficiencies of lysosomal enzyme[107–109]. A new variation of the PUMPT concept was presented with PGA, where unmasking and subsequent protein release relies on the cleavage of a reduction sensitive linker in specific sites of the body[104]. In this study lysozyme was used as model protein recovering after polymer unmasked almost all proteolytic activity.

Degradation of DEX, HA or PGA requires the presence of a determined enzyme (α-amylase, hyaluronidase and cathepsin B, respectively) in significant amounts in the biological compartment where the wrapped protein has to be unmasked, ensuring the specificity of the delivery. These enzymes may not be necessarily involved in many crucial

processes of the body such as inflammation, response to the presence of a tumor, arthritis, tissue regeneration or wound healing among others. Importantly, a drop in the pH has been observed during these processes around the affected area. Therefore, alternative solutions to this so-restricted unmasking step must be explored in order to expand the applicability of this technology.

Polyacetals are macromolecules that can be achieved under gentle conditions by an acid catalyzed addition of a diol to divinyl ether. Stability of the acetal moiety both, at basic and at neutral pH arises from the lack of chemical mechanism of replacement of any of the substituents of acetal carbon. However, protonation in acid media of the oxygen enables the disruption of the polymeric chain with a pH-dependent kinetics rate[11,78–80,110].
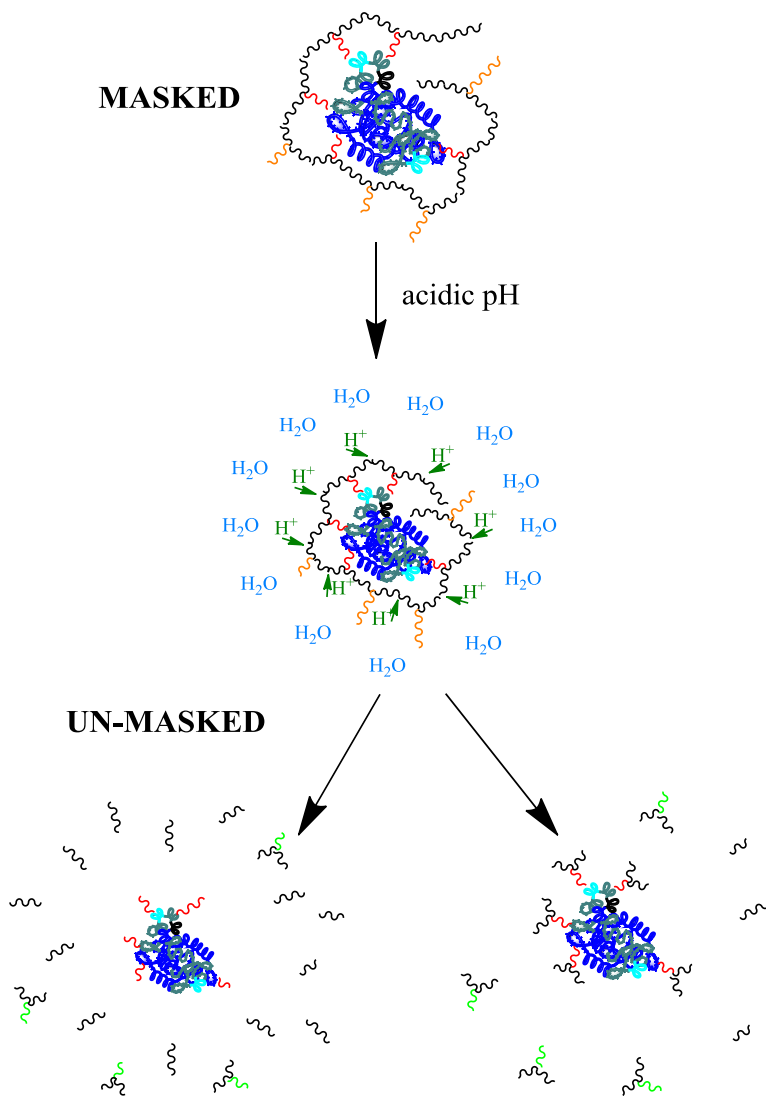
Figure 4.1. Scheme of PUMPT mechanism based on polyacetals degradation triggered by acidic pH.

Additional interesting physico-chemical properties of the main polymer chain can be tuned by the use of conveniently chosen diols. Copolymerization with functionalized diols allows the insertion of reactive centers in the backbone that can be used for multiple bioconjugation of a drug or a biologically active protein and to increase their payload. Reaction of the divinyl ether with short molecular weight PEG based diols ensures the water solubility of the resulting polyacetal as well as the retention of most of the other PEG-related properties above mentioned, while the polymer keeps the ability of self-degradation at acidic pH. This fact clearly overcomes the problem of PEGylated nanodrug accumulation in chronic treatments.

The aim of this study was to develop a degradable PEG-mimicking PUMPT system capable of unmasking the protein only under acidic conditions. Functionalized new PA backbones (containing fragments of PEG-diol 4000 Da units and serinol moieties with adequate functionalities) have been synthesized and physico-chemically characterized. Trypsin has been used as a model enzyme in order to build our PUMPT. Influence of linker (succinoylated PA) and the effect of the proportion of polymer to protein in the masking/unmasking capability of the PA have been investigated. The biological activity of the masked and unmasked protein has been assessed using N-benzoyl-L-arginine-p-nitroanilide (L-BAPNA) as a substrate. Finally, the ability of the protein to recover its full initial activity after the PUMPT process has been evaluated.

PEG-trypsin conjugate has been also synthesized in order to directly compare this FDA approved non-biodegradable polymeric carriers with the newly synthesized pH-responsive PA-trypsin conjugate.

4.2. Methodology

4.2.1. Synthesis and Characterization of Polyacetals (PA)

4.2.1.1. Synthesis of amino-pendant PolyAcetals

- Synthesis of Fmoc-2-amino-1,3-propanediol (Fmoc-serinol, 1)

Fmoc-Serinol (1) was synthesized following the methodology reported by Tomlinson et.al. Basically, serinol (0.0820 g, 7.500 mmol) was dissolved in aqueous Na_2CO_3 (10% solution in water, 20 mL). Dioxane (15 mL) was added, the mixture was cooled down (4 ºC), and Fmoc-Cl (0.0290 g, 7.500 mmol) was added carefully. Reaction was carried out at 4ºC (4 h) and then at room temperature (12 h). After that, mixture was poured in water (100 mL). To recover the final product, it was extracted from with ethyl acetate (3 x 100 mL). The organic phase was dried, filtered off and concentered. Finally, the product was washed in a large excess of hexane to yield a white loose powder.

Yield 80%. ^{1}H NMR [(δ (ppm), 300 MHz, $CDCl_3$]: δ 7.68 (d, J = 6.2 Hz, 2H, ArCH-), 7.54 (d, J = 6.2 Hz, 2H, ArCH-), 7.38 (t, J = 6.0 Hz, 2H, ArCH-), 7.31 (td, J = 6.2, 1.0 Hz, 2H, ArCH-), 5.74 (s, 1H, R'': R'-O_2CNH-R'''), 4.91 (d, J = 5.2 Hz, 2H, R': R-CH_2-R''), 4.72 (t, J = 5.5 Hz, 1H, R: Ar-CHR'-Ar), 4.35 (dd, J = 21.4, 12.2 Hz, 5H, R''': CH_2CHR''CH2), 2.80 (s, 4H, -OH)

- Synthesis of amino-pendant Fmoc-serinol protected (PAFS, 2) and de-protected (PANH$_2$, 3) PolyAcetals,:

PANH$_2$s were synthesized by copolymerization of diol monomers (Fmoc-serinol and PEG4000, Mw ≈ 4000 g/mol) with ethylene groups of TEGDVE through addition reaction catalyzed in acidic conditions, following the protocol published by Gimenez et. al.[11] based on the procedure described by Tomlinson[78,79]. Briefly, PEG4000 (1.0100 g, 0.25 mmol,) and Fmoc-serinol (0.1170 g, 0.375 mmol) were dried under high vacuum (15 min) in a Schlenk tube. Dried anhydrous 1,4-dioxane (Dioxane, 6 mL) was added under inert atmosphere conditions. Then, pTSA (1 mL of a previously prepared 2mg/mL solution in dioxane, 0.0023 g, 0.010 mmol) was dropped over the reaction mixture, which was then warmed (60 ºC) until complete dissolution of the reactants. The system was left stirring until cooled down at room temperature (21ºC) and then TEGDVE (128 µL, 0.1264 g, 0.625 mmol) was carefully added. The solution was covered from light and left reacting for 1h. After this time the polymer obtained was the Fmoc-serinol amino-pendant polyacetal (**PAFS, 2).** Small sample was isolated to be analyzed by ^{1}H NMR in order to follow the reaction and to determine the amount of Fmoc protected amino group moieties present in the polymer main chain. Once quantification was performed, the reaction was quenched with KOH (2mL, 1M in methanol) to ensure the complete deprotection of the amino group as well as the total neutralization of catalyst, pTSA. The solution was poured over a mixture of hexane: diethyl ether, 4:1 (100 mL), and the precipitate obtained was washed three times by re-dissolving it in

ethyl acetate and precipitating it in ether. The suspension was centrifuged and the pellet dried under a N_2 stream. The obtained amorphous white solid was identified as the amino-pendant polyacetal (**PANH₂, 3**) (0.6510 g, yield: 78%). Polymers were characterized by 1H-NMR (identity and reaction success) and GPC (to determine the Mw). Ninhydrin assay showed that the amount of amino groups loaded in the polyacetal.

PAFS (2): ^{1}H NMR (300 MHz, Acetone) δ 7.86 (d, J = 6.0 Hz, 2H, ArCH-), 7.71 (d, J = 7.4 Hz, 2H, ArCH-), 7.42 (dd, J = 12.0, 5.0 Hz, 2H, ArCH-), 7.34 (dd, J = 12.8, 5.5 Hz, 2H, ArCH-), 4.76 (dd, J = 10.5, 5.3 Hz, 3H, acetal-CH-), 4.34 (d, J = 15.3 Hz, 2H, R-CH$_2$-R), 4.24 (s, 1H, Ar-CH-Ar), 3.85 – 3.78 (m, 3H), 3.78 – 3.39 (m, 420H, PEG-CH$_2$-O), 3.39 – 3.29 (m, 3H), 2.52 (s, 1H), 2.30 (d, J = 2.4 Hz, 1H), 2.26 (qt, J = 4.4, 2.2 Hz, 1H), 1.86 – 1.82 (m, 1H), 1.25 (d, J = 1.6 Hz, 4H, acetal-CH$_3$), 1.24 (d, J = 1.5 Hz, 5H, acetal-CH$_3$). Mw 12257 g/mol; Mw/Mn = 1.9.

PANH₂ (3): ^{1}H NMR [(δ (ppm), 300 MHz, Acetone]: δ 4.85 – 4.56 (m, 3H, acetal CH), 3.97 – 3.22 (m, 337H, PEG -CH$_2$-CH$_2$-), 1.38 (s, 1H), 1.26 (t, J = 7.7 Hz, 12H, acetal -CH$_3$). GPC (PBS 100mM, pH 7.4, T=35∘C) Mw 10889 g/mol; Mw/Mn = 1.8. TNBSA assay reveled the amount of amino groups loaded in the polyacetal was 1.6wt%.

- Synthesis of PASucc (4):

PASucc (4) was obtained by succinoylation of **PANH₂ (3)**. Briefly, 0.5000 g of **PANH₂** 10889 g/mol, 0.4946 g, 0.0065 mmol-equivalent of NH$_2$,) was dried in the *Schlenk tube* under high vacuum and N_2 atmosphere for 10 min; then it was dissolved in anhydrous THF

recently distilled (10mL), followed by the addition of succinic anhydride (0.0125 g, 0.125mmol) and DMPA (0.0153g, 0.125mmol). Reaction mixture pH was adjusted to 8 with Et$_3$N and left reacting under vigorous stirring and N$_2$ atmosphere (24h, 21ºC). A white powder was obtained after precipitation of the reaction mixture in hexane: diethyl ether (4:1, 100mL). The solid was isolated by centrifugation, re-dissolved in THF (10mL) and precipitated as describe in the previous step. This process was repeated 3 times. The resulting solid was dried under a N$_2$ stream, dissolved in milliQ water (15mL) and concentrated with centrifugal concentrators tubes (Vivaspin^{TM}) (20mL MWCO 10000, 6000 rpm, 25º fixed angle rotor, 4ºC, 3x). The concentrated solution (5mL) was freeze dried. The product was recovered and characterized by ^{1}H NMR. 90% Yield. ^{1}H NMR [(δ (ppm), 300 MHz, Acetone]: δ 4.69 (qd, J = 5.3, 1.8 Hz, 1H acetal CH), 3.86 – 3.18 (m, 138H), 2.61 – 2.35 (m, 1H succinoylate CH$_2$-CH$_2$), 1.27 – 1.19 (m, 3H acetal CH$_3$). GPC (PBS 100mM, pH 7.4, T=35∘C) Mw=10512 g/mol, Mw/Mn=1.4). Carboxylic group content was 2.3 wt%, determined by titration with NaOH (0,02mM).

- Synthesis of PACOOH (5):

PACOOHs (5) were synthesized following a similar copolymerization process but, replacing serinol by 2,2-tris (hydroxymethyl) propionic acid (BHMPA) as monomer to obtain a novel carboxylic pendant polyacetal. Briefly, PEG4000 (1.0151 g, 0.250 mmol), BHMPA (0.0335g, 0.250 mmol) and pTSA (0.0024 g, 0.01 mmol) were dried in the *Schlenk tube* under high vacuum and N$_2$ atmosphere for 10 min. Dioxane (5mL) was added, mixture was stirred and warmed (60ºC) until completely

dissolution of the reactants. The solution was left cooling down to room temperature. TEGDVE (0.1112 g, 112 µL, 2.200 mmol,) was then added. The reaction was left covered from light (21ºC room temperature, vigorous stirring) until the complete consumption of free TEGDVE, followed by disappearing of quadruple signal of free TEGDVE at 6.5 ppm monitored by ^{1}H NMR in CDCl$_3$ (1 h in this case). The mixture was quenched with KOH (2 mL, 1M in MeOH). The final product was purified and dried as describe above for PANH$_2$. A white powder was obtained and identified as PACOOH. 80% yield. ^{1}H NMR [(δ (ppm), 300 MHz, ^{6}d-DMSO]: δ 4.75 – 4.50 (m, 4H acetal CH), 3.96 – 2.92 (m, 637H CH$_2$-CH$_2$-O), 1.31 – 1.06 (m, 9H acetal CH$_3$), 0.89 (t, J = 3.2 Hz, 3H acetal CH$_3$). GPC (PBS 100mM, pH 7.4, T=35°C) showed Mw 10307 g/mol; Mw/Mn=2.1. Carboxylic content was 1.3wt%, determined by titration with NaOH (0.02mM).

4.2.2. Synthesis and characterization of Polyacetal-Trypsin conjugates.

Polyacetylation of the trypsin was achieved through a condensation reaction between amino (NH$_2$) groups from the lysine amino acids of the protein and the carboxylic groups of polyacetals (4) and (5).

In both cases, carboxylic moieties of polyacetals (4) and (5) were activated in DMF (1mL) with EDAC (1.5 mol excess respect to COOH mol, for 10min) and Sulfo-NHS (1.5 mol excess respect COOH mol, another 45 more min). Then, protein was added to the reaction mixture (dissolved in 0.1M Borate Buffer solution pH 9.2). The amount of protein used for each reaction was calculated taking in account a

determined molar ratio between functional groups in polyacetals (20 mmol, 40 mmol or 60 mmol of COOH groups) and in trypsin (by 1 mmol of NH$_2$ groups). Reactions were carried out during 16h at 4ºC. The conjugates from each type of polyacetal were purified with centrifugal concentrators tubes (Vivaspin™) (20mL, MWCO 10000, 6000 rpm, 25º fixed angle rotor, 4ºC), diluting the reaction mixture with d.d.H$_2$O up to 15mL. Samples were concentrated to 5mL and re-diluted to 15 mL. This step was repeated twice, and the last 5 mL of concentrated products were freeze dried. White powders were obtained. Products were characterized by ^{1}H-NMR, GPC in aqueous phase, FPLC with PBS 100mM solution as mobile phase, DOSY-NMR, and CD.

PASucc-T [(δ (ppm), 300 MHz, [6]d-DMSO]: 8.50 – 6.24 (m, ar-CH, aromatic amino acid of trypsin), 4.94 – 4.41 (m, acetal CH), 3.78 – 3.47 (m, PEG CH$_2$), 1.18 (d, J = 5.3 Hz, acetal CH$_3$). GPC (Mw=26531g/mol, Mn/Mw=1.3)

PACOOH-T ^{1}H NMR [(δ (ppm), 300 MHz, [6]d-DMSO]: 8.77 – 6.47 (m, ar-CH, aromatic amino acid of trypsin), 5.80, 4.67 (dt, J = 20.7, 10.4 Hz, acetal CH), 4.23 , 3.98 – 3.06 (m, PEG CH$_2$), 1.47, 1.17 (dd, J = 10.2, 5.2 Hz, acetal CH$_3$). GPC (Mw=27400 g/mol, Mn/Mw=1.7)

Trypsin ^{1}H NMR [(δ (ppm), 300 MHz, [6]d-DMSO]: 8.58 – 6.36 (m, 30H, aromatic amino acid of trypsin), 4.91 (s, 4H), 4.42 (d, J = 84.6 Hz, 17H), 3.83 – 2.63 (m, 146H), 2.56 – 2.36 (m, 57H), 2.30 – 0.51 (m, 62H). GPC (Mw = 23650 g/mol, Mn/Mw = 1.2)

Total amount of protein conjugated to each kind of polyacetal was quantified by UV spectroscopy (with BCA assay and with nanodrop, absorbance read at 280nm) using the native trypsin solution as standard for calibration curve (0.1-0.7 mg/mL). Conjugation efficiency was determined by SDS-PAGE (12.5% A.A., 100V) and FPLC (1mL of sample, 5mg/mL protein equivalent, PBS 1X, pH 7.4, flow 0.5, Sephacryl S-300, 20ºC), by comparison between the peak area of trypsin conjugate with free trypsin. Conjugation efficiency was also evaluated by quantification of free amino groups of lysine present in Trypsin before and after the conjugation reaction, using the standard protocol for TNBSA assay[111]. Briefly, PA-Ts samples with known trypsin concentration (50µg/mL) were prepared in 0.1M Sodium Bicarbonate (NaHCO$_3$) pH 8.5. Stock solution 0.2mM of Glycine in the same buffer was used for calibration curve (0.016 – 0.2 mM). Then, 500 µL of sample/standard were added to 1.5mL microtubes, followed by 250 µL 0.01% TNBSA solution. Samples and standards were incubated at the same time for 2h at 37 ºC. Finally, 250 µL 10% SDS solution and 125µL 1N HCl were added. Mixture was stirred 5s and absorbance was read at 340 nm. Structural integrity of protein after conjugation was verified through circular dichroism (CD). With this porpoise samples of naked and conjugated trypsin were dissolved in phosphate buffer solution 100 mM, with the same trypsin-equivalent concentration. Analyses were carried out at 20 ºC in a Jasco V-630 UV/Vis spectrophotometer. DOSY analyses were done as complementary studies to determine whether more than one macromolecular structure could be detected by diffusion within a magnetic field.

4.2.3. Study of PUMPT effect with PA-T conjugates.

4.2.3.1.   Determination of PUMPT effect with PA-T conjugates

Trypsin (T) enzymatic activity was the property selected in order to determine if PA-T conjugated systems showed masking-unmasking (PUMPT) behavior. L-BAPNA assay was used to determine the enzymatic activity.

 The same protocol was followed for native naked T and its conjugates. L-BAPNA was used as trypsin specific substrate. The hydrolysis of L-BAPNA released p-Nitroanilide (pNA), making possible to follow the progress of this reaction in time by measuring the absorbance increase of this small molecule. Reaction was followed during the first 10 min in a Victor UV reader plate, with filter of 405nm, at 37ºC.

The range of substrate concentration study was between 0.16-1.0 mM of L-BAPNA. Stock solution L-BAPNA (10 mL, 1.609 mM) was prepared dissolving first the solid L-BAPNA in DMSO (1mL, 7mg/mL) and finally diluting with 0.1M Tris buffer solution and 0.02 M $CaCl_2$, pH 8.2 (9 mL).

Protein concentration was kept constant for all experiments (20µL, 1mg/mL trypsin equivalent, final volume 200 µL, final T concentration 0.1mg/mL)

According to literature the unit of activity is defined as the amount of enzyme that hydrolyses 1µmol of substrate (L-BAPNA) by unit of time (min).

Unit of activity (unit/mg) = (ΔAbs_{410nm} x f x l)/(ϵ x m) Equation 4-1 [32]

ΔAbs_{410nm} =measure of absorbance

f, Factor of conversion = 1000, from mmol to μmol

l, Light path length = 1cm

ϵ = 8800 (L/mol.cm) L-BAPNA Molar absortivity,

m = (mg) protein mass.

Trypsin from porcine pancreas Type IX-S, lyophilized powder (Sigma Aldrich)

17000 units/mg protein or 17000units/mg solid

Enzymatic activity was expressed as relative percentage in comparison with native T activity under the same condition of incubation. In order to calculate the kinetic parameters, a Lineweaber-Burk plot model was applied. Native T and PA-T conjugates were incubated under the same conditions and then enzymatic activity was measured and compared.

First, samples of naked T as well as PA-T with equivalent amount of T were dissolved and incubated in 100mM PBS pH 7.4 at 37°C for 2h. After that enzymatic activity of each sample was measured and compared among them.

Second, new samples of naked T as well as PA-T with equivalent amount of T were dissolved and incubated in 100mM PBS pH 5.5 and 6.5 at 37°C for 2h. After that, enzymatic activity of each sample was measured and compared among them.

4.2.3.2.   Effect of PA/T ratio

Family of **PASucc-T** conjugates was synthesized in order to study the influence of polyacetal/T ratio over the masking-unmasking effect. Three different molar ratios between PA functional groups (COOH) and Trypsin functional groups (NH_2) were evaluated (COOH-PA/NH_2-T molar ratios = 20:1, 40:1, 60:1). The enzymatic activity of conjugates was determined using the L-BAPNA assay, following the procedure described in the previous section, keeping constant the relative amount of trypsin to be able to establish an appropriate comparison among them.

4.2.3.3.   Effect of linker presence

According to the results of experiments from section 2.4.4, the PA/T molar ratio with best results was chosen for **PACOOH-T** synthesis, with the porpoise to determine the influence of having or not a linker between polyacetal main chain and trypsin over the masking-unmasking effect keeping constant the amount of COOH groups by NH_2 groups of trypsin. Samples of conjugates and naked trypsin (1mg/mL equivalent of trypsin) were incubated at pH 7.4, 6.5 and 5.5, for 2 h. Enzymatic activity was measured before and after incubation, with L-BAPNA assay, to compare PACOOH-T and PASucc-T behavior among them and with naked trypsin.

4.2.4. PEGylated systems

4.2.4.1. *Synthesis of Trypsin-PEG conjugates.*

Trypsin was chosen as a model protein because its structure and activity is well known, this makes easier to follow it through the conjugation process and evaluate if it is able to keep the activity. Also it is a good model because it has a molecular weight similar to some proteins with specific biological activity (such as IL-6) that could be used later in wound healing applications. Using a similar Mw will allow the optimization of conjugate and scaffold parameters preventing us from the elevated cost of important proteins such as IL-6. PEG was chosen because it is a semitelechelic non-biodegradable polymer

A modification of the synthetic protocol reported by Duncan et al. was used here[32]. MeO-PEG-OH and MeO-PEG-COOH both with molecular weight 2000 Da were used as polymeric carrier in order to obtain the desired PEG-trypsin conjugates. Trypsin (23000Da) was selected as the model protein. A molar ratio of 1:5 Trypsin:PEG$_{2000}$.

Two different strategies were followed for each kind of PEG.

For strategy 1, applied for **MeO-PEG-COOH**, the reaction synthesis is summarized in figure 4.2

Briefly, EDAC(0.0158g, 8.29×10^{-2}mmol, and 0.00317g, 1.658×10^{-2}mmol) was added as solid to an aqueous solution (8mL) of **MeO-PEG-COOH** (2000 Da; COOH; 0.008g, 4.14×10^{-2}mmol of COOH) and left to stir for 10 min at RT) then sulfo-NHS (0.001g, 8.29×10^{-2}mmol and) was added also as solid, and let to stir for further 40min at RT.

Trypsin (0.02g, 8.29×10^{-3} mmol) was dissolved in ddH$_2$O (5mL) and added drop by drop over the reaction mixture and the pH was adjusted to 8 with NaOH 1M. The reaction was left to react by 18h at RT. Same equivalents of EDAC and Sulfo-NHS were added after this time in order to enhance reaction yields, the pH was readjusted to 8 and the reaction let to react for further 8 h.

The precipitated urea was filtered off and the conjugate solution further first by ultrafiltration (membrane Mw cut off 10000 DA, rpm min). DdH$_2$O was added to the upper layer (3x) for exhaustive subproduct removal PBS (1 M, pH 7.4) (volume, v = 2 mL, final concentration 5 mg/mL) was added to the concentrated aqueous trypsin solution (total volume, vt = 20mL)

Final product was freeze dried and storage at -20ºC to be used latter.

Figure 4.2. Scheme of strategy 1 for PEG-Trypsin conjugation reaction

Strategy 2 for conjugation reaction of Trypsin with MeO-PEG-OH was based on the procedure propuosed by Zarafshani et al.[112]

Reaction synthesis is summarized in figure 4.3

First, **MeO-PEG-OH** succinoylation was accomplished. Briefly, **MeO-PEG-OH (**1.00g, 5.00×10^{-4} mol) was dried by azeotropic distillation with toluene. Then, **MeO-PEG-OH** was dissolved in anhydrous DMF (1.00g, 0,5mmol; MeO-PEG-OH 2000 MW, 10mL). Following, succinic anhydride was added in a molar ratio 4 times bigger than **MeO-PEG-OH** (para MeO-PEG-OH$_{2000}$: 0.20g, 2mmol) followed by DMAP in the same proportion than succinic anhydride (0.24g, 2mmol). This solution was stirred by 16h at room temperature, following the reaction progress by Thin Layer Chromatography (TLC) using the mixture of solvents (BuOH/AcOH/H$_2$O in volume proportion 4:1:1).

After the reaction time was completed, the mixture was purred into ether in order to precipitate the succinoylated PEG, which was recrystallized twice in a mixture of CH$_2$CL$_2$/Ether (1:40).

Acid groups in PEG-Succinoylated were quantified by titration with a standard solution of NaOH 1.00×10^{-4}M and Bromothymol blue (also known as bromothymol sulfone phthalein and BTB) as pH indicator.

Next step was trypsin PEGylation. Fist, **PEG-Succinoylated** (200mg/mL; 0.2315g, 1.10×10^{-4} PEG-Succinoylated) was dissolved in DMF (N,N-Dimethylmethanamide, 1.16mL). Then EDAC was added in a molar proportion 4 times bigger than the amount of trypsin which was going to be conjugated (0.0038g, 2.00×10^{-2}mmol) and mixture was

stirred by 10 min. Then sulfo-NHS (Hydroxy-2,5-dioxopyrrolidine-3-sulfonicacid sodium salt, 0.0043g, $2.00*10^{-2}$mmol) and all was stirred by 45min.

Finally, **trypsin** (0.1151g, $4.8*10^{-3}$mmol) was added dissolved in aqueous borate buffer (borax/HCl, pH 9 at 20ºC, 2.97mL, final concentration of trypsin 40mg/mL) previously cooled at 4ºC.

Both solutions were mixed adding drop by drop the trypsin solution over the PEG-succinoylated solution.

Reaction mixture was stirred at 4ºC by 4h and latter 2h more at room temperature.

The precipitated urea was filtered off and the conjugate solution further first by ultrafiltration (membrane Mw cut off 10000 DA, rpm min). DdH_2O was added to the upper layer (3x) for exhaustive subproduct removal PBS (1 M, pH 7.4) (v= 2 mL, final concentration 5 mg/mL) was added to the concentrated aqueous trypsin solution (vt=20mL)

Final product was freeze dried and storage at -20ºC to be used latter.
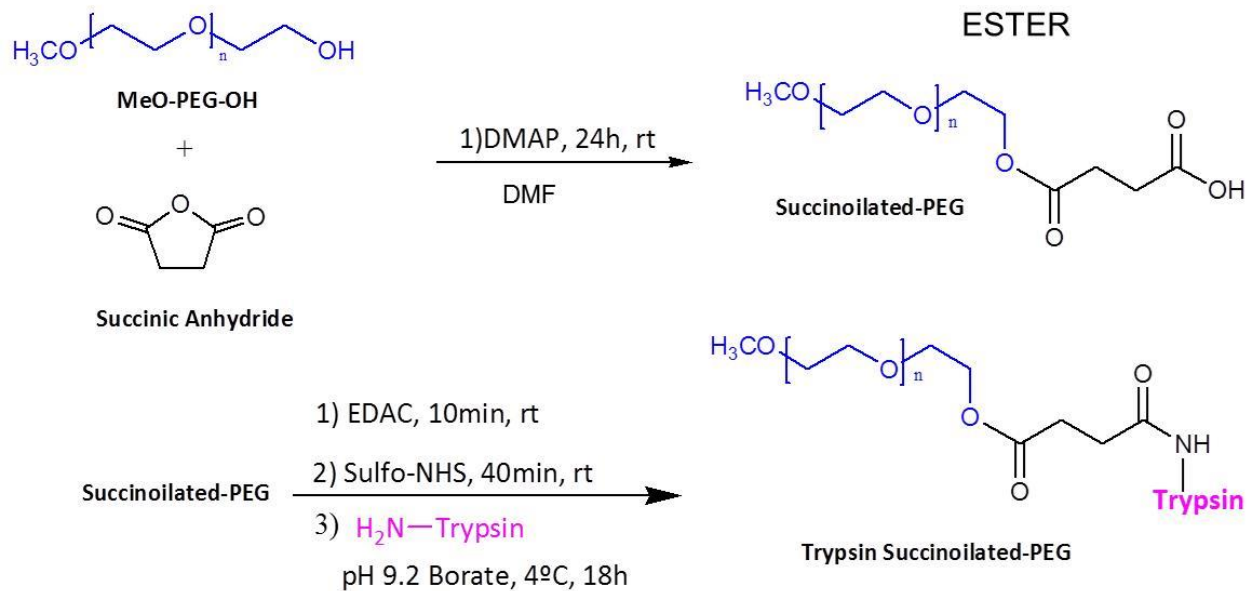
Figure 4.3. Scheme of Trypsin-PEG conjugates reaction synthesis

Characterization of PEG-trypsin conjugates and trypsin, by FPLC, SDS-PAGE electrophoresis and enzymatic activity

As explained before for PUMPT conjugates, total amount of protein conjugated was quantified by UV spectroscopy with BCA assay using the native trypsin solution as standard for calibration curve (0.1-0.7 mg/mL). Conjugation efficiency was determined by SDS-PAGE (12.5% A.A., 100V) and FPLC (1mL of sample, 5mg/mL protein equivalent, PBS 1X, pH 7.4, flow 0.5, Sephacryl S-300, 20ºC), by comparison between the peak area of trypsin conjugate with free trypsin.

The experiment was made preparing SDS polyacrylamide gels at 12.5% with 0.75mm of thickness. Gels were made as follow: Special equipment from BIORAD was used. Two glasses plate (outer and inner glasses) were assembling into the casting frame, it was put into the casting stand to fill up glasses with water to check the water tightness.

 Water was removed and introduced Resolving buffer (10 mL, composition: 3.54mL ddH$_2$O, 2.5 mL TRIS pH 8.8 1.5M, 3.75mL Bis-acrylamide 40%, 0.1 SDS 10%, 0.1mL APS 10%, 0.01mL TEMED), added 50 µL of butanol and let polymerization developed (10 min). Then butanol was removed and washed with ddH$_2$O.

 Glasses were filled up with Stacking buffer (4mL, composition: 4.42mL ddH$_2$O, 1ml TRIS pH 6.8 0.5M, 0.5mL Bis acrylamide, 0.04 SDS 10%, 0.04 APS 10%, 0.004 mL TEMED) and immediately put the plastic comb until polymerization (10 min). Plastic comb was removed and washed with water the glasses were introduced into clamping frame

and electrode assembly and finally introduce it in the electrophoresis box. Running buffer 1x (1L, composition: 100mL Running buffer 10x, 5mL SDS 20%, 895mL ddH$_2$O (Running buffer 10x composition: 1L, 0.25M Trizma Base, glycine 1.92M, ddH$_2$O)) was added.

Conjugates (1mg/mL in dd H$_2$O), and control sample of free trypsin (1mg/mL in dd H$_2$O) were prepared by dilution (1:1) with a denaturing solution (loading buffer composition: 3.8mL of H2O, 5mL; 0.5Mtris HCl (pH6.8), 8mL 10% w/v SDS, 4mL of glycerol, 2mL 2-mercaptoethanol, 0.4mL of bromophenol blue 1% w/v) and heated for 7min at 95ºC. Samples and Mw marker were loaded (10µL) into the gel and let running for 15min at 90V and the last 45min at 130V. The gel was then rinsed and stained (1h) with Coomassie blue, cleared in distaining buffer (35% methanol/ 5% acetic acid) for 24h and then rehydrated in a solution composed by 5% methanol/7% acetic acid.   Finally, the gel was rinsed with ddH$_2$O.

Enzymatic activity was also measured after PEGylation following the L-BAPNA assay protocol describe previously in section 4.2.3.1, in order to compare how much biological activity was lost as consequence of this chemical process.

4.3. Results

4.3.1. Synthesis and Characterization of Polymer conjugates

4.3.1.1. Synthesis of amino-pendant PolyAcetals, PAFS (2) and PANH₂ (3)

Amino-pendant polyacetals, were synthesized following a modification of the methodology proposed by Tomlinson et al.[79] as describe previously. Before stop the reaction, a sample was taken in order to characterize the Fmoc-protected product (**PAFS, (2)**) to be able to quantify by ^{1}H NMR the amount of NH_2 groups loaded in the main chain. The sample was isolated and precipitated in ether as a white loose powder. ^{1}H-NMR analysis confirms the desired compound. See Figure 4.4.
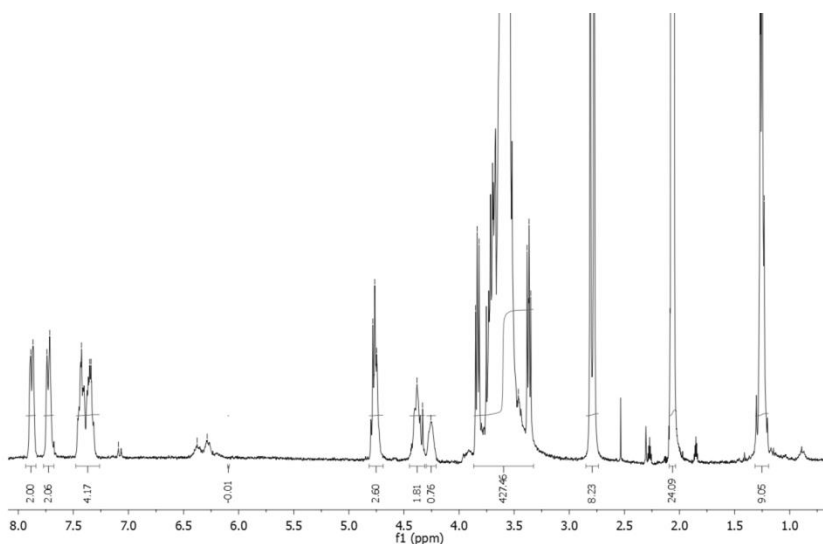
Figure 4.4. ^{1}H-NMR of isolated aliquot of PAFS (2) in Acetone-*d6.*
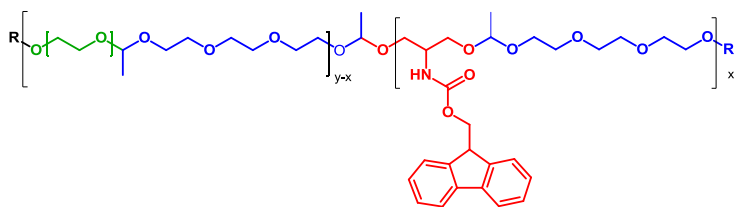
Figure 4.5. Scheme of chemical structure of PAFS.

Then, reaction was stopped by adding a solution of KOH (2M) in MeOH, consequently deproteccting the product. Final solution was poured into ether to obtain a white loose powder. Total deprotection was confirmed by ^{1}H-NMR (see figure 4.6,). This product was identified as **PANH$_2$ (3)**.
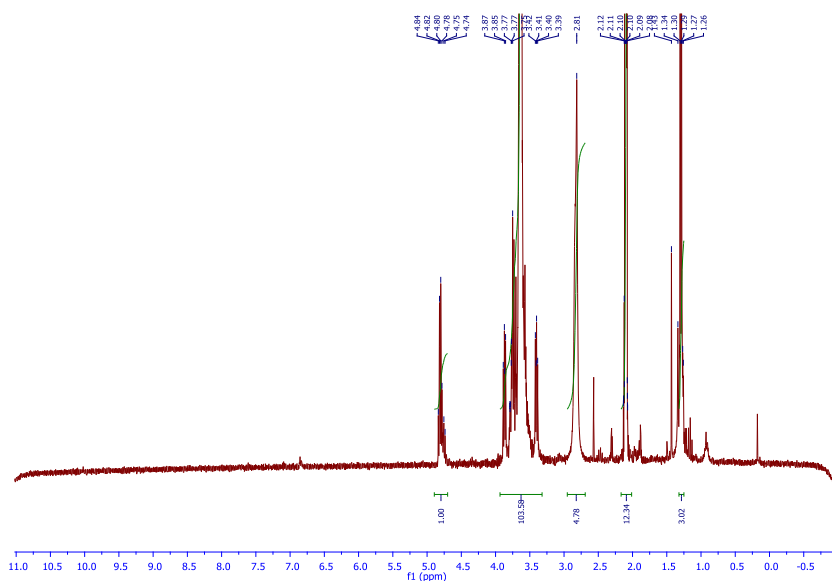
Figure 4.6. ^{1}H-NMR of isolated PANH$_2$ (3) in Acetone-*d6*.
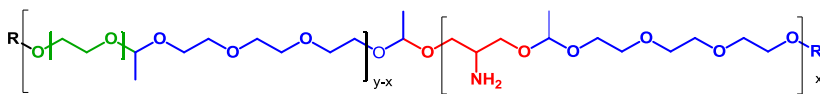
Figure 4.7 Scheme of chemical structure of PANH₂.

A summary of the polymers obtained with their assigned Mw by GPC and the amino groups loading in the polyacetal is depicted in the following table 4-1.

Table 4-1 Comparison of Molecular weight and amount functional groups in PAFS (2) and PANH₂ (3)

Polymer	Mw* (g/mol)	PDI	FS content (wt%)**	NH₂ content (wt%)***
PAFS (2)	12257	1.9	20	-
PANH2 (3)	10889	1.8	-	21

* Determined by GPC
** Determined by Colorimetric assay 300nm
*** Determined by Ninhydrin assay
FS: Fmoc-serinol

4.3.1.2.   Synthesis of PASucc (4)

Next step was the succinoylation of amino groups in polyacetals, **PASucc (4)**. After total deprotection of amino groups in PAFS (2), the amount of NH_2 (expressed as NH_2 molar %) was the same as Fmoc-Serinol molar % in PAFS (2). According to this, there was 21% molar of NH_2 in PANH₂ (3) polymer main chain. Average MW for polyacetal was calculated (3324g/mol).   The amino groups were derivatized with

succinic anhydride in order to introduce a suitable linking moiety to be attached to the protein through the amino groups of peripheral lysines. The succinoylation reaction was done in proper conditions to achieve the total functionalization of all free amino groups present in **PANH$_2$ (3)**. Reaction was successfully accomplished with 100% succinoylation of NH$_2$ groups, corroborated by ^{1}H NMR analysis, were characteristic multiplet of CH$_2$-CH$_2$ belonging to succinoylated side chain was observed at 2.61-2.35 ppm. Qualitative amino test with ninhydrin was also performed, which resulted negative for free amino groups in succinoylated product and positive for PANH$_2$.
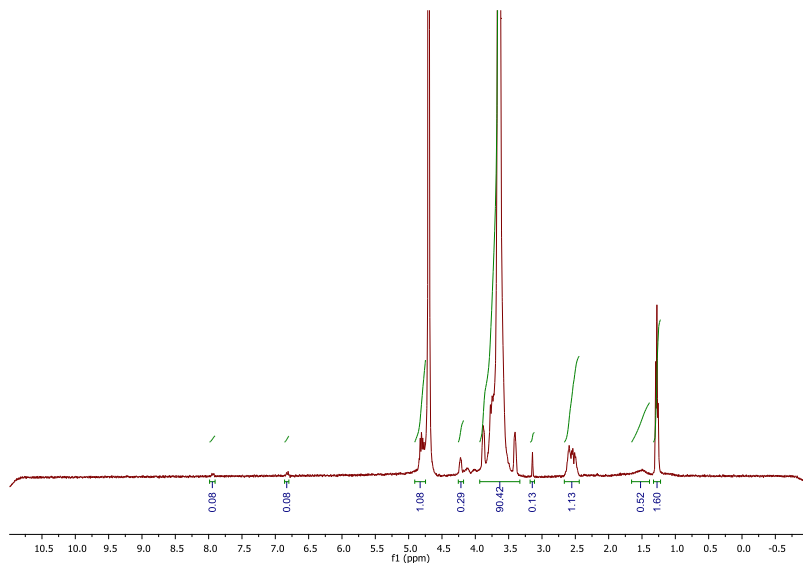
Figure 4.8 ^{1}H-NMR of isolated of PASucc, 300MHz
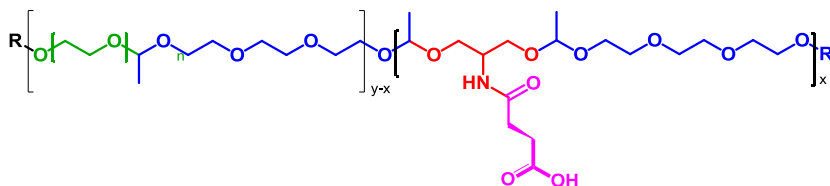
Figure 4.9 Chemical structure of PASucc (4)

4.3.1.3.   Synthesis of PACOOH (5)

The COOH-pendant polyacetals PACOOH **(5)** were synthesized as describe previously in Materials and Methods and characterized by ^{1}H NMR and GPC (6mg/mL). Quantification of COOH in the polymer main chain was performed by titration with NaOH standard solution ([]=2,1*10-5M) resulting to be 1.3 wt% of COOH groups. This novel carboxylic-pendant polymer from the polyacetals family had similar MW than its equivalent amino-pendant, as expected. The resulting polymer was completely soluble in a wide range of solvents (aqueous, DMSO, Chloroform…) and proven to be stable, as solid (weeks) as well as in aqueous solution, under normal atmospheric condition. An example of 1H-NMR of PACOOH (5) is shown in Figure 4.10.
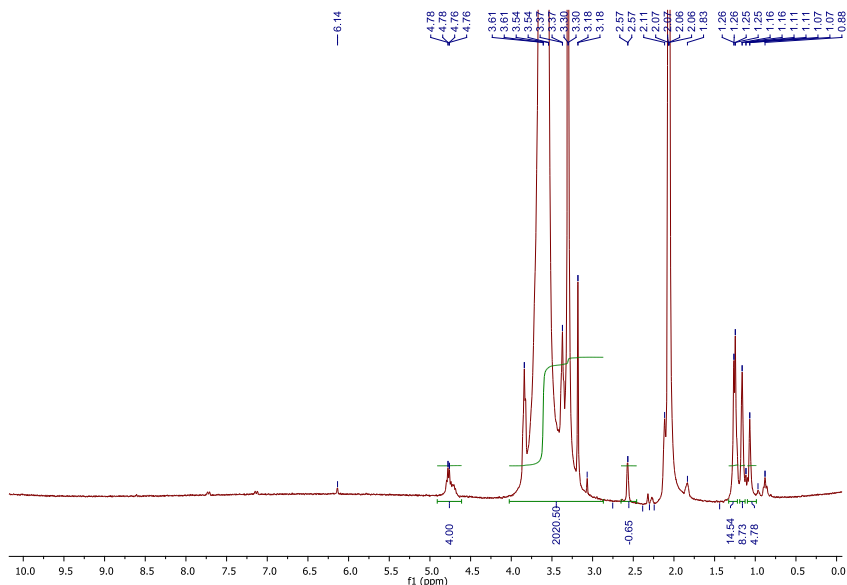
Figure 4.10. ^{1}**H-NMR of isolated PACOOH (5) in Acetone-*d6*, 300MHz.**
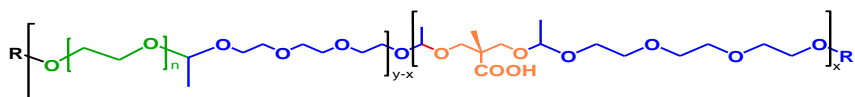
Figure 4.11 . **Chemical structure of PACOOH (5)**

4.3.2. Synthesis and characterization of PA-T conjugates

Next step was the synthesis of a family of trypsin-polyacetals, PASucc-**T (6)** and PACOOH-**T (7)**. The protein trypsin (T) was loaded by linking the amino group of available lysine residues in the protein to the carboxylic groups pendant to polymer main chain, in case of PACOOH (5), or in the lateral chains for PASucc (**4**). Figure 4.12 shows the reaction scheme of protein conjugation.
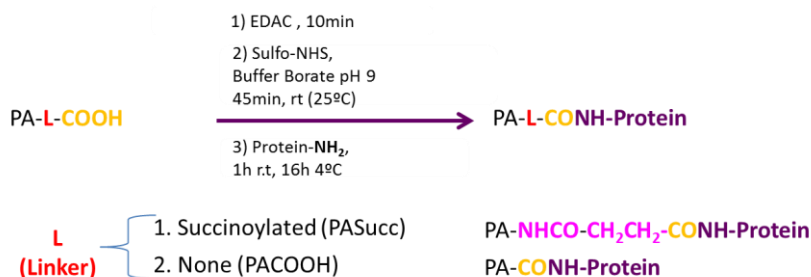
Figure 4.12. Synthetic scheme to reach PA-Trypsin conjugates.

To confirm the conjugation of trypsin with the polymers (PASucc-T, 6 y PACOOH-T, 7), different physico-chemical characterization was performed.

Firstly, SDS-PAGE electrophoresis (SDS-PAGE 10% A.A., 10ug **T** equivalent by well) and FPLC (in PBS 100mM pH 7.4, flow 0.5ml/min column Sephacryl S300 16/60) were used to confirm the reaction efficiency and the relative amount of free protein, in case it was present in the final product.

SDS-PAGE showed that conjugates were obtained in all cases, as expected. Also, reveals that degradation of trypsin under reaction conditions is diminished upon conjugation.
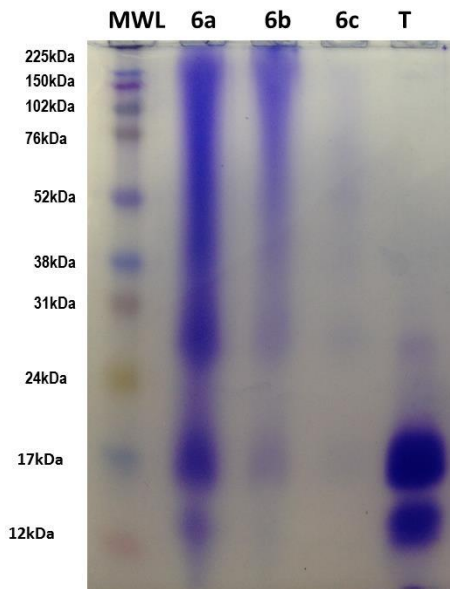
Figure 4.13. SDS-PAGE 12.5% A.A., 10ug T **equivalent by well, 6a) PASuc-T 20/1; b) PASuc-T 40/1, c)) PASuc-T 60/1, T) naked Trypsin**
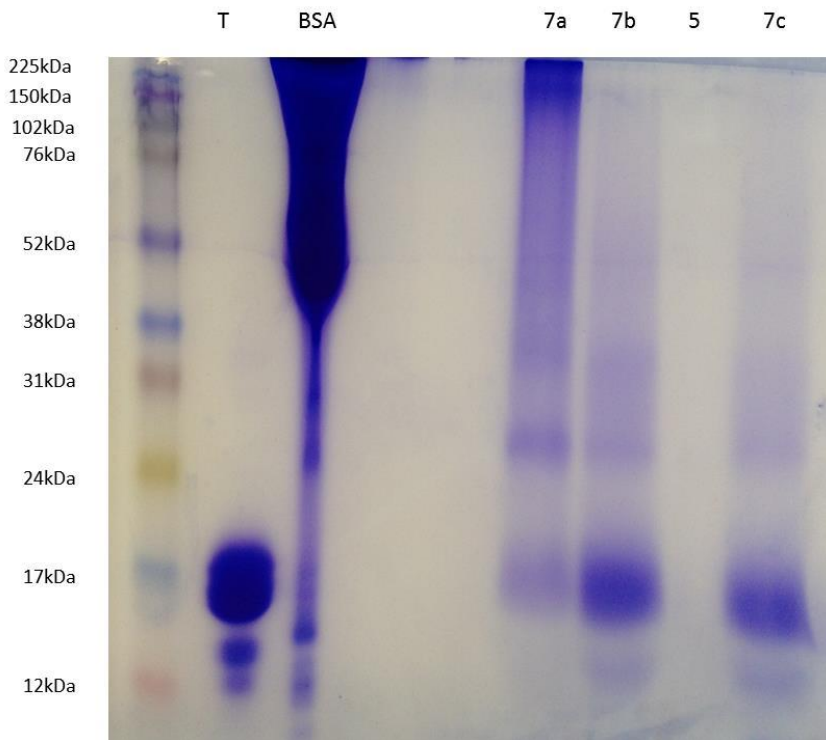
Figure 4.14. SDS-PAGE 12.5% A.A., 10ug T equivalent by well, 7a) PACOOH-T 20/1; b) PACOOH-T 40/1, c)) PACOOH-T 60/1, T) naked Trypsin, BSA) Bovine serum albumin, 5) PACOOH

FPLC analyses showed that all conjugates presented almost the same retention volume (Vr) as shown in figure 4.15 at the same analytical conditions than naked trypsin. Values of retention volume for conjugates were higher than retention volume of naked trypsin, revealing that conjugated had bigger hydrodynamic ratio than trypsin, as expect when conjugation is accomplished.
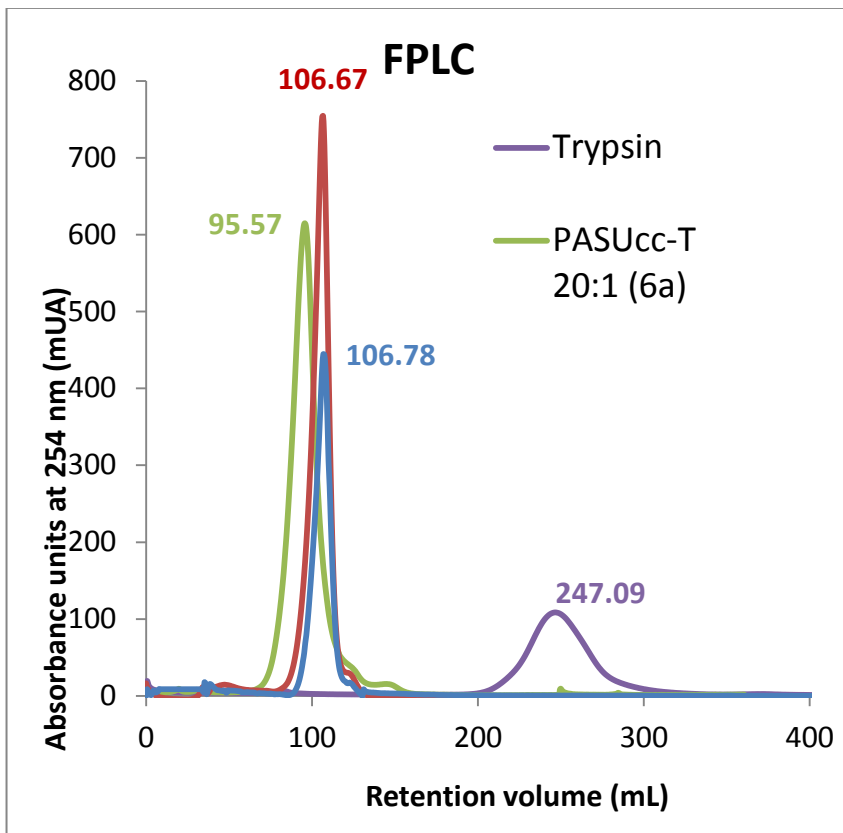
Figure 4.15. FPLC analysis of a) Trypsin; b) PASucc-T 20:1 (6a) c) PASucc-T 40:1 (6b) and d) PASucc-T 60:1, in PBS 100mM pH 7.4, flow 0.5ml/min, column Sephacryl S300 16/60, sample loaded: 1mL, 5mg/mL T equivalent.
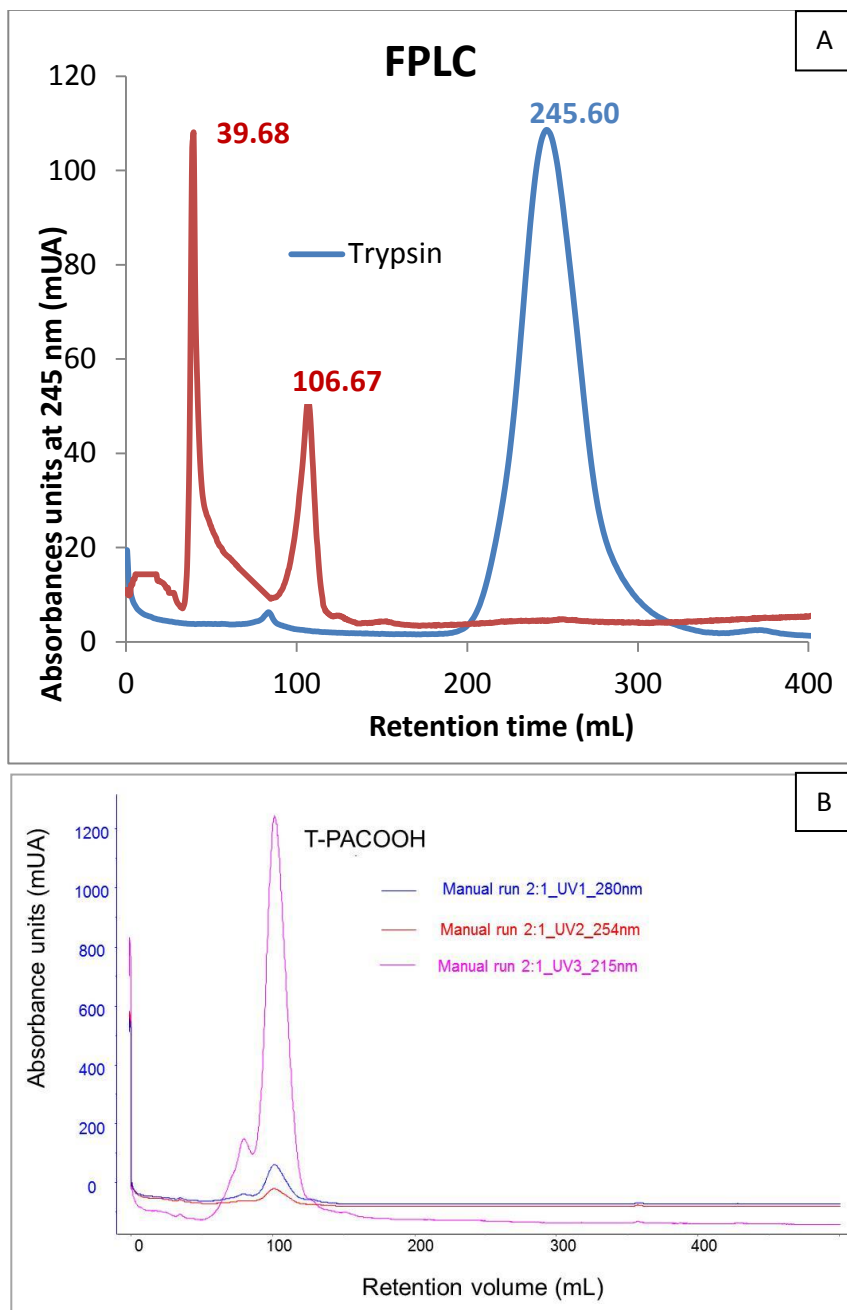
Figure 4.16. FPLC analysis of A) Trypsin and PACOOH-T (7) samples; B) puried PACOOH-T (7). Analytical conditions: in PBS 100mM pH 7.4, flow 0.5ml/min, column Sephacryl S300 16/60, sample loaded: 1mL, 5mg/mL T equivalent.

Likewise, Conjugates **PACOOH-T (7)** also showed higher retention volume (Vr) than naked trypsin at the same analytical conditions, corroborating that protein conjugation was accomplished successfully.

According to the FPLC analyses, there are no detectable amounts of free trypsin, and degradation products from trypsin hydrolysis have been removed. The most relevant observation is that the evident increase of the hydrodynamic ratio of polymers shows that protein has been conjugated to the polyacetals.

GPC analyses were also performed in aqueous conditions to compare the MW increase of Trypsin conjugates with respect to naked T.

Results are summarized in table 4-2.

Table 4-2 Comparison between MWp of naked T, PASucc, PACOOH, PASucc-T and PACOOH-T.

	Mw (g/mol)[a]	PDI[a]
T	23650	-
PASucc (4)	10512	1.4
PACOOH (5)	10307	2.1
PASucc-T (6)	26531	1.3
PACOOH-T (7)	27400	1.7

a. As determined by Gel Permeation Chromatography (GPC)

Following, chemical structure of **PASucc-T (6)** and **PACOOH-T (7)** were analized by ^{1}H NMR.

In Figure 4.17 draws attention the peak that appears around 5.5ppm upon conjugation between PASucc and Trypsin (PASucc-T). Although further experiments should be performed to ratify this effect (2D NMR such as TOCSY), it seems there is a displacement of the acetalic −H from the serinol (4.6 ppm) due to the shielding induced by the presence of conjugated trypsin, this peak is absent in the physical mixture. Therefore, it could be said that the conformation adopted by the conjugate really induce an important structural change, also observed in CD analysis (Fig. 4.18).
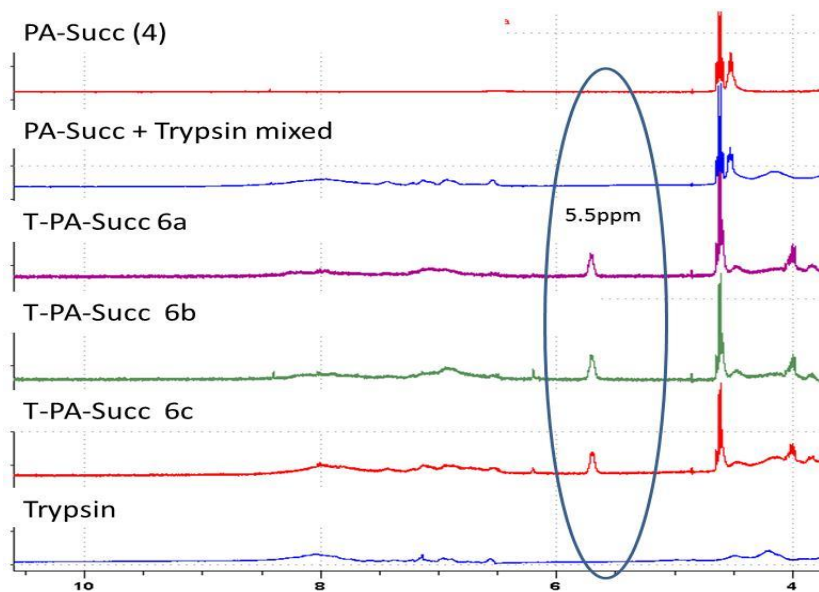
Figure 4.17. ^{1}HNMR analysis of a family of PASucc-T, according to ratio PA/T: 6a=20/1 , 6b=40/1, 6c=60/1, conjugates by ^{1}HNMR in DMSO d[6], 300MHz.

Instead, the PACOOH-T (7) ^{1}H-NMR spectrum did not show the mentioned peak a 5.5pmm. This observation indicates that electron delocalization that presumably occurs with linker mediated polyacetal (PASucc, 4) an trypsin, is not taking place when direct bounding is performed, as in case or PACOOH (5) and trypsin. Again, further experiments should be performed to unravel this phenomenon (2D NMR such as TOCSY),
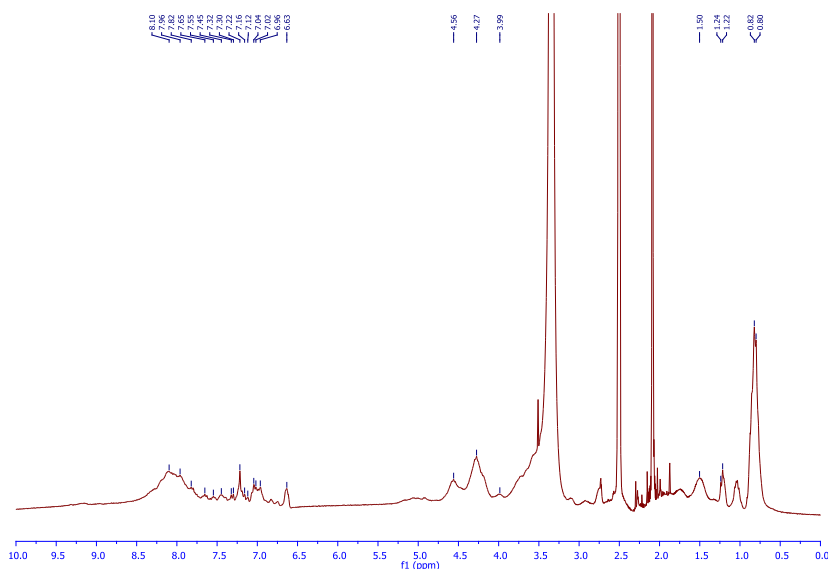
Figure 4.18. ^{1}HNMR analysis of PACOOH-T (7) conjugate by ^{1}HNMR in DMSO d[6], 300MHz.

The total protein content in the conjugate was quantified by UV-Vis spectroscopy using the colorimetric quantitative assay Bradford, commonly used for total protein quantification.

Results summarized in table 4.3, show that conjugation was accomplished in all cases, and that it is possible to modulate the amount of protein linked to the polyacetalic carrier. In this case it is a great advantage that polyacetal are virtually invisible to UV detector at 280nm and they do not cause any interference, which simplify the total protein quantification procedure. Besides, conjugation efficiency was 100% in all cases according to FPLC and SDS-PAGE gels showed that conjugation increase the stability of T in comparison to naked T under the same environmental conditions, as expected.

Table 4-3. Quantification of protein content and free amino groups available in PASucc-T conjugates

	Ratio PA(nCOOH) / T(nNH$_2$)	% Total protein (wt%±5) *	Ratio n NH2/n protein (n ±2) **
T	0	100	14
PASucc-T 6a	20	35	2
PASucc-T 6b	40	22	2
PASucc-T 6c	60	20	2
PACOOH-T 7	20	35	2

*Method of quantification applied: Bradford

**Determined by TNBSA.

Regarding the structural integrity of trypsin after conjugation, CD spectra showed there were no significant differences between naked and conjugated T under the same aqueous saline solution conditions.
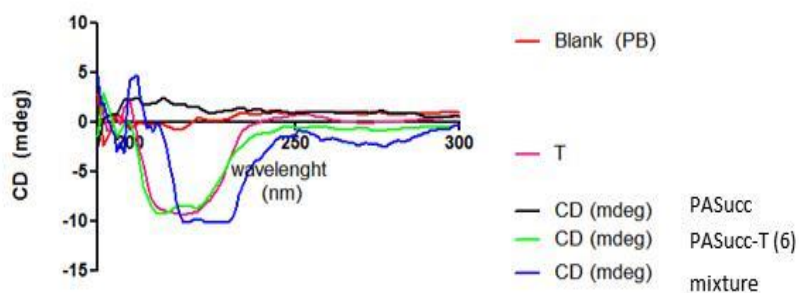
Figure 4.19. **Circular Dichroism analysis for naked T, PASucc (4) and PASucc-T (6a).**
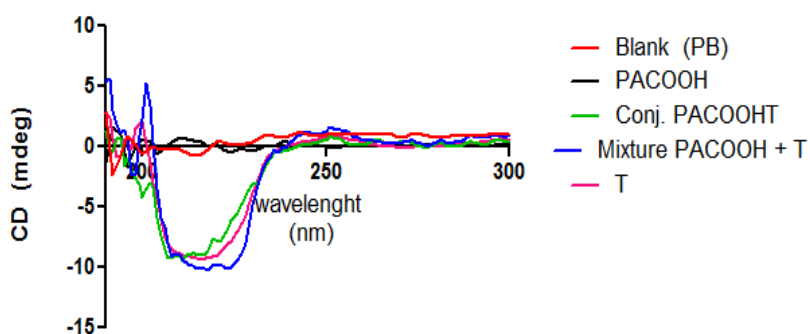
Figure 4.20. **Circular Dichroism analysis for naked T, PACOOH (5) and PACOOH-T (7).**

On the other hand, diffusion experiments by NMR (DOSY analyses) did not show any relevant information about the possible existence of different macromolecular structures, however further studies should be performed in this context.

4.3.3. Study of PUMPT effect with PA-T conjugates

The enzymatic activity of T, naked and conjugated, was studied first in comparison with PASucc conjugates in order to proof the PUMPT concept with polyacetals, which is the main contribution of this study. In this case, protein unmasking was supposed to be triggered by change of pH, from neutral to acidic conditions, as require to achieve the hydrolysis of acetal bounds in the polymer main chain, making possible the protein release.

4.3.3.1.   Determination of PUMPT effect in PA-T conjugate

As it can be seen in **figure 4.21**, there is actually a clear change in the enzymatic activity profile when T is conjugated to PASucc in comparison to naked T when both samples are incubated at pH 7.4, for 10 min at 37ºC. PASucc-T enzymatic activity is very much lower than naked T activity.   This is clear evidence that protein activity was masked by the polyacetal.

On the other hand, when samples of naked T and PASucc-T are incubated in the same acidic conditions, PBS solution pH 6.5, for 10 min at 37ºC, both samples showed almost the same enzymatic activity profile, proving that T was release or un-masked from polyacetal and

protein recovers its original activity. PUMPT effect was achieved with T and polyacetal conjugation.

4.3.3.2. *Effect of PA/T ratio with PASucc-T conjugate*

At the same time, the influence of $nCOOH/nNH_2$ ratio over the activity was evaluated by comparison of T activity from PASucc-T, 6a, 6b, and 6c, before and after incubation at different pH. All samples had the same concentration of trypsin equivalents, they were incubated during the same period of time, and treated in neutral (pH 7.4) and acidic (pH 6.5) conditions, mimicking the physiological pH, present in healthy and wounded tissue, respectively, thinking in a possible application. The results are summarized in **table 4-4** and **figure 4.20**, were it can be notice that enzymatic activity of **T** was partially suppressed at pH 7.4, when it was conjugated, in comparison with naked T at the same condition. This means that proteins, or at list the active sites, are shielded by polyacetals which are covalently linked to lysine residues of trypsin, making possible to observe the masking effect of polymer over the enzymatic activity.

Besides, it was possible to recover the activity after incubation of conjugates at pH 6.5 for 2h. It is interesting to remark that activity was recovered in all systems keeping the **T** protected to the acidic degradation. These results prove that protein was unmasked by effect of acidic pH, responsible of hydrolysis of PASucc 2 main chain.
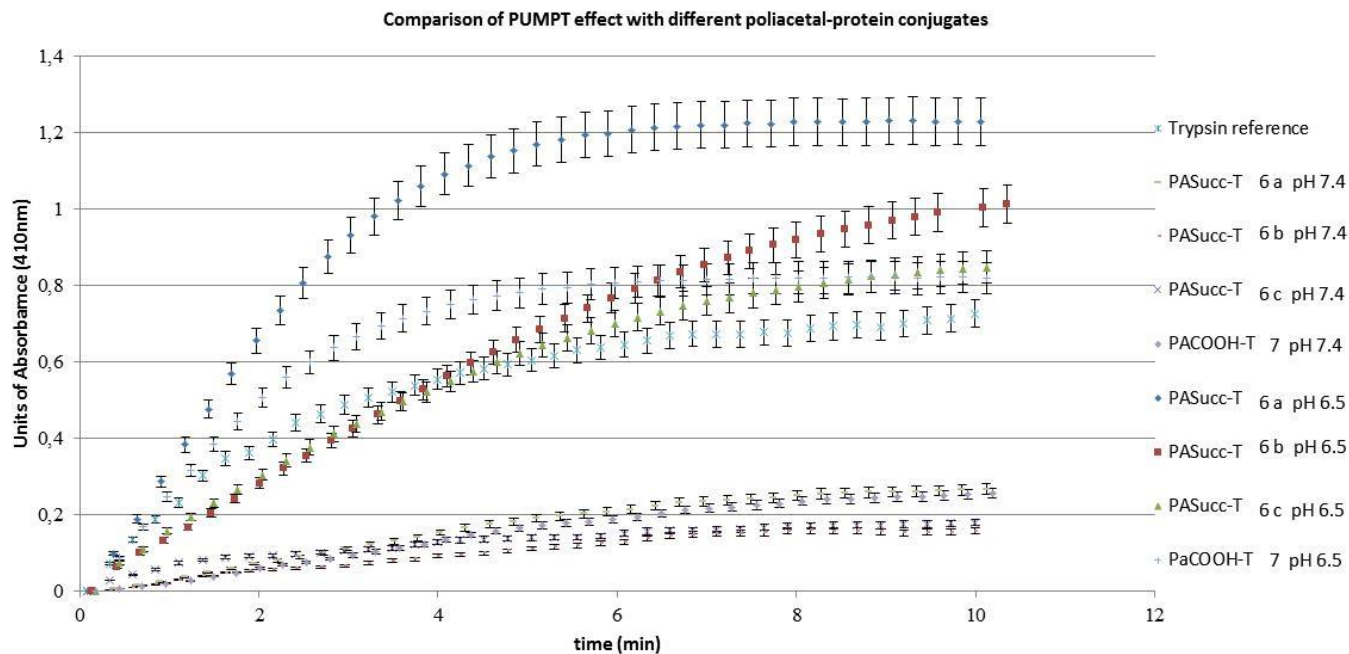
Figure 4.21 Comparison of PUMPT effect with different polyacetal-protein conjugates. Enzymatic Activity of Trypsin using L-BAPNA as substrate at different pH and at 37ºC.

Table 4-4. Comparison of enzymatic activity between naked T and PASucc-T at different pH (t=2h). Data as mean ± SD (n>3)

Compound	% Enzymatic Activity (0.2mg protein/mL)	
	pH 7.4* (masked)	pH 6.5* (unmasked)
PASucc-T 6a	17 ± 5	132 ± 5**
PASucc-T 6b	16 ± 5	71 ± 5
PASucc-T 6c	20 ± 5	77 ± 5

* % Activity relative to naked T enzymatic activity at pH 7.4
**See discussion

4.3.3.3. Effect of the polymer-protein linker: Determination of PUMPT effect in PACOOH-T conjugate and comparison with PASucc-T

According with the results summarized in table 3-5, both systems were able to hide efficiently the enzymatic activity of trypsin, with the possibility to recover the protein activity even increased in comparison with naked trypsin under de same conditions. These observations make possible to conclude that there are not a significant effects when protein in attached to the polymer by linkers or not.

Table 4-5   Comparison of PUMPT effect with PASucc-T 6a and PACOOH-T 7 after 2h. Data as mean ± SD (n>3)

Compound	Protein Content wt%	% Enzymatic Activity*	
		pH 7.4* (masked)	pH 6.5* (unmasked)
PASucc-T 6a	35	17	132
PACOOH-T 7	35	28	233

*Assay condition: [S]:1.64mM LBAPNA, [E]: 0.2mg/mL trypsin, T: 37ºC, t: 10min of incubation, stirred at 450rpm%. Activity relative to naked T enzymatic activity at pH 7.4

4.3.3.4.   *Study of PUMPT effect over Kinetic parameters of T enzymatic activity under different reaction conditions*

Data from experiments in section 2.4.3 were used to choose the best candidate for kinetic studies, which resulted to be PACOOH-T conjugates. The enzymatic activity of trypsin, masked and unmasked, was measured using LBAPNA assay, following the same procedure previously described. Incubation temperature (37 °C) and trypsin-equivalent concentration were kept constant. Experimental conditions used as variables were: i) substrate concentration (L-BAPNA, 0.20 mM, 0.40 mM, 0.80 mM, 1.2 mM), ii) incubation time (0h, 0.25h, 0.5h, 1h, 6h, 8h, 24h), iii) incubation pH (5.5, 6.5, 7.4).

Table 4-6. Study of PUMPT effect with PACOOH-T (5) at different incubation time at pH 7.4

T(h)	T (% relative enzymatic activity respect naked T)	PACOOH-T (%relative enzymatic activity respect naked T)
0	100	11
0,5	150	17
1	105	93
5	63	10
8	28	5
24	34	36
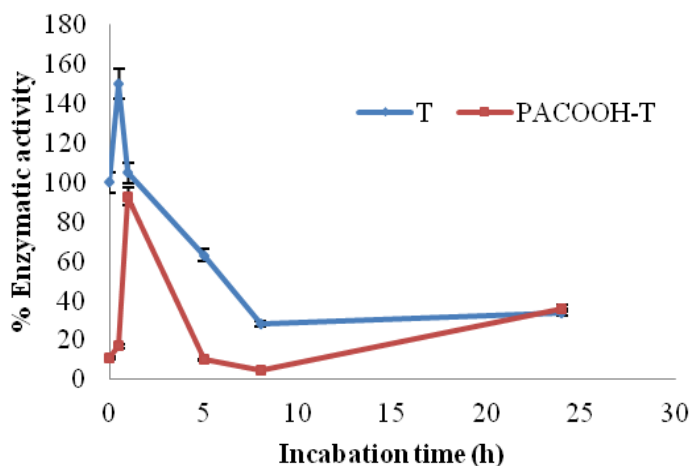
Figure 4.22 PUMPT effect with PACOOH-T (5) at different incubation time at pH 7.4

Table 4-7. Study of PUMPT effect with PACOOH-T (5) at different incubation time at pH 6.5

T (h)	T (%relative enzymatic activity respect naked T)	PACOOH-T (%relative enzymatic activity respect naked T)
0	82	28
0,5	89	49
1	103	34
5	62	32
8	55	45
24	56	62
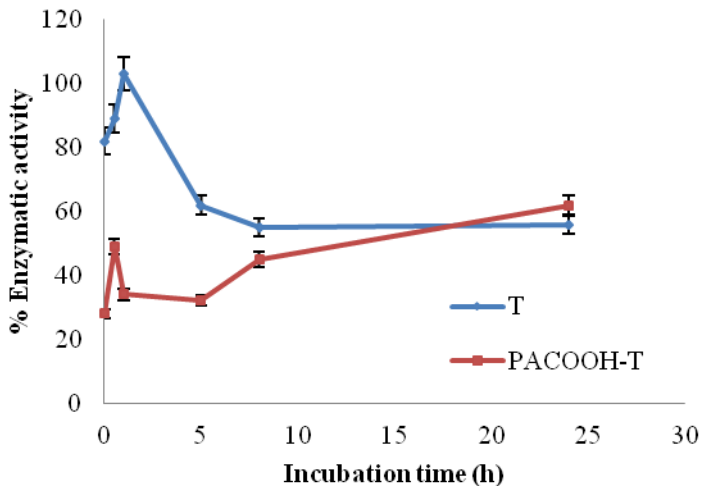
Figure 4.23 PUMPT effect with PACOOH-T (5) at different incubation time at pH 6.5

Table 4-8. Study of PUMPT effect with PACOOH-T (5) at different incubation time at pH 5.5

T (h)	T (%relative enzymatic activity respect naked T)	PACOOH-T (%relative enzymatic activity respect naked T)
0	222	23
0,5	157	83
1	107	65
5	100	49
8	71	55
24	46	84
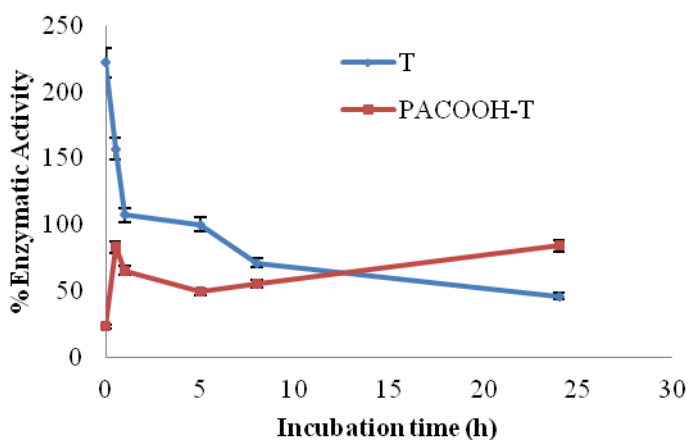
Figure 4.24 PUMPT effect with PACOOH-T (5) at different incubation time at pH 5.5

4.3.4. Synthesis and characterization of PEG-Trypsin conjugates.

It is expected that PEG-Trypsin conjugates protect the protein from degradation once it was loaded into the membranes and prevent the loss of biologic activity. Studying the activity of trypsin before and after PEGylation, and finally after encapsulation and release from the scaffold, it will be possible to estimate the behavior of another proteins with specific application in tissue regeneration.

Bicinchoninic acid (*BCA*) *assay* kit was used to quantify protein content in the conjugates, always using Trypsin standards.

Table 4-9. Quantification of Trypsin conjugates to PEG polymers determined by BCA

Trypsin conjugate	Wt% trypsin
MeO-PEG-Succ-T	20±1
MeO-PEG-COOH-T	26±1

SDS-PAGE electrophoresis was used to assess if trypsin PEGylation was accomplished as well as the presence of free trypsin after the reaction.
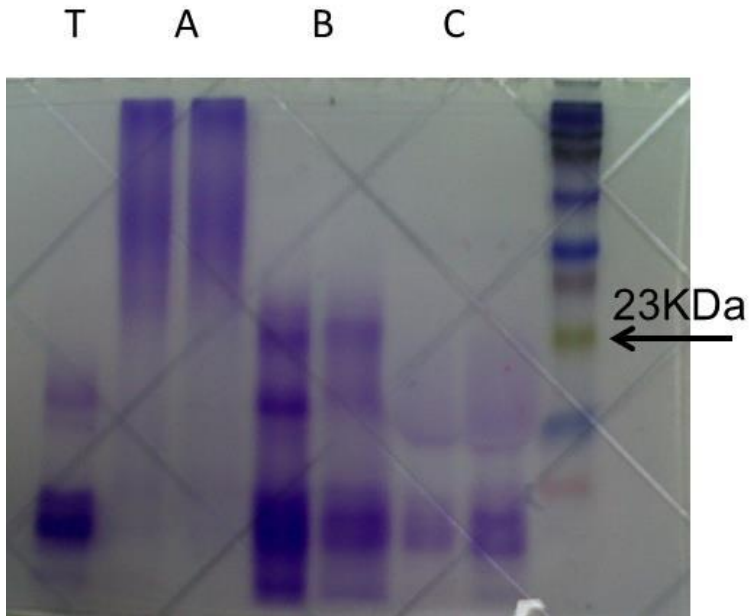
Figure 4.25 SDS-PAGE electrophoresis with 15% of Acrylamide with 0.75mm of thickness, running for 15min at 90V and the last 45min at 130V, and stained with Coomassie blue Volume of each sample: 10 µL. **T: free Trypsin, A: PEGylated trypsin with MeO-PEG-OH MW 2000 Da, C: PEGylated trypsin with MeO-PEG-COOH MW 2000 Da (B), and mixture of T and MeO-PEG-OH 2000**

SDS-PAGE (figure 4.25) revealed that only the strategy 2, for MeO-PEG-Succ-T conjugation was successful without free trypsin. Therefore, the following experiments of encapsulation were carried on using only this conjugate.
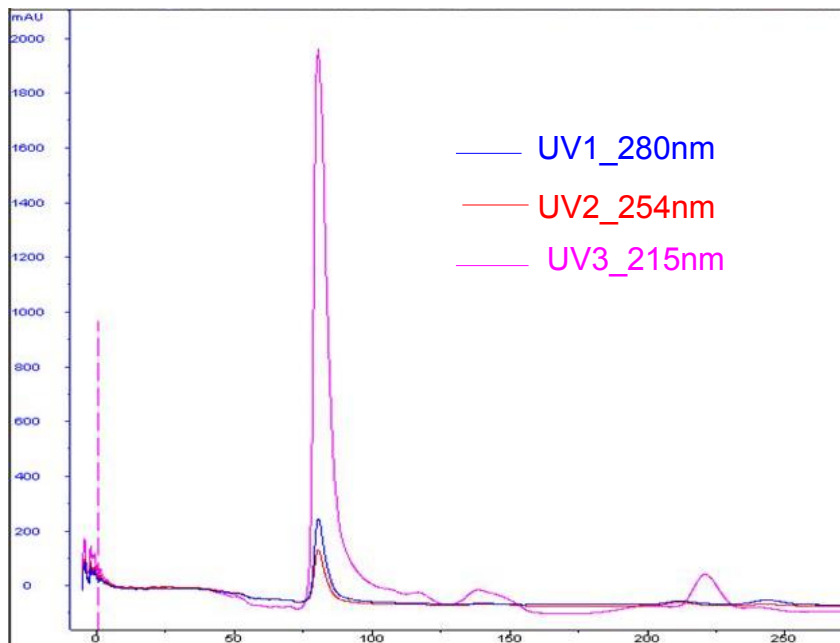
Figure 4.26. FPLC analysis of a) Trypsin; b MeO-PEG-Succ-T**, in PBS 100mM pH 7.4, flow 0.5ml/min, 215, 254 and 280nm, column Sephacryl S300 16/60, sample loaded: 1mL, 5mg/mL T equivalent**

FPLC chromatogram showed there was not free trypsin after conjugation and purification processes. This results also demonstrated that PEGylation reaction was accomplished successfully.

Structural integrity of protein after conjugation was corroborated by circular dichroism as well as it was done with PUMPT conjugates 4.2.2.

As it can be seem in figure 4.27, PEGylation do not seem to have had a completely change the conformation of protein tertiary structure, keeping alfa-helix and random coil proportion similar to free trypsin,

but the second peak in PEG2000-T profile reveals that tridimensional arrangement of protein structure was modified in some grade.
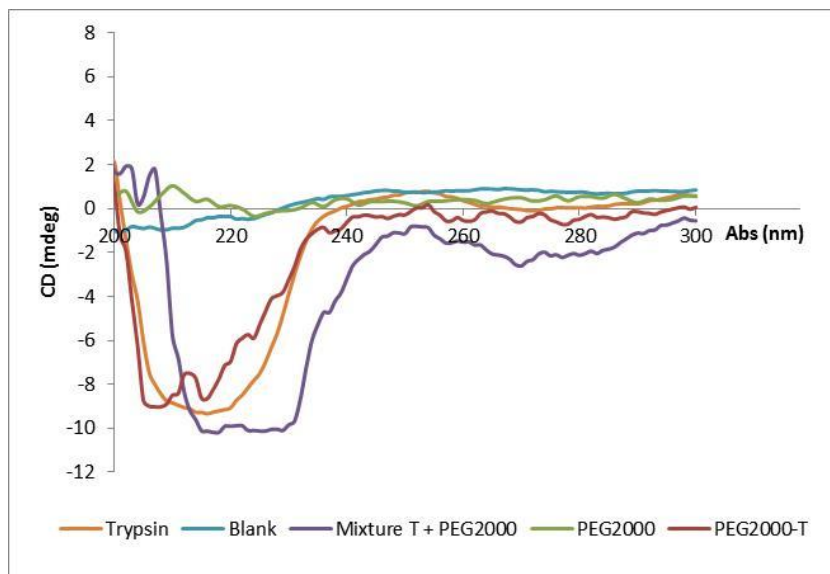
Figure 4.27. Circular Dichroism analysis for not conjugated Trypsin (T), PEGylated trypsin with MeO-PEG-OH MW 2000 Da (PEG2000-T), MeO-PEG-OH MW 2000 Da (PEG2000), and physical mixture of MeO-PEG-OH MW 2000 Da and trypsin.

In order to corroborate the influence of this structural change over the biological activity of the protein, L-BAPNA enzymatic activity assay was also accomplished, following the same procedure previously described in section 4.2.3.1.

After PEGylation the enzymatic activity of trypsin decreased considerably. Even thought, the enzyme is still active, and therefore could be useful for proteolysis of other proteins always that concentration of enzyme was enough to accomplish its porpoise in the selected environment of application.

The esterase activity of trypsin was calculate and compared with the activity of the conjugate applying the equation of Lineweaver-Burk:

$$\frac{1}{V_o} = \frac{K_m}{V_{max}[S]} + \frac{1}{V_{max}}$$

Equation 4-2

Table 4-10. Activity of trypsin and trypsin-PEG conjugates with L-BAPNA as substrate. Kinetic parameters of native and PEG-trypsin conjugates

	(µg/mL)	Residual activity (%)	K_M (mM)	V_{max} (min)	K_{cat} (s^{-1})	K_{cat}/K_M ($s^{-1} mM^{-1}$)
Trypsin	0,50	100	1,43	0,08	0,21	0,15
PEG$_{2000}$-T	0,91	64	1,11	0,03	0,50	0,45

According to these results trypsin activity diminish when it is conjugate with PEG. It is interesting that conjugates with PEG also have lower Km values indicating a higher affinity for the binding site of trypsin, and in fact the increase in the molecular weight is related directly with a decrease of kinetic parameters. This behavior has been observed before by Treetharnmathurot (2008)[32]. As it was coment before, applications the used of PEGylated proteins as in this case implies that it would be necessary to find an strategy to protect the protein and modulate the localized release of protein during an especific period of time. Therefore it is necessary to test if residual activity before and after release would be enouth to provide the thapeutic effect and be able to make the adjusments in doses administration.

4.4. Discussion

NMR analyses demonstrated that all polyacetals were successfully synthesized. Also conjugates with both types of polyacetals (**4** and **5**) with trypsin were obtained, according to SDS-PAGE and FPLC analyses. The last ones showed there were no detectable amounts of free trypsin. Besides, the clear difference between conjugate elution times vs. free trypsin provides evidence of increase in hydrodynamic ratio, as expected for these polymer-Trypsin conjugates.

On the other hand, the comparison among PASucc-T (6) family of compounds about the influence of the variation of the ratio between NH_2-T/PASucc-COOH functional groups with respect to efficiency of conjugation and size, is not providing an important difference in terms of size. These results are coherent with the experimental fact that after the conjugation reaction the amount of free amino groups available, determined by TNBSA is the same for the three products. Remember that each trypsin molecule have 14 amino groups from lysines (quantified previously by TNBSA assay) available to react with activated carboxylic groups from PA.

Taking into account these results, it was decided to synthesize new conjugates with T and PACOOH as the masking polymer. The chosen ratio NH_2-T/PACOOH was 1:20. Results similar to those observed previously for PASucc-T family was observed with ^{1}H NMR, SDS-PAGE and FPLC analyses. In this case, it was necessary to use the same kind of column for FPLC but smaller, in order to be able to inject small amount of sample (200µL) without loss of sensibility. Here the peak

corresponding to conjugate PACOOH-T (5) sample was bigger enough to be distinguished clearly from naked trypsin. Notice, the ratio T/Vr for PA-T, which is 3/1, was the same for both families of PA-T compounds (4 and 5), which suggest they are in the same range of molecular weight.

Summarizing, results previously described revealed that succinoylated linker between polyacetal main chain (2) and trypsin is not providing a clear advantage in comparison to the conjugate without linker (3).

Therefore, novel polyacetal PACOOH seems to be a better alternative for PUMPT because, a) the synthesis is one step instead two as in case of PASucc, reducing loss of row material and save time with less purification steps; and b) once the proteins are unmasked the residues that could remain linked to their amino groups in the primary structure are significantly smaller than the residues that could be left from PASucc, reducing the risk of possible change in the third structure of proteins, induced by hydrophilic/hydrophobic interactions, which could cause occurrence or increase of hindrance effects between such residues with other aminoacid residues or small molecules like water.

In this manner, possible increase of inactivation of the active site of proteins, in case of enzymes, is prevented, as well as the inhibition of site recognition in case of proteins with action over the cell membrane surface receptors.

The sum of all the above issues leads to a very promising system, with synthetic and maybe physicochemical advantages pointing to simplify

the scale up processes that is critical to be able to go into medical applications.

It was possible to observed that the used of linker do not produce specific influence on the accomplishment of the PUMPT effect.

Nevertheless, the PA/T ratio do have an influence, making necessary to take into account the optimization of this proportion, that in this study was demonstrated to be 40/1 in PA/T.

The study of PUMPT effect over kinetic parameters of enzymatic activity of T in comparison with PACOOH-T under different reaction conditions demonstrated that under neutral pH T and PA-T show similar kinetics but under acidic conditions T tend to lose activity, while PA-T activity was increasing continuously.

These behaviors are coherent with expected because trypsin suffers degradation by self-proteolysis at neutral pH and due to hydrolysis under acidic pH.

Instead, PA-T was unwrapping trypsin gradually, making possible to keep the protein activity for longer even under acidic conditions.

PEGylated proteins were also obtained, being the most efficient strategy the use of Succinoylated MeO-PEG-OH instead of MeO-PEG-COOH.

SDS-PAGE as well as FPLC analyses demonstrated the successful PEGylating reaction, with 20wt% of total protein loading. Also enzymatic activity was evaluated and it was observe that pegylation

process reduce the activity as expected according to previous studies, published for other researches[32]

PUMPT system proposed in this chapter may provide an alternative to PEGylation in those cases where pH could be used as trigger for protein release, offering the possibility to improve the biological activity perform of conjugated proteins.

4.5. Conclusions

We have successfully designed a novel polymeric system capable of a) protect and mask the protein activity under normal pH physiological environment, and b) that is completely able to recover its activity in a time-dependent manner once arriving to acidic condition similar to those proper of damage tissue for example suffering from inflammation processes.

PEGylation of trypsin was accomplished and the obtained product is stable enough as to be used in the next step of experimentation that is the encapsulation into microparticles.

Conjugation of proteins with interesting biological activity for tissue repair, like IL-6 is currently ongoing in our laboratory and the biological evaluation of protein-polyacetals conjugates will be carried out in primary cell cultures and in the appropriate in vivo models.

5. SYNTHESIS AND CHARACTERIZATION OF CURCUMIN POLY(ACETAL)S

5.1. Introduction

As mentioned in the general introduction, nanomedicines known as "Polymer therapeutics" (PT) constitute a relatively new technology for controlled drug delivery which has become a useful tool for treatment and diagnosis of several diseases during the last years, but it is still an emerging field with enormous potential to explore. As can be deduced by the name, big part of "the secret behind the success" lies in the properties of the polymers used to synthesize them and polyacetals are members of this special family.

With 40 products already in the market and more than 70 in cancer clinical trials[113], the nanomedicine field has experienced a great exponential growth within the last decade. This fact is due to its potential to serve as a candidate solution for the urgent requirement of dealing with unsolved pharmaceutical and clinical needs in life-threating diseases[114]. In the recent years, nanomedicine has gained special attention in different research areas, especially for drug and gene delivery, in diagnostics and molecular imaging as well as in tissue repair and engineering[115] amongst other uses.

Nature and virtues of polymer therapeutics were previously described in general introduction. Therefore, in this chapter we are going to highlight some aspects particularly interesting for this study.

5.1.1. Polyacetals as carriers.

Polyacetals are well-known polymers since 1980 when Heller et al[77] published their synthesis by the reaction of divinyl ether and polyols. Their main qualities are that the synthesis is performed under mild conditions and products are water soluble, stable in neutral pH but degradable under mild acidic conditions and absolutely biocompatible. Latter, Tomlinson and co-workers[78,79] saw the opportunity to take profit of these qualities and published the synthesis of functionalized amino-pendant drug-loaded polyacetals as alternative to water soluble, high molecular weight, non-biodegradable polymers used as carriers for conjugation of bioactive agents, in order to provide a solution to the problem of polymer accumulation in the lysosomes[116].

Tomlinson et al. [78,79] demonstrated that these polymers were able to i) be stable at physiological pH (~7.4); ii) be able to improve drug delivery to cancer cells *in vitro* and iii) be biodegradable under acidic pH, showing pH dependent drug release kinetics, allowing to control drug release in acidic cellular compartments such as endosome (pH 6.5) and lysosomes (pH5.5). In 2006 Vicent et al.[80] described for the first time, the synthesis of polyacetals with the drug diethylstilbestrol (DES) directly linked to the polymer backbone through acetal bonds. Such systems demonstrated enhanced *in vitro* antitumor activity in comparison with the drug alone. The versatile synthesis described by Vicent and co-workers allows to easily introduce diol-bearing drugs without the need of complex linking strategies. From the same group, Gimenez et al. [81] applied similar strategies to synthesized novel polyacetal-drug conjugates, specially emphasizing the influence of

polymer architecture in the biological performance. Furthermore, England et al.[12] have recently demonstrated the power of polyacetal-based combination therapy (two drugs in the same polymer) designed for antitumor application with very promising *in vitro* and *in vivo* results. Tang and co-workers[82] have also published their results regarding the synthesis of a battery of curcumin-bearing polymers as anticancer conjugates following the same strategy by means of curcumin introduction within polymer backbone. Among their polymer structures, polyacetals represented the best candidates for their applications as anticancer therapies according with their *in vitro* and *in vivo* activity.

5.1.2. Chronic wounds and Curcumin as model drug.

On the other hand, during the last years, Curcumin, a natural polyphenol extracted from *Curcuma longa* (turmeric) and with ancestral use in traditional Asian medicine, caught the attention of researchers due to the wide spectrum of biological activities that has demonstrated to possess, including antioxidant, anti-inflammatory, antiviral, antimicrobial and anticancer agent. Curcumin (diferuloylmethane) is a polyphenolic compound derived from turmeric spice from curcuma longa[117]. Naturally occurring curcuminoids are a mixture of curcumin (77 %), demethoxycurcumin (DMC) (17 %), and bisdemethoxycurcumin (BDMC) (3 %)[118]. (See Figure 5.1.).

Curcumin antagonizes many steps in the inflammatory cascade, including activator protein-1 transcription, activation of nuclear factor-kB, iNOS, and JNK[119–121].

Curcumin

Demethoxycurcumin

Bisdemethoxycurcumin
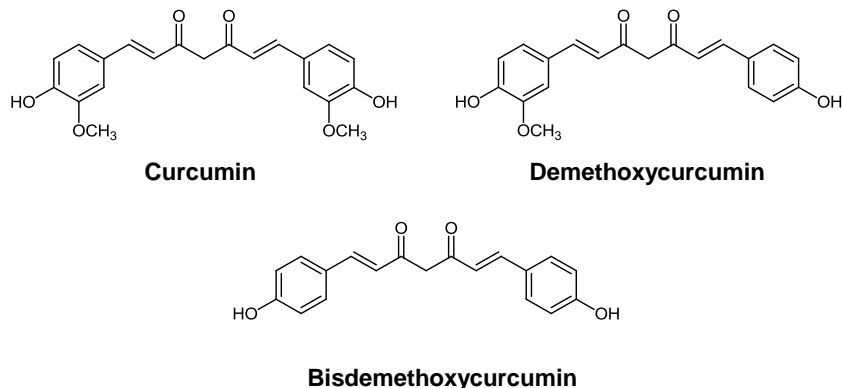
Figure 5.1. **Structure of the different curcuminoids present in curcuma turmeric spice from curcuma longa.**

It also exerts a potent antioxidant activity for NO-related radical generation[122] In fact, to date curcumin has become in a very attractive candidate for applications related with the treatment of various cancers, neurodegenerative deceases and of course, wound healing.

In this work, PACur conjugates were chosen as candidates for tissue repair/regeneration applications, concretely, for wound healing of chronic injuries. As it was previously explained in general introduction, this pathology is related with aging diseases among other aspects and is characterized by occurrences of inflammation and subsequent infection of the injury[45]. Interestingly, during inflammation stages the pH of the tissue becomes slightly acidic, around 6[39]. Therefore a rational design of a localized drug delivery system may include a polymer-drug conjugate composed by polyacetals because they are

biodegradable, biocompatible and their degradation depends on pH changes; and curcumin because of its potential antioxidant, anti-inflammatory and antimicrobial activity.

5.2.   Methodology

5.2.1.   Synthesis and Characterization

Curcumin polyacetals (PACur) were synthesized following a modification of the methodology proposed by Giménez et al.[12,81] applying Schlenk techniques. Briefly, diol-polyethylene glycol (diol-PEG$_{4000}$) (1.257mmol, 5.030g) used as monomer and p-Toluenesulfonic acid p-TSA (0.074mmol, 0.014g) used as a catalyst for the addition reaction, were weighted and added 100mL Schlenk tube (A). Curcumin, the second monomer (1.0832mmol, 0.339g) was weighted separately in another Schlenk tube (B). Both flasks were purged 3 cycles of dry N_2 and vacuum at room temperature and finally completely dried under high vacuum (20min). The contents of each flask were dissolved in anhydrous dioxane (20mL for A and 10mL for B). Flask A was heated up to 80ºC to dissolve completely the solids and it was left to cool down until room temperature (25ºC). Then, the curcumin solution was transferred under inert N_2 atmosphere with the aid of a cannula. Once they were completely mixed, the last monomer, Triethyleneglycol-Divinylether, TEGDVE (2.1538mmol, 0.44mL) was added dropwise. The reaction was carried out under N_2 atmosphere, stirring for 3h. After that, pH was adjusted to 8 with triethylamine (0.2mL) in order to quench the reaction (by neutralizing pTSA) and finally the product was separated by precipitation into a large excess of hexane: diethyl ether (ratio 4:1) and filtered off. The product

recovered was purified by recrystallization in hexane: diethyl ether (3x, 100mL) and dried under vacuum. The final product was isolated as a yellow loose powder and it was stored at -20ºC for further analyses.

5.2.1.1. Structural Characterization by NMR

Structural characterization of products was carried out by NMR spectroscopy. Samples were dissolved in DMSO-d6, Spectra were recorded in a Bruker 300 BRUKER ADVANCE AC-300 (300 MHz,) spectrometer and NMR data was processed using the programs Topspin 1.3 (Bruker GmbH, Karlsruhe, Germany) and MestreNova v6.0.2-5475 (MestreLab Reseach S.L., Galicia, Spain). The chemical shifts of the nucleus are reported as s (singlet), d (doublet), t (triplet), q (quartet) or m (multiplet) and expressed by δ (ppm) taking as an intern reference the tetramethylsilane signal (TMS) 0.00 ppm, and the intermediate signal in the quintuplet (49.86 ppm) in the carbon spectra. The J-coupling constants are expressed in hertzios (Hz). Besides ^{1}H and ^{13}C NMR experiments, two-dimensional NMR experiments were also performed, concretely, 2D-Correlation spectroscopy (COSY).

5.2.1.2. Determination of Molecular weights and polydispersity by GPC

Molecular weight and polydispersity of all products obtain after polymerization reactions with curcumin, PEG4000 and TEGDVE, were determined by GPC in aqueous (PBS 1X, pH 7.4) phase. Samples were dissolved in PBS and injected in the GPC instrument as explained previously in general methodology section. Polymer solution (6mg/mL in PBS) was injected in GPC using two TSK Gel columns in series G2500 PWXL and G3000 PWXL with a Viscotek TDA^{TM} 302 triple detector 87

with UV detection coupled. The mobile phase used was PBS 0.1 M, flow 1 mL min^{-1}.

5.2.1.3. Quantification of free drug and total drug loading

Total drug loading in PACur was determined by UV spectroscopy. First, maximum absorbance wavelengths for curcumin were identified by registering the UV-Visible spectrum of curcumin in the absorbance range between 220nm at 600nm in Acetonitrile ACN, ethanol and PBS 1X pH 7.4. For quantification, a calibration curve ranging from 0.2-20 µg/mL of curcumin was performed at fixed wavelengths of at 260nm, 405nm and 418nm, using quartz cuvettes of 1mm of length path. To do that, a mother solution of curcumin in ethanol was prepared at 1mg/mL and from there; the different concentrations were adjusted by diluting with PBS 1X pH 7. In order to establish curcumin loading within the PACur, samples were measured at 6mg/mL under the same conditions used for the calibration curve. Total drug loading (TDL) was determined as percent in weight from total polymer mass, using the calibration curve to translate absorbance in curcumin concentration.

$$Total\ drug\ loading\ (\%) =$$

$$\frac{amount\ of\ curcumin\ measured\ in\ PACur\ polymer\ (mg)}{mass\ of\ PAcur\ polymer\ (mg)} x100$$

Equation 5-1. **Total drug loading determination by UV-Vis.**

Free drug amount was determined by RP-HPLC, from a PACur solution in ACN (6mg/mL), using the gradient mode, with a ramp

70A:30B/30A:70B (A:ACN;B:PBS 1X 7.4) in 20 minutes run. Retention time of curcumin was 6.6min. Non acidic or basic additives were used in any of both mobile phases to prevent sample decomposition due to a decrease or increase in pH. For HPLC analysis 50µL of standard and sample solution were injected with a 1mL/min flow, into a C18RP column. Calibration curve ranging from 0.2-20 µg/mL of curcumin was performed under these conditions. UV-Vis detector was used to register HPLC signals, at 260nm, 405 and 418nm. Calibration curves were built following the same protocol than used for UV spectroscopy.

$$Free\ drug\ content\ (\%) =$$

$$\frac{amount\ of\ free\ curcumin\ measured\ in\ PACur\ polymer\ (mg)}{mass\ of\ PAcur\ polymer\ (mg)} x100$$

Equation 5-2 Free drug content determination by HPLC analysis.

5.2.2. Hydrolysis of PACur and Curcumin Release kinetics

3mL solutions of PACur conjugate (6mg/mL) were prepared using PBS buffers at different pH: 5.5, 6.5 and 7.4 and incubated up to 5 days at 37ºC. Aliquots (200µL) were taken and frozen immediately in liquid nitrogen at selected time points (0, 15, 30min, 2h, 8h, 24h, 48h, 72h, 96h, 120h, 260h) and stored at -80ºC until analysis. Before the analysis, acidic samples were neutralized with a solution of ammonium formate 0.1M and the volume of all samples was adjusted with PB pH7.4 in order to keep the same concentration. Samples were analyzed by HPLC and GPC.

For HPLC analysis, 50µL of sample were injected using same condition as described above for total and free drug content.

For GPC analysis 100µL of sample were injected and analyzed as described in general methodology.

5.2.3. Cytotoxicity of Cur and PACur

Cell viability is defined as the percentage of live cells compared with untreated controls. Therefore, cytotoxicity of free Curcumin and PACur conjugates was determined in a human fibroblast cell line and using the standard MTS assay (3-(4,5-dimethylthiazol-2-yl)-5-(3-carboxymethoxyphenyl)-2-(4-sulfophenyl)-2H-tetrazolium) to measure cell viability. Cells were cultured in Dulbecco's Modified Eagle Medium, DMEM (Fisher, Spain), with 4.5 g/l D-glucose, supplemented with 10% de fetal bovine serum FBS (Fisher), 1% of penicillin/streptomycin and 1% of L-glutamine (Lonza, Switzerland). Cells were used in their exponential phase of growth.

Briefly, fibroblast cells were seeded onto 96-well plate with a density of 10.000 cell/cm^2 (100µL) and incubated at 37ºC, in a humidified atmosphere with 5% CO_2 (v/v) up to 24h to allow cells were properly adhered. Then the medium was replaced by different concentrations of drug (alone or conjugated to the polymer), dissolved in culture medium from 0.5 to 38 µg/ml drug-equivalent.

After 72 h with treatment, combination of MTS/PMS was used to assess cell viability after treatments. In brief, after cell incubations, 10 µL of manufacturer solution of MTS/PMS (20:1) was added to each

well, and the cells were incubated for a further 2 hours. Mitochondrial dehydrogenase enzymes of viable cells converted MTS tetrazolium into a colored formazan product. The optical density of samples was measured at 490 nm. Absorbance of the optical density of the solution was determined spectrophotometrically in a Perkin Elmer precisely 1420 Victor 3[TM] multi-label counter using a microtiter UV plate reader.

5.3.   Results

5.3.1. Synthesis and Characterization

PACur reaction yield was 5.42g, 2.3603mmol, 41%. Total drug loading in the polyacetals were 9.5 wt.% with less than 0.2 wt.% of free drug, according to UV and HPLC analyses, respectively. Polyacetals had a M_p 17106 g/mol; Mn=19526g/mol; Mw=51302 g/mol; M_w/M_n=2.6 as determined by GPC in PBS.
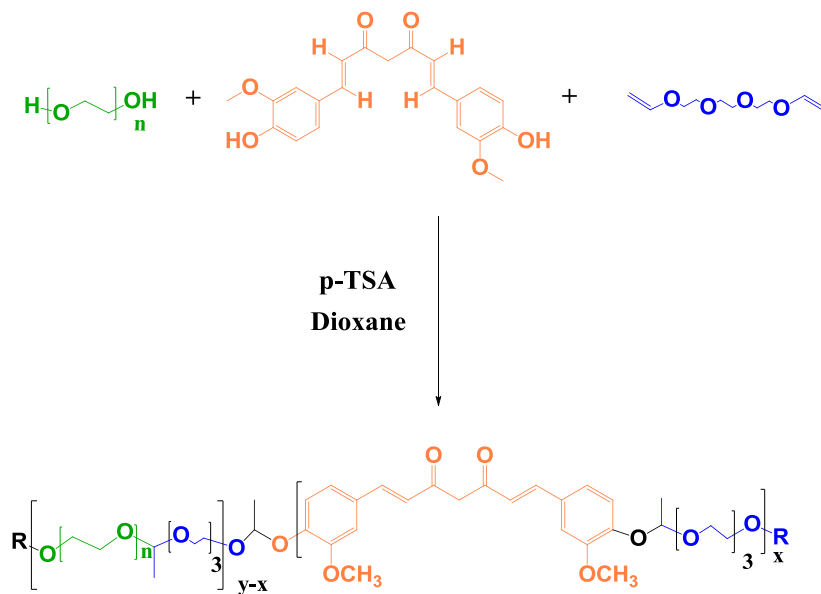
Figure 5.2   PACur synthesis from PEG, curcumin and TEGDVE monomers.
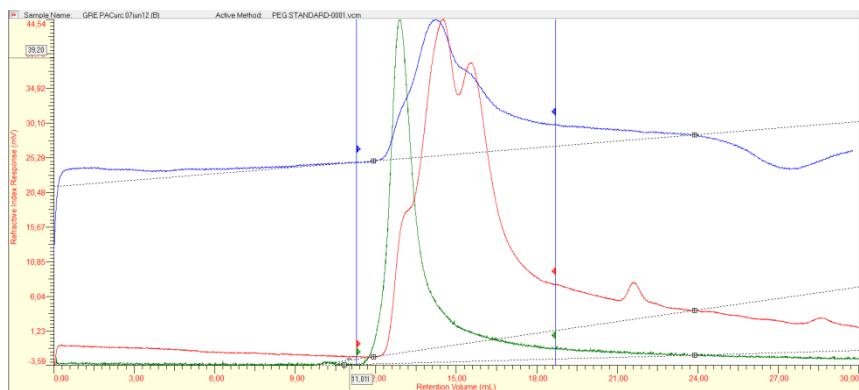
Figure 5.3 GPC Chromatogram of Polyacetal-curcumin (PACur) conjugate, analyzed in PBS 1X, pH 7.4, at 30ºC, 35min running, sample concentration 6mg/ml, flow 1mL/min. Detectors: Refractive Index, Right angle light scattering, viscometer

The ^{1}H NMR (300 MHz, Acetone) spectrum (Figure 3.3) revealed the following chemical shift for main groups in PACur sample: δ 8.28 – 8.06 (m, 1H, -OH), 7.62 (d, J = 15.8 Hz, 3H, HC$_d$=C), 7.34 (s, 3H, H-ArC$_b$), 7.19 (s, 5H, H-ArC$_a$), 6.89 (dd, J = 8.1, 2.4 Hz, 2H, H-ArC$_c$), 6.83 – 6.66 (m, 2H, C= HC$_e$), 6.00 (d, J = 13.8 Hz, 1H, C$_f$H$_2$), 5.51 (s, 2H, Acetal $_j$CH), 4.76 (dd, J = 10.5, 5.2 Hz, 5H, , Acetal $_i$CH), 3.95 – 3.88 (m, 9H, $_g$CH$_3$-O), 3.86 – 3.31 (m, 590H, CH$_2$-CH$_2$, PEG+TEGDVE), 1.47 (d, J = 5.2 Hz, 6H, CH$_3$-AcetalC$_j$), 1.25 (d, J = 5.2 Hz, 15H, CH$_3$-AcetalC$_i$).

COSY NMR bi-dimensional experiment spectrum of PACur (Figure 4.3) conjugate shows the relation between the groups to make clearer the assignments**.**
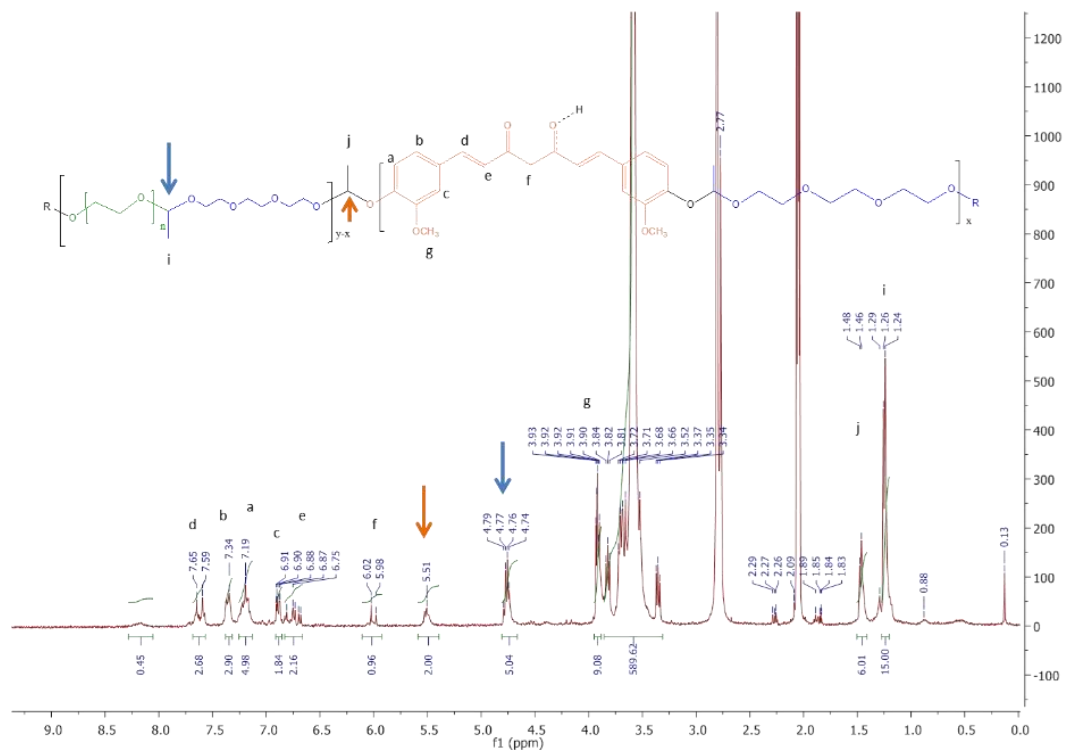
Figure 5.4 ^{1}H NMR spectrum of Polyacetal-curcumin (PACur) conjugate, acquired in DMSO-d6, at 300.5K, 300 MHz.
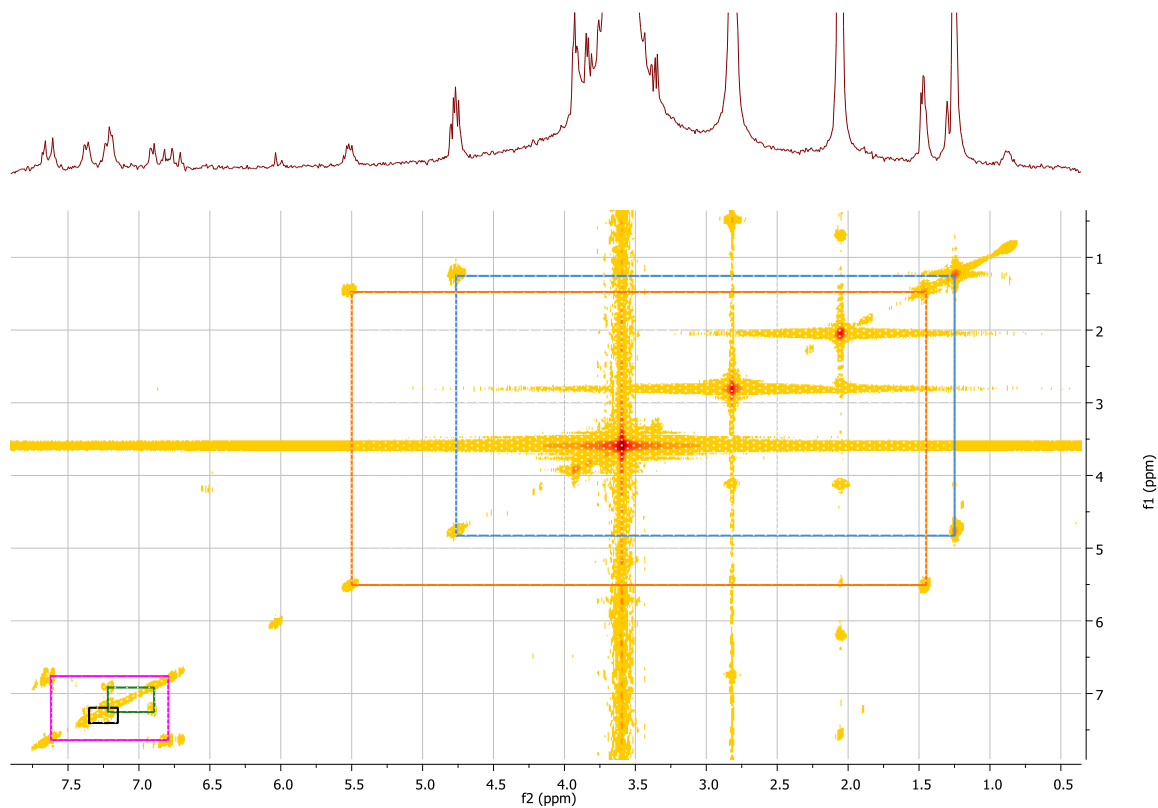
Figure 5.5 COSY NMR bi-dimensional experiment spectrum of Polyacetal-curcumin (PACur) conjugate, acquired in Acetone-d6, at 300 MHz,. Blue square shows relation between CH-Acetal(PEG-TEGDVE) and CH_3-CHAcetal(PEG-TEGDVE). Orange square shows relation between CH-Acetal(Cur-TEGDVE) and CH_3-CAcetal(Cur-TEGDVE). Magenta, green and black squares belong to Curcumin double bonds and aromatic protons.

5.3.2. Hydrolysis of PACur and Release kinetics

After 266h (11 days) in observation, it was determined that curcumin polyacetals are able to release curcumin faster at pH 5.5, as expected, with an initial burst of 4% on the first 30 seconds, followed by a fast released during the next 6 hours until reach 59% of drug release. Then, the system seems to be stabilized, showing a progressive release of curcumin at a relatively constant rate until 168h (7days). After that time, a slight increase in rate is observed until 266h (11 days) reaching 85% of total drug release. Some precipitated was observed at that time, and the sampling was finished at that point in order to avoid mistakes due to drug decomposition or saturation of the solution analyzed with the drug released.

Meanwhile, the release at pH 6.5 was also fast at the beginning, starting with a bust of 30% and reaching a 34% of drug release during the first 7 hours. Then as observed at pH 5.5, the release rate slows down and after 11 days only 52% of the total drug loaded was found to be released.

On the other hand, at pH 7.4 curcumin-bearing polyacetals behaved as a relatively stable construct. After an initial burst of 7%, only 13% of drug was released during the first 8h and then rate release became slower during the next hours. From 24h and beyond the rate remains stable achieving around 25% release after 266h (11 days).
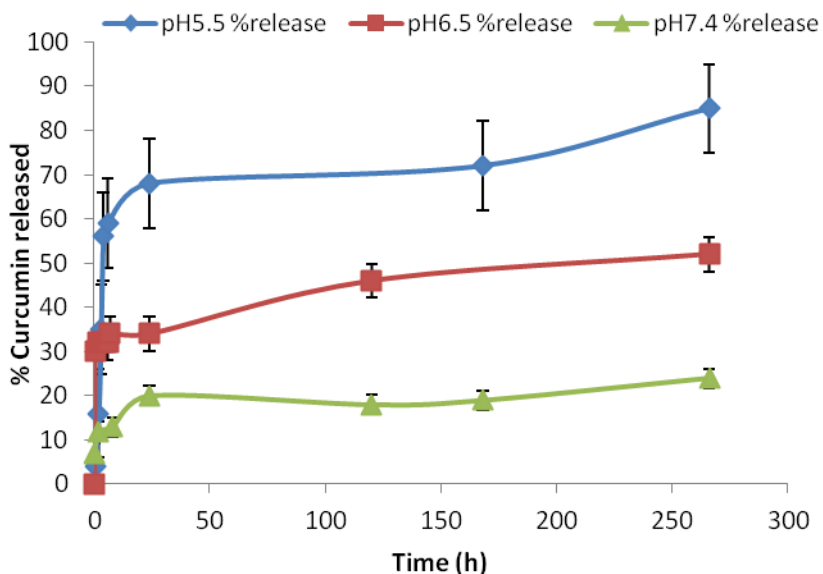
Figure 5.6   Drug release kinetic profile of Curcumin from polymer conjugates at different pH.

5.3.3. Cytotoxicity of Cur and PACur

Fibroblast cells of human origin were used to screen the cytotoxicity of PACur conjugates and free curcumin for comparison. Results were expressed as % Cell Viability vs Curcumin-equivalent concentration determined by MTS assay. Conjugates were found to be slightly more cytotoxic than de drug by itself at 72h of treatment, as can be appreciated in Figure 5.7. From this data IC_{50} values were calculated: IC_{50} of free curcumin was 36 µg/mL, while PACur IC_{50} was 24 µg/mL.
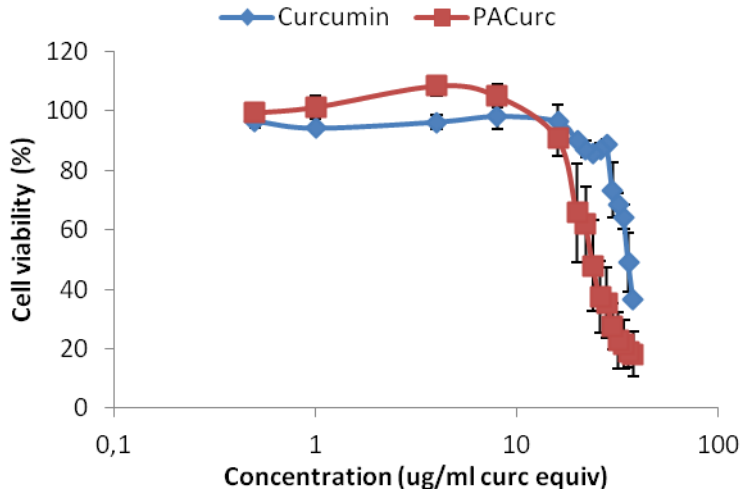
Figure 5.7 Cytotoxicity of free curcumin and polyacetal-curcumin conjugated (PACurc) measured in a human fibroblast cell line, 72h of treatment at 37ºC, in humidified atmosphere with 5% CO_2. Mean ± SD, n>3 independent experiments.

5.4. Discussion

5.4.1. Synthesis and Characterization

In the present chapter, the synthesis and characterization of novel Polyacetal-Curcumin conjugates (PACur) with potential application in wound healing approaches have been addressed. PACur were easily obtained by applying a mild polymerization method involving the reaction of diols with divinyl ethers. This strategy allowed the incorporation of drugs with bis-hydroxyl functionalities (such as curcumin) into the polymer main chain. Provided the biodegradable character of PAs, such drugs introduced would be released under acidic environment by degradation of the polymer backbone, without the need for the use of biodegradable linkers.

Concretely, our strategy was based on the use of cationic addition reactions catalyzed by acidic medium (use of pTSA). The mechanism of the polymerization reaction performed is depicted in the Figure 5.8.

i) Initiation

p-TSA (initiator)

TEGDVE

starting chain
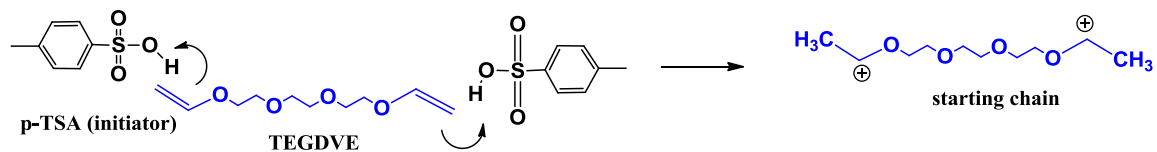
ii) Propagation

iii) Termination

Triethylamine

OH-R-OH =

or
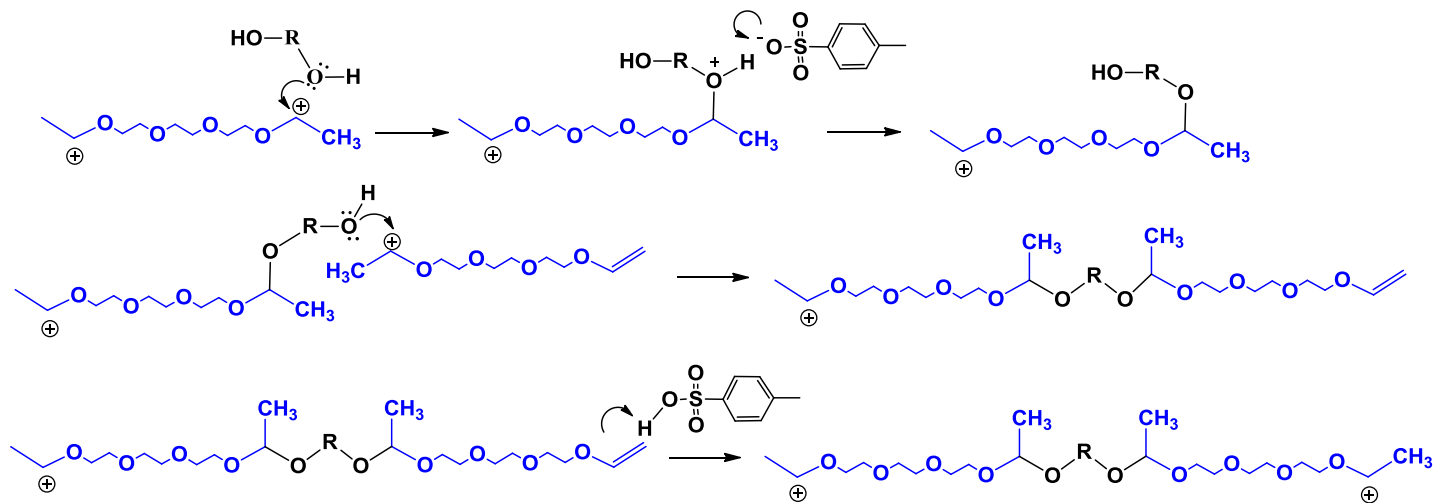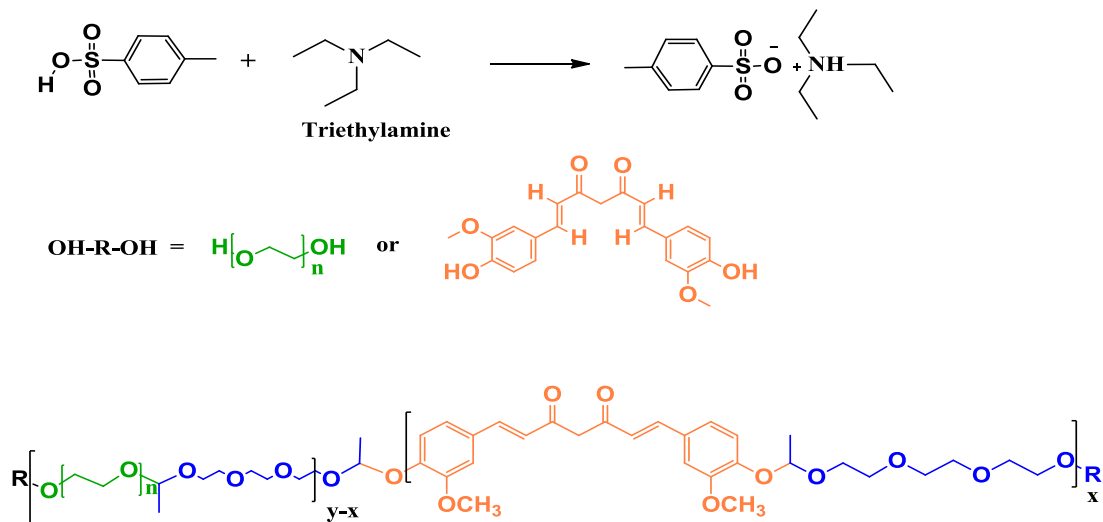
Figure 5.8 Mechanism of polymerization by cationic additions

Polymerizations were successfully accomplished yielding well-defined PACur conjugates with up to 10.8 wt.% total curcumin loading and less than 0.2 wt.% of free drug contain as determined by UV-VIS and HPLC techniques. Although the drug loading obtained of the highly hydrophobic drug curcumin were considerably high, the PACur obtained showed complete solubility in aqueous solutions.

According to GPC, the molecular weight (MW) obtained was in the range of 17000-20000 g/mol with a PDI around 2.6 as could be expected from the inherit limitations of this polymerization method. This MW is suitable in this desired application due to the fact that, even if not all the system is degraded, the MW is under renal clearance threshold (below 40000 g/mol).[116,123]

^{1}H NMR and COSY experiment confirmed the reaction success (Figures 5.4 and 5.5), where curcumin molecules were shown to be clearly linked to polyacetals backbone. As already stated in Results section from this chapter, the ^{1}H NMR spectrum shows the appearance of two different multiplets at different chemical shift corresponding to the area of the acetal peaks. The first one at 4.74 - 4.79 ppm can be assigned to PEG-TEGDVE acetal bond, and the second at 5.51 - 5.53 ppm was assigned to Cur-TEGDVE acetal bond. The PEG-TEGDVE acetal bond peak showed a bigger integration than the other, pointing out that polymerization reaction might occur preferentially with PEG. This behavior was expected since PEG monomers are better nucleophiles than curcumin monomers. This can be attributed to the fact that, in the case of PEG, the two hydroxyl groups have their negative charge density localized over the oxygen atoms, making these electrons more

available to attract protons, necessary in the initiation step of the polymerization. Instead, hydroxyl groups in curcumin are actually phenols, where the negative charge density of oxygen atoms is delocalized through the aromatic ring, making this OH groups bad nucleophiles in comparison with OH from aliphatic alcohol. For that reason, catalyst activates more PEG chains than curcumin molecules, resulting in a polymer with a higher proportion of PEG acetal. However, despite that line of reasoning, reactivity of curcumin was acceptable and the ratio obtained between both kind of acetals (Curcumin:PEG) was 1:2.52.

5.4.2. Hydrolysis of PACur and Release kinetics

Polyacetals are pH responsive polymers, soluble in water. They are designed to be hydrolyzed under acidic conditions. This kind of polymers has been successfully used (*in vitro*) as drug carriers, improving the pharmacokinetic and pharmacodynamic profiles of the free drug and providing mechanisms to stablish a sustained and controlled drug release[12,81]. Ideally, this system should make possible to reduce the number of doses and frequency of drug's administrations, resulting in the improvement of treatment efficacy and patience comfort. On the other side, Curcumin is a natural phenol with a lot of potential therapeutic properties, including anti-inflammatory and antioxidant activities, but its applications has been limited because of its hydrophobicity and therefore poor water solubility, relatively low bioavailability and low stability in solution.[124]

Drawing from this premise it was expected that through the conjugation of curcumin with polyacetal, it should be possible to obtain hydro-soluble polymer conjugates, more stable in solution than curcumin alone, opening the door to a wide range of therapeutics uses, including wound healing.

As explain before in the introduction of this chapter, inflammation is one of the phases that takes place during the process of chronic wounds and it is known that pH of injured area changes from neutral (pH 7.4) to slightly acidic (pH around 6) during this inflammatory stage.

Such conditions make polyacetals one of the best choice as polymer carriers since it is expected to be able to tailor drug release by controlling pH changes in the specific environment.

It has been demonstrated that curcumin-polyacetals conjugates synthesized through the present methodology explained in this chapter are completely soluble in water, because dilutions of different concentration between 3 a 25mg/mL were prepared as part of procedures for drug loading quantification. Hydrolysis experiments demonstrated that the highest drug release takes place at pH 5.5 as expected, followed by the release at pH 6.5 while the lower release was observed at pH 7.4 (Figure 5.6).

Acidic pH made possible the hydrolysis of acetal bond through the protonation of oxygen atoms, probably following the mechanism proposed below in Figure 5.9. Basically, a protonated molecule of water, acts as the acid that initiate the hydrolysis, protonating one of the oxygen atoms in acetal bond. Probably, in the first step of the

mechanism the phenolic group (in case of curcumin or aliphatic hydroxyl in case of PEG chain) is recovered and a pseudo-carbocation (δC+) is formed. In this case, δC+ is in a secondary carbon with a $-CH_3$ adjacent. In the second step δC+ promotes the elimination of one of the proton from methyl group next, which is passed to another molecule of water, then a double bond (-C=C-) is formed between them. This mechanism is similar to the bimolecular Elimination mechanism used to explain the olefin synthesis by alcohol dehydration in presence of acid as catalyst but in this case, heating is not necessary[125]. Polyacetals can be hydrolyzed at 37ºC, natural body temperature, as shown in this experiment. Nevertheless, it is logical to expect that an increase in temperature produce an acceleration of this reaction. This fact represents an advantage to our systems in our desired application since inflammation also is companied by a slight raise of body temperature.
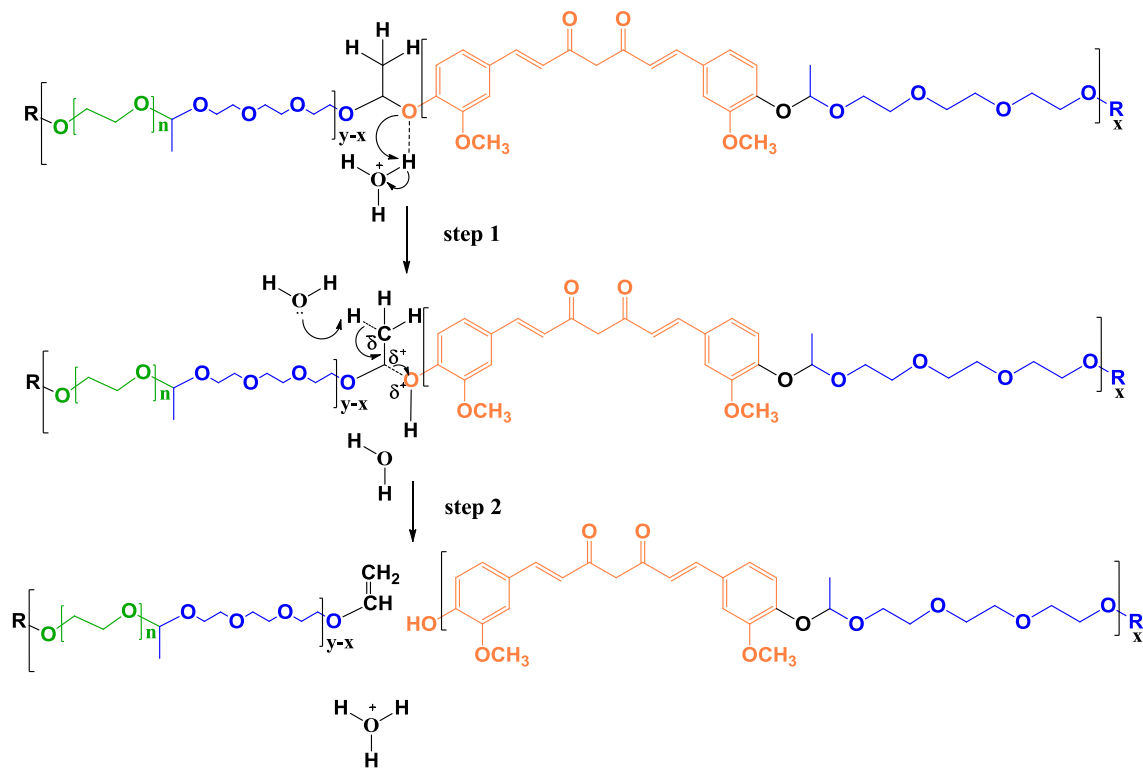
Figure 5.9 Proposed PACur mechanism of hydrolysis under acidic conditions.

Hydrolysis reaction takes place in a random way cleaving all acetal bonds yielding oligomers and finally the parent monomers: free curcumin, PEG and TEGDVE.
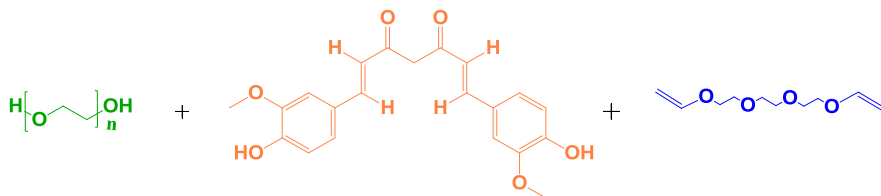
Figure 5.10   Final products of PACur total hydrolysis

It is evident that, in this case, drug release kinetic is directly related to polymer degradation, because curcumin is loaded in polyacetals as part of the main chain of the polymer. Therefore, when acetal bonds that link curcumin molecules to TEGDVE are broken, polymer molecular weight diminishes and curcumin is been released.

In situ degradation of polymers is another positive aspect of this system, because prevents their accumulation in the lysosomal compartments of cells. Furthermore, the biggest non-biodegradable fragments are PEG_{4000}, that are under the maximum MW (40 kDa) of renal elimination.

5.4.3.   Cytotoxicity of Cur and PACur

Curcumin was selected as a drug for this study because of its anti-inflammatory and antioxidant properties. In addition, it is believed that it can protect tissues from oxidative damage improving wound healing[126]. However, due to the other roles of curcumin and

curcuminoids related to anti-proliferative activity in cancer applications[127,128], curcumin dosing in regenerative medicine must be carefully control in order to not induce unexpected toxicities.

As mentioned in the general introduction, repair of injured tissues occurs as a sequence of events which include inflammation, proliferation and migration of different cell types. In the inflammatory phase, bacteria and debris are phagocytized and removed. In addition, neutrophils migrate to the wound site. This kind of cells generate free radicals, producing oxidative stress leading to local lipid peroxidation, DNA breakage and enzyme inactivation. Due to the fact that free radicals are produced during inflammatory phase, antioxidants like curcumin may inhibit inflammation allowing regeneration.

Cytotoxicity assays in human fibroblasts were performed in order to ensure safety of our PACur at the concentrations to be used in wound healing applications. Such experiments revealed that PACur conjugates are slightly more cytotoxic than curcumin alone. However, these findings could not be necessary bad, because the PACur IC_{50} is still high enough to be sure that we can work in a safety concentration for wound healing applications, provided that only low concentrations are needed to provoke beneficial effects. Recent studies reveal that a concentration of 2μM of free curcumin is enough to reduce ROS in an acellular system (without cells) to measure antioxidant activity of curcumin[129]. As a second example, another study published that a maximum doses of 8.5μg/ml of curcumin released from nanoparticles (chitosan-PEG400) during 24h is enough to promote tissue regeneration in a model of murine burn injure[29].

5.5. Conclusions

In this part of the thesis, versatile polymer-drug conjugates based on the biodegradable polyacetals and the antioxidant curcumin have been effectively synthesized. Curcumin molecules were incorporated into a poly(ethylene glycol) (PEG) based polyacetal system using a reaction of short PEG chains with triethyleneglycol-divinylether (TEGDVE) units and an acid catalyst, without the need for biodegradable linkers. With an improved polyacetal synthesis strategy we obtained high yields of water soluble polymer conjugates with desirable drug loadings (total drug loading of 10.8 wt% and less than 0.2wt% of free drug) and tailored molecular weights (Mw 17,000–20,000 g/mol) with acceptable polydispersities.

These polymers were found to be hydrolytically cleaved under acid conditions (such as those found in endosomes, lysosomes or the extracellular fluid of some inflamed areas) yielding the free drug curcumin. Additionally, they were found to be stable over prolonged periods of time at pH 7.4 mimicking blood plasma.

Cytotoxicity assays performed as a proof of safety ensured that PACur conjugates are not toxic within the therapeutic window for curcumin applications in wound healing.

6. SYNTHESIS AND CHARACTERIZATION OF HYALURONIC ACID MICROPARTICLES

6.1. Introduction

HA is a natural polyelectrolyte based on repeating disaccharides of β1-4 D-glucuronic acid and β1-3 D-N-acetyl glucosamine ([β-1,4-GlcUA-β-1,3-GlcNAc]$_n$). Sahiner et al. highlight that it is present in the extracellular matrix (ECM) of all higher animals and plays vital roles regulation the ECM organization, in cell adhesion, cell motility, and cancer metastasis beside its inherent biocompatibility and biodegradability makes it an attractive biomaterial in drug delivery and tissue engineering.[130–133]

Also, HA, an important component of the extracellular matrix, has been used as a viscoelastic biomaterial for medical purposes, in cosmetics because of its high water retention capacity and in drug delivery systems because of its non-toxicity, biodegradability, and biocompatibility.[44]

Most studies with HA are directed to hydrogel films or scaffolds fabrication[93,132,134–145] due to its amazing biocompatibility and because it is a naturally occurring biodegradable polymer with a variety of applications in medicine, including scaffolding for tissue engineering, dermatological fillers and viscosupplementation for osteoarthritis treatment[133].

Nevertheless, there are also interesting researches about the use of HA for fabrication of micro and nanoparticles. For example, Lee et al.[51] studied a laminin-modified infection-preventing collagen membrane containing silver sulfadiazine–hyaluronan microparticles. They prepared hyaluronan-based microparticles containing silver sulfadiazine (AgSD) incorporated into the two collagen layers (AgSD content 50mg/cm2) and found that the laminin-coated AgSD-medicated collagen membrane demonstrated a higher wound size reduction and vessel proliferation and lower inflammation than the polyurethane control, suggesting that the laminin AgSD-medicated collagen membrane substantially improves dermal wound healing.[51]

HA-based hydrogel microparticles are attractive materials for biomedical applications because they can provide bigger surface area that will improve tissue integrating and facilitate drug delivery[130].

Another interesting approach in this field is the encapsulation of nanomedicine like polymers conjugated to drugs or proteins, because in is expected that conjugation not only protect the molecules conjugated but also increase their potential therapeutic activity[146].

Lately, curcumin has kept the attention in this field as candidate to be encapsulated into HA films, vesicles, nanoparticles and microparticles[147,148] with promising burn-wound healing potential.

For this reason in this part of the project it was explore the possibility to obtain this kind of interested combine systems design for drug delivery.

6.2. Methodology

6.2.1. Synthesis of MPs and encapsulation of model drugs and Polymer-drug conjugates

6.2.1.1. Synthesis of HA MPs

Microparticles of hyaluronic acid (MPs-HA), were obtained following a modification of the methodology proposed by Sahiner and co-workers[130] using the synthesis of microparticles by single reverse emulsion, a water-in-oil micro emulsion system. At the beginning, MPs-HA without loading was fabricated in order to find the best parameter for the synthesis, and also keep this batch of MPs-HA as reference for comparison with loaded MPs.

Theoretical cross-linking was calculated to be 90% as function of available reactive groups in HA chains as is shown in the equation

$$\% Crosslinking = \left(\frac{mol\ DVS}{mol\ unid\ HA}\right) x 100 \quad \textbf{Equation 6-1}$$

Amount of DVS was calculated as shown in the following example:

$$\boldsymbol{x - gHA = 10gsoln\ HA\ x\frac{5g}{100g\ soln\ HA} = 0.5} \quad \textbf{Equation 6-2}$$

$$x - mol\ Unid\ HA = 0.5g\ HA\ x\frac{1\ mol\ unid\ HA}{401g}$$

$$= 0.00125 mol\ unid\ HA$$

$$x - mol\ DVS = \frac{100\% crosslinking\ x\ 0.00125 mol\ HA}{100} \quad \textbf{Equation 6-3}$$

$$\mu L\ DVS = 0.00112 mol\ x\frac{118.15g}{1mol}x\frac{1mL}{1.177g}x1000 = 112.9\mu L$$

Equation 6-4

Briefly, an aqueous solution of HA 5% wt/v, (12 mL) was prepared dissolving the HA powder (0.6 mg, Mw=1000KDa) in a solution of 0.2N NaOH (12mL). The mixture was left in 24h at 27º on a back-and-forth plate with slow motion, to avoid polymer degradation. Next day, the microemulsion was prepared into a cylindrical flat bottom glass vessel reactor of 400 mL of volume capacity, couplet to the stirring system, which was constituted by one stainless steel propeller stirrer with 4-bladed, connected to a digital overhead stirrer (IKA, OST 20 basic digital IKA Yellow [line] or model Eurostar 40 digital).

The steel stirrer was put into the vessel and the height was adjusted to keep the propeller as close as possible to the bottom without touching it. Then the top of the reactor was fixed and sealed with a metallic ring to prevent solvent evaporation.

Following, a volume of dichloromethane (DCM, 100mL) which is the dispersant phase used in this case, was transferred into the reactor through one of the access in the top of the reactor, followed by accurately measured amounts of sodium bis(2-ethylhexyl)sulfosuccinate (AOT 1.34g, mmol) and 1-heptanol (1-HP, 1.7mL, mmol). The mixture was stirred at 500 rpm until all components were completely dissolved. Then stirring rate was adjusted, from 1300rpm to 1500 rpm to select the best condition.

Once the stirring rate was stabilized to avoid turbulence in the system, HA solution was loaded in a plastic syringe and the aqueous solution (10mL) was dropped into the system using a syringe pump at constant

flow of 1 mL/min. When the addition was completed, the obtained emulsion was stirred by 1h to stabilize it and let the microparticles to be formed, then cross linker divinyl sulfone (DVS, 112 µL) was added to the system keeping the stirring rate constant for 2h more at room temperature (25ºC) to allow cross-linking reaction to take place *in situ* and completing the MPs formation.

Figure 6.1 MPs stirring system

Following, the reaction mixture was poured into acetone (300mL) to precipitate the microparticles. The suspension was filtered through stainless steel sieve (Φ=0.050mm of light) to separate the desired MPs from bigger particles and residues of HA gel. MPs-HA suspended in the supernatant were led to sediment in a 500mL beaker cover with plastic film at 4ºC by 16h. Latter, the suspension was shaken mechanically and distributed into four centrifuge tubes of 50 mL of volume capacity. MPs were separated from liquid phase by

centrifugation (4000 RCF, 25 ºC, 5 min, in centrifuge Eppendorf model 5804, with swinging rotor A-4-44, with four holders for tubes of 50 mL). This procedure was repeated until the whole MPs were collected from the total volume of suspension. Once MPs were concentrated (to 10 mL) on each one of the four tube of centrifuge, clean acetone (30x5 mL) was added on each tube, shaken and centrifuge again in the same conditions than before, in order to extract any residual amount of reactants.

The whole process was accomplished under the fume hood to prevent the inhalation of toxic substances.

Finally, MPs were left in a minimum amount of acetone, barely wet, frozen at -20ºC 4h and then at -80ºC 16h before been freeze-dried by 24h. Product was a white lose powder.

Samples were weighted and stored at -20ºC until further analyses.

6.2.1.2.   Synthesis of MPs-HA loaded with Curcumin

To be able of loading curcumin, that is a completely hydrophobic compound and degradable under basic pH, into the HA-MPs it was necessary to use an additional step.

First, curcumin (5 mg) was dissolve in DCM (1 mL), then this organic solution was emulsify with 12mL of HA solution in 0.2N NaOH, stirring at 12000 rpm by 3min at 25ºC with an stirred model IKA T-25-ULTRA TURRAX.

Immediately, this o/w emulsion was loaded in a syringe and the following procedure was the same described previously, but in this case it was obtain a double emulsion system o/w/o. After freeze-drying process it was obtain a pale yellow lose powder. Samples were weighted and stored at -20ºC until further analyses.

6.2.1.3.   Synthesis of HA MPs loaded with PACurc

In this case, the procedure was easier than with curcumin because PACur conjugates are completely soluble in water and protecting curcumin from degradation under basic pH.

Therefore, PACur (52.63 mg equivalent to 5 mg Cur) was added to the solution of HA 5% wt/v in 0.2N NaOH (10 mL) and it was completely dissolved.

Following, the procedure was exactly the same that the one describe for the synthesis of MPs-HA. After freeze-drying process it was obtain a light yellow lose powder. Samples were weighted and stored at temperature -20ºC until further analyses.

6.2.1.4.   Synthesis of HA MPs loaded with Trypsin and PEG-Trypsin

In this case, the procedure was similar to PACur conjugates because both Trypsin and PEG-Trypsin conjugates are completely soluble in water and relatively stable under basic pH. Therefore, Trypsin (5mg trypsin by 500mg HA) and PEG-Trypsin (20%wt of Trypsin, 25mg of PEG-T equivalent to 5 mg Trypsin), were dissolved in their respective

solution of HA 5% wt/v in 0.2N NaOH (10mL). Following, the procedure was exactly the same that the one describe for the synthesis of MPs HA.

In both cases, after freeze-drying process it was obtain a white lose powder. Samples were weighted and stored at -20ºC until further analyses.

6.2.2. Characterization of loaded and un-loaded MPs systems

6.2.2.1. Morphology by SEM

The particles surface was analyzed with Scanning Electron Microscopy (SEM) using an equipment JEOL model JSM-6300 (JEOL Ltd., Tokyo, Japan). Samples were previously sputtered-coated with gold under vacuum. Analyses were carried out at 15kV of acceleration voltage and 15mm of distance working.

6.2.2.2. Particle Size Distribution

The particles distribution and average size was measured with laser diffraction technique, using an instrument model Mastersizer 2000, Laser light scattering, based on Mie and Fraunhofer scattering analytical methodology. Data Analysis was accomplished with Malvern Software Mastersizer 2000 v.5.60.

6.2.2.3. Encapsulation Efficiency an Total Drug Loading

To be able to determine the total drug loading (TDL) in MPs-HA it was necessary to degrade them completely. With this porpoise, a known

amount of MPs were suspended in a volume of 0.01M acid chloride solution and heated at 80ºC overnight.

In case of curcumin systems, due to curcumin is hydrophobic and stable in acidic medium, ACN was added to prevent free drug precipitation and warranty that all free curcumin was dissolved in the aqueous phase. Notice that in case of PACur loaded HA-MPs, polyacetals should have been completely degraded in acid medium so curcumin would be free too. Samples of un-loaded HA-MPs and both, PACur and Cur loaded HA-MPs where processed this way. Then, solutions were analyzed and curcumin concentration was determined spectroscopically. Samples were measured at 260 nm with an UV-Vis double-beam equipment model Jasco UV-670. Samples were analyzed in quartz cuvettes with a light path 1mm.

Alternative methodology was also tried. Total drug loading (TDL) was determined dissolving completely an accurately measure amount (5 mg) of loaded MPs-HA in a solution of 0.2N NaOH (900µl) and ethanol (100 µL) to improve the solubility of free curcumin. The suspension was centrifuge at 18000 rcf in an Eppendorf centrifuge model 5804 with fix angle rotor. Supernatant was separated and diluted with PBS the curcumin concentration was determine spectroscopically. Samples were measured at 260 nm with an UV-Vis double-beam equipment model Jasco UV-670. Samples were analyzed in quartz cuvettes with a light path 1mm. Curcumin calibration curve (from 1 to 30 µg/mL) dissolve in the same condition than sample was used to do quantification calculus.

In case of trypsin systems, total degradation of MPs were also accomplished in the same conditions because trypsin is stable under acidic conditions (between pH 3 and 6.5); not only it is not denaturized but also its proteolytic activity is reduced. Quantification was performed using BCA kit with a calibration curve made with the same trypsin used in the experiments.

In all cases, the encapsulation efficiency (E.E.) in HA MPs was calculated from the actual loading with respect to the theoretical loading of drug/protein in the MPs.

6.2.3. Drug Release Kinetic studies from loaded HA-MPs

To study drug release kinetics in microparticles un-loaded and loaded HA-MPs samples were analyzed. Previously all samples were dried under vacuum at 60ºC and weighted but 24h, then suspended in a volume of 1.5 ml of PBS solutions.

In case of MPs HA unloaded, and loaded with curcumin or PACurc it was desire to study the influence of pH in the system, because PACur is susceptible to be degraded under acidic conditions, so it was expected to observe difference in the system's release kinetic under neutral and slightly acidic conditions. Therefore, they were used two different PBS 1X solution at pH7.4 and pH=6.5, respectively.

In case of Trypsin and PEG-Trypsin loaded system they were studied only at pH 7.4 because PEG-T conjugate was also stable under acidic pH, so difference in behavior would not be related with change of pH

In all cases, every suspension was tempered at 37ºC and 1 ml was taken out in different times and replaced with 1 ml of fresh solution.

Curcumin concentration in samples was determined by UV-Vis spectroscopy following similar procedure describes before for TDL. In this case, curcumin was previously dissolved in ethanol, and then dilutions in PBS pH 6.5 and 7.4 were done to prepare the calibrations curves.

In case of trypsin systems, quantification was performed using BCA kit with a calibration curve made with the same trypsin used in the experiments.

6.3.   Results

6.3.1. Synthesis of MPs and encapsulation of model drugs and Polymer-drug conjugates

The methodology proposed made possible to obtain microparticles of hyaluronic acid both un-loaded and loaded.

Following, characterization of products is presented.

6.3.2. Characterization of loaded and un-loaded MPs systems

6.3.2.1.   Curcumin systems

- Morphology by SEM

Surface analysis by SEM showed that HA MPs are spherical and not completely regular, also, they look polydisperses. Particles sizes

clearly increase when loading process is accomplished as well as polydispersity.

HA MPs un-loaded are smaller and more homogeneous, but particles surface is rough. HA MPs loaded with curcumin, show a less rough surface but broader range of sizes. Nevertheless, the smallest particles seem to be in the same order of magnitude but the main difference is reflexed in the size of bigger particles that are produced. In any case, o/w/o emulsions do not affect significantly the morphology.

HA MPs loaded with PACur were the biggest of three groups and higher polydispersity, but particles shape is uniform, spherical, and softer than un-loaded HA MPs. Amphiphilic nature of loaded compound has a clear effect on microparticles morphology, with respect at size and polydispersity, but particles have still the appropriate shape and size for the desire approach.

SEM 1500X   SEM 3500X

HA MPs

a

b

HA-MPs Curcumin

c

d

HA-MPs PACurc

e

f
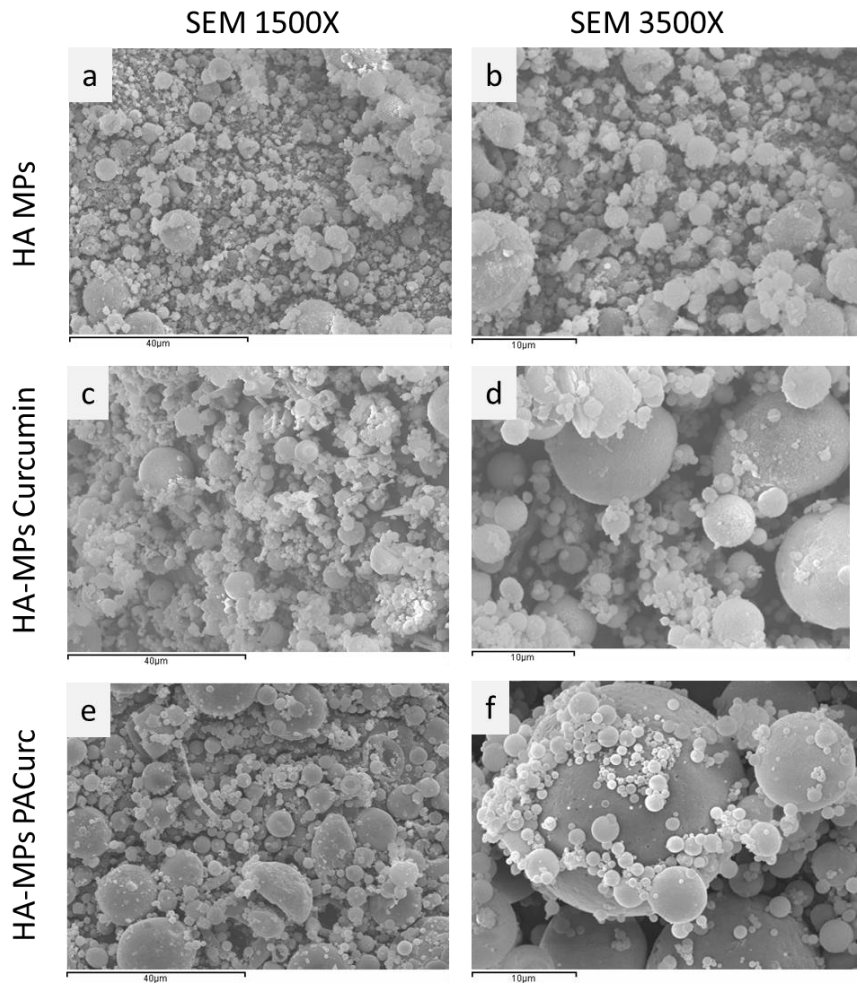
Figure 6.2 MPs surface morphology analyzed by SEM

- <u>Particle Size Distribution</u>

Particles size analyses with laser diffraction support the information provided by SEM.

HA MPs unloaded are the smallest of three groups, with average size of 6.441 µm when measure in acetone, which is a solvent where MPs are not swollen (figure 6.4 a).

A sample of the same HA MPs was suspended in water (double distilled water) and measured after 10s of sonication, and swollen effect was immediately produced as can be clearly appreciated in lower panel (b) of fig 6.4.

Particles average size increased to reach 42.518 µm; 6.6 times their original size. This behavior was expected due to HA is a hydrogel, but the fact that MPs were able to remain their structural integrity shows that cross-linking process works, making possible to keep the MPs after swollen.

Cross-linking was accomplished by DVS reaction with hydroxyl groups of HA, through an Oxa-Michael addition mechanism (figure 6.3). According to some authors, it could be expected that the reaction occurs mainly on the hydroxyl of C6 of the N-acetylglucosamine moiety of HA, because of the better accessibility of reagents to primary alcohols[149,150].

 Hydroxyl groups are negatively charged under basic condition, as is the case when HA is dissolved in NaOH 0.2N solution.
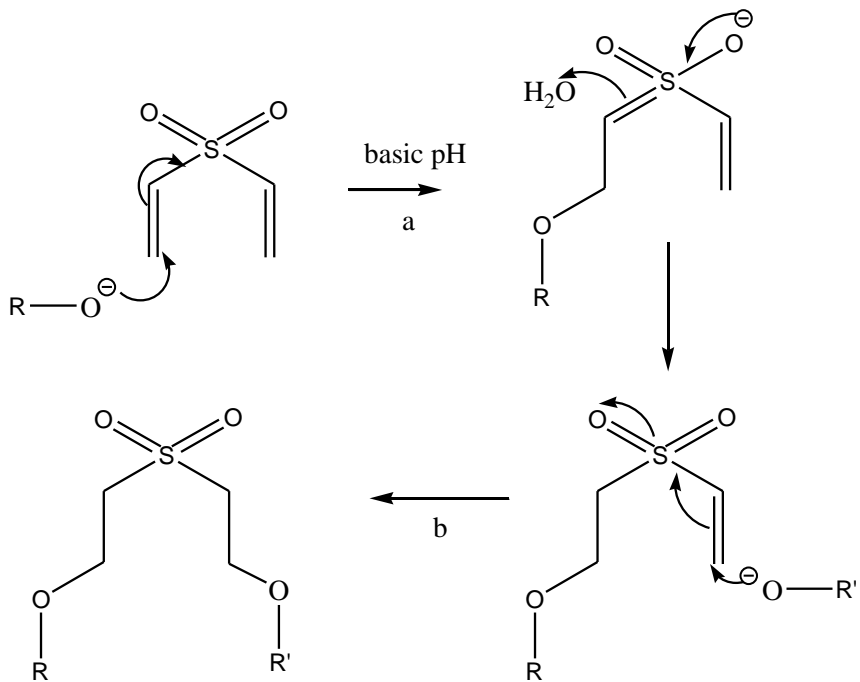
Figure 6.3. Oxa-Michael addition mechanism proposed for DVS crosslinking with HA in basic medium[23].

Then, $^-$OH performs a nucleophilic attack over the double bonds promoting electronic delocalization through -SO$_2$ functional group. Negative charge is compensated with a proton from water molecules of the solution. This way, step "a" is completed, then process stars

over again by the other double bond of DVS (step "b") in the same way as happened in step "a".
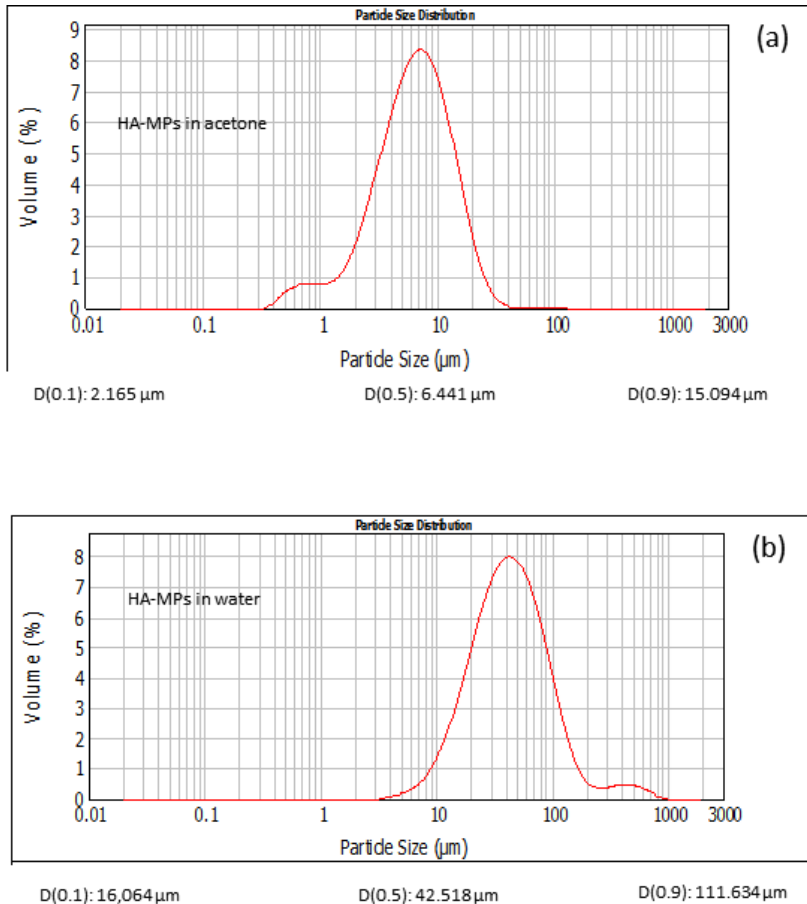
Figure 6.4 Comparison of Particle size analyses of HA MPs Systems by laser dispersion HA-MPs in acetone and water

This technique was also used to measure de size distribution of HA MPs loaded with Curcumin and PACur only with water as dispersive medium. The stability of microparticles after been sunk, swollen and

sonicated in water demonstrated that these groups of microparticles are crosslinked too (Figure 6.5).

D(0.1): 16,064 µm   D(0.5): 42.518 µm   D(0.9): 111.634 µm

D(0.1): 20.286 µm   D(0.5): 47.091 µm   D(0.9): 113.020 µm

D(0.1): 12.885 µm   D(0.5): 41,634 µm   D(0.9): 202.086 µm
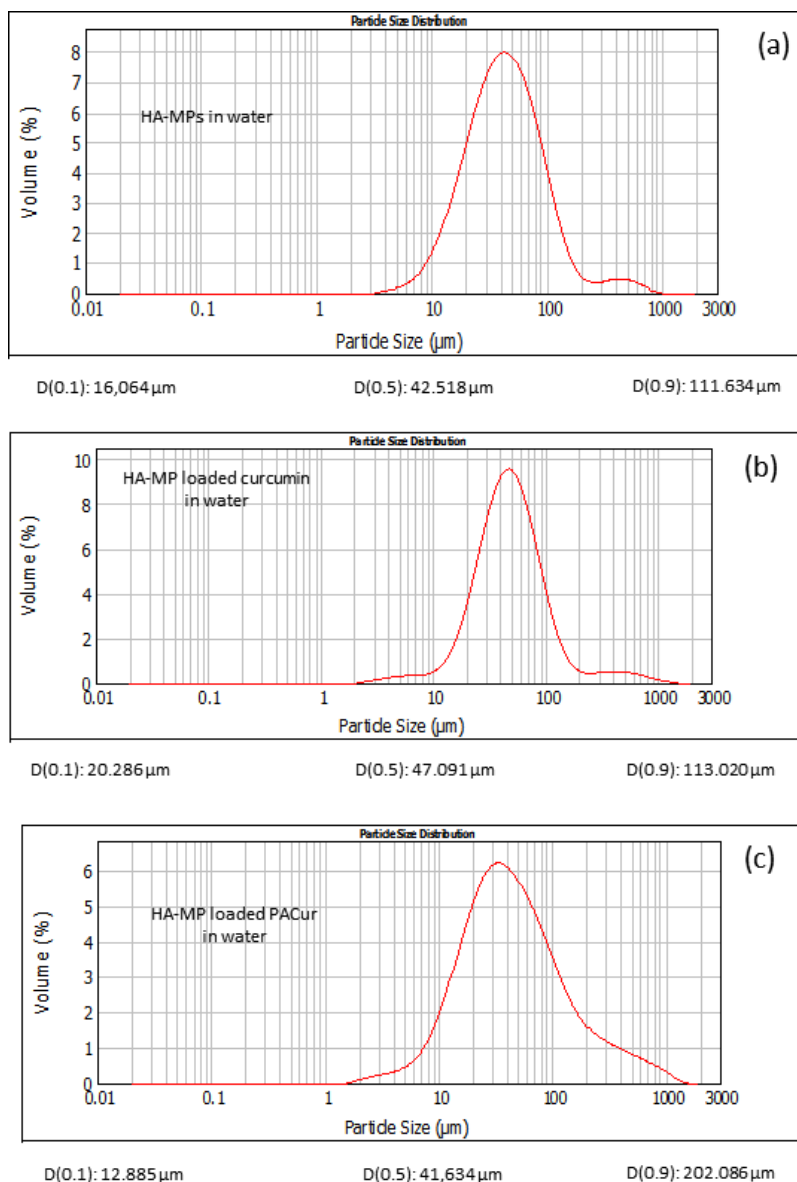
Figure 6.5 Particle size analyses of HA MPs Curcumin and PACur Systems by laser dispersion in water

- <u>Encapsulation Efficiency an Total Drug Loading</u>

Encapsulation efficiency was determined accurately following the methodology previously described, and it was possible to obtain the following values.

Table 6-1. Total drug loading and encapsulation efficiency for different systems of MPs HA loaded with curcumin and PACur.

	TDL (%)	EE (%)
MPsHA2%-Curcumin	0.23±0.04	23±4
MPsHA2%-PACur	0.44±0.03	40±3
MPsHA5%-Curcumin	1.0±0.3	82±24
MPsHA5%-PACur	1.1±0.1	90±11

- **Drug Release Kinetic studies**

Due to one of the possible application of the propose system is for local administration of therapeutic agents to contribute with wound healing, the sensitivity to pH is an important property to take in account because it is crucial for transdermal delivery systems. It is reported that the pH of the skin surface, or stratum corneum (SC), is typically in the range 5.0–6.0[151]. And it is very important to keep the homeostasis of the system during the treatment.
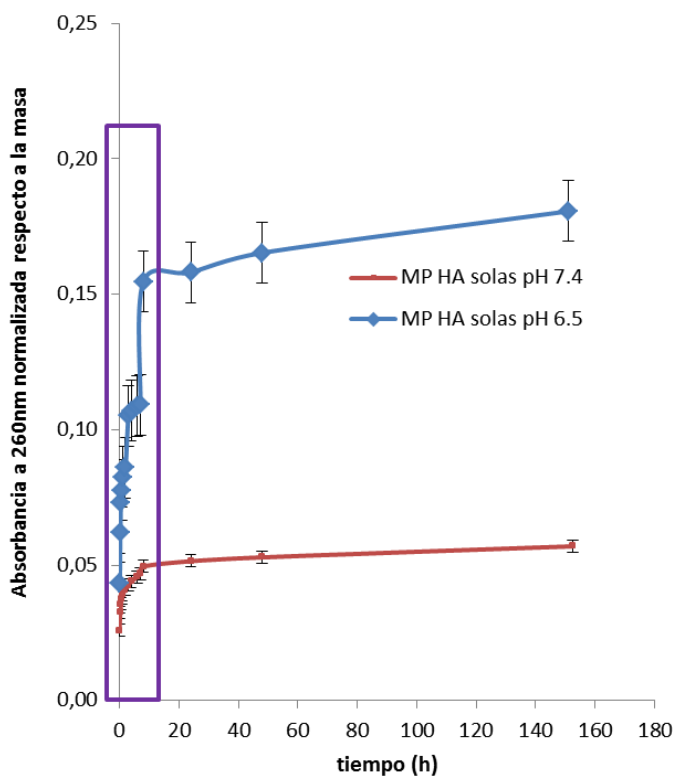
Figure 6.6 Profile of MPs-HA degradation at pH 6.5 and pH 7.4 after 180h
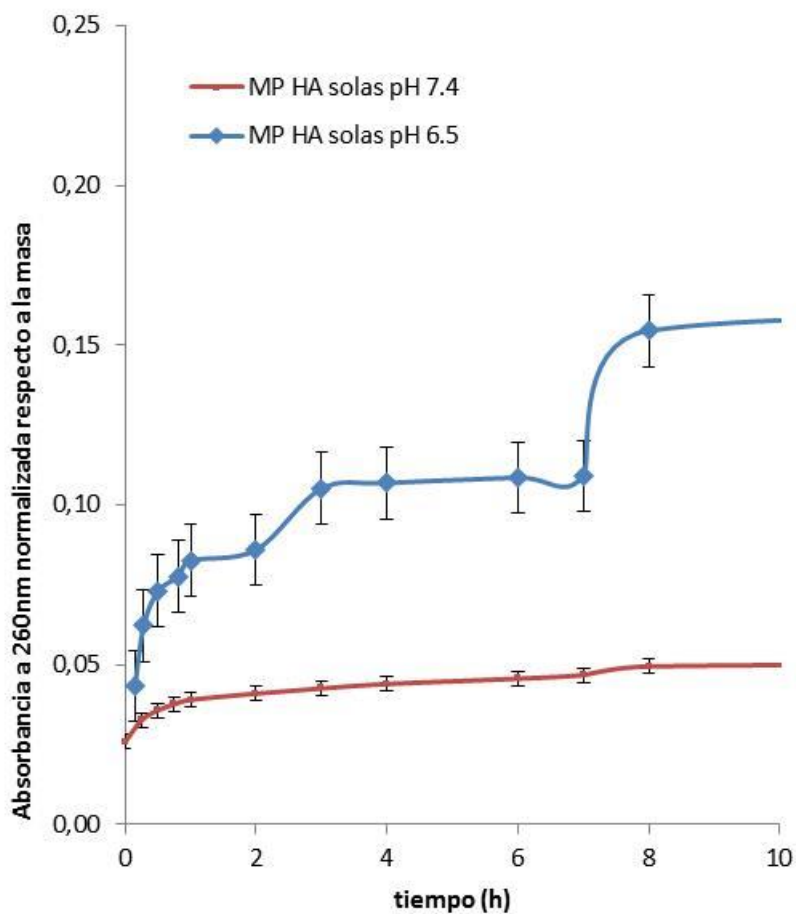
Figure 6.7 Profile of MPs-HA degradation at pH 6.5 and pH 7.4 after the first 8h.

Because of that it was decided to evaluate the behavior of MPs-HA at two different pH, which are similar to physiological conditions.

First, a qualitative evaluation of MPs-HA degradation was carried on under the same conditions that drug release was going to be studied.

According to these results, MPs-HA are degraded faster under acidic pH than under neutral pH. Possible explanation is that acidic medium promotes the hydrolysis of glycosaminoglycan polymer chain or the bond with DVS.

It has been described in literature[151] that HA is a linear polysaccharide composed of repeating units of β-1,4-linked N-acetyl-D-glucosamine and glucuronic acid. The pKa of the carboxyl groups of the HA is in the range 3–4, and these groups are ionized at pH 7. This explains why HA is capable of binding to peptides, matrix proteins, and growth factors. Besides, HA is a hydrophilic polymer that can absorb large quantities of water and can contain up to 1000 fold more water than its solid volume, due to formation of the hydrogen bonding between carboxyl, and N-acetyl groups of HA with water[151].

Nevertheless, deeper analyses are required to provide a better explanation to this observation.

Taking in account this information, release experiment data were analyzed.

As shown in figure 6.8, drug release from both systems of microparticles at different pH was collected and represented. According to the profiles describes on each case, there is not a big difference on release kinetic between MPs loaded with curcumin or PACur under acidic pH, reaching the equilibrium at the same time. In the other hand, at pH 7.4 the amount of drug release is three times smaller when MPs-HA are loaded with PACur in comparison with MPs loaded with curcumin without conjugation.

It has been reported that when increasing pH levels, the carboxyl groups of the HA residue can become ionized, forming carboxylate groups (-COO⁻). The negative charge of the carboxylate leads to electrostatic repulsion, increasing the pore size in the hydrogel network. Furthermore, the negatively charged group forms a hydrated membrane, which increases water binding, leading to an ability to absorb large quantities of water[151].

In the systems that were studied in this work it seems that the swelling ratio is also related with the increase of the pH levels and in consequence with the drugs release kinetic.

When pH is slightly acidic, pH 6.5, carboxylic groups are less ionized, therefore interaction with other groups would be hydrogen bonds, making narrow the pore size in hydrogel. Besides, curcumin that is hydrophobic is going to diffuse to the outside. On the other hand, PACur is degraded under pH 6.5, then it is possible that curcumin was been released from polymer conjugated this is de reason of the similar behavior. The difference is that during the first hours, there was no burst in system loaded with PACur, contrary to the system loaded with Curcumin, because during this time PACur is starting to be degraded.
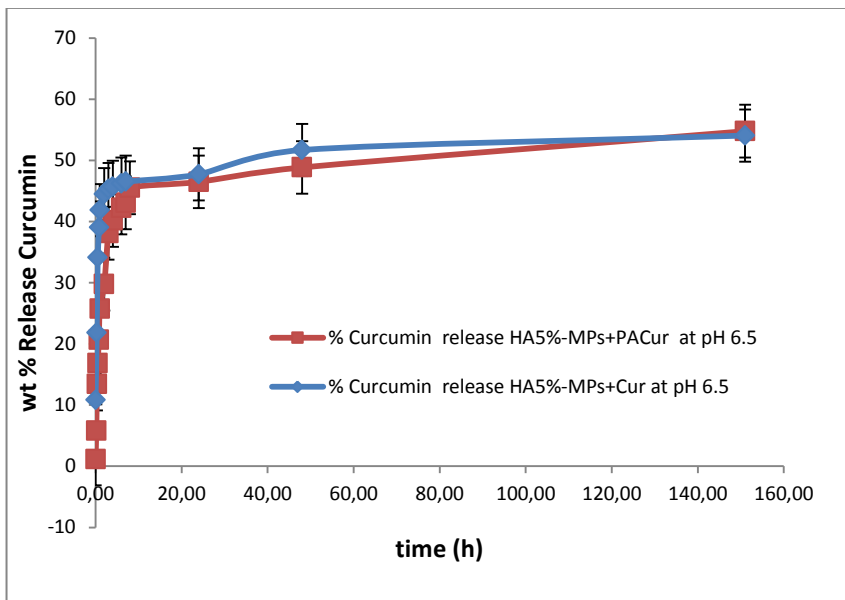
Figure 6.8 Profile % drug release from MPs-HA loaded with curcumin in comparison with MPs-HA loaded with PACur at pH 6.5
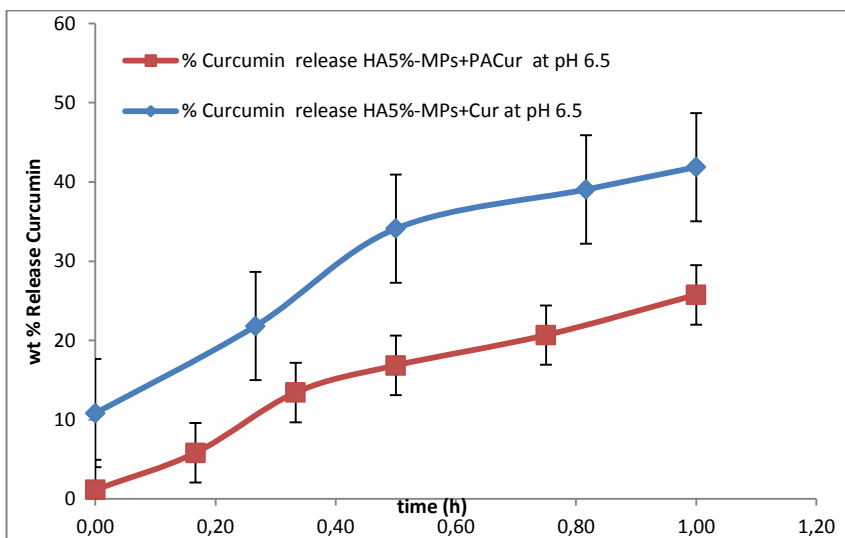
Figure 6.9 First hour of Profile % Curcumin release from MPs-HA loaded with curcumin in comparison with MPs-HA loaded with PACur at pH 6.5

Due to swelling process happened almost immediately, fickian diffusion model could be used to better understand this behavior[134]

Taking in account the shape the corresponding equation for Fick law[152] is:

$$\frac{Mt}{M\infty} = 6\left[\frac{Dt}{a^2}\right]^{1/2} - 3\frac{Dt}{a^2}$$

Equation 6-5

Where:

Mt= masa a tiempo t
M∞=masa en el equilibrio
D= coeficiente de difusión
t= tiempo
a= radio de la MP

Then:
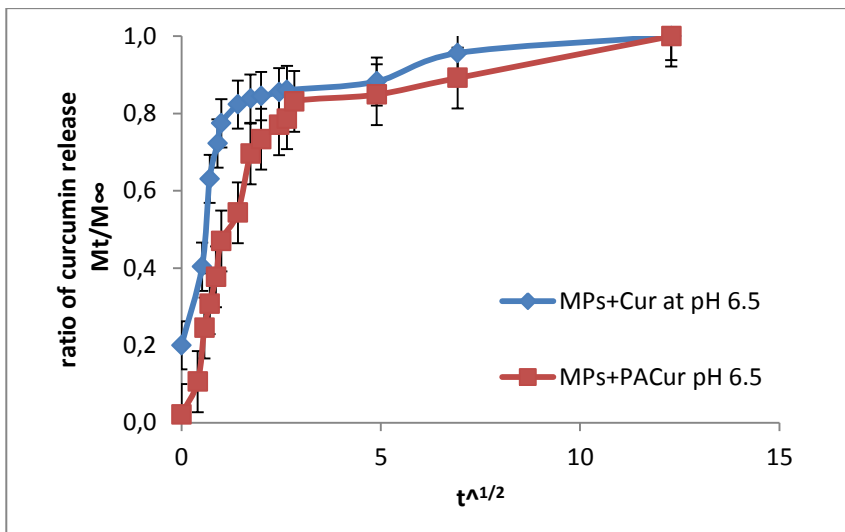
Figure 6.10 Profile of diffusion for drug release from MPs-HA loaded with curcumin in comparison with MPs-HA loaded with PACur at pH 6.5

On the other hand, when pH is 7.4, carboxylic groups are ionized and in consequence the hydrogel is going to be able to interact with more molecules of water and is going to absorb more water.

But in this case, the curcumin is going to diffuse to outside as happened at pH 6.5 because it is repelled by water at p<h 7.4 as well as pH 6.5 because it is highly hydrophobic.

Instead, PACur is not going to diffuse so fast, because at pH 7.4 PACur is not degraded so fast as it happened at pH 6.5. Besides, PACur is hydrophilic, possibly interacts with ionic groups as well as with the polar chain or glicosaminoglycans, remaining stack inside the microparticles longer time, as can be appreciated in figures 6.11 and 6.12.
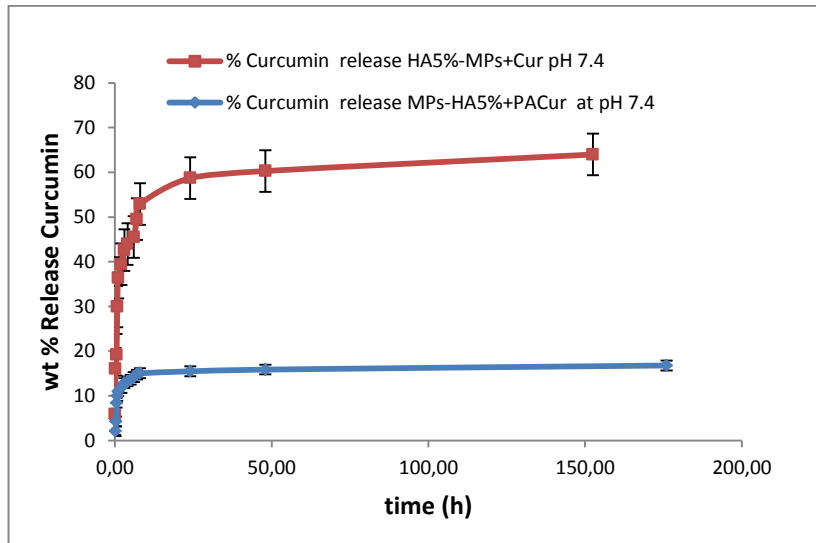
Figure 6.11 Profile % drug release from MPs-HA loaded with curcumin in comparison with MPs-HA loaded with PACur at pH 7.4
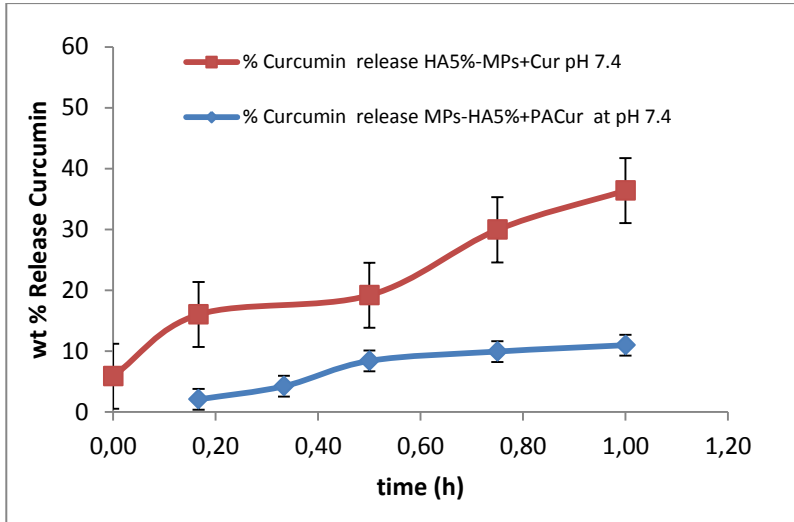
Figure 6.12 First hour % drug release from MPs-HA loaded with curcumin in comparison with MPs-HA loaded with PACur at pH 7.4

Again, it is possible to represent these data following the model of fickinan diffusion as it was done before with pH 6.5

Similar profile as expected because it is possible that curcumin was the specie release in both cases, but when it is conjugated it do not reach the 100% of release.

These pH sensitive behavior could be exploited to release a pharmaceutical agent at a specific pH in a controlled manner, that is one of the objectives of this research.
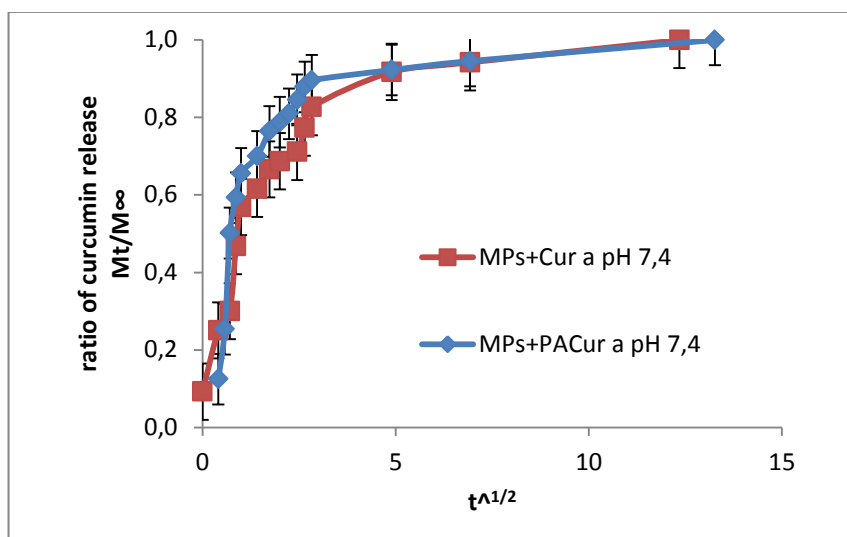
Figure 6.13 Profile of diffusion for drug release from MPs-HA loaded with curcumin in comparison with MPs-HA loaded with PACur at pH 6.5

Table 6-2 Fick diffusion coefficient for trypsin and PEG-Trypsin

	D [$\mu m^2/h$]	
	pH 6.5	pH 7.4
Curcumin	0.697	0.393
PACur	0.203	0.484

6.3.2.2. Trypsin systems

- ## Morphology by SEM

Images from SEM show clearly that MPHA loaded with trypsin are much bigger than unloaded MPsHA, MPsHA loaded with curcumin and MPsHA loaded with PACur.

Nevertheless, MPsHA loaded with PEGylated Trypsin, PEG-T, are significantly smaller than MPsHA loaded with naked Trypsin. In fact, they are almost in the same range of the other two kind of loaded MPsHA. Another interesting difference between these two systems is the polydispersity size distribution. MPsHA loaded with trypsin seem to present less polydispersity than those loaded with PEG-T
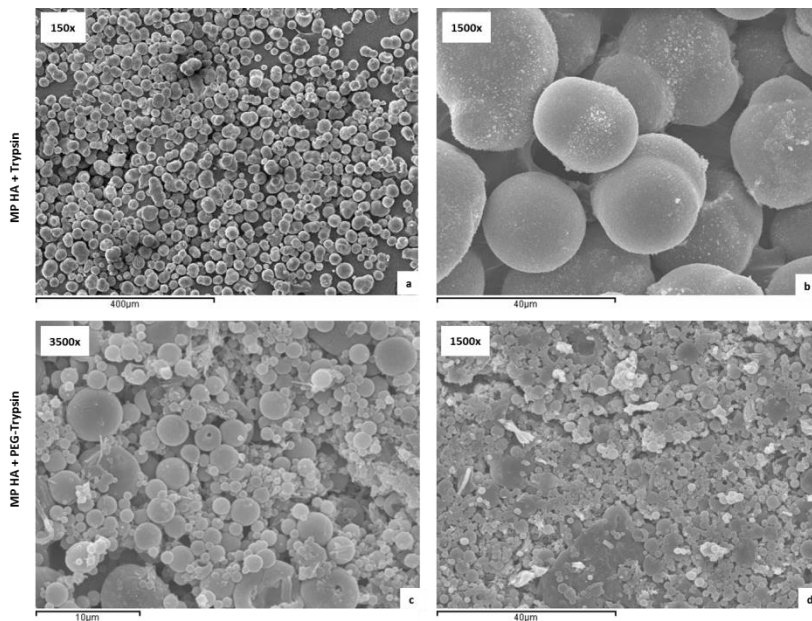
Figure 6.14 MPs surface morphology analyzed by SEM at different magnification taken at 15KV and 9 mm of wd : (a-b) MPs HA + Trypsin. (c-d) MPs HA + PEG-Trypsin

- <u>Particle Size Distribution</u>

Particles size analyses with laser diffraction technique support the information provided by SEM.

Average size of MPsHA-T is 30.6µm, measured in acetone and dispersive medium. In comparison to unloaded MPsHA analyzed in the same conditions, the system with trypsin is almost 5 times bigger than unloaded system.

In case of MPsHA loaded with PEG-T the analysis showed a bimodal distribution, where most of MPs have a particle average sizes of 4.3, even smaller than unladed MPsHA. Bigger sizes particles could be adjudicated to the presence of aggregates.
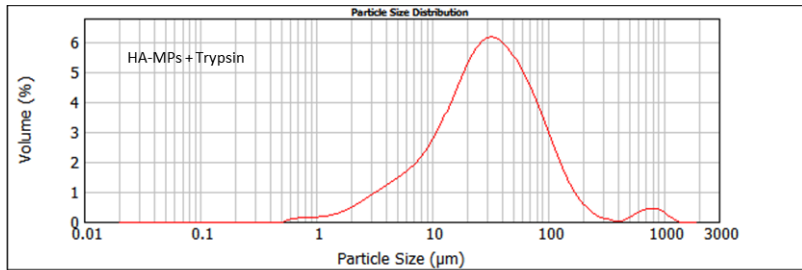
D(0.1): 6.391 µm   D(0.5): 30.591 µm   D(0.9): 103.411 µm
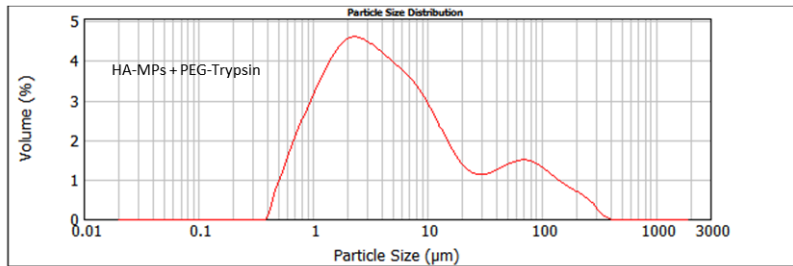
D(0.1): 1.003 µm   D(0.5): 4.285 µm   D(0.9): 66.689 µm

Figure 6.15 Particle size analyses of HA MPs Trypsin and PEG-Trypsin Systems by laser dispersion in acetone

- <u>Encapsulation Efficiency an Total Drug Loading</u>

Encapsulation efficiency was properly determined and obtain values are shown in the next table

Table 6-3   Total drug loading and encapsulation efficiency for different systems of MPs HA loaded with curcumin and PACur.

	TDL (%)	EE (%)
MPs HA + Trypsin	1.0±0.3	99±1
MPs HA + PEG-Trypsin	1.0±0.3	97±1

- <u>Drug Release Kinetic studies</u>

Again, drug release seems to follow the same kinetic mechanism during the first hour, after this time, rate of release becomes slower for PEG-T system, and finally, MPs loaded with trypsin were able to release almost 80% of total loading while MPs loaded with PEG-T only release almost 40% of total loading in the same time.
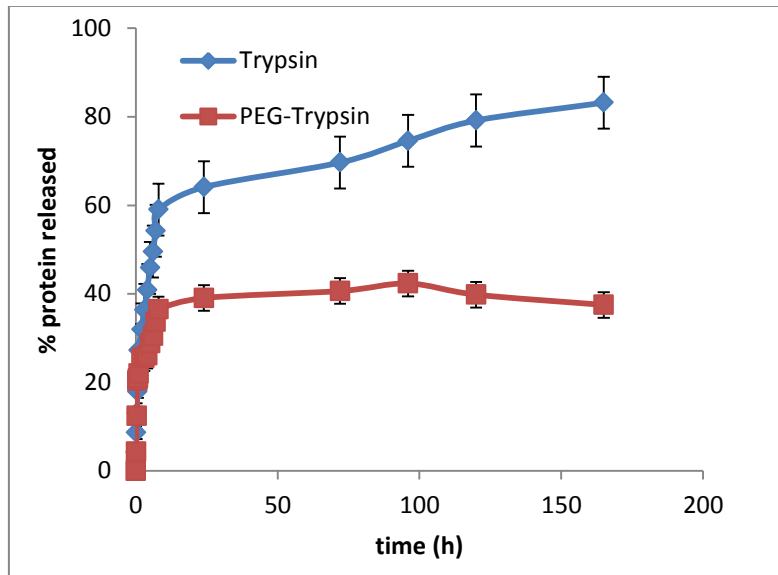
Figure 6.16 Release Kinetic of Trypsin and PEG-Trypsin from MPs HA in PBS 1x pH7.4 at 37º
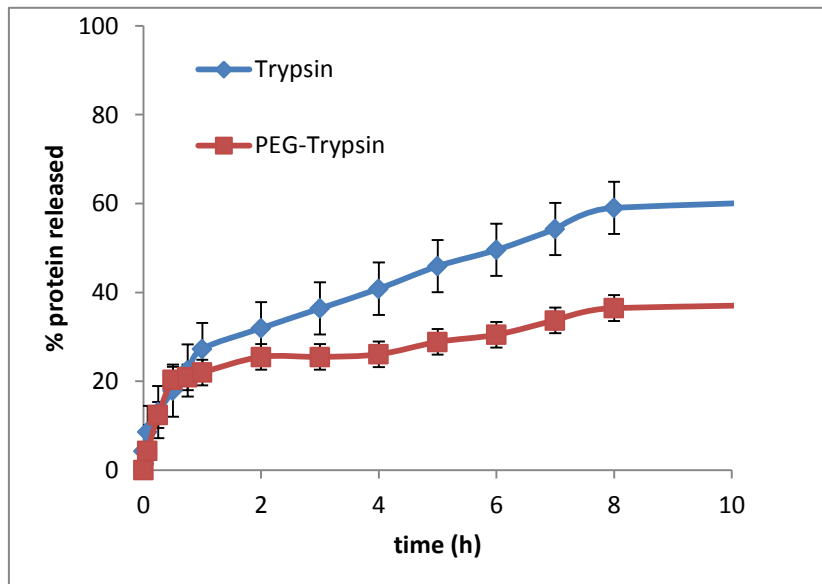
Figure 6.17 Release Kinetic of Trypsin and PEG-Trypsin from MPs HA in PBS 1x pH7.4 at 37º
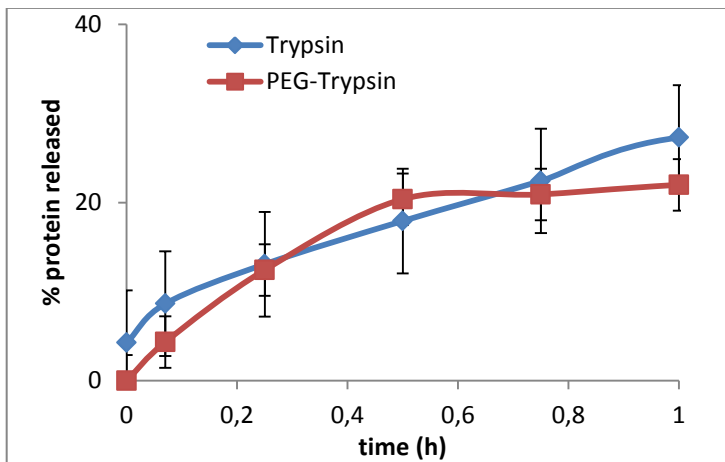
Figure 6.18 Release Kinetic of Trypsin and PEG-Trypsin from MPs HA in PBS 1x pH7.4 at 37º

Table 6-4 Fick diffusion coefficient for trypsin and PEG-Trypsin

	D [$\mu m^2/h$]
Trypsin	0,071
PEG-Trypsin	0,097
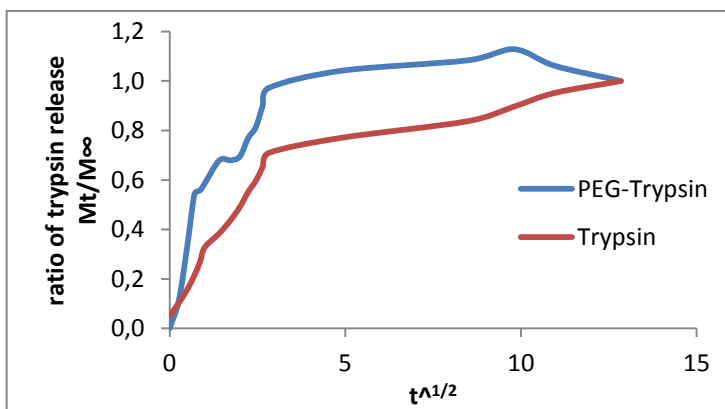
Figure 6.19 Profile of diffusion for drug release from MPs-HA loaded with curcumin in comparison with MPs-HA loaded with PACur at pH 6.5

6.4.   Discussion

The result presented previously demonstrated that stirring rate is a crucial parameter to define MPs size, as expected. But there are other parameters that also affect the morphology of the final product.

Loading process implies the addition of components which nature affects the interactions of HA molecules when final emulsion is formed. Because of that when loaded compounds are hydrophobic, it is possible than most of the molecules try to migrate to organic phase of emulsion, causing a low drug loading. Nevertheless, as probable their interaction with HA chain are weak it does not affect the size and polydispersity so much.

In the other hand, amphiphilic compounds as PACur and T-PEG are able to dissolve completely in aqueous phase, improving the drug loading. They probable have more interaction with polar groups of HA chain but not enough to interfere in MPs formation, but produce an increase in size a polydispersity of the product.

In case of trypsin, it is possible that the process condition modify the tertiary structure of the protein, or even produces the denaturing of some amount of protein added; modifying the characteristic of the emulsion, and this result in bigger MPs despite the rate stirring was the same in all the experiments

When release kinetic was studied, it was observed a fast release in all cases. This behavior was expected because HA is a hydrogel that swells immediately in aqueous medium.

It was expected than smaller molecules were released faster. Nevertheless, it was observed that under acidic pH, release kinetic was independent of the size of loaded compound. This behavior could be attributed to HA will be more restricted in shape, positive charge formed will repel each other and there is not going to be interaction between loading compound and HA MPs walls, so the compounds inside will be release and rate will depend only of swelling.

In case of neutral pH, affinity of loading compounds affect the rate of release, the molecules closer to the MPs surface will be release immediately, but those close to the middle could interact with functional groups of HA and released will be delay.

6.5.   Conclusions

Stirring rated, organic solvent used for final emulsion, as well as chemical nature and hydrophilicity of loaded compound affect the morphology of resulting microparticles.

Release kinetic of MPs-HA systems depends on pH of aqueous medium

In neutral pH interaction of loaded compounds with MPs-HA matrix defined the release kinetic of the system

7. POLYMERIC COMPOSITE SYSTEM DESIGNED TO PROMOTE A LONG LASTING, STABLE, LOCALIZED AND CONTROLLED DRUG RELEASE

7.1. Introduction

ES technique is so versatile than it can be successfully adapted to elaborate 3D-scaffolds for the healing and repair of diseased musculoskeletal tissues, that is a very complex matrix rely on many signaling pathways, involving numerous growth factors and their receptors. One of the great challenges in this field, according to Tao Jiang et al, is to mimic closely the hierarchical architecture and properties of the extracellular matrices (ECM) of the native tissues [38]

However, not always cell adhesion is a property desirable in some application. This is the case of the work published by Arnal-Pastor[64] and colleagues. They accomplished to elaborate electrospun adherent–antiadherent bilayer membranes based on cross-linked hyaluronic acid for advanced tissue engineering applications where was sought to transplant cells on a tissue surface and keep them protected from the environment. To be more specific, the concept was to obtain a patch to prevent post-surgical adherences, which are a major issue in many surgeries. *In vitro* assays with L929 cell line of mouse fibroblasts shows very promising results. Their materials resulted to be not cytotoxic. Furthermore, the PLLA nanofiber face was cell friendly and promotes cell attachment and spreading therefore it could be used as a cell supply vehicle, while the HA face hindered cell

adhesion and thus might prevent undesired adherences. Co-axial electrospinning technique was used in this case.

Likewise, during the last years several studies have been published that supports the fact that electrospun fibers can be associated with angiogenic and/or vasculogenic factors, epidermal factors and molecules with anti-inflammatory and antimicrobial properties to favor and enhance skin regeneration[19,21,38,58,59,65–69]. Taking into account the wide range of opportunities, we decided to explore the possibilities of composites material which combine ES with encapsulation of therapeutic agents directly into de fibers or inside a vehicle such as microparticles to promote tissue regeneration/repair.

Several recent studies have focus their attention on the encapsulation of curcumin into nanofibers of PLLA or blend of other polymers with PLLA [61,62,74,153], due to the multiples therapeutic applications of this compound, since carcinoma treatment to neurodegeneration and cutaneous wound healing. For this reason it was consider appropriated the use of this molecule as model drug for the present study.

Variations of nanofibrous films made by electrospinning have also been study as improved alternative biomaterials. For example, Ionescu et al.[73] in 2010 designed a fabrication technique to entrap drug-delivering microspheres within nanofibrous scaffolds to obtain an anisotropic nanofiber/microsphere composite with controlled release of biomolecules to promote musculoskeletal tissue regeneration. Their results showed that microspheres ranging from 10 ~ 20 microns in

diameter could be electrospun in a dose-dependent manner to form nanofibrous composites. In this case, the release profiles of the composite structures were similar to free microspheres, with an initial burst release followed by a sustained release of the model molecules over 4 weeks.

Taking in account all this interesting experiences, it was decided to embrace the challenge to propose a n alternative methodology for the fabrication of a novel composite material based in these previous technologies with the objective to obtain a new biomaterial which work as platform for control and localized delivery of nanodrugs like polymer conjugates, with the porpoise to promote tissue regeneration, for example, with application in wound healing among other possible therapeutic targets.

7.2. Methodology

7.2.1. Synthesis of Poly(L-lactic) acid membranes by electrospinning and encapsulation of model drugs and polymer conjugates

Ultra-thin nanofibers microporous membranes were obtained by the electrospinning technique.

The objective in this part of the work was the production of two different kinds of materials. First, PLLA random nonwoven fibers membranes, loaded with a model drug, which were describe with the name of "simple membranes" for practical reasons in this research. Second, PLLA nonwoven fibers membranes with micro particles inserted among or inside the fibers also loaded with a model drug. The resulting material was designated in this work with the name of "composite membranes".

The electrospinning process was carried out using a device composed by: a) a syringe pump, b) a syringe of 12mL of volume capacity (14.72 mm of inner diameter), c) with a metallic tip, which was a flat end needle of 25G and 0,5x16mm (electrode), d) a metallic sheet covered with aluminum foil (counter-electrode) to collect the fibers, and e) a high voltage source power, to generate the electric field. The whole setup was located in a fume hood previously prepared to avoid undesired electric discharges.

The parameter optimized to obtain PLLA random nonwoven fibers with nanometric diameters were: a) PLLA solution concentration, b)

the voltage applied, c) distance between the needle tip and the collector, and d) feeding rate.
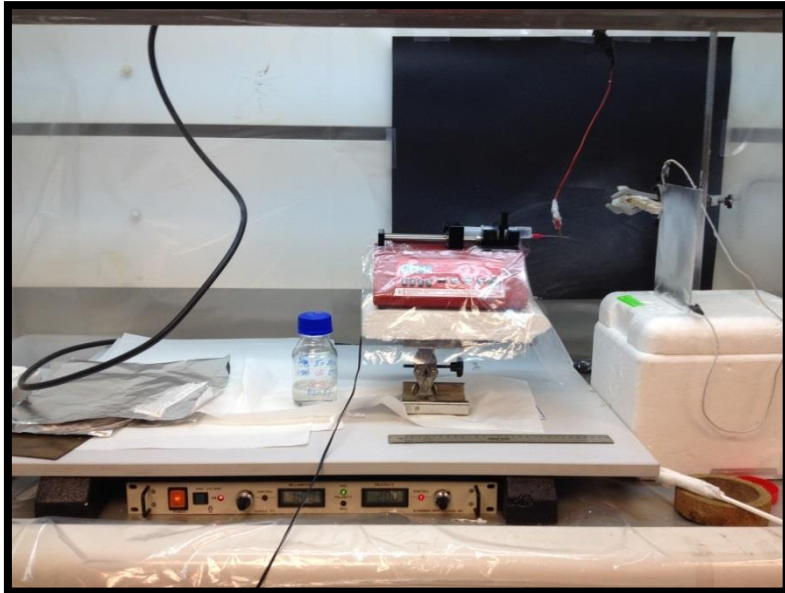
Figure 7.1. Picture of Electrospinning device used to produce the simple and composite membranes

The procedure was accomplished at room temperature (25 to 26 ºC). The needle tip was in perpendicular position with respect to the collector sheet; this is called a perpendicular spinning configuration.

PLLA solution concentration was from 3 to 9 wt%, using dichloromethane (DCM) as solvent.

The applied voltages were: 17, 20, and 27 kV, driven by a high voltage power supplied.

 Fibers were collected on an electrically grounded aluminum foil, place at 15 – 20 cm from the needle tip.

Feeding rate were 0.01mL/min, 0.02mL/min, 0.1mL/min, 1mL/min

The process was carried out until the required thickness of the fibrous mats (scaffold) was reached (from 5min to 1h).

Samples were previously observed with optic microscope as regular control of the procedure and finally analyzed by scanning electron microscopy (SEM).

Fist the procedure was used to produce membranes of PLLA alone. When optimal working conditions were fixed for this material, these were used as initial conditions to produce materials loaded with drugs and polymer conjugates. This membrane made of PLLA, was the first in the family of simple membranes (since now named ES01) and it was used as reference to compare the properties of the others simple and composite membranes.

Model drug used for these experiments was curcumin, and PACur was the polymer conjugate. It was desired to obtain membranes with final drug loading of 1wt% of Curcumin.

Therefore to obtain the simple membrane of PLLA loaded with curcumin (named as ES05 from this point in this work), it was dissolved 0.05g of Curcumin and 5.00g of PLLA in 100mL of DCM.

To obtain the simple membrane of PLLA loaded with the polymer conjugated with curcumin, PACur, it was dissolved 0.53g of PACur (9.5 wt% of Curcumin) and 5.00g of PLLA in 100mL of DCM. This simple membrane is going to be named as ES04 since this moment for this work.

Both, curcumin and PACur, are completely soluble in DCM, therefore, to obtain the starting solution for electrospinning experiments, an accurately weighted amount of Curcumin or PACur was added to the PLLA solution with the selected concentration (12 mL, in DCM).

Summarizing, three different materials, called simple membranes type, were produce:

ES01: random nonwoven fiber membranes of PLLA

ES04: random nonwoven fiber membranes of PLLA loaded with PACur

ES05: random nonwoven fiber membranes of PLLA loaded with Curcumin

7.2.2. Synthesis of polymeric composite systems: thin membranes loaded with microparticles.

The methodology propoused by Hongxu Qi and co-workers was used as reference[71] to develop our own procedure.

The fist material produce was the composite membranes of PLLA with unloaded HA-MPs. Optimal working conditions found for this system were used as starting condition to produce composite membranes with HA-MPs loaded with curcumin or PACur.

Preparation of Mixture for electrospinning:

Two different strategies were followed to obtain the mixture necessary to manufacture the composite system.

a) First method: Mixture in Two steps

Step 1: Synthesis of microparticles in reverse emulsion.

First step was the production of HA micro particles (HA-MPs) following the protocol describe in chapter 5.

HA-MPs were poured in acetone and washed. Resulting microparticles were stored in a 50 mL plastic conical-bottomed centrifuge tube suspended in 20mL of acetone in order to be dehydrated and preserve their structure until mixing with PLLA.

Step 2: Inclusion of HA-MPs into the PLLA fibers by electrospinning.

Second step was the production of membranes made of PLLA fibers with micro particles included in the mat.

With this porpoise, HA-MPs (0.060 g) obtain in the first step were separated from acetone by centrifugation and decantation. Remaining solid was carefully mixed with a PLLA solution in DCM (12 mL, 5 wt.%). Mixture was stirred with a magnetic stirrer at 300rpm by 5 min and loaded in a syringe with 10 mL volume capacity, ready to by electrospun.

b)   Second method: Mixture in One step of production

In this case the procedure started also with the formation of HA-MPs, following the same procedure described in chapter 5 but without microparticles precipitation.   After 1h from DVS addition, PLLA pellets (5g, to achieve a final concentration of 5 wt %) were incorporated to the emulsion and dissolved in the organic phase (100 mL, DCM). Subsequently, the electrospinning protocol was carried out.

Inclusion of HA-MPs into the PLLA fibers by electrospinning and
Membrane production

The electrospinning process was carried out at RT in a diagonal and perpendicular spinning configuration using a different needles (25G 0.5x16mm, G21 0.8x25mm and G18 1.2x40mm) flat end needle. The applied voltages were 15KV, 17, 20, 25 and 27KV, driven by a high

voltage power supplied. Fibers were collected on an electrically grounded aluminum foil place at 15 or 20cm from the needle tip. The process was carried out until the required thickness of the fibrous mats (scaffold) was reached. Samples were analyzed by optic microscope and scanning electron microscopy (SEM).

Summarizing, three different materials, called composite membranes type, were produce:

ES02: random nonwoven fiber membranes of PLLA with MPs-HA unloaded

ES03: random nonwoven fiber membranes of PLLA with MPs-HA loaded with PACur

ES06: random nonwoven fiber membranes of PLLA with MPs-HA loaded with Curcumin

a) Method 1 step

HA-MP

PLLA
(fiber forming
material)

b)Method 2 steps

Core material

HA, AOT, 1-Hp,
DVS, CH_2Cl_2

1. Emulsification

2. Dissolution

Pump

Jet ejection

Taylor cone

Solvent rapid
evaporation

Receptor

High voltage generator   V

4. Harvesting

3. Electrospinning
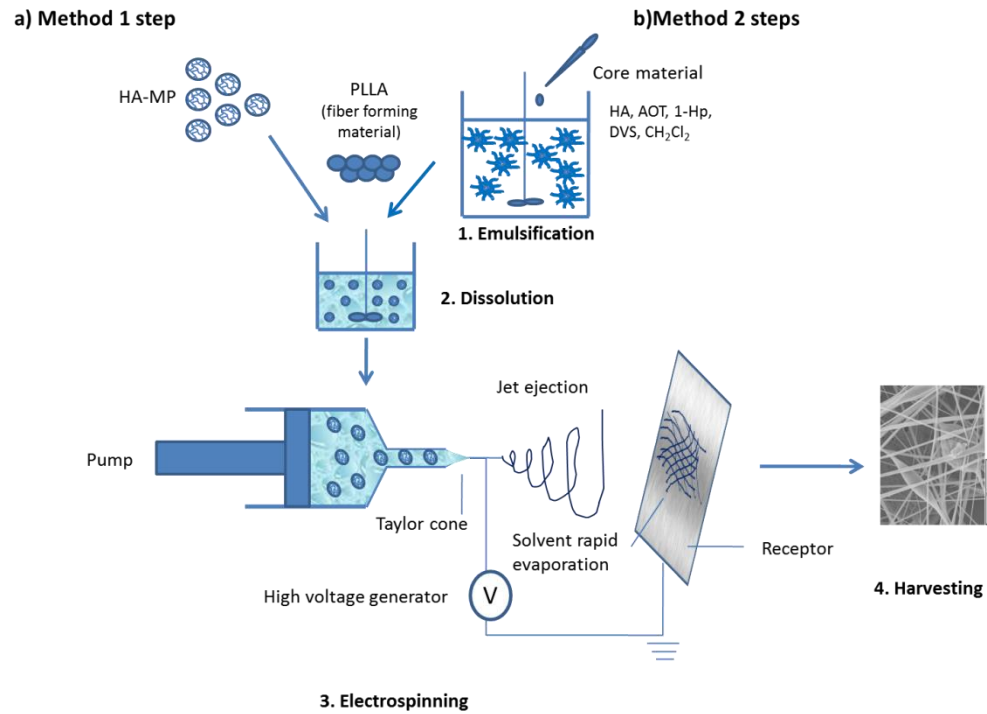
Figure 7.2. Sketch of composite membrane production procedure

7.2.3. Characterization of Poly(L-lactic) acid membranes and composite systems

7.2.3.1. Characterization of membranes morphology by SEM

The membranes surfaces were analyzed with Scanning Electron Microscopy (SEM) using an equipment JEOL model JSM-6300 (JEOL Ltd., Tokio, Japan). Samples were previously sputted-coated with gold under vacuum. Analyses were carried out at 15kV of acceleration voltage and 15mm of distance working (wd).

7.2.3.2. Analysis of membrane thermal properties and composition by TGA and DSC

Thermogravimetric analyses (TGA) were performed to determine the composition of all membranes (simple and composites) and compared this results those obtain by spectroscopic technique. The equipment used was a METTLER-TOLEDO model TGA/SDTA 851 operated through the software provide with the device STARe. Samples were weighted in platinum crucibles and scanned from 30ºC to 800ºC at 10ºC/min under N_2 flow of 20 mL/min.

Differential scanning calorimetry (DSC, model 823e (Mettler-Toledo Inc., Columbus, OH, USA) was used to measure the effect of the emulsification and cross-linking process on the thermal properties of empty and drug-loaded microparticles. Approximately 3 mg samples were heated in a pierced aluminum pan under nitrogen atmosphere, in a range of temperature of -20 to 300 ºC, with a heating rate of 10 ºC/min.

7.2.3.3. Study of Membranes wettability by Contact angle measurement

The wettability of simple and composite type membranes was determined by measuring the contact angle of a water drop on the surface of the samples. A Dataphysics OCA instrument was used for these analyses. Double distilled water was used for the experiments. To ensure the reproducibility of results 10 drops of water were analyzed for each material. Samples were previously dried under vacuum at 40ºC by 24h.

7.2.3.4. Study of Mechanic Tensile properties of membranes

The stretching assay of electrospun mats were performed in a stress-strain machine model Microtest SCM3000 95 (Microtest SA, Madrid, Spain). Samples were cut as rectangles of 0.5 x 1.5 cm^2 approximately. Stress rate was 0.2mm/min until fracture. Row data was process and plotted as stress (σ) vs strain (ϵ), in order to calculate the elastic moduli from the slope of the linear region of the curves. Final value is the average of at least 5 measures.

7.2.3.5. Determination of Total Drug Loading and Encapsulation Efficiency

To be able to determine the total drug loading (TDL) in membranes it was necessary to degrade them completely. With this porpoise, a known amount of material was suspended in a volume of DCM and stirred by 5min.

Then, solutions were analyzed and curcumin concentration was determined spectroscopically. Samples were measured at 260 nm with an UV-Vis double-beam equipment model Jasco UV-670. Samples were analyzed in quartz cuvettes with a light path 1mm.

Curcumin calibration curve (from 1 to 30 µg/mL) dissolve in the same condition than sample was used to do quantification calculus.

7.2.3.6. Drug Release Kinetic studies

To study drug release kinetics from membranes samples all materials were analyzed. Previously all samples were dried under vacuum at 60ºC and weighted after 24h, then suspended in 1.0 ml of PBS solutions pH 7.4.

In all cases, every suspension was tempered at 37ºC and 1 ml was taken out in different times and replaced with 1 ml of fresh solution.

Curcumin concentration in samples was determined by UV-Vis spectroscopy following similar procedure describes before for TDL.

7.2.3.7. Preliminary studies of simple and composite membranes degradation

Degradation studies were accomplished by comparison of SEM images at different times: 0, 1, 7, 28, and 90 days. Samples of each kind of material were weighted and put in a well of a P48 plate. Then, they were immersed in 1 mL of PBS solution 1X, pH 7.4 at 37ºC.

After each time the samples were remove from the well, washed with distilled water to remove the residues of salts and dried under vacuum at 40ºC by 24h.

Samples of each material were analyzed by triplicate for each time.

7.2.4. Preliminary Biologic Evaluation though *in vitro* assays

7.2.4.1. *Study of Membranes Cytotoxicity*

Cytotoxicity experiments by indirect contact were undergone. The L929 cell-line of mouse fibroblasts in its 13th passage was used for these purposes. In order to obtain the extracts, samples were immersed overnight in a Dulbecco's Modified Eagle's Medium (DMEM; high glucose (4.5 g L^{-1}) Invitrogen), supplemented with 10% fetal bovine serum (FBS; Fisher) and 1% penicillin-streptomycin (P/S; Fisher), 0.1 g of sample per ml of medium. Complete medium was used as positive control and extract of latex was employed as negative control.

In parallel, L929 fibroblasts were seeded at a density of 10^4 cells on the bottom of each well in 96-well plates with the medium described above and incubated in a humid atmosphere with 5% CO_2 at 37ºC for 24 h. Next, this culture medium was replaced by the extracts of the different samples, or of latex in the negative controls. The medium was changed by fresh medium in the positive controls.

The MTT assay was performed with an MTT-based toxicology assay kit (Sigma Aldrich, M5655) after 24 and 48 h. At each time, the medium in the wells was removed and the cells were incubated in 100 µl of a 90% DMEM and 10% MTT (1 mg/mL) mixture for 2.5 h in the dark in 5% CO_2 at 37°C. Next, the MTT solution was replaced by 120 µl of isopropanol and plates were shaken for 1 min. 100 µl of each well were transferred to a new 96-well plate to read its absorbance at 550 nm in a Victor Multilabel Counter 1420 (Perkin Elmer, Waltham, MA; USA). Three replicates of each material were tested.

7.2.4.2. Study of cellular adhesion and morphology

- Analysis of Cellular Density and morphology by Immunofluorescence

After culture, cell proliferation and distribution were observed by fluorescence (Leica DM6000) or confocal laser scanning microscopy (Olympus, FV1000). Previously, the samples were rinsed with PBS, fixed with 4% paraformaldehyde (PFA; Panreac) for 20 min at room temperature, and washed twice with PBS for 5 min. Cells were permeabilized with 0.1 vol.% Triton X-100 for 30 min at room temperature. After two rinses with DPBS, the samples were incubated with BIODIPY-FL phalloidin (Invitrogen, 1:200) for 1 h at room temperature in the dark, then washed twice with DPBS and counterstained for 5 min with 4,6-diamidino-2-phenylindole dihydrochloride (DAPI; Sigma, 1/ 5000). For microscopy observation, the slices were mounted with Fluorsave reagent (Calbiochem).

- Analysis of cell proliferation and distribution by Immunofluorescence and Scanning Electron Microscopy (SEM)

The morphology of L929 fibroblasts and ADSCs after culture on the substrates was analyzed by SEM. After 7 days of incubation, culture medium was removed and samples were rinsed with PB. Fixation of the samples was carried out with a 3% glutaraldehyde (GA; Electron Microscopy Science, 25% purity) solution in PB for 1 h, followed by a rinse with PB. Post-fixation was performed with 1% osmium tetroxide in PB, along with a smooth shaking for 1 h at room temperature, and followed by four rinses with distilled water. Then, samples were dehydrated through a series of graded ethanol (30º, 50º, 70º, 96º, and 100º) at 4ºC for 10 min each. Finally, samples were sequentially desiccated with hexamethyldisilazane (HMDS; Sigma Aldrich) at proportions of 1:2, 1:1 and 1:0 with absolute ethanol at 4ºC for 10 min. HMDS was allowed to evaporate at room temperature overnight. After sputter-coating samples with gold, they were examined in a Hitachi S-4800 SEM at 25 kV and 15 mm of working distance (wd).

7.3. Results

7.3.1. Synthesis and characterization Poly (L-lactic) acid membranes and composite systems

After a systematic evaluation of different operative conditions it was determined that the best parameters to obtain PLLA random nonwoven fibers by electrospinning were:

a) PLLA solution concentration: 5%

b) Flat end needle 25G 0.5x16mm

c) Voltage applied: 27KV

d) Distance between the needle tip and the collector: 15cm in perpendicular spinning configuration

e) Feeding rate: 0.02mL/min

With these conditions already established to produce PLLA membranes by electrospinning, it was possible to find the best operative conditions for the manufacture of PLLA membranes loaded with Curcumin and PACur.

It was found that best conditions to produce PLLA loaded with 1wt% of Curcumin are:

a) PLLA solution concentration: 5%

b) Flat end needle 25G 0.5x16mm

c) Voltage applied: 25 KV

d) Distance between the needle tip and the collector: 20cm in perpendicular spinning configuration

e) Feeding rate: 1mL/min

Same condition were appropriate for elaboration of PLLA membranes loaded with PACur (1wt% of total drug loading with respect to curmumin)

In the other hand, composite membranes resulted to present better quality (minimum amount of beats, regular distribution of MPs through the mat) under the following conditions:

a) Mixture for electrospinning formed following the "in one step" methodology.
b) Flat end needle 25G 0.5x16mm
c) PLLA solution concentration: 2.5%
d) Voltage applied: 25 KV
e) Distance between the needle tip and the collector: 20cm in perpendicular spinning configuration
f) Feeding rate: 0.1mL/min

7.3.1.1. Characterization of membranes morphology by SEM

Fibers´ size and distribution were determined analyzing the images obtained by SEM with the software ImageJ 1.50a.

With this porpoise, it was measured the diameter of 100 fibers by image on three different pictures taken by SEM with 1500X (ES01 and ES03), 3500X (ES02) 300X (ES04) 100X (ES05) or 5000X (ES06) magnification.

Likewise, in composite systems the amount and distribution of microparticles was determined following a similar procedure but measuring the diameter of at least 30 particles on three different images with 1500X (ES02 and ES06) or 300 X (ES03) magnifications. These results are represented in the following frequency histograms.
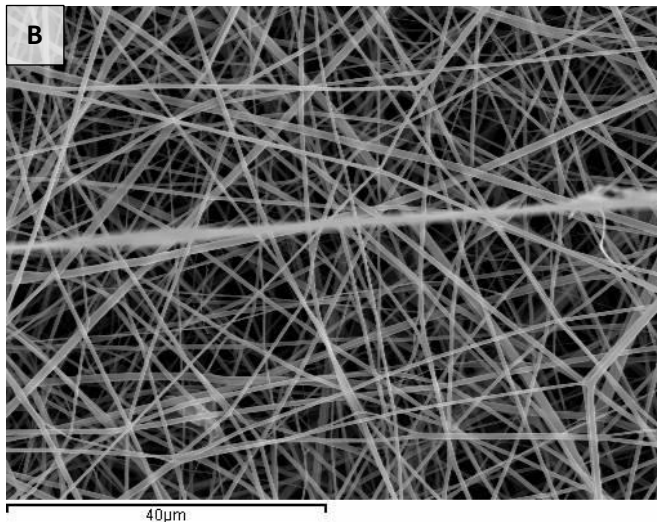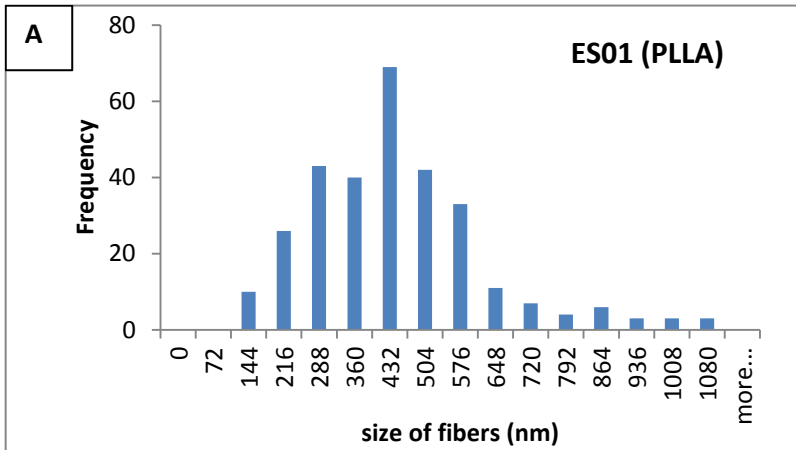
Figure 7.3. A) Histogram of frequency for fibers size in material ES01: ES simple membrane made of PLLA B) Scanning Electron Microscopy image of ES01 carried out at 1500X, 15mm wd and 15KV.
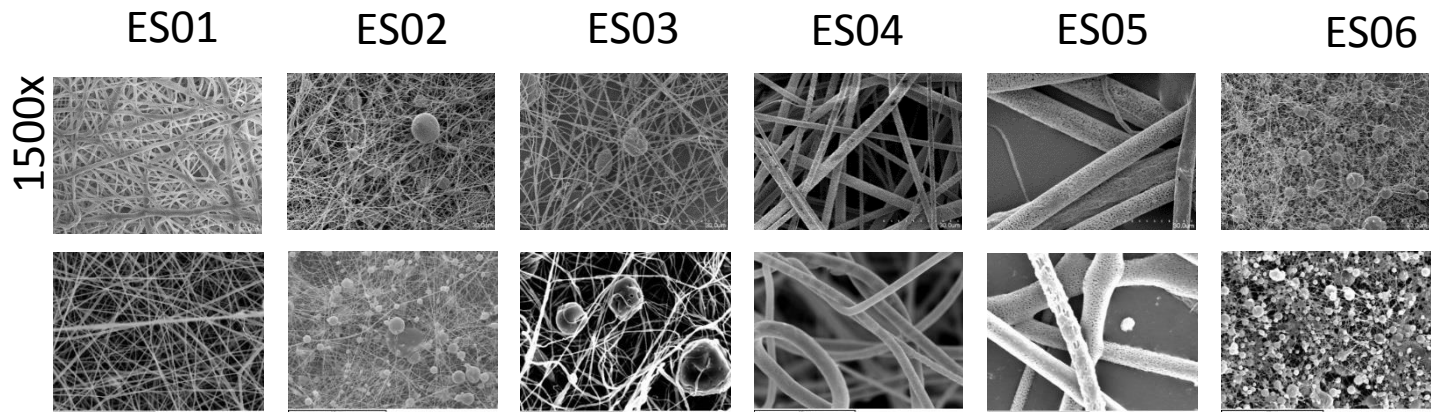
Figure 7.4. Comparison of SEM images of the different materials obtained by electrospinning, taken at 1500X magnification for analysis of fiber size distribution and microparticles distribution.

ES01: Simple membrane of PLLA; **ES02**: Composite material of PLLA fibers and HA microparticles; **ES03**: Composite material of PLLA fibers and HA microparticles loaded with PACur; **ES04:** Simple membrane of PLLA loaded with PACur; **ES05:** Simple membrane of PLLA loaded with curcumin; and **ES06:** Composite material of PLLA fibers and HA microparticles loaded with curcumin.
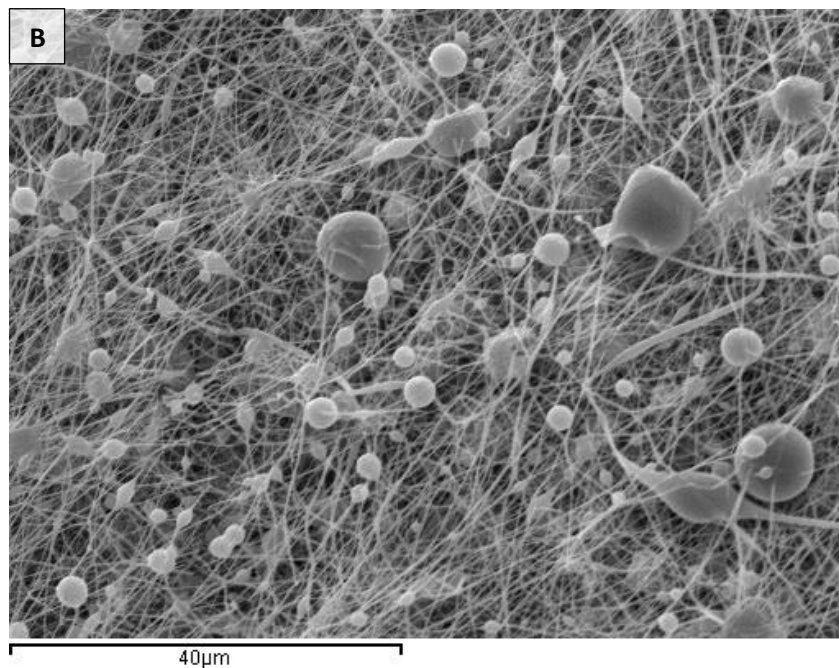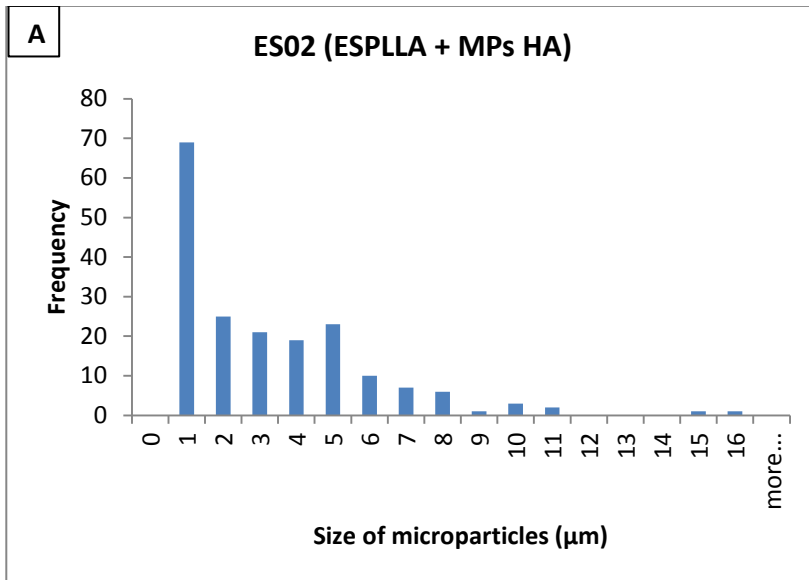
Figure 7.5. A) Histogram of frequency for microparticles size in material ES02: ES composite membrane made of PLLA fibers and MPs of HA B) Scanning Electron Microscopy image of ES02 carried out at 1500X, 15mm wd and 15KV.
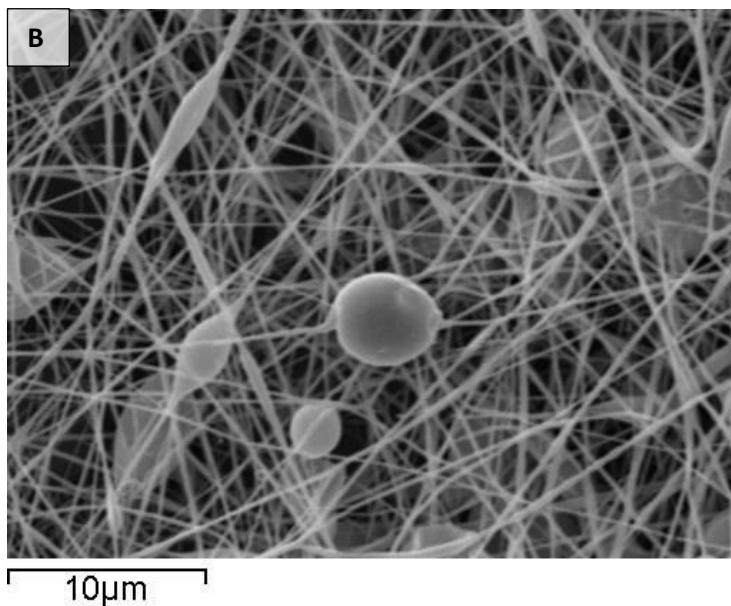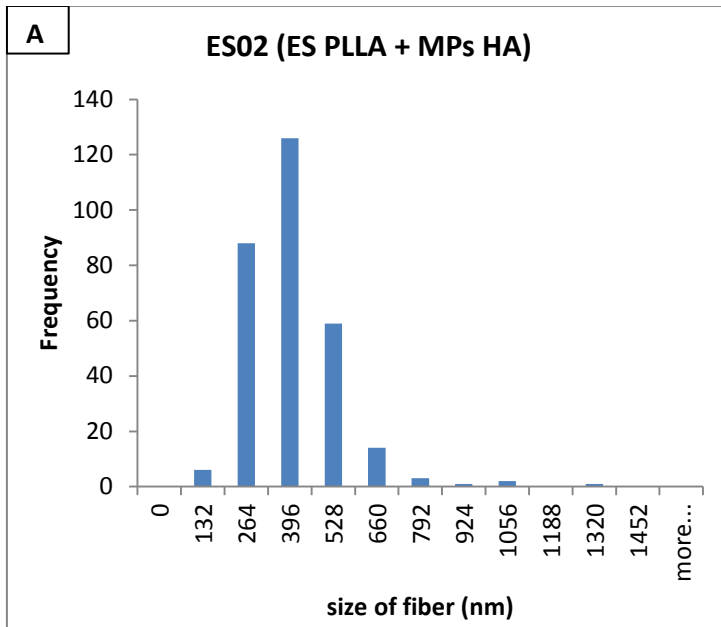
Figure 7.6. A) Histogram of frequency for fibers size in material ES02: ES composite membrane made of PLLA fibers and MPs of HA B) Scanning Electron Microscopy image of ES02 carried out at 3500X, 15mm wd and 15KV.
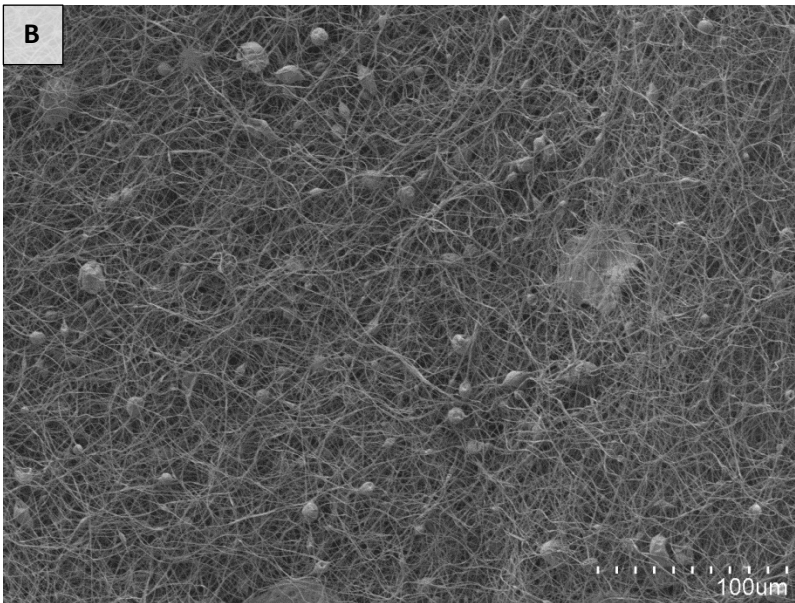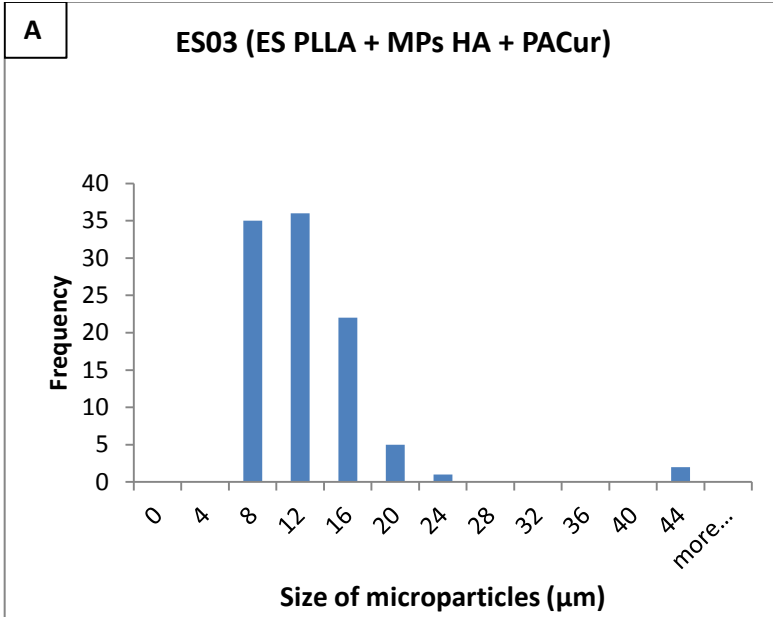
Figure 7.7. A) Histogram of frequency for microparticles size in material ES03: ES composite membrane made of PLLA fibers and MPs of HA loaded with PACur **B) Scanning Electron Microscopy image of ES03 carried out at 300X, 15mm wd and 15KV.**
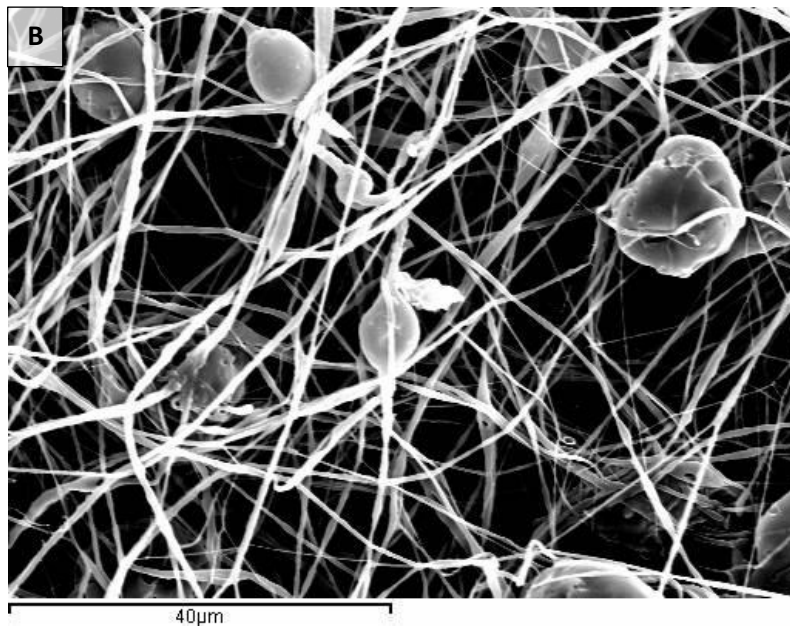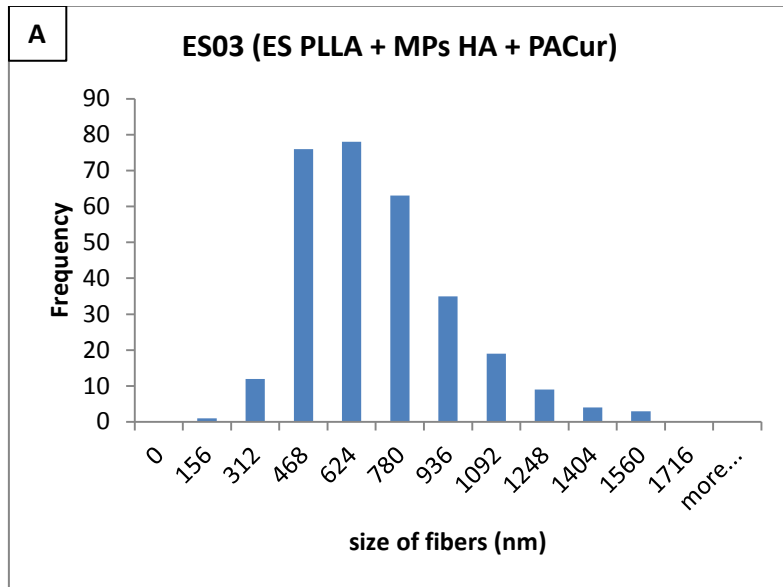
Figure 7.8. A) Histogram of frequency for fibers size in material ES03: ES composite membrane made of PLLA fibers and MPs of HA loaded with PACur B) Scanning Electron Microscopy image of ES03 carried out at 1500X, 15mm wd and 15KV.
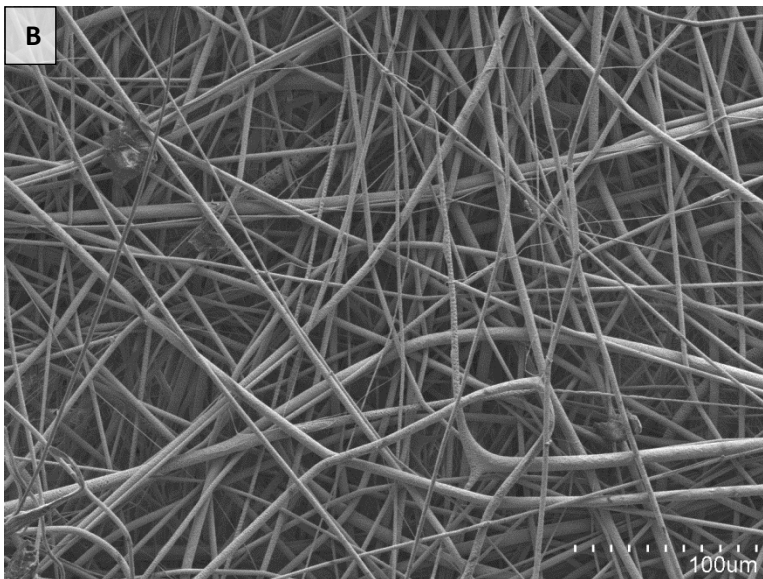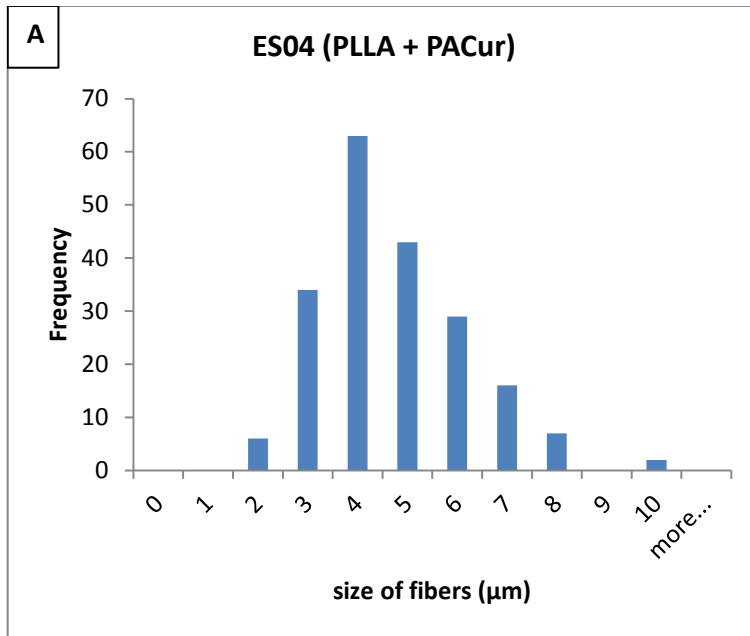
Figure 7.9. A) Histogram of frequency for fibers size in material ES04: ES simple membrane made of PLLA loaded with PACur B) Scanning Electron Microscopy image of ES04 carried out at 300X, 15mm wd and 15KV.
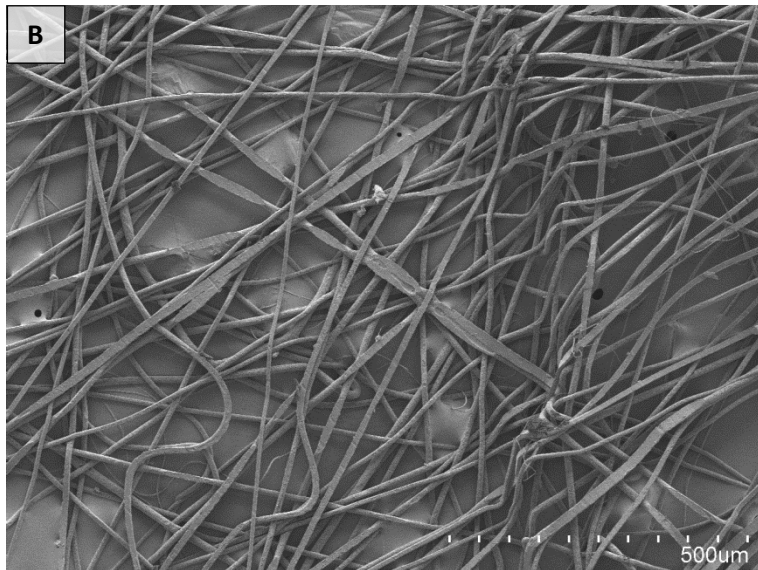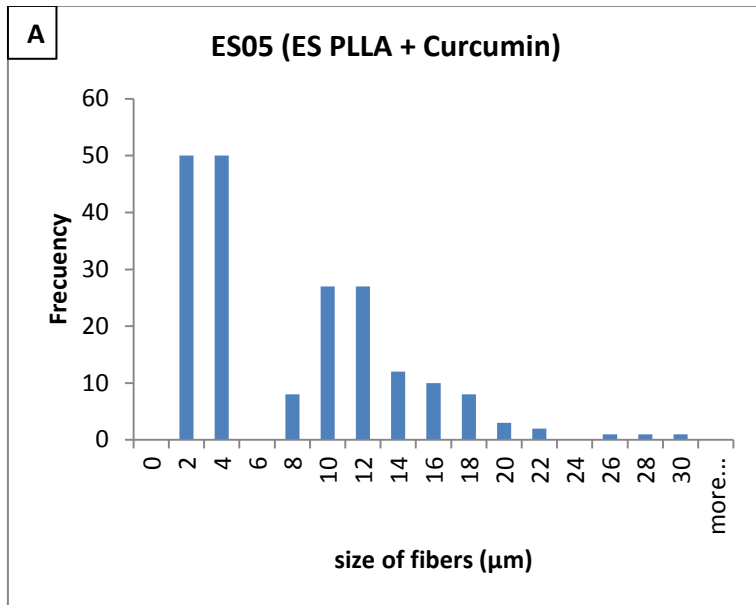
Figure 7.10. A) Histogram of frequency for fibers size in material ES05: ES simple membrane made of PLLA loaded with Curcumin B) Scanning Electron Microscopy image of ES05 carried out at 100X, 15mm wd and 15KV.
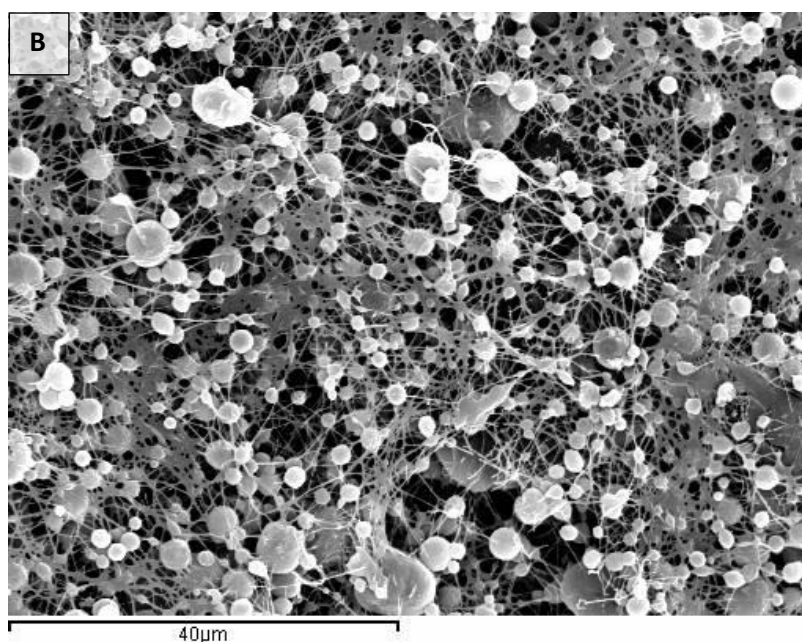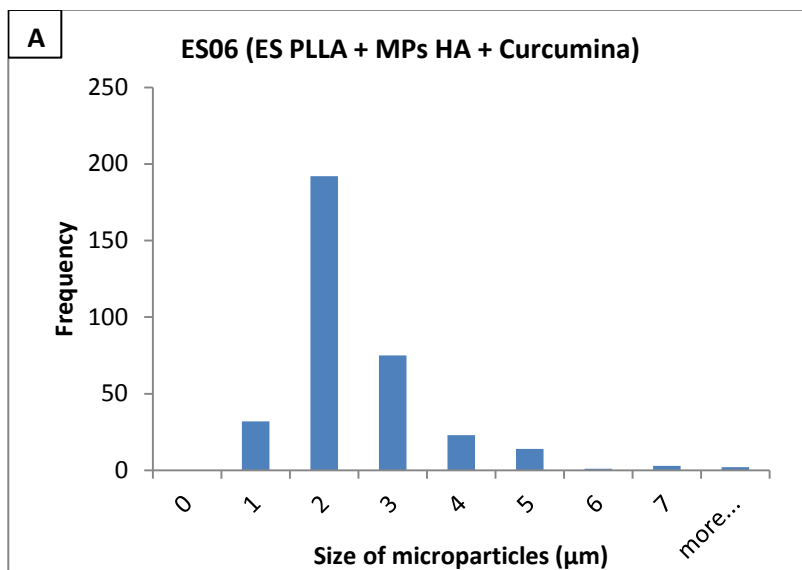
Figure 7.11. A) Histogram of frequency for microparticles size in material ES06: ES composite membrane made of PLLA fibers and MPs of HA loaded with Curcumin B) Scanning Electron Microscopy image of ES06 carried out at 1500X, 15mm wd and 15KV.
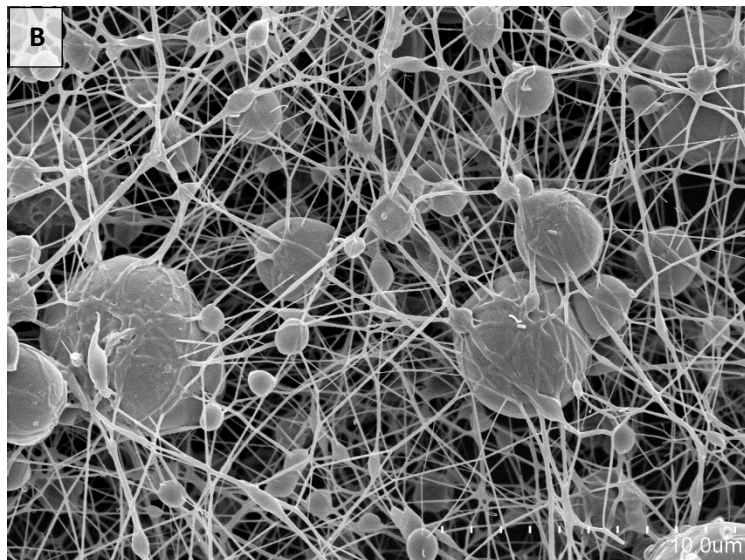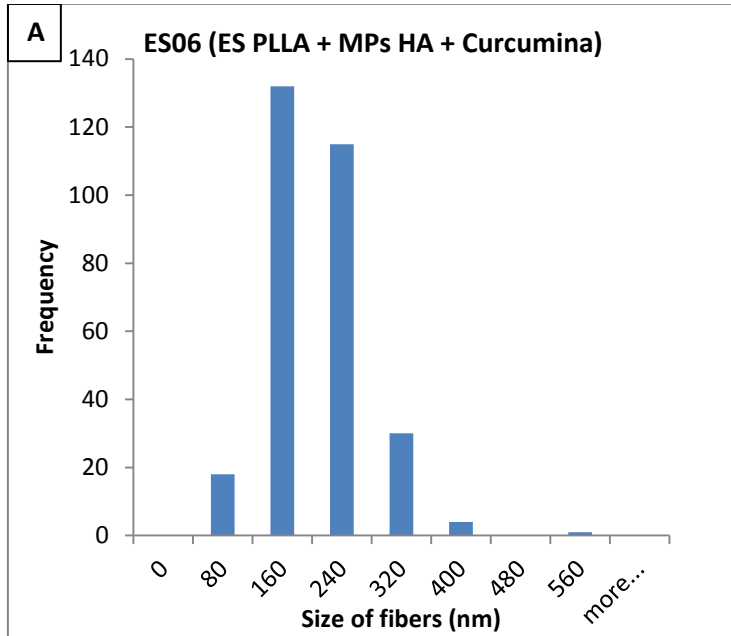
Figure 7.12. A) Histogram of frequency for fibers size in material ES06: ES composite membrane made of PLLA fibers and MPs of HA loaded with Curcumin B) Scanning Electron Microscopy image of ES06 carried out at 5000X, 15mm wd and 15KV.

7.3.1.2. Determination of membrane composition and thermal properties by TGA and DSC

Thermal stability of raw materials, model drugs and all materials produced for this part of the research was analyzed by thermogravimetric analysis (TGA).

These graphics summarized the thermal behavior of all different systems analyzed.
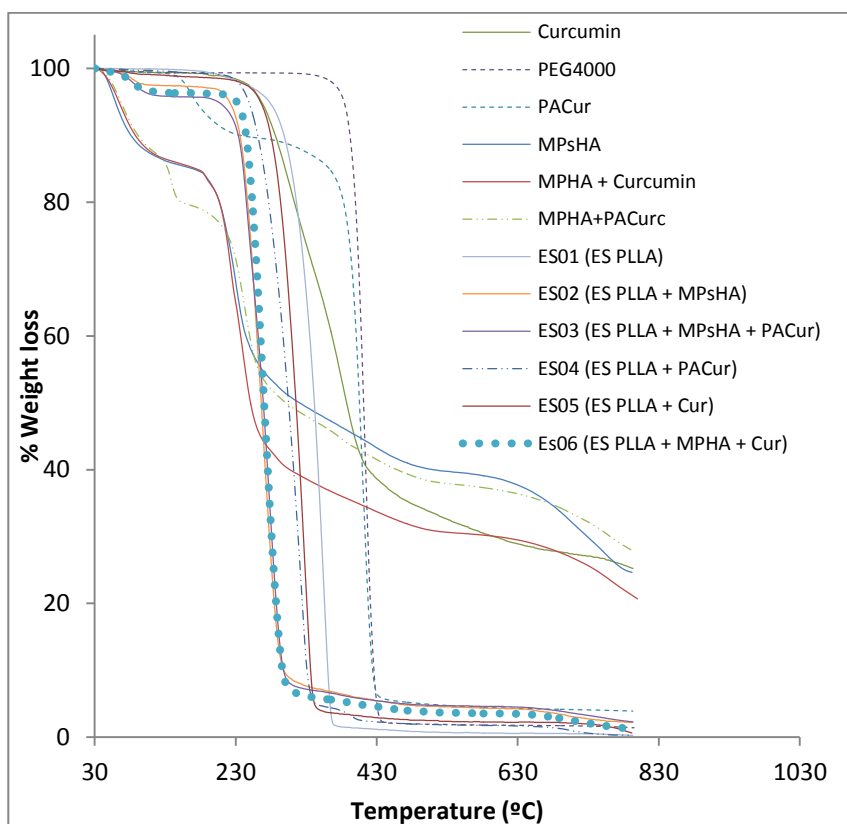
Figure 7.13 Profiles of weight loss obtained by Thermogravimetric Analyses of raw materials, simple and composite systems

As it can be seen in figure 7.13, there are significant differences between the raw material weight loss profiles and the simple or composite systems.

Following, the results for particular cases are going to by describe.
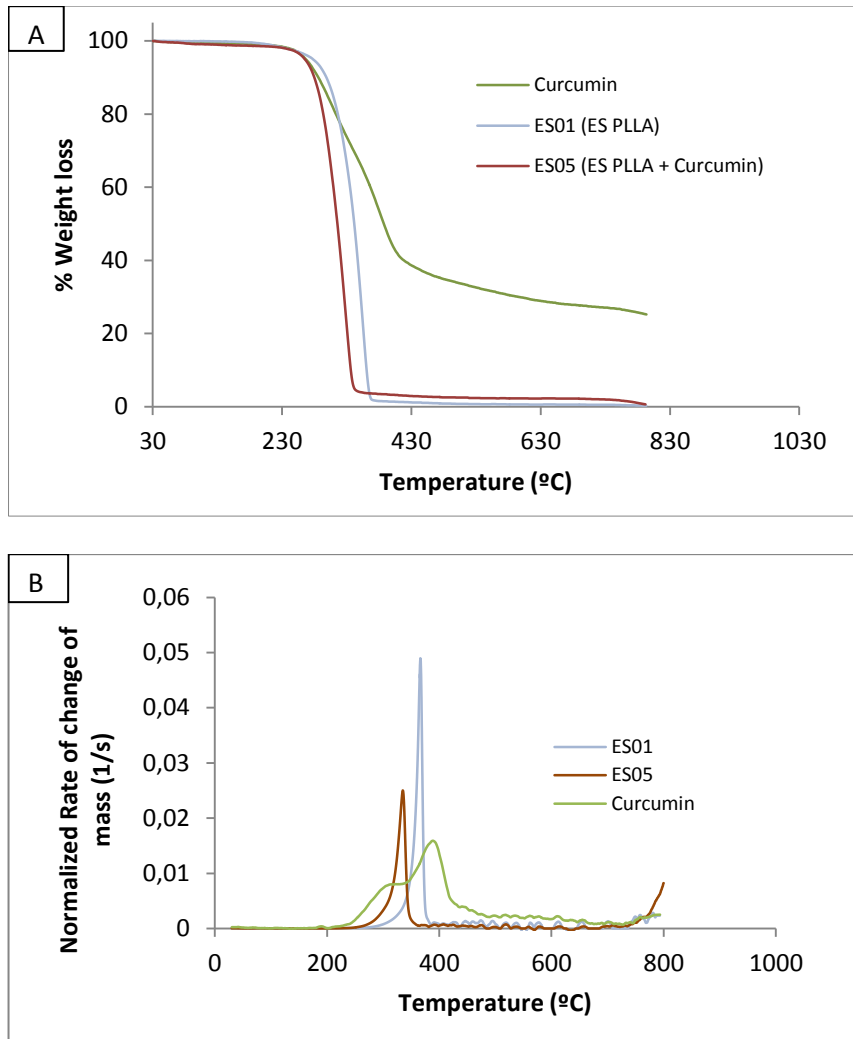
Figure 7.14 Comparison among thermogravimetric analyses of simple membrane systems ES01 and ES05: A) % weight loss curve B) Derivative Thermogravimetric curve (DTG).

Curcumin, was used as model drug for release kinetic studies. Therefore, it was necessary to analyze the thermal stability of this compound by itself, as starting point to be able to stay comparisons between the simple and composite membrane systems which contain this substance.

Result of thermogravimetric analyses of Curcumin are presented in in figure 7.14, together with the results for to simple membrane material: **ES01** and **ES05**.

It is observed in figures 7.14.A and 7.14.B that **curcumin** presents two process of weight loss. First, curcumin suffers a decomposition reaction at 300ºC, and later at 400ºC took place a second process, identified as the pyrolysis of the resulting solid that left 27% of residues.

In the other hand, **ES01**, that is a membrane made by electrospinning composed only by PLLA, was pyrolized in a single step process between 250 and 400ºC as shown in figure 7.14A. The DTG profile of ES01 in figure 7.14 confirmed this observation.

In the case of the simple membrane **ES05**, made of PLLA and loaded with Curcumin, it was observed a degradation pattern with similar trend to **ES01** but at slightly lower temperature. According to DTG curve of **ES05** (Figure 7.14B), this material did not undergo decomposition as happened with curcumin but a single step of pyrolysis as is clearly observed in figure 7.14B. The onset temperature was 240ºC and complete pyrolysis was achieved at 350ºC. Besides, the solid residue left after the pyrolysis (2.2 %wt) was higher than the

residues left by ES01 (0.6 %wt), and it should come from curcumin present in the fibers.

The composition of **ES05** was calculate using the data of fraction mass obtained from the isothermal at 500ºC in the graphic of weight loss. The following equations were applied:

Fraction mass equation

$$1 = x_a + x_b + \cdots + x_n \qquad \textbf{Equation 7-1}$$

$$x_n = mass\ fraction\ of\ each\ component$$

Total weight loss, which can be defined as:

$$\Delta m_T = \Delta m_a * x_a + \Delta m_b * x_b + \cdots + \Delta m_n * x_n \qquad \textbf{Equation 7-2}$$

Where:

$$\Delta m_T = Total\ weight\ loss\ of\ combine\ material\ at\ temperature\ T$$

$$\Delta m_n = weight\ loss\ of\ pure\ component\ at\ temperature\ T$$

$$x_n = mass\ fraction\ of\ each\ component$$

In case of ES05, it is constituted by two components: PLLA (a) and Curcumin (b).

It was traced an isotherm at 500ºC in the graphic % weight loss (Figure 7.14A), and corresponding values of Δm total and of each components were taken and substituted in equation 7.2. Then, the values of x_n where calculated, solving the system of equation with Equation 7.1 and equation 7.2. Results are summarized in table 7.1.

ES04 is a single membrane, similar to ES05, made of PLLA fibers but loaded with the polymer conjugated with curcumin (PACur). In this case it was used the same procedure to determine the composition of this material, using the information given by the profiles of weight loss shown in figure 7.15A.

As well as ES05, membranes of material ES04 suffer pyrolysis at lower temperature in comparison with ES01, revealing the influence of the payload over the thermal properties of both kinds of membranes.
DTG curves (Fig 7.15B) corroborate these results. It is interesting to highlight that a closer sight of DTG curve in Figure 7.16 provides very important information about the chemical nature of the different materials.
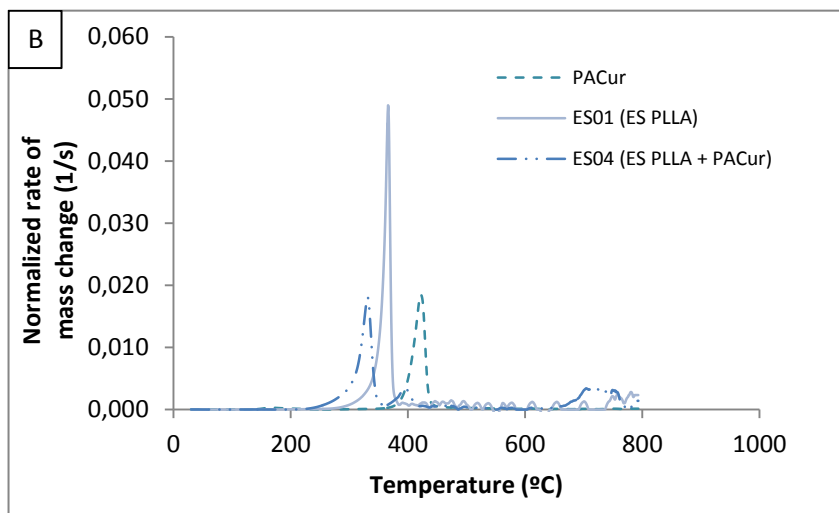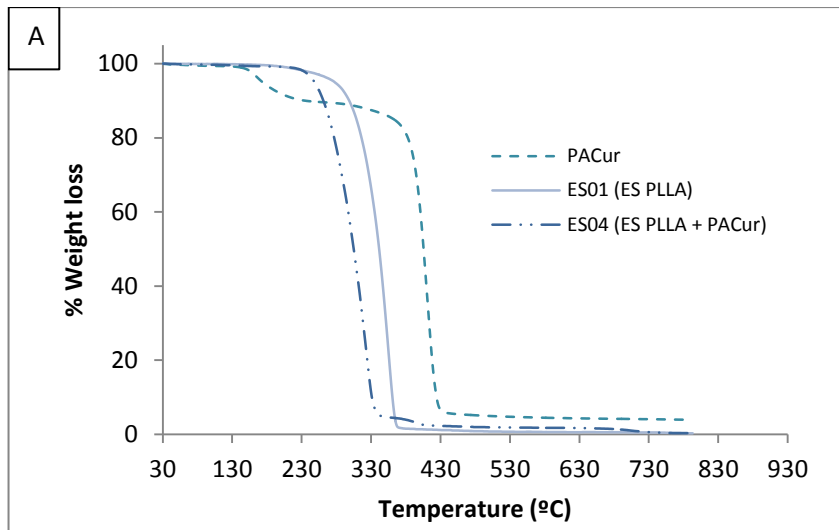
Figure 7.15 Comparison among thermogravimetric analyses of PACur and the simple membrane systems ES01 and ES04: A) % weight loss curve B) Derivative Thermogravimetric curve (DTG).
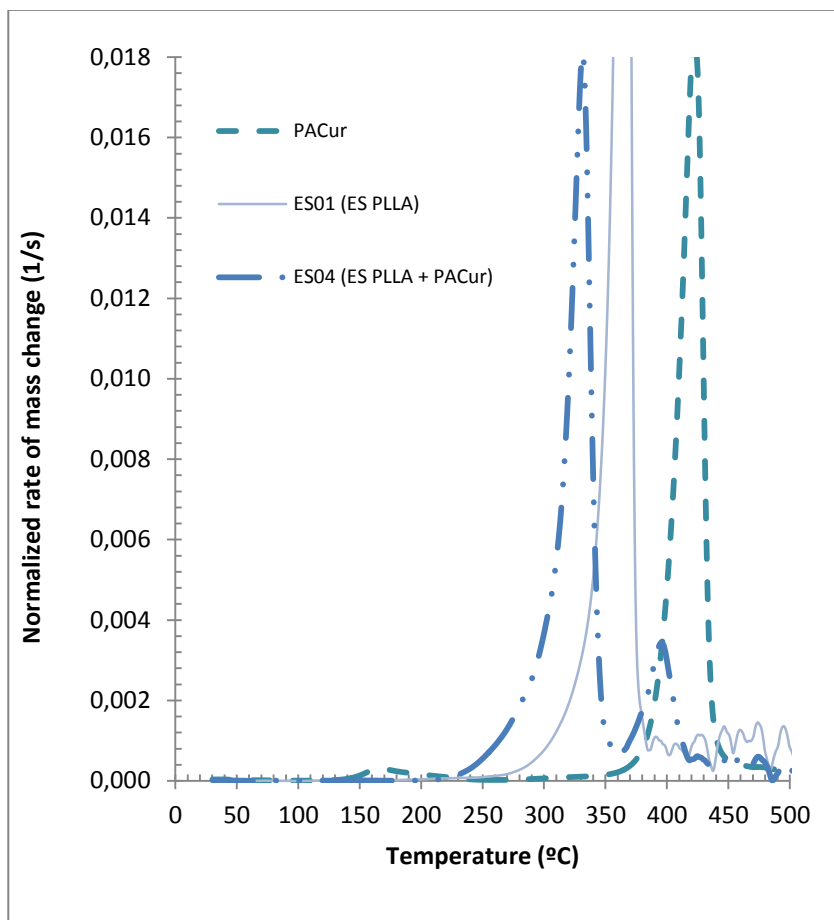
Figure 7.16 Closer view of Comparison among derivative Thermogravimetric (DTG) curve of PACur and the simple membrane systems ES01 and ES04

For example, unlike **ES05** membranes which are loaded with curcumin, the **ES04** membranes, which are loaded with the polymer conjugated PACur, presented a two steps thermal decomposition. This material was pyrolized mainly in step 1 (onset temperature 210ºC) and left only 4% of residue. Step two (onset temperature 365ºC) was shorter than the first, and left 1.6% of residue.
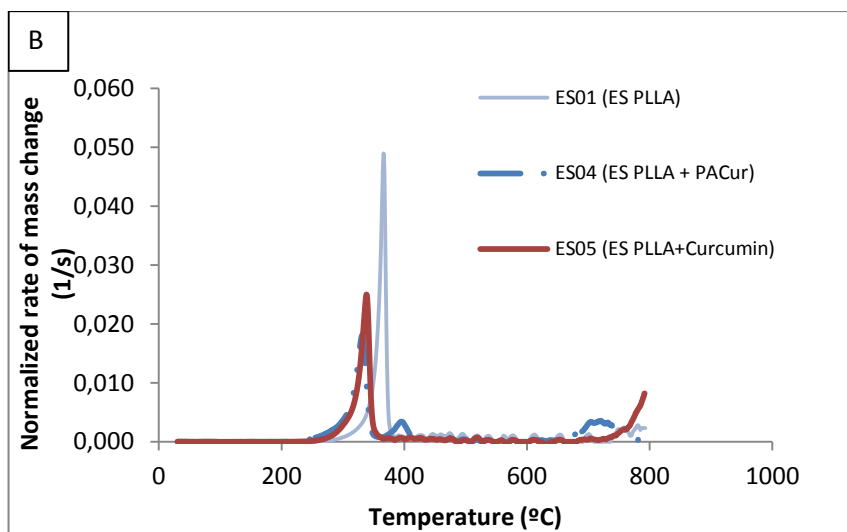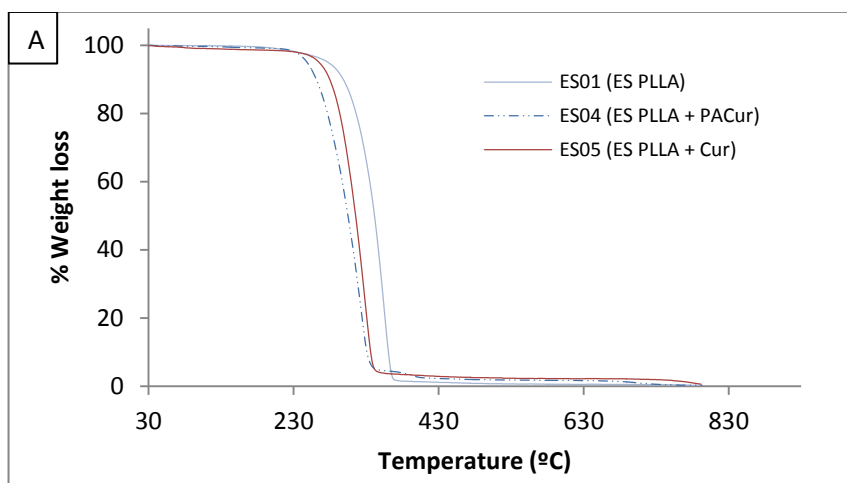
Figure 7.17 Comparison among thermogravimetric analyses of simple membrane systems ES01, ES04 and ES05: A) % weight loss curve B) Derivative Thermogravimetric curve.

Nevertheless, the fact that ES04 as well as ES05 experienced the maximum grade of pyrolysis in one step means that there is one principal component, PLLA, which is responsible of these behaviors.

On the other hand, the variation observed among the three different simple membranes, ES01, ES04 and ES05, are related to the presence or absence of payload. The loss of weight in both loaded membranes present similar trend, and suffer pyrolysis at slightly lower temperature with respect to unloaded simple membrane, that is composed only of PLLA

In other to obtain a better understanding about the payload influence on PLLA fibers thermic resistance, curcumin and PACur where analyzed individually.

Figure 7.18A and B show that **curcumin** started to lose weight at 160ºC. The pyrolysis took place gradually apparently in one step with a gentle slope.   DTG curve (figure 7.18B) reveals that actually there are two different process overlapped between 200 and 432ºC, and another one between 160 and 200ºC. After 800ºC there is still 27% of residue.

Instead, **PACur**, which is a copolymer of polyethylene glycol and curcumin, underwent thermal decomposition in two steps clearly differentiated as it can be appreciated in figure 7.18A. Step 1 has the onset temperature at 130ºC with 90% of residue and step two has the onset in 330ºC with 2% of residue.   If it is compared with polyethylene glycol weight loss profile it seems that in the first step the copolymer is broken and in the second step all PEG is pyrolized quickly, therefore residue should come mainly from curcumin.
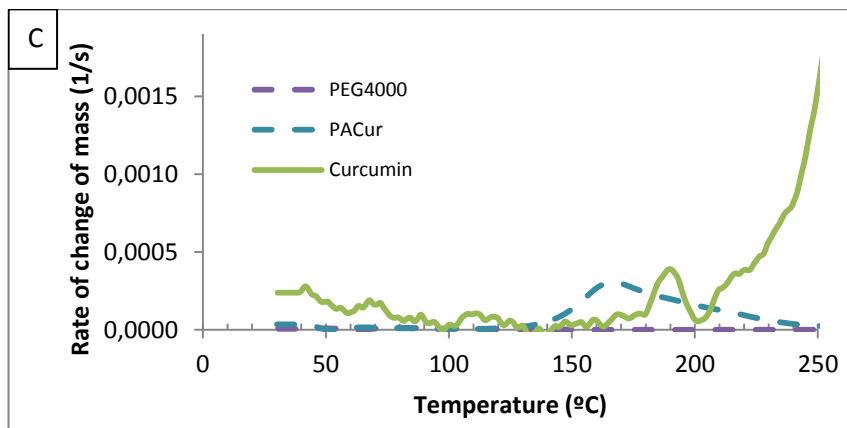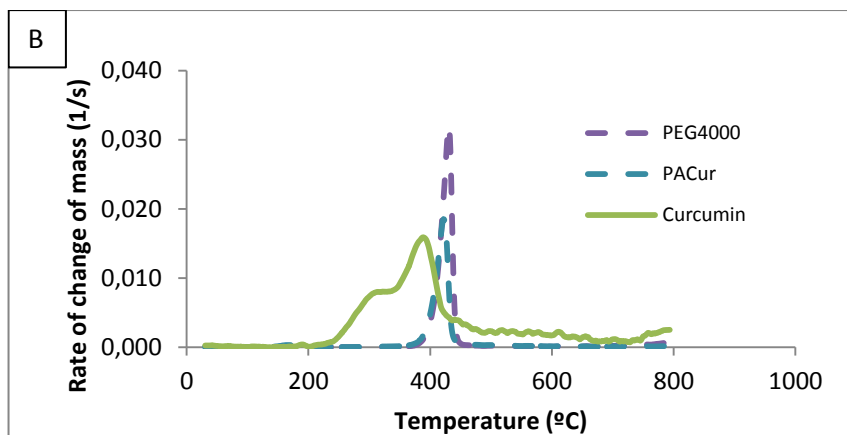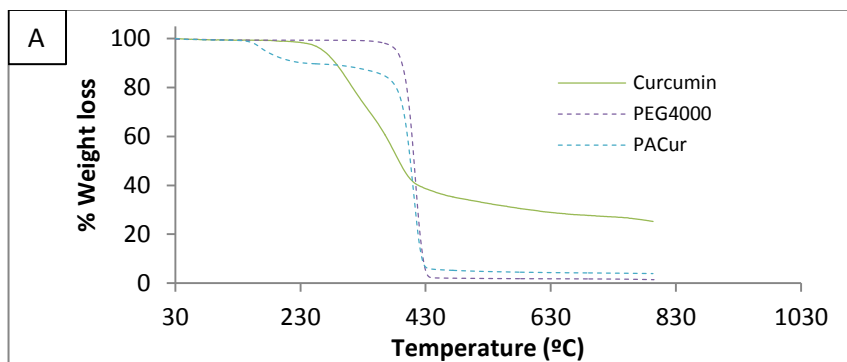
Figure 7.18 Comparison among thermogravimetric analyses of curcumin, PEG4000 and PACur: A) % weight loss curve B) Derivative Thermogravimetric curve C) Zoom of (B) between 0 and 250ºC.

Composite membranes where also analyzed in order to determine their composition and verify if the desire component ratio was achieve.

The first composite membrane analyzed was **ES02**, which is constituted by PLLA fibers and microparticles of hyaluronic acid (MPs HA). Results are shown in figure 7.19.
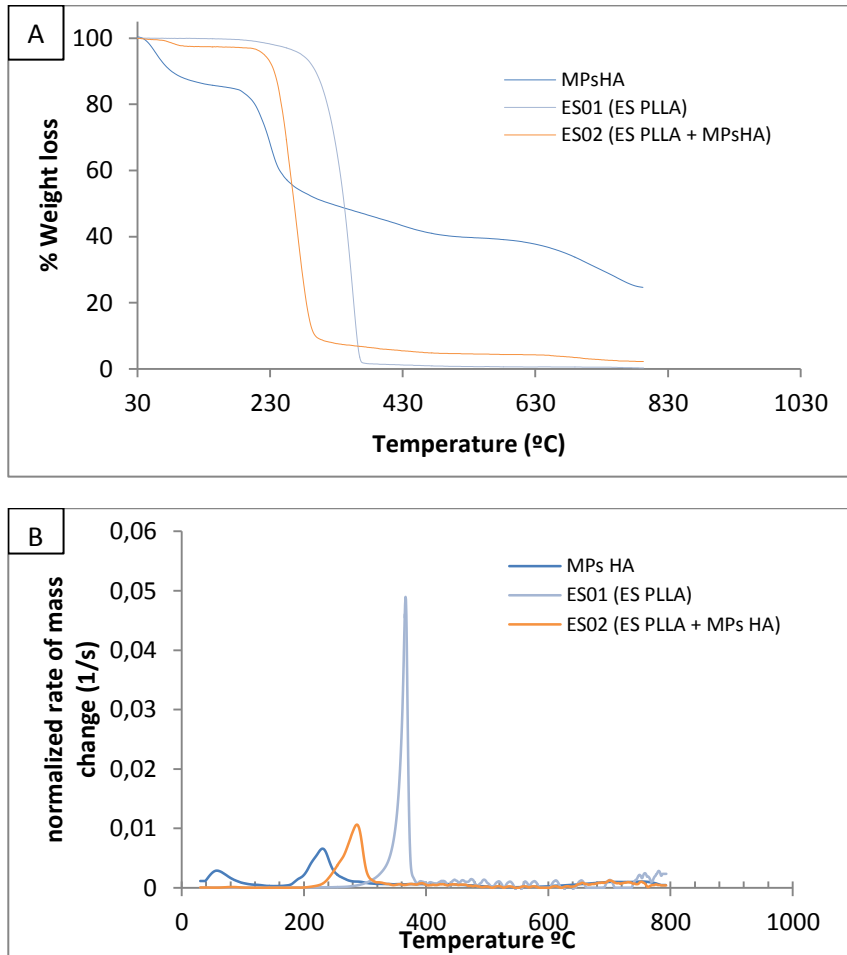
Figure 7.19 Comparison among thermogravimetric analyses of simple membrane systems ES01, with microparticles of HA (MPs HA) and the composite membrane system ES02: A) % weight loss curve B) Derivative Thermogravimetric curve.

The weight loss profile (figure 7.19A) shows that **MPs HA** suffered and initial loss due to the presence of water in the material. According to these experiments the water content in these microparticles after drying is around 24% of total mass.

The second step correspond to hyaluronic acid pyrolysis which was degraded up to 55% between 160 and 260ºC, then remains relatively stable, and finally it was obtained 25.5% of residue at 800ºC.

ES02, the composite membrane that is supposed to be constituted by PLLA fibers and microparticles of hyaluronic acid (MPs HA) shows a small initial weight loss with onset temperature of 54ºC. This belongs to water present in the material. Then, pyrolysis took place in one step, with similar slope to ES01 membranes, which are made with PLLA, but the onset temperature of ES02 (200ºC) is lower than the onset temperature of ES01 (250ºC). Likewise, after 500ºC ES02 presented 4.6% of residues while ES01 only presented 0.8% at the same temperature. These results corroborates the presence of MPs HA together with PLLA in the composite material. Composition was calculated as explained before for ES05.

ES03, is also a composite membrane, similar to ES02, but in this case MPs HA were loaded with PACur. Figure 7.20 shows the results for TGA experiments.

ES03 suffered pyrolysis process in two steps. First step is related to the presence of water in the membrane despite it was dried previously. Second step showed similar profile than ES01 but with lower onset temperature (210ºC) as it was observed for ES02.
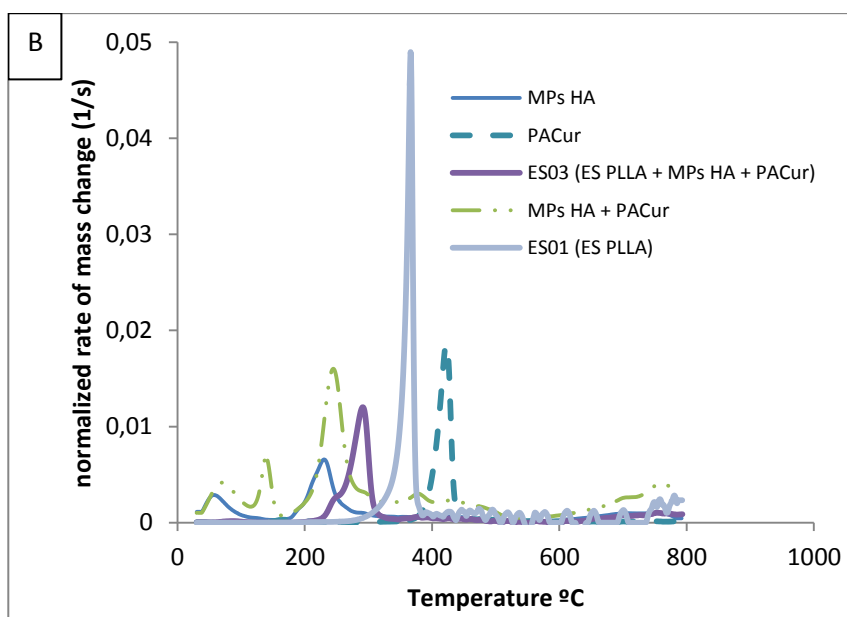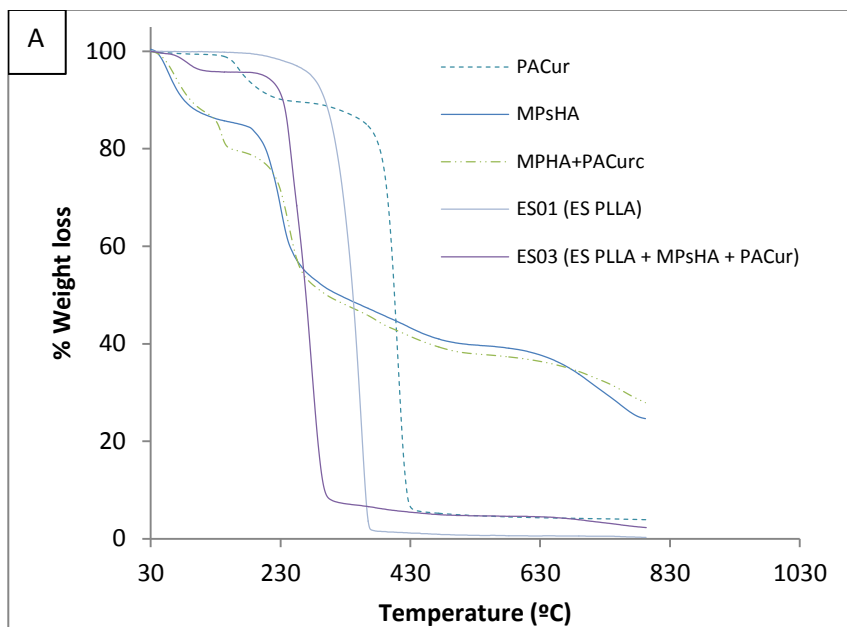
Figure 7.20 Comparison among thermogravimetric analyses of simple membrane systems ES01, with microparticles of HA (MPsHA), PACur and the composite membrane system ES03: A) % weight loss curve B) Derivative Thermogravimetric curve.

Also the amount of residues after 500ºC were higher for ES03 (4.8%) than the residues for ES01 (0.8%) at the same temperature.

These results corroborated the presence of PLLA and MPs HA. The amount of curcumin in this case was too small to produce a particular variation in the weight loss profile of the material.

Nevertheless, a sample of MPs HA loaded with PACur, as those included in the PLLA fibers of ES03, where analyzed by separated, as cam be seen in figure 7.20.

The results demonstrated the presence of an additional step with onset temperature at 107ºC, which was not observed in unloaded MPs HA that corresponded to PACur encapsulated into the MPs HA.

Figure 7.20B shows clearest the different processes that took place on each material.

The last composite membrane material analyzed was **ES06**, which is made of PLLA fibers with MPs HA loaded with curcumin.

The results were similar than obtained for ES03, as can be appreciated in figure 7.21. Following the same logical reasoning than before with ES03 it was determined that ES06 was composed by PLLA and MPs HA loaded with curcumin.

When the results obtained for the three composite membranes were compared, it was observed that the curves were overlapped as can be seen in Figures 7.22 and 7.23, with small differences, related to the kind of substances loaded in the microparticles.

Composition were estimated using the procedure explained for ES05 but including de values of two or more different isotherms to solve the system of equation with the help of the tool "solver" included in the software EXCEL. Calculation results are summarized in table 7-1.
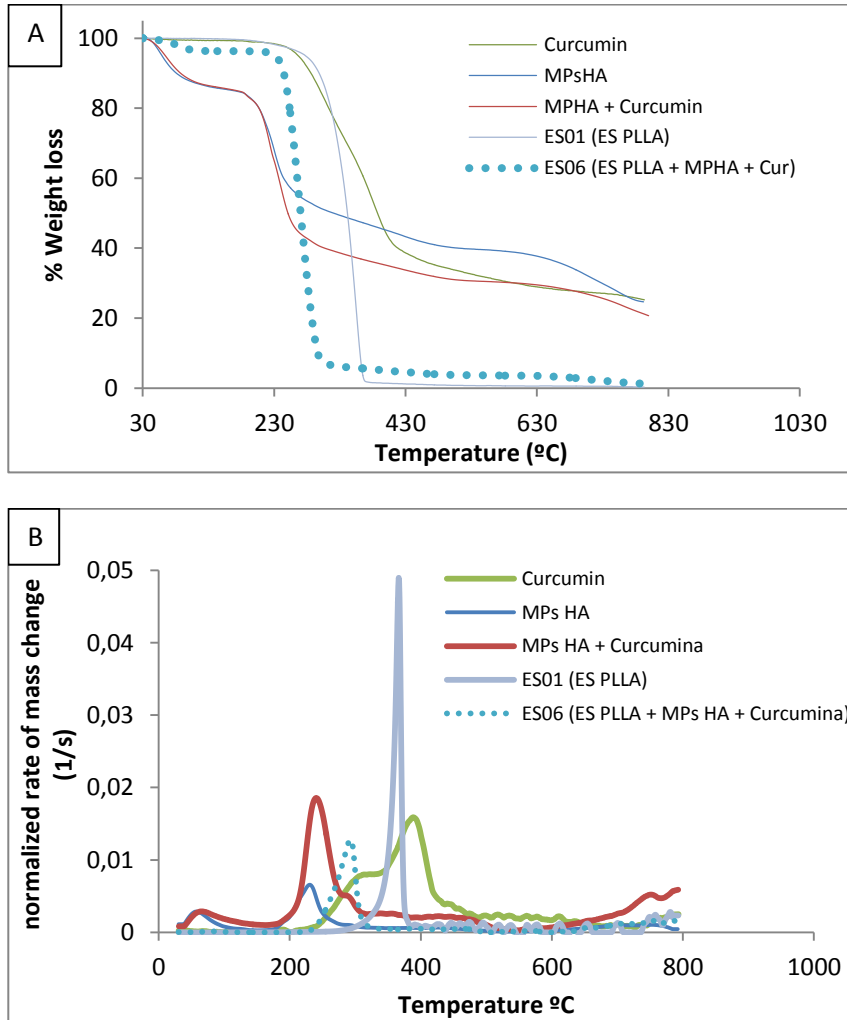
Figure 7.21 Comparison among thermogravimetric analyses of simple membrane systems ES01, with microparticles of HA (MPsHA), Curcumin and the composite membrane system ES06: A) % weight loss curve B) Derivative Thermogravimetric curve.
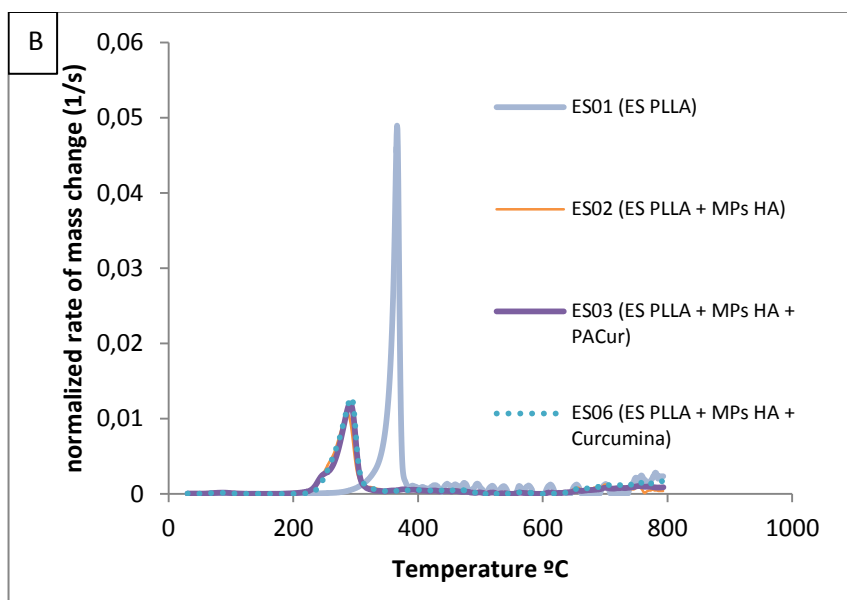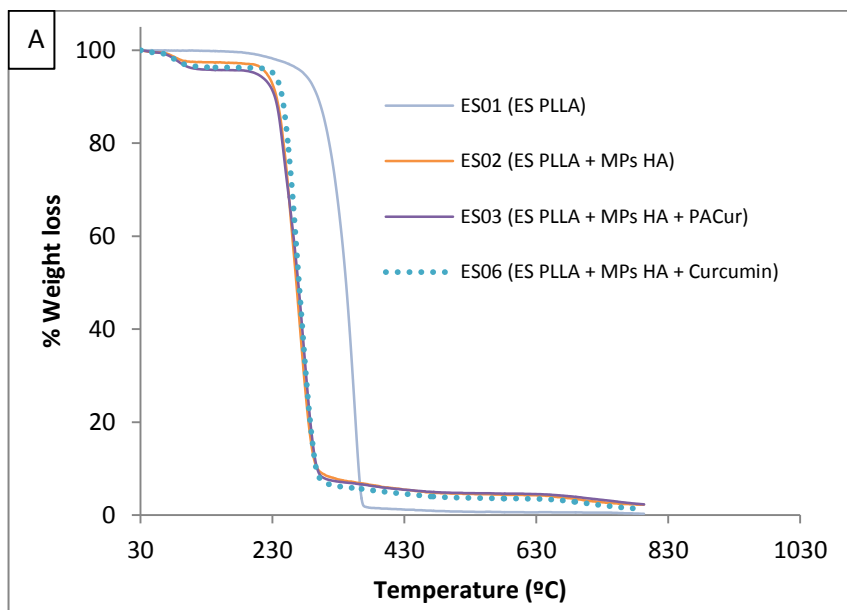
Figure 7.22 Comparison among thermogravimetric analyses of simple membrane ES01 and composite membrane systems ES02, ES03 and ES06: A) % weight loss curve B) Derivative Thermogravimetric curve.

271
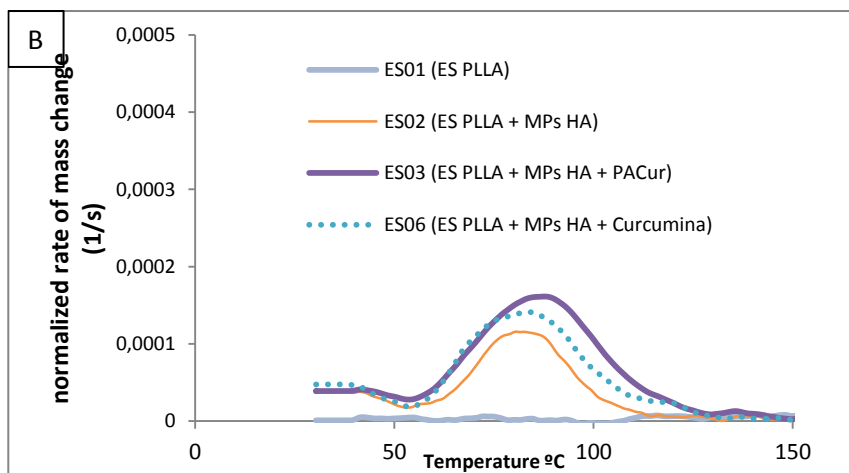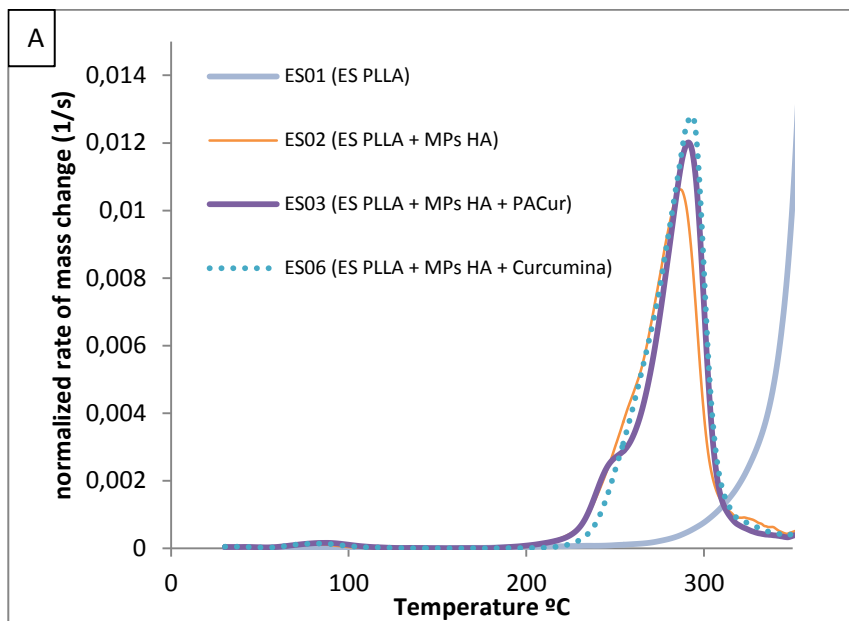
Figure 7.23 Closer view of comparison among thermogravimetric analyses of simple membrane ES01 and composite membrane systems ES02, ES03 and ES06: A) Derivative Thermogravimetric curve between 0 and 350ºC B) Derivative Thermogravimetric curve between 0 and 150ºC

Table 7-1 Composition calculated from data obtain by Thermogravimetric Analyses

Material	% PLLA	% HA	% Cur
PACur	-	-	9.2
ES01 (ES PLLA)	100	-	-
ES02 (ES PLLA + MPHA)	90	10	-
ES03 (ES PLLA + MPHA + PACurc)	90	9.7	0.3 (PACur) 0.02 (Curcumin)
ES04 (ES PLLA + PACur)	71.8	-	28.0 (PACur) 2.5 (Curcumin)
ES05 (ES PLLA +Curcumin)	95	-	5
ES06 (ES PLLA + MPHA + Curcumin)	88	7	5

The influence of the different composition of the simple and composite membranes was also studied by dynamic scanning calorimetry (DSC).

The thermograms obtained are represented in figure 7.24 and the values of different thermodynamic parameters are summarized in table 7.2.

As can be appreciated in figures 7.24 and 7.25 crystallization temperatures as well as melting temperature are moved with respect the pure PLLA fibers membrane, demonstrating the influence of additional components: MPs HA, Curcumin and/or PACur.
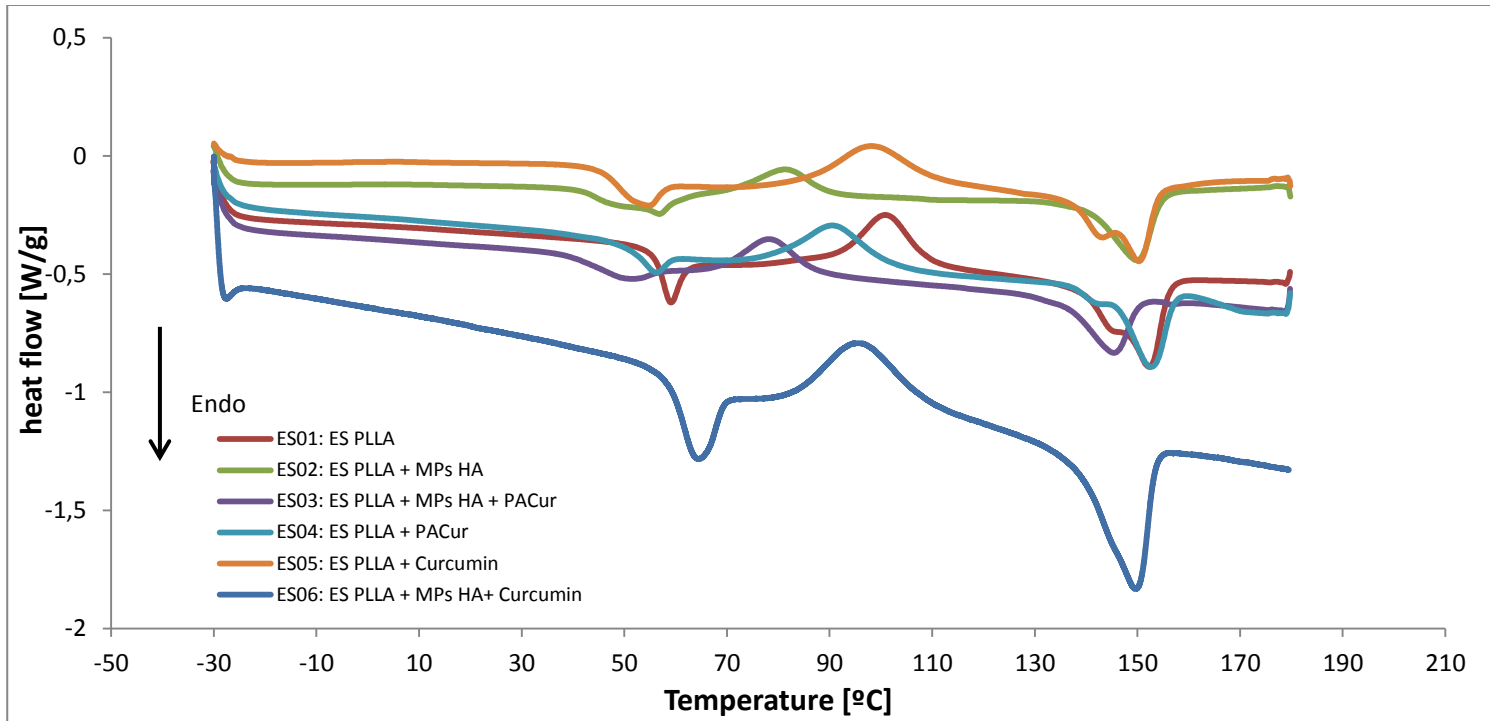
Figure 7.24 Thermograms obtained after the first heating cycle by Dynamic Scanning Calorimetry (DSC) analyses of simple and composite systems
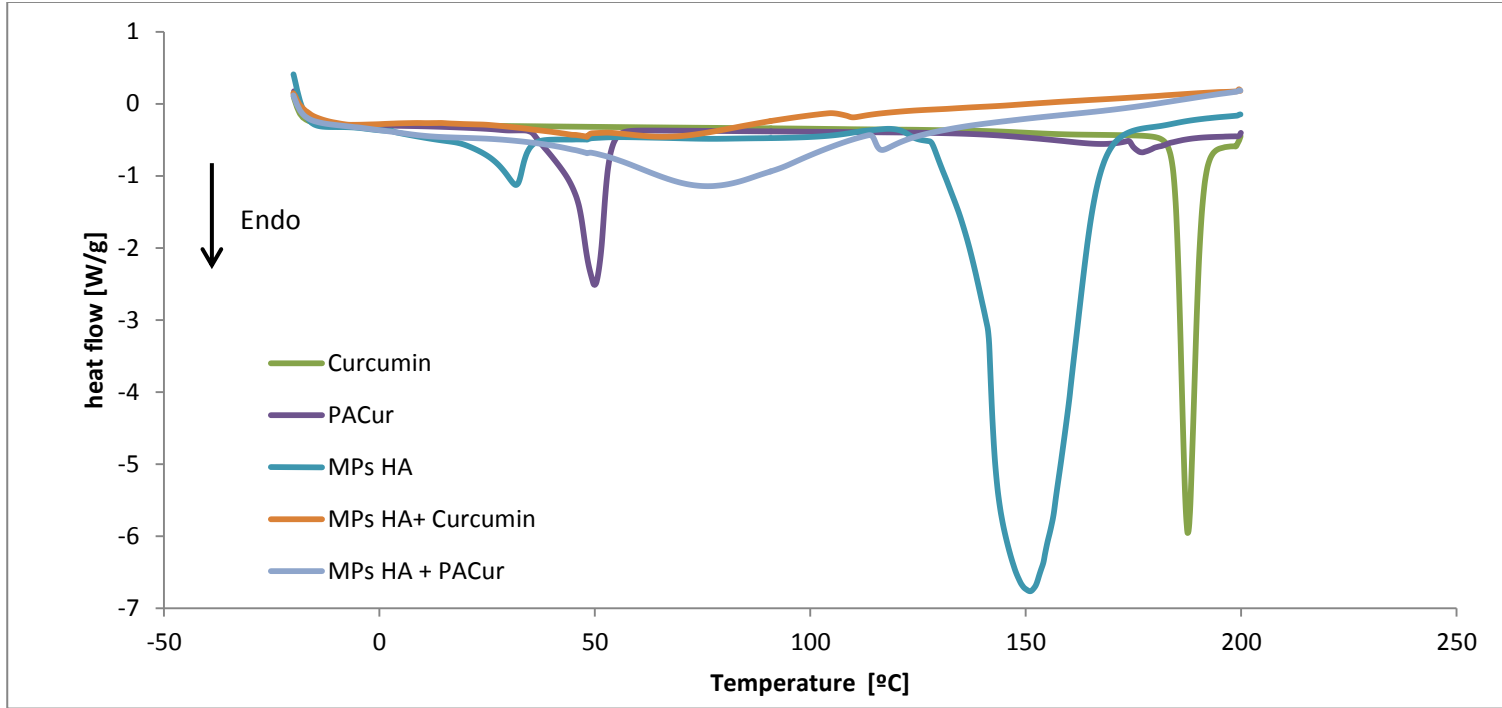
Figure 7.25 Thermograms obtained after the first heating cycle by Dynamic Scanning Calorimetry (DSC) analyses of hyaluronic microparticles, curcumin and PAcur

Table 7-2 Values of Thermodynamic properties determined by the experiments of Dynamic Scanning Calorimetry (DSC)
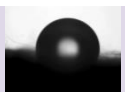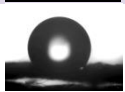
Material	Tm [ºC]	ΔHm [J/g]	Tg (ºC)	ΔCp [J/(g K)]	Tc [ºC]	ΔHm [J/g]
ES01 (ES PLLA)	59.09	5.94			100.93	13.6
	152.27	22.86				
ES02 (ES PLLA + MPHA)	56.98	1.06	41.27	0.375	81.48	7.62
	149.98	16.6				
ES03 (ES PLLA + MPHA + PACurc)	50.08	3.76			78.25	10.01
	145.42	12.48				
ES04 (ES PLLA + PACurc)	56.1	4.52			90.6	14.75
	152.77	11.2				
ES05 (ES PLLA +Curcumin)	54.65	6.49	8.03	0.024473	98.15	18.91
	150.49	4.01				
	150.32	22.96				
ES06 (ES PLLA + MPHA + Curcumin)	64.30	9.50			96.06	12.04
	149.55	20.87				

7.3.1.3. *Study of Membranes wettability by Contact angle measurement*

The behavior of water drops in contact with membranes surface was different for simple and composite materials.

In some cases it was impossible to register a measurement due to the sample absorbed immediately the water drop.

Table 7-3 Values of contact angles measured between drops of water and the surface of simple and composite membranes

Material	Contact angle		Drop of water
	Left	right	
ES01 (ES PLLA)	109.4	109.4	
ES02 (ES PLLA + MPHA)	-	-	
ES03 (ES PLLA + MPHA + PACurc)	-	-	
ES04 (ES PLLA + PACurc)	117.7	117.4	
ES05 (ES PLLA +Curcumin)	121.3	120.9	
ES06 (ES PLLA + MPHA + Curcumin)	-	-	

7.3.1.4. *Mechanic Tensile properties of membranes*

The study of mechanic tensile properties of simple and composite membranes provides interesting information about the resistant of the different material to some kind of mechanical stress, that is necessary to a better idea of the suitability of these systems for future application in the field of regenerative medicine as for example, wound healing.

The modulus of longitudinal elasticity – the Young's modulus (*E*) – defines the relation between stress (σ) and strain (ε) in elastic materials.

The modulus characterizes materials resistance to elastic elongation. This dependence is generally presented by the Hooke's Law: ε = *E*/σ. In the elastic range the relationship between stress and strain is linear and the factor of proportionality is expressed by the Young's modulus[154].

The values of Young modulus (E) were calculated from the slope of the elastic (initial, linear) portion of the stress–strain curve shown in figure 7.26, which was the result to apply the equation 7-3 to the row data collected with the tensile experiments.
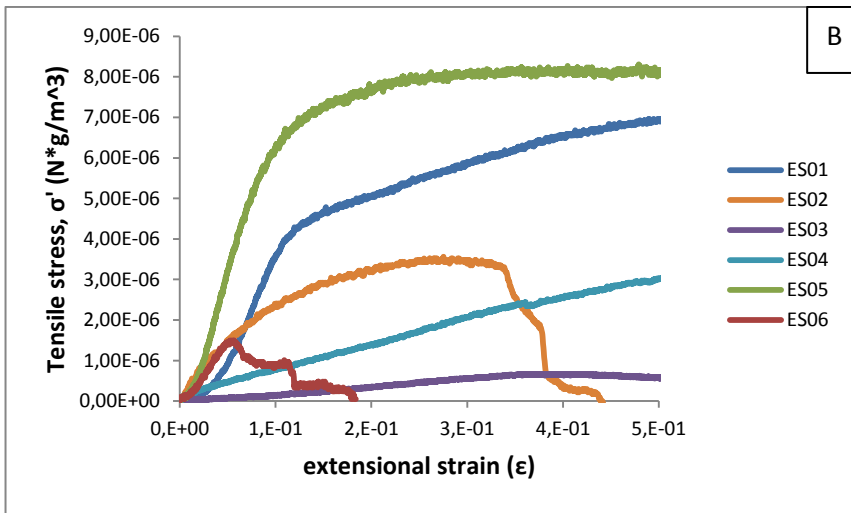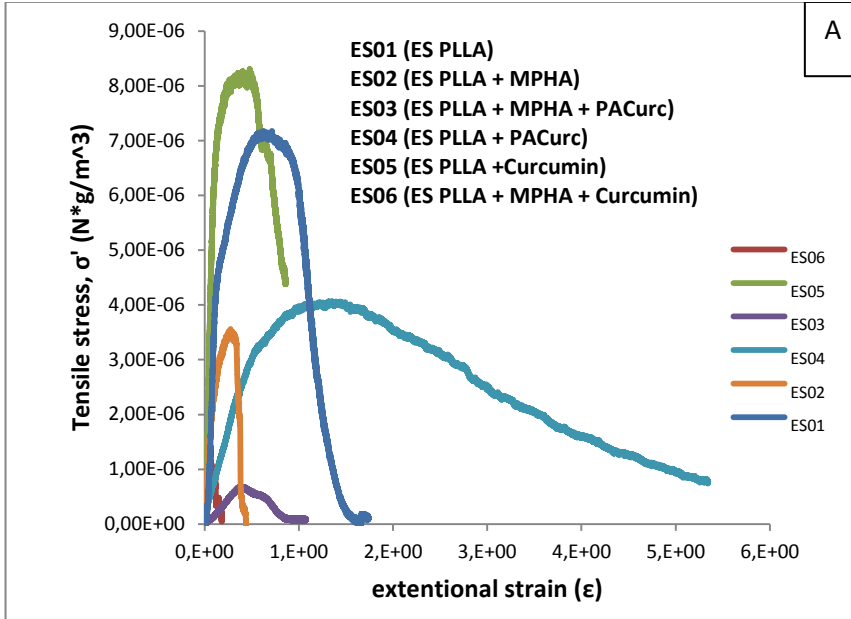
Figure 7.26 Tensile Stress (σ') – extensional strain (ε) curves for different simple and composite membranes: A) complete profiles, B) closer view of strength –stain curves.
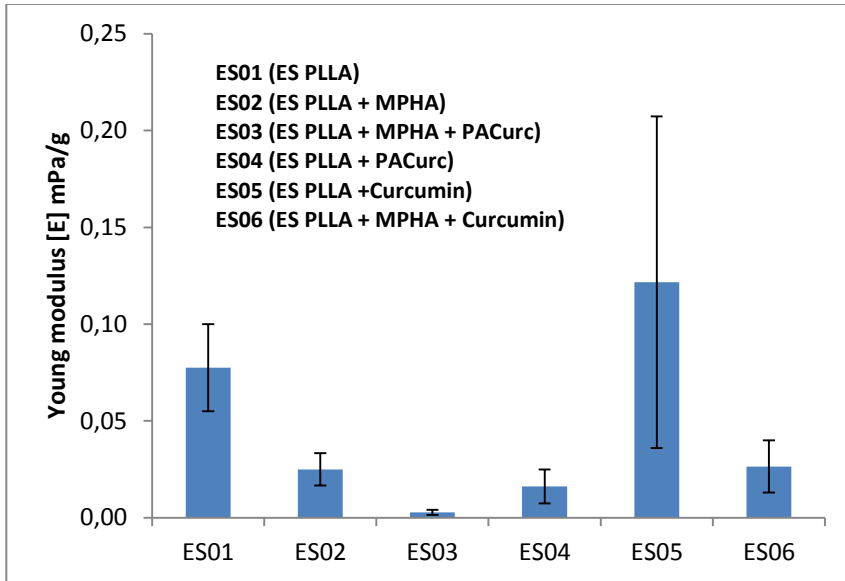
Figure 7.27 Comparison of Young moduli values calculated for simple and composite membranes.

$$E \equiv \frac{tensile\ stress\ (\sigma)}{extensional\ strain\ (\varepsilon)} = \frac{\left(\frac{F}{A_0}\right)}{\left(\frac{\Delta L}{L_0}\right)} = \frac{FL_0}{A_0\Delta L} \quad \text{Equation 7-3}$$

Where

     E: Young's modulus (modulus of elasticity)
     F: force exerted on an object under tension
     A_0: initial cross-sectional area through which the force is applied
     ΔL: amount by which the length of the object changes
     L_0: initial length of the object

In order to be able to establish an appropriate comparison among the E values of the different membranes a variation was introduced in equation 7-3, dividing the registered strength by the samples wide (w) and the surface density (sd) determine experimentally for each sample, as shown in equation 7-4.

$$sd = \frac{cross\ sectional\ area}{mass} \qquad \textbf{Equation 7-4}$$

Analyses were done with five independent samples of each kind of material.

Finally, the equation used to build the stress-strain curve was:

$$E \equiv \frac{tensile\ stress\ (\sigma\prime)}{extensional\ strain\ (\varepsilon)} = \frac{\left(\frac{F}{sd*w}\right)}{\left(\frac{\Delta L}{L_O}\right)} \qquad \textbf{Equation 7-5}$$

As can be appreciated in figure 6.26 the composite materials presented the lowest elastic moduli and there was no significant difference between the values of the composites ES02 and ES06, instead ES03 resulted to have the less elastic modulus of all six materials analyzed.

In the other hand it was observed that simple membrane ES04, composed by PLLA fibers loaded with PACur, presented the lower elastic modulus in comparison with the other simple membranes ES01 and ES05. ES04 had similar elasticity than the composite systems.

ES01, ES04 and ES05 do present significant difference among their E values. ES04 was the most elastic, followed by ES01 (PLLA), and the less elastic of all six materials was ES05 (PLLA + Curcumin).

Similar tendency was observe for breaking strength and maximum strain.

These results can be explain because the heterogeneity of composite makes them more elastics but also weaker. Instead the structure of

simple membranes is more homogeneous, but their mechanical properties are related to influence of PACur and Curcumin over the PLLA fibers.

Curcumin made PLLA fibers less elastic and harder, instead PACur made them more elastic and soft as cotton.

Intermolecular interactions between curcumin and PLLA, or PACur and PLLA, in the solid phase are responsible of these behaviors.

Table 7-4 Values of Young Modulus, Breaking Strength and maximum strain determined for simple and composite membranes with tensile strength assays

	Young Modulus (mPa/g)	err	Breaking Strength $(N*g/m3)*10^{-6}$	err	ε maximum strain	error
ES01 (ES PLLA)	0.08	0.02	12	3	0.6	0.1
ES02 (ES PLLA + MPHA)	0.025	0.008	3	1	0.19	0.07
ES03 (ES PLLA + MPHA + PACurc)	0.003	0.001	0.5	0.2	0.35	0.05
ES04 (ES PLLA + PACurc)	0.016	0.009	6	2	1.3	0.2
ES05 (ES PLLA +Curcumin)	0.12	0.09	8	1	1.2	0.5
ES06 (ES PLLA + MPHA + Curcumin)	0.03	0.01	1.2	0.3	0.06	0.02

7.3.1.5. *Quantification of Total Drug Loading and Encapsulation Efficiency*

The encapsulation efficiency was determined by UV spectroscopy. Results are summarized in table 7-5.

These values are different to obtain by TGA, maybe due to the limitation associated to each technique. Amount of drug loaded were too small to by properly detected by TGA.

In any case it was observe that the elaboration procedure of drug loaded membranes resulted to have a high efficiency except in case of ES03, which must be improved.

Table 7-5 Encapsulation Efficiency and Total Drug Loading

	wt % Total drug loading Curcumin (TDL)	Efficiency	Theoretic loading
ES03 **(ES PLLA + MPHA + PACurc)**	0,04	44	0,1
ES04 **(ES PLLA + PACurc)**	0,10	99	0,1
ES05 **(ES PLLA +Curcumin)**	1,22	81	1,5
ES06 **(ES PLLA + MPHA + Curcumin)**	0,09	100	0,1

7.3.1.6. Release Kinetic studies

Release kinetic profiles of different simple and composite membranes were represented in figure 7.28.
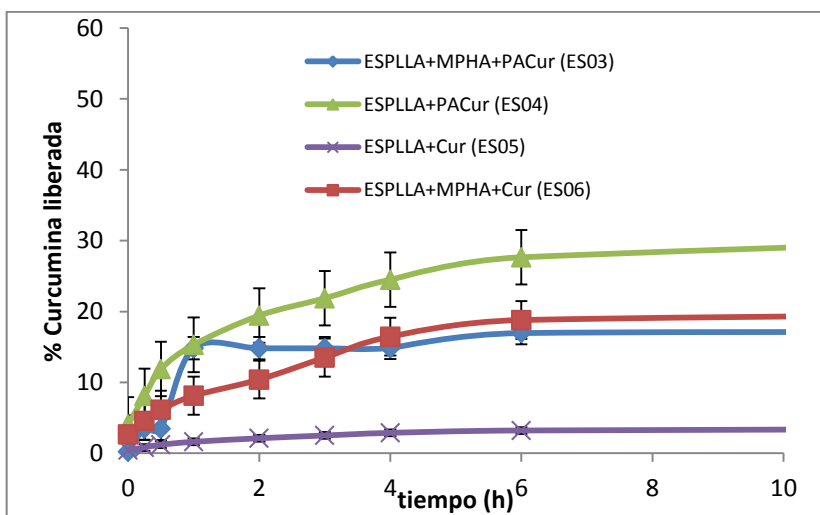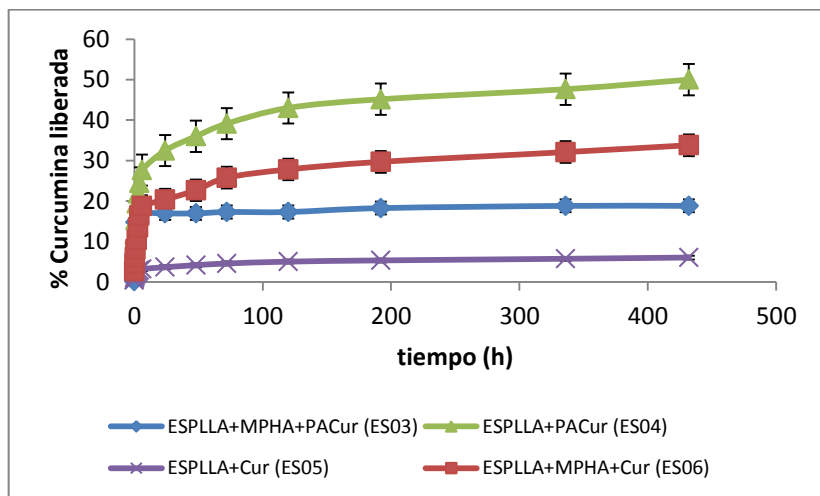
Figure 7.28 A) Complete profile of curcumin release kinetic from ES PLLA membranes and composite systems. B) Closer view of the curcumin profile release kinetic from ES PLLA membranes and composite systems

It was observed that **ES05**, the membrane of PLLA fibers loaded with curcumin was the slowest system, follow by the two composite membranes, **ES03** (PLLA fibers with MPs HA loaded with PACur) and **ES06** (PLLA fibers with MPs HA loaded with Curcumin) which present very similar profiles, and finally, **ES04**, composed by PLLA fibers loaded with PACur resulted to be the fastest system of release.

It is interesting to mention that, in comparison with the profile of drug release obtained from MPs HA, there was no significant difference between the composite material loaded with PACur (**ES03**) and the MPs HA loaded with PACur when released is study at pH 7.4 a 37ºC.

Instead, the composite system loaded with curcumin (ES06) did slow down the releases of the drug in comparison with the MPs HA loaded with curcumin, when released is study at pH 7.4 a 37ºC.
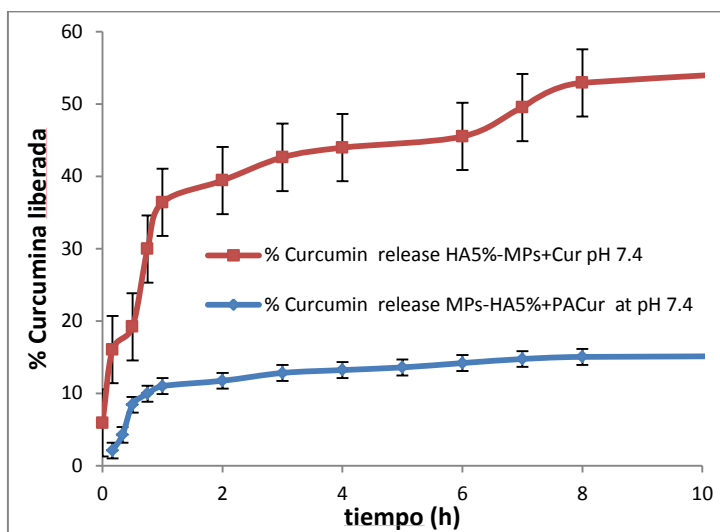
Figure 7.29 Closer view of the curcumin profile release kinetic from MPs HA systems

7.3.1.7. Preliminary studies of simple and composite membranes degradation

Time of degradation is a very important parameter to be taken into account to establish the suitability of materials for a specific biomedical application.

For this reason, a preliminary degradation study was carried on simulating the most basic physiological condition in wet environment: aqueous PBS solution 1X concentration and pH 7.4 at 37ºC. Enzymatic degradation was not included in this study.

ES01: PLLA simple membranes

As can be appreciated in figure 7.30, PLLA fibers of this material did not experience significant change in fibers morphology after 7d. Fibers kept the same dimensions; there is no evidence of breaking or wear.
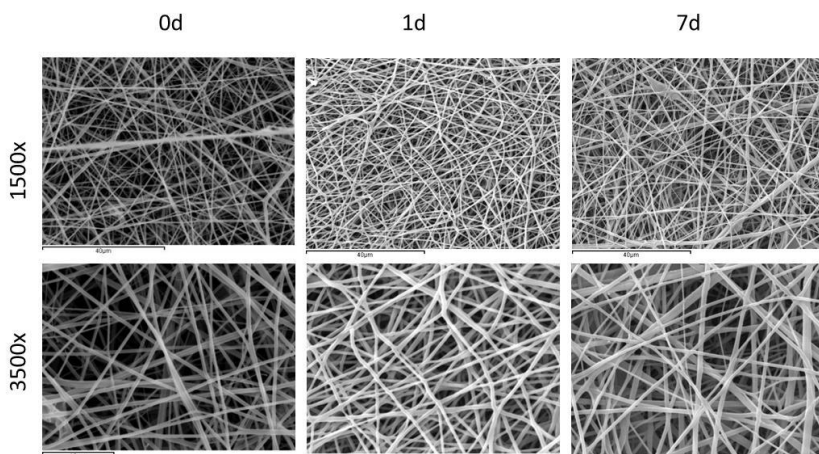
Figure 7.30 Comparison of change in PLLA fibers morphology of ES01 membranes after different times of soaking in PBS 1X at pH 7.4 and 37ºC, by SEM images taken at 15KV and 9mm of working distance

ES02: Composite membranes of PLLA fibers with MPs HA

Composite membranes ES02 did not show any significant change after 7 days of soaking as far as can be observed in figure 7.31
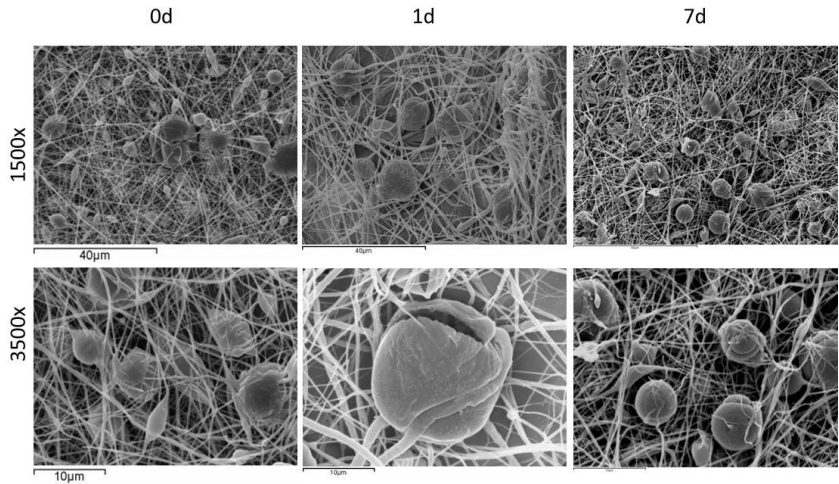
Figure 7.31   Comparison of change in PLLA fibers and MPs HA morphology of ES02 membranes after different times of soaking in PBS 1X at pH 7.4 and 37ºC, by SEM images taken at 15KV and 9mm of working distance

ES03: Composite membranes of PLLA fibers with MPs HA loaded with PACur

SEM images in figure 7.32 show that composite membrane ES03 a slight increase in fiber sizes, but there is any signal of degradation.
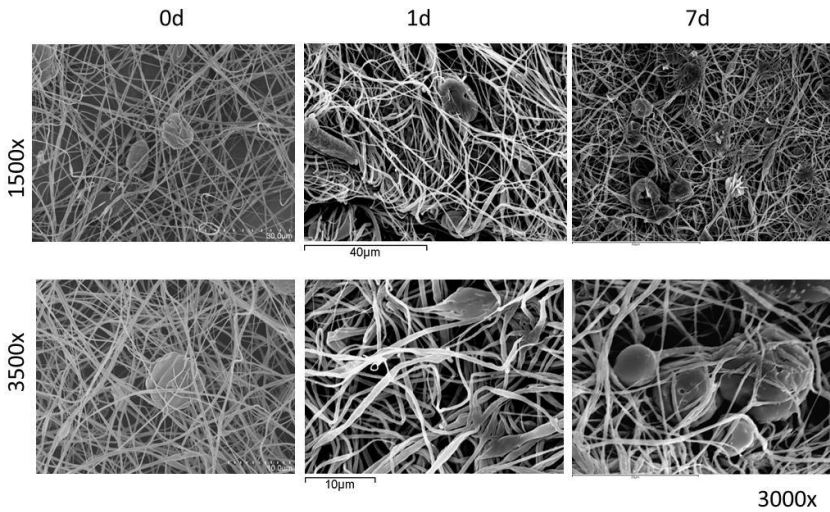
Figure 7.32   Comparison of change in PLLA fibers and MPs HA morphology of ES03 membranes after different times of soaking in PBS 1X at pH 7.4 and 37ºC, by SEM images taken at 15KV and 9mm of working distance

ES04: PLLA simple membranes loaded with PACur

Fibers stayed without change after 7 days in PBD at pH 7.7 and 37ºC
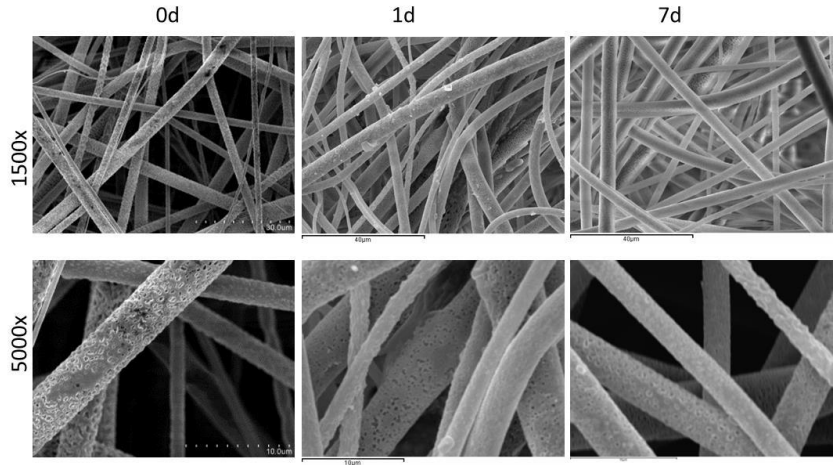
Figure 7.33 Comparison of change in PLLA fibers morphology of ES04 membranes after different times of soaking in PBS 1X at pH 7.4 and 37ºC, by SEM images taken at 15KV and 9mm of working distance

ES05: PLLA simple membranes loaded with PACur

PLLA fibers of ES05 kept the same appearance since time cero until 7days in aqueous solution.   Any hydrolysis or degradation was observed.
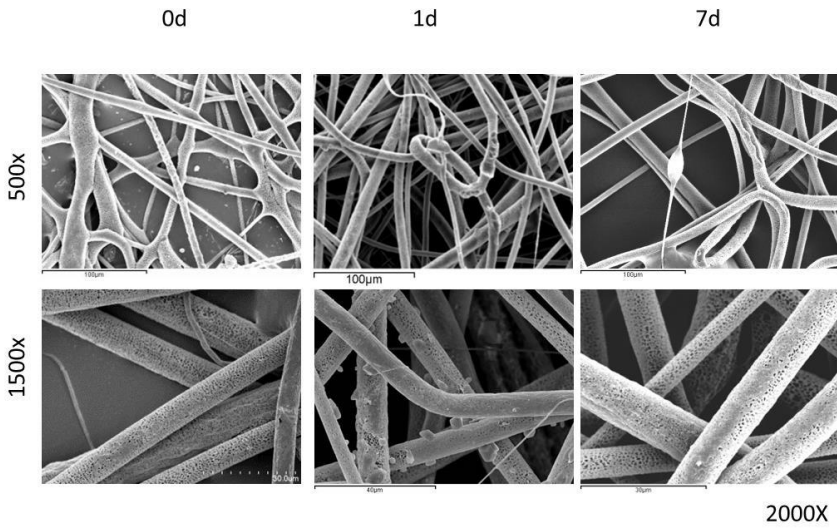
Figure 7.34 Comparison of change in PLLA fibers morphology of ES05 membranes after different times of soaking in PBS 1X at pH 7.4 and 37ºC, by SEM images taken at 15KV and 9mm of working distance

ES06: Composite membranes of PLLA fibers with MPs HA loaded with Curcumin

SEM images in figure 7.35 did not give evidence of degradation after 7days of study.
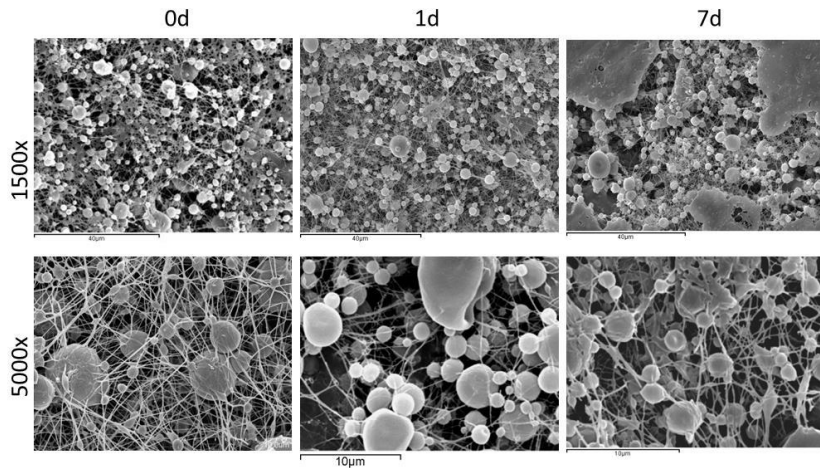
Figure 7.35   Comparison of change in PLLA fibers and MPs HA morphology of ES06 membranes after different times of soaking in PBS 1X at pH 7.4 and 37ºC, by SEM images taken at 15KV and 9mm of working distance

According with these results, all the six system are stable after seven days of soaking in aqueous solution of PBS 1X at pH 7.4 and 37ºC.

This behavior was expected because it is well known that PLLA is a material highly resistant to aqueous hydrolysis at neutral pH.

7.3.2. Preliminary Biologic Evaluation though *in vitro* assays

7.3.2.1. Study of Membranes Cytotoxicity

Cytotoxicity experiments were undergone by indirect contact. Results shown that after 48h cell viability was over 70%, which means that any of the systems analyzed were cytotoxic.
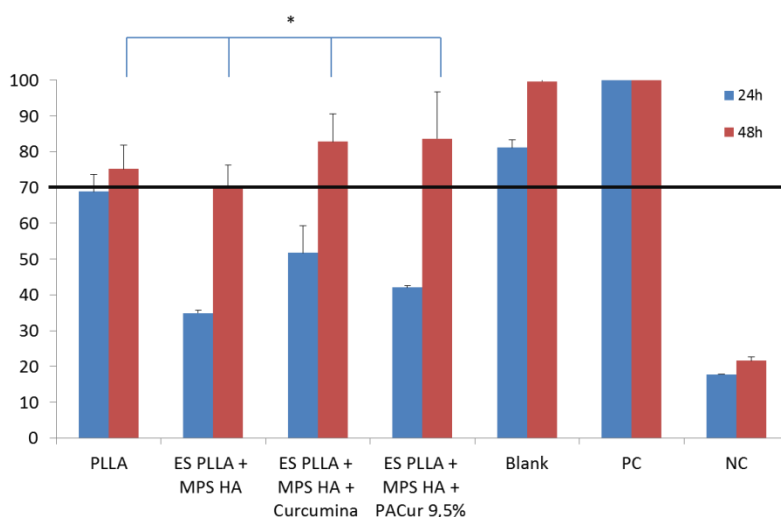
Figure 7.36 Cytotoxicity comparison for different composite systems. ES01: membrane of PLLA fibers; ES02: composite membrane of PLLA fibers with MPs HA; ES03: Composite membranes of PLLA fibers with MPs HA loaded with PACur; ES06: Composite membranes of PLLA fibers with MPs HA loaded with Curcumin. (*) No statistical significant difference

Result demonstrated that after 48h there are not significant differences statistically among any of the systems analyzed. That means that composite membrane materials are not cytotoxic in any case.

7.3.2.2. *Study of cellular adhesion and morphology*

- Analysis of Cellular Density and morphology by Immunofluorescence

L929 fibroblast cells were seeded onto the materials. To determined cellular density microscopy of fluorescence was used, staining the nucleic acid with DAPI. Besides, to determine how were distributed the cells the cytoskeleton was stained with Phalloidin to determined roundness by confocal microscopy.   Images are shown in the next figure.
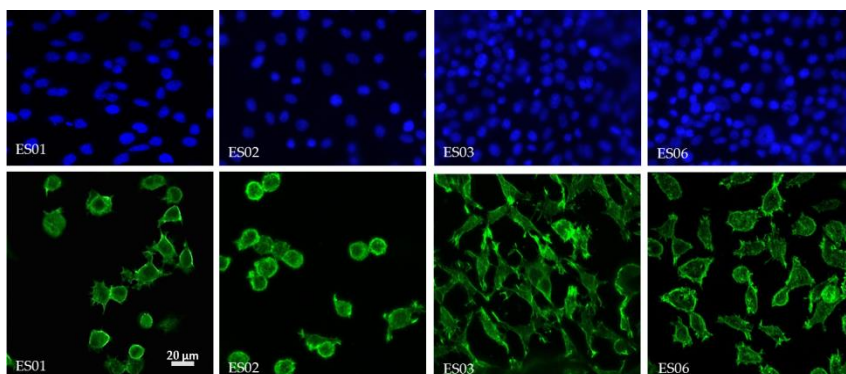
Figure 7.37 Images taken by fluorescence microscopy to estimate the cellular density and cellular distribution of L929 cells after 1d of culture on different composite materials. Nuclei stained in blue with DAPI, images with 10X magnification. Cytoskeleton stained in green with Phalloidin, images with 40X magnification. ES01 (A, A'): Simple membrane of PLLA; ES02 (B, B'): Composite material of PLLA fibers and HA microparticles; ES03 (C, C'): Composite material of PLLA fibers and HA microparticles loaded with PACur and ES06 (D, D'): Composite material of PLLA fibers and HA microparticles loaded with curcumin.

Using ImageJ software for image analyses, the following results were obtained.

As can be appreciated in figure 7.38, cellular density resulted to be bigger in composite systems loaded with curcumin and PACur. It was determined that there is a statistically significate differences between drug loaded composite materials and the unloaded. Also demonstrate the favorable influence of curcumin, conjugated or not, over cell proliferation morphology.
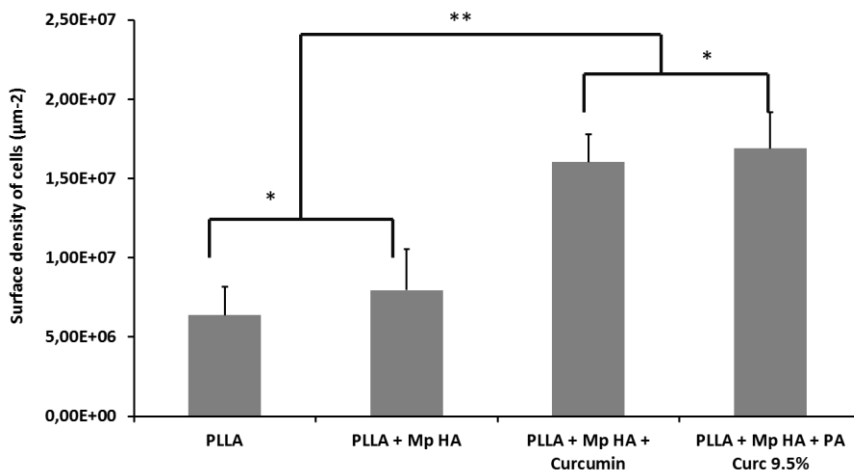
Figure 7.38 Cellular density of L929 cells on different composite systems. (*) no significant differences statistically, (**) significant statistical difference

Likewise, cellular distribution happens to be better in the same both composite materials which are loaded with curcumin (**ES06**) or PACur (**ES03**). There were no significant difference between **ES03** and **ES06**,

which means that conjugation of curcumin do not produce any additional effect on cell proliferation under these conditions.

On the other hand, cell proliferation on **ES01** (ES PLLA) and **ES02** (ES PLLA + MPs HA) was statistically equal between them, but significantly lower in comparison que the drug loaded composite material.

That means that morphology of composite material by itself did not have an additional effect on the rate of proliferation of cells L929, but it was clear that curcumin, conjugated or not is having an additional effect on this cells proliferation. The higher proliferation observed in ES03 and ES06 composite membranes was due to curcumin and PACur influence on cells behavior.

Results shown in figure 7.39 corroborated the observations previously mention.

Cell morphology, in terms of the shape that cells adopt in contact with the materials was also affected mainly by the presence or absence of drugs (Curcumin o PACur without significant difference between them) more that the topology of the material surface under the conditions on these preliminary *in vitro* assays.

According to the graphic of cell roundness (Figure 7.39) cells were more extended when composite membranes were loaded with curcumin or PACur in comparison with cell observed in **ES01** (ES PLLA) and **ES02** (ES PLLA + MPs HA), where cells adopted a spherical shape, as can be appreciated in figure 6.36.
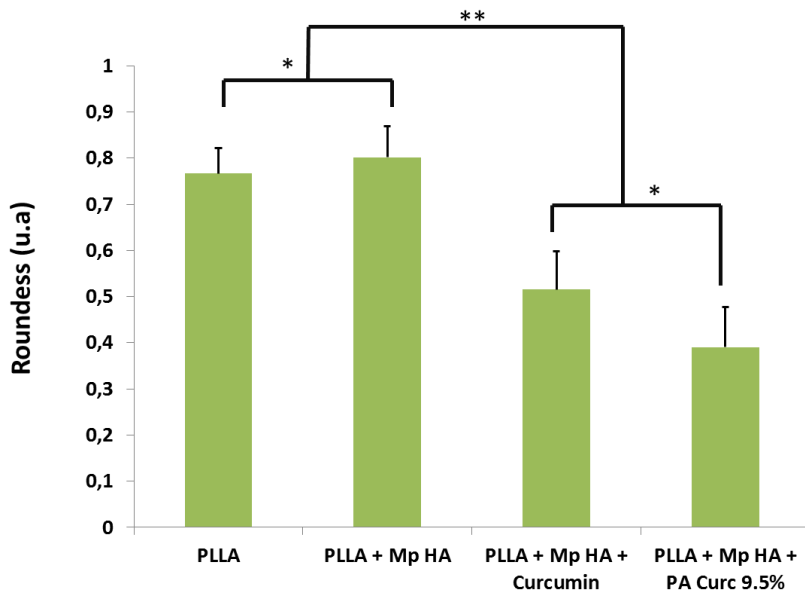
Figure 7.39 Cellular distribution of L929 cells on different composite systems. (*) no significant differences statistically, (**) significant statistical difference

- <u>Analysis of cell proliferation and distribution by Immunofluorescence and Scanning Electron Microscopy (SEM)</u>

After 1 day, confocal microscopy images (Figure 7.40) demonstrated those fibroblasts are growing in all membranes but with special affinity a higher rate over composite materials with Curcumin and PACur.
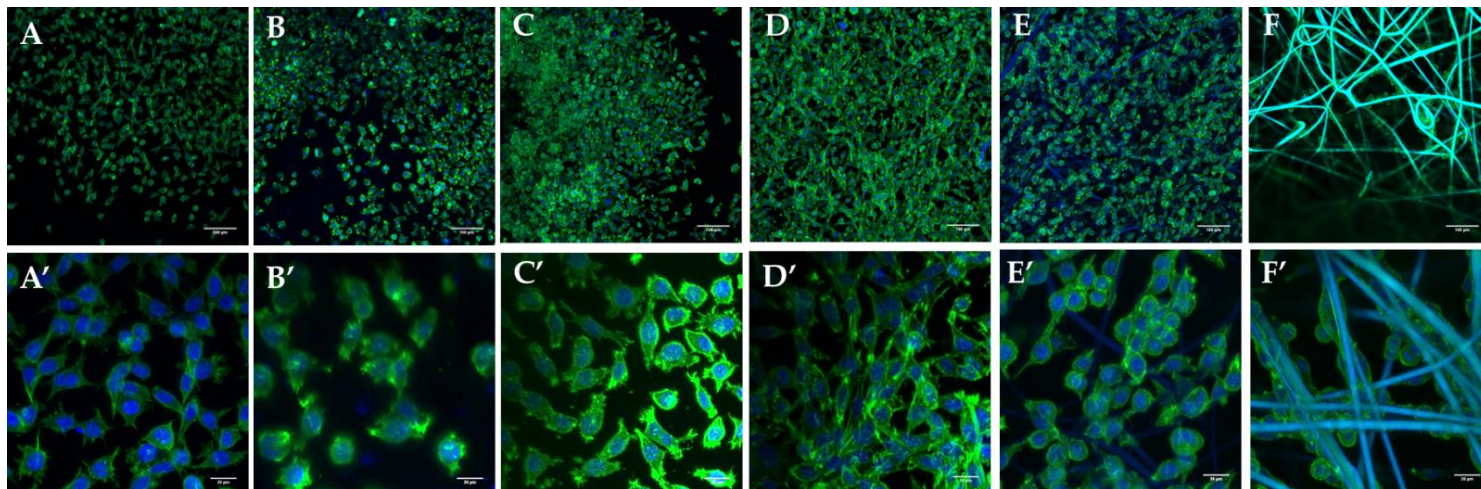
Figure 7.40. Comparison of confocal microscopy images of the different simple and composite materials after 1day of culture with fibrobroblasts L929 cells with phaloydin (green) to stain the cytoskeleton of cells and DAPI (blue) to stain the nuclei. Images were taken at to magnification 10X (A-F) and 40X (A'-F')

ES01 (A, A'): Simple membrane of PLLA; **ES02 (B, B')**: Composite material of PLLA fibers and HA microparticles; **ES03 (C, C')**: Composite material of PLLA fibers and HA microparticles loaded with PACur; **ES04 (D, D'):** Simple membrane of PLLA loaded with PACur; **ES05(E, E'):** Simple membrane of PLLA loaded with curcumin; and **ES06 (F, F'):** Composite material of PLLA fibers and HA microparticles loaded with curcumin.
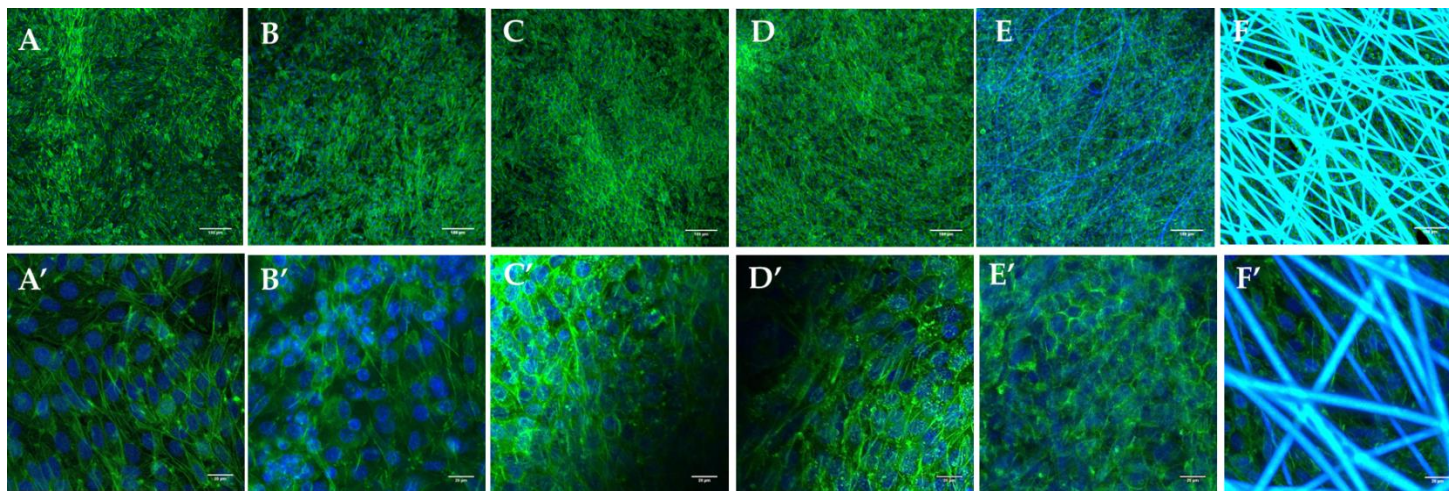
Figure 7.41. Comparison of confocal microscopy images of the different simple and composite materials after 7 day of culture with fibrobroblasts L929 cells with phaloydin (green) to stain the cytoskeleton of cells and DAPI (blue) to stain the nuclei. Images were taken at to magnification 10X (A-F) and 40X (A'-F')

ES01 (A, A'): Simple membrane of PLLA; **ES02 (B, B')**: Composite material of PLLA fibers and HA microparticles; **ES03 (C, C')**: Composite material of PLLA fibers and HA microparticles loaded with PACur; **ES04 (D, D'):** Simple membrane of PLLA loaded with PACur; **ES05(E, E'):** Simple membrane of PLLA loaded with curcumin; and **ES06 (F, F'):** Composite material of PLLA fibers and HA microparticles loaded with curcumin.

After 7 days fibroblast had completely covered the surface of all simple and composite membranes (Figure 7.41). Nevertheless, it was difficult to observe the cells seeded on simple membranes **ES04** (ES PLLA + PACur) and **ES05** (ES PLLA + Curcumin) due to the self-fluorescence of the fibbers which interfered with the cells fluorescence.

Scanning Electron Microscopy images of the same samples provides more information about the changes in cells morphology seeded in these materials after two different times: 1day and 7d.

Images n figure 7.42 corroborated the observations described for **ES01** (ES PLLA: A, A') simple membrane and the composites (**ES02:** B, B', **ES03:** C, C' and **ES06:** D, D'). In all tis cases, cells are extending by the whole mats surface.   Different behaviour was observed in simple membranes of PLLA fibbers loaded with curcumin (**ES05:** F, F')   and PACur (**ES04:** E, E'). In these cases, it was observed that cells were growing not only adhered to the fibbers but along the fibbers.

SEM images of samples after 7d to have been seeded (figure 7.43) showed that the simple membranes **ES01** and **ES04**, as well as the composites membranes (**ES02, ES03** and **ES06**) were almost completely covered by cells which look like a "cell carpet".

In contrast to these observations, cells seeded onto **ES05** (ES PLLA + Curcumin) made a different structure with channels. Fibbers were gathered by the cells and adopted a completely different arrangement in comparison with the other systems.
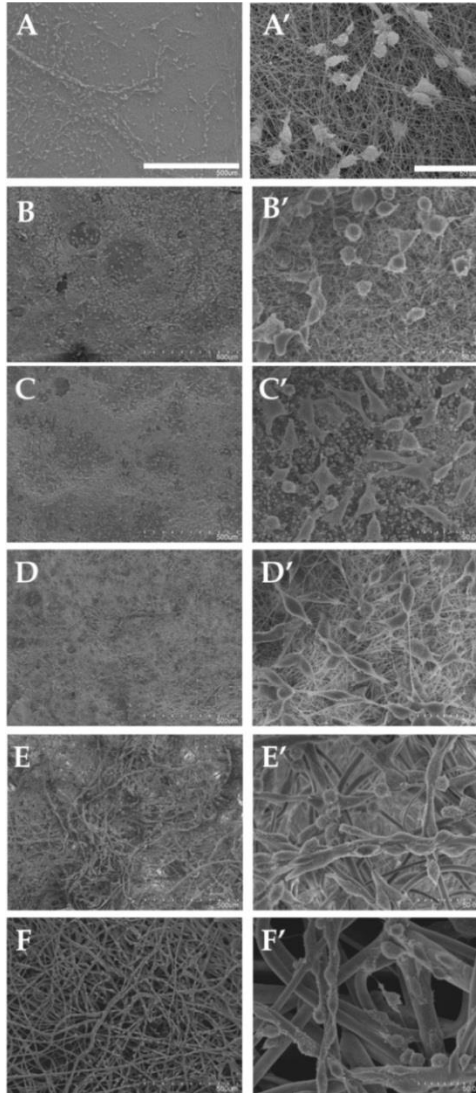
Figure 7.42   Comparison of scanning electron microscopy images of the different simple and composite materials after 1 day of seeded with fibroblasts L929 cells.   Condition: 10kV and WD=9mm. Images were taken at to magnification 100X (A-F) and 700X (A'-F').

ES01 (A, A'): Simple membrane of PLLA; ES02 (B, B'): Composite material of PLLA fibers and HA microparticles; ES03 (C, C'): Composite material of PLLA fibers and HA microparticles loaded with PACur; ES06 (D, D'): Composite material of PLLA fibers and HA microparticles loaded with curcumin. ES04 (E, E'): Simple membrane of PLLA loaded with PACur; and ES05 (F, F'): Simple membrane of PLLA loaded with curcumin
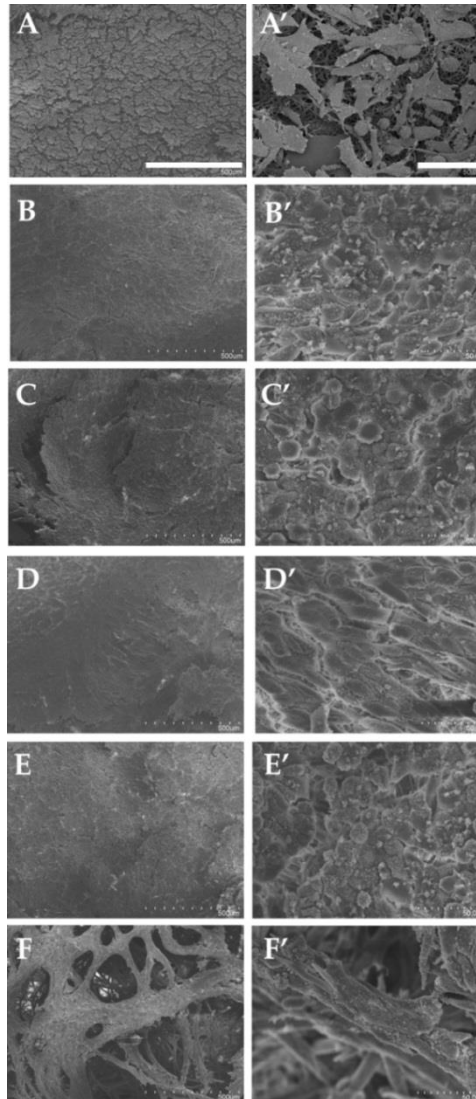
Figure 7.43   Comparison of scanning electron microscopy images of the different simple and composite materials after 7 day of culture with fibroblasts L929 cells.   Condition: 10kV and WD=9mm. Images were taken at to magnification 100X (A-F) and 700X (A'-F').

ES01 (A, A'): Simple membrane of PLLA; ES02 (B, B'): Composite material of PLLA fibers and HA microparticles; ES03 (C, C'): Composite material of PLLA fibers and HA microparticles loaded with PACur; ES06 (D, D'): Composite material of PLLA fibers and HA microparticles loaded with curcumin. ES04 (E, E'): Simple membrane of PLLA loaded with PACur; and ES05 (F, F'): Simple membrane of PLLA loaded with curcumin

7.4. Discussion

7.4.1. Synthesis and characterization Poly (L-lactic) acid membranes and composite systems

According with the results showed in the previous section, it was possible to obtain "simple membranes" as well as "composite membranes" following the methodology proposed in this work.

As expected, each system require specific condition of operation to be able to produce materials with the desire characteristics, which are fibers with nanometric diameter size, very few defects as beats, and in case of composite materials, relative homogeneous distribution of microparticles through the mat.

Likewise, images obtain by SEM microscopy showed that the "one step procedure" is more efficient than "the two steps procedure" methodology for mixture preparation.

These results are very interesting because demonstrate that the original emulsion plays a relevant function to obtain the composite membranes.   The emulsion not only guarantee that HA-MPs will preserve their spherical, dehydrated structure but also that the will be well disperse and distributed in the final mixture.   This condition is critical to be able to electrospun the MPs, otherwise, MPs could aggregate and form sediments before it was possible to for the fiber, making as consequence that only a few amount or nothing of MPs were present in the final material after electrospinning process.

Besides, the "One step procedure" guaranties that even the drug that was not possible to encapsulate into de microparticles is going to be retained in the second structure, constituted by the ES PLLA fiber mat. Also, loss of material is reduced, because HA MPs do not need to be separated from the emulsion, preventing aggregation of smaller microparticles during the purring step in acetone.

The main disadvantage of this methodology is that resulting membranes must be carefully washed to eliminate any possible residue of any toxic reactive used during the fabrication procedure.

7.4.1.1. Characterization of membranes morphology by SEM

Image analyses of SEM pictures reveals that it was possible to obtain nanometric fibers with very few defects with PLLA alone, and then it was also possible to include microparticles in the net, which were enveloped by the PLLA fibers, providing an additional point of control for the release kinetic of drug molecules encapsulated into de microparticles.

It is important to notice that the addition of curcumin or PACur to PLLA solution produced a very big difference among the morphology of the fibers of those called as "simple membranes materials".

ES01, which is composed 100% by PLLA present very thin fibers, the surface is smooth, and the weave was tighter than the weave of **ES05** or **ES06**.

ES05 was the result of a ternary solution composed by dichloromethane (DCM) as solvent, PLLA and Curcumin as solutes.

Both PLLA and curcumin are completely soluble in DCM, so in this case we have dissolution similar to the PLLA in DCM.

Viscosity was not measure but, even though, it is possible to expect to this value should be similar because the polymer is in higher concentration than curcumin and therefore PLLA is going to be the main responsible of the value of this property.

Nevertheless, the presence of curcumin molecules in the solution caused that it was necessary to increase the feeding rate during the electrospinning process, because it was observed that under the same condition used for PLLA solution electrospun, it was impossible to obtain fibers.

Similar behavior was observed with **ES04**, which came from a ternary dissolution of PLLA and PACur in DCM.

Notice that PACur is an amphiphilic compound. These polyacetals are completely soluble in organic non-polar solvent, as DCM, as well as, in polar solvents as water.

PACur is not able to form micelles, but due to the polar chain of PEG present in their structure it is able to interact with polar molecules like water.

Curcumin molecules in the main chain represent the hydrophobic moiety, increasing the affinity of PACur with non-polar solvents.

ES04 and **ES05** have in common that the fibers obtain by electrospinning are much bigger that fibers of PLLA alone, besides they have porous.

It is possible that during the electrospinning process when solvent is evaporated a phase separation took place, PLLA and Curcumin (or PACur) become solid again, then the low affinity between them due to their different chemical nature (PLLA is hydrophobic and PACur is hydrophilic), the way they interact may be responsible of producing the porosity in the fibers.

But this microscopic characteristic is not the only important difference when the "simple membranes" are compared.

Macroscopically there are clear changes from one material to the other.

The most obvious is the color. Curcumin is bright yellow, so, **ES05** is also bright yellow, **ES04** is pale yellow despite PACur is dark yellow, and **ES01** is white as PLLA powder.

But the really interesting difference is in texture, mechanical properties and wettability.

These aspects will be considered later on following sections.

At this point we it could be said that incorporation of curcumin to the PLLA solution modifies the fiber properties in comparison with PLLA fibers alone. Also, conjugation of curcumin as PACur, print similar

behavior for electrospinning process, similar microscopic morphology but clear different macroscopic characteristic.

In the other hand, it was observed when composite membranes were compared that the main difference in the microparticles density. **ES06**, the membrane with PLLA fibers and HA-MPs loaded with curcumin is the material with the higher density of MPs, followed by **ES02**, the membrane with PLLA fibers and HA-MPs without load, and finally, ES03 the membrane with PLLA fibers and HA-MPs loaded with PACur.

In this case the presence of PACur seems to have an unfavorable effect over the system. Even though, the microscopic morphology is very similar for the three materials, with thin fibers in the same order of magnitude but MPS from **ES03** are much bigger than MPs in **ES02** and **ES06.**

Nevertheless, macroscopic properties seem to be very similar, as shown in next sections.

7.4.1.2. *Determination of membrane composition and thermal properties by TGA and DSC*

TGA analyses corroborated that in all cases for composite systems the main component is PLLA, as expected, always around 95-72% for PLLA, 10-7% for HA and 5-0.3% for curcumin conjugated or not.

Taking in account this results, information from DSC analyses could by better understood.

PLLA Tm remains with relative small variation, but melting enthalpy values change significantly when MPsHA loaded and unloaded are present in the system as well as in simple system where PLLA is mixed with curcumin or PACur, as expected because on each case the mass fraction of PLLA in the system is bigger than the other components.

7.4.1.3. *Mechanic Tensile properties of membranes*

Composition also affects the mechanical properties of these materials. As shown in result section there is a very clear relation between the presence of MPs and the increase or decries of tensile strength. But it is absolutely clear than in simple systems the additions of curcumin increase considerably the tensile strength of the mat in comparison with PLLA alone, due to it high hydrophobicity y bigger size of the fiber this material results easier to handle in comparison with PLLA ES with equivalent dimensions. Also, **ES04** (ES PLLA + PACur) are very easy to handle but its texture in similar to cotton and is very hydrophilic, able to absorb water as a cotton patch.

7.4.1.4. *Encapsulation Efficiency and Total Drug Loading*

As explain before, TGA and DCS analyses corroborate that membranes are loaded with curcumin or PACur, depending on the system analyzed.

Direct measures by UV spectroscopy support the previous results.

Nevertheless, the composite system with MPsHA loaded with PACur resulted to have the worst encapsulation efficiency. That means that the protocols still need to be improved for this kind of system.

7.4.1.5. Release Kinetic studies

As can be observed in the graph of profile release, the slower is the system composed by the mixture of PLLA and Curcumin. This is logical because curcumin is hydrophobic; therefore these molecules possess higher affinity for PLLA fiber than for the aqueous medium surrounding.

On the other hand, the system with the mixture PLLA and PACur is the faster because PACur in amphiphilic, by possess high affinity for aqueous medium, so these molecules will diffuse throw the surface of fibers, taking advantage of the high porosity of this fibers, which is product of this mixture.

Finally, systems with microparticles of HA loaded with curcumin seem to present an initial fast release, maybe due to the heterogeneity of the system, but immediately adopt the same kinetic than system with MPHA loaded with PACur. This could be explained because both loaded components are into the matrix of MPS and they should wait until PLLA shell led them diffuse to the surface.

That is why the behavior observed when only loaded MPs release kinetic are compare at pH 7.4 is different to the behavior of those when MPs are into the PLLA fiber.

7.4.1.6. Preliminary degradation studies

SEM images revealed that the six materials produced by the proposed procedure, the simple membranes as well as the composite

membranes are stable in aqueous medium when pH is 7.4 and mild temperatures as 37ºC, similar to the internal human body temperature.

Supernatant in contact with samples at different times where analyzed by GPC and RP-HPLC in order to determine degradation products dissolved in the aqueous medium, but any kind of compound was detected. Samples of each time of degradation where weighted after drying under vacuum at 40ºC by 24h and weight loss was not detected.

This behavior can be attributed to PLLA high stability in front to hydrolysis under neutral conditions and mild temperatures. As demonstrated through thermogravimetric analyses, the main component in all membranes is PLLA, and the absence of change in surface morphology of MPs HA present in the composite materials point at MPs are inside the PLLA fibers as it was desired to be able to provide and additional point of control in the release kinetic of drug loaded, besides a matrix to keep MPs immobilized in the membranes.

7.4.2. In vitro studies

Cytotoxicity study demonstrated that any of the analyzed materials resulted to be cytotoxic; therefore it is possible to conclude that the procedure proposed for simple as well as composite membranes do not left any toxic residual substance.

On the other hand, there were clear differences with respect the cell affinity when surface density and cell distribution it are compared among the different materials.

Another interesting result was the influence of curcumin, conjugated or not, on cells proliferates. Surface materials did not show any particular difference when membranes are unloaded. Instead, cells showed a significant higher proliferation in drug loaded simple as well as composite materials. In fact cells are able to adopt extended shape, similar to the elongate shape describe in literature for fibroblast morphology in normal skin tissue. Besides, seeded cells were able to completely cover the surface material, that it a desirable characteristic for system design for wound healing.

Particularly interesting was the case of structures formed be the cells after 7 days in material **ES05**, the simple membrane constituted by PLLA fibers loaded with curcumin.

Some kind of channels were built by cells which were growing along the fibers, then cells created links among them until forming micro structures through the membrane, joining the PLLA fibers intro wide columns envelop by cell's shells.

More biological studies should be done in order to unravel the entire biologic and biomechanics potential of these materials and as well as e better understanding of how curcumin is influencing the cells proliferation.

7.5. Conclusions

One step methodology was corroborated as the most efficient technique for fabrication of composite systems based of combination of microparticles with electrospinning membranes.

Image analyses of SEM pictures reveals that it was possible to obtain nanometric fibers with very few defects with PLLA alone, and then it was also possible to include microparticles in the net, which were enveloped by the PLLA fibers, providing an additional point of control for the release kinetic of drug molecules encapsulated into de microparticles

This technique makes possible to obtain relatively homogenous systems with typical thermal properties of materials that could be used as parameters for quality control for standardized fabrication.

At this point we it could be said that incorporation of curcumin to the PLLA solution modifies the fiber properties in comparison with PLLA fibers alone. Also, conjugation of curcumin as PACur, print similar behavior for electrospinning process, similar microscopic morphology but clear different macroscopic characteristic.

Mechanical properties are dramatically affected for different composition of the system.

It was corroborated that the six systems of membranes studied are stable after seven days of soaking in aqueous PBS 1x pH 7.4 and 37ºC.

It was possible to modulate the drug released kinetic from the different systems. As expected, the composite material provides an additional point of control on the release kinetic of loaded molecules in comparison with the release from microparticles by themselves, but only with the non-conjugated drug.

The conjugation of Curcumin do not exerts a significant influence on the release from "composite membranes" but it does have difference when it is release from "simple membranes". In the last case, the higher affinity of PACur with aqueous medium promotes the diffusion of conjugate molecules from the fibers to outside.

Biological *in vitro* studies demonstrated that composite system are non-cytotoxic, and promotes fibroblast proliferation with cell morphology similar to normal tissue

Composite membrane materials loaded with curcumin or PACur promotes fibroblast to adopt an elongated morphology, in contrast with unloaded composite membrane, demonstrate the influence of drug loaded into the material.

Simple membranes loaded with Curcumin and PACur also allowed the proliferation of fibroblast but with preferment orientation longwise the fiber.

Morphological difference observed between the fibroblast cultured on "composite membranes" and those cultured on "simple membranes" reflex the influence of mechanical properties of the surface over the

interaction with cells independently from the biochemical stimuli from drugs loaded.

Composite systems proposed in this research could be good candidates to by evaluated *in vivo* models for promoting wound healing.

8. GENERAL DISCUSSION

Current approaches for the replacement of damaged tissues/organs based conventional treatment and strategies lack of effectiveness in many clinical situations. Thus, there is an urgent need for alternatives to overcome most of the limitations of existing techniques. In this context, innovative approaches including tissue engineering or regenerative medicine, controlled drug delivery systems and nanomedicines (such as Polymer Therapeutics) are emerging as promising options to solve this problem. Moreover their combination offers countless advantages and a myriad of possibilities to face a vast range of disease targets that will not be possible with a single technology.

With that in mind, the aim of this thesis was to design intelligent composite system for tissue regeneration through the combination of biomaterial science and nanoconjugate synthesis, in order to have a structure with double control on drug release kinetics, and with the possibility to be used on different clinical applications, such as implants in damage tissue. We combine the use of Polymer Therapeutics with an appropriate scaffold made with innovative techniques aiming to obtain an innovative construct to be used as topic or surgical implants able to promote tissue regeneration with the aim of both act as support for cellular growth, and as therapeutic device by the local release of bioactive agents. This novel biomedical device consisted on composite systems composed by three main elements: Polymer conjugates (Polymer-Protein Trypsin and/or

Polymer-Drug Curcumin conjugates); biodegradable polymeric micro-particles (MPs) of hyaluronic acid (HA) and biodegradable polymeric membranes of Poly(L-lactic acid). The combination of these complex systems will result in a novel structure with particular physico-chemical, mechanical and biological properties, which are characteristics of a new biomaterial.

In order to accomplish the already exposed goals of this highly ambitious project, the initial efforts were devoted to the synthesis optimization of biodegradable polyacetals to be used as polymer carriers for the development of both, Polymer-Protein Conjugates and Polymer-Drug Conjugates.

On one hand, Polymer-Protein Conjugates were developed by applying two different approaches: a) Protein PEGylation, as example of system with non-biodegradable polymer carriers and b) Protein conjugation with polyacetals, as example of system with a biodegradable polymeric carrier under acidic conditions. The second one, pursued to develop the so called polymer-masking-unmasking-protein therapy (PUMPT), described first by Duncan et al[87,99,101–104,155,156]. This latter strategy will enable the protein protection while traveling to the therapeutic target and/or will allow controlled release at the target site promoted by the polymer degradation.

Regarding the first strategy, it consisted on the PEGylation of the model protein Trypsin[32,33,112,157] with MeO-PEG-COOH and succinoylated MeO-PEG-OH both with the same molecular weight (2000 g/mol) in order to compared the possibility to have two

different linkers with PEG chain: a) biodegradable ester link (succinoylated PEG-OH) and b) not biodegradable amide link (PEG-COOH). Reaction was successfully accomplished with MeO-PEG-OH succinoylated, achieving a Trypsin loading of 20wt% of total conjugate weight. Although the enzymatic activity of Trypsin was shown to be reduce upon conjugation (64% of total activity for Trypsin-PEG$_{2000}$), this system resulted to be stable enough to be used as model for its encapsulation in HA microparticles.

For the PUMPT strategy, polyacetals functionalized with COOH groups following different strategies and based on fragments of PEG-diol 4000 Da units were synthesized and physico-chemically characterized. Once again Trypsin has been used as a model protein. Two different PA-COOH were obtained, one of them including a succinoylated linker in order to study the linker influence in the PUMPT effect. Moreover, different conjugates with various polymer to protein ratios were developed with total protein contain ranging from 20-35wt%, in order to study the influence of such ration in the masking/unmasking capability of the system.

The biological activity of the masked and unmasked protein was assessed using N-benzoyl-L-arginine-p-nitroanilide (L-BAPNA) as a substrate. This way, the ability of the protein to recover its full initial activity after the PUMPT process could be studied. Results obtained showed that enzymatic activity of Trypsin was partially suppressed at pH 7.4, when it was conjugated, in comparison with naked protein at the same condition. Moreover, Trypsin activity could be recovered after incubation of the conjugates at pH 6.5 for 2h, regardless the

linker used. These results proved that protein was unmasked by effect of acidic pH, responsible of hydrolysis of polyacetals.

On the other hand, polymer-drug conjugates based on the biodegradable polyacetals and the antioxidant drug curcumin have been effectively synthesized and physico-chemically characterized. Curcumin molecules were incorporated into a poly(ethylene glycol) (PEG) based polyacetal carrier by applying an improved polyacetal synthesis. This approach consisted on the reaction among short PEG-OH chains, curcumin and triethylene glycol-divinylether units using p-toluensulfonic acid as acid catalyst, without the need for biodegradable linkers. With this strategy we were able to obtained high yields of water soluble polymer conjugates with desirable drug loadings (total drug loading of 10.8 wt% and less than 0.2wt% of free drug) and controlled tailored molecular weights (Mw 17000–20000 g/mol) with acceptable polydispersities. Controlled drug release under acidic pH was obtained with this system since PACur were found to be hydrolytically cleaved under acidic conditions (such as those found in endosomes, lysosomes or the extracellular fluid of some inflamed areas) yielding the free drug curcumin. Additionally, they were stable over prolonged periods of time at pH 7.4 mimicking blood plasma scenario. Additionally, cytotoxicity assays were performed as a proof of safety of these constructs for their application in wound healing/tissue repair. The tested PACur resulted to be non-toxic within the therapeutic window for curcumin application in wound healing, validating its application.

Once our Polymer-Protein/Drug Conjugates were synthesized and properly characterized, the next stage involved their encapsulation into hyaluronic acid microparticles (MPs-HA). HA was selected due to its multiple roles in nature, as well as its inherent biocompatibility and biodegradability what makes HA an attractive biomaterial in drug delivery and tissue engineering.[130–133,148,158–162] In our concrete final system, HA microparticles can provide bigger surface area that could presumably improve tissue integrating and facilitate drug delivery[130].

Two different model systems were developed at this stage: on one side, MPs-HA were loaded with the polymer-drug conjugate PACur and free Cur[148]. These systems were physico-chemically characterized, and their drug release profiles were evaluated under acidic and neutral pH. From the results obtained, it could be concluded that as expected, a controlled drug release was only possible with MPs-HA loaded with PACurc. In this system, a sustained release of curcumin is achieved at pH 6.5 (up to ~60% drug release) while the system is relatively stable at pH 7.4 (only 15% drug release). In the case of MPs-HA loaded with Curcumin, the same release profile (up to ~60% drug release) was obtained in both cases. These results validated our system for the purposes of this thesis dissertation.

On the other hand, hyaluronic acid microparticles were loaded with the polymer-protein conjugate PEG-Trypsin and free Trypsin. These systems were also physico-chemically characterized, and their drug release profiles were evaluated only at neutral pH due to Trypsin degradation at acidic pH. In this case, a sustained release was obtained, validating our MPs for the controlled delivery of Trypsin. The

next step would be the encapsulation of our PUMPT conjugates that will provide additional benefits regarding protein stability and controlled release under acidic pH, our real scenario.

Once hyaluronic microparticles were preliminary validated, the following step was their inclusion in our final device, based on a polymeric composite system. In order to accomplish our goal, the versatile methodology utilizing electrospinning techniques (ES) was optimized for our purposes. Poly (L-lactic acid) (PLLA), a biodegradable and biocompatible polymer, was exploited to generate nonwoven fiber membranes which will provide a second point of control for a controlled and sustained drug release in our dually-controlled final system.

First, the synthesis of PLLA random nonwoven fibers with nanometric diameters was optimized by varying different parameters: a) PLLA solution concentration, b) the voltage applied, c) distance between the needle tip and the collector, and d) the feeding rate.

Then, in order to validate the PLLA technology, PLLA random nonwoven fibers membranes were loaded with the model drug Curcumin[61] or PACur (*simple membranes*) or with micro particles loaded with Cur or PACur, inserted among or inside the fibers (*composite membranes*[71]). The introduction of MPs into the PLLA fibers was performed by means of two methodologies: one direct approach without MPs precipitation, and a two-step approach that includes MPs isolation. The first approach resulted to be the most efficient.

A complete and exhaustive physico-chemical characterization was performed through the subsequent analysis: (i) membrane composition and thermal properties by TGA and DSC, (ii) membranes wettability by contact angle measurement, and (iii) mechanic tensile properties of membranes systems.

Selected membranes were evaluated in terms of drug release profile obtaining adequate drug release profiles for membranes loaded with MPsHA-Cur and MPsHA-PACur at pH 7.4. Furthermore, as membrane degradation time is a highly important parameter to be taken into account to establish the suitability of materials for a specific biomedical application, membrane degradation profile was also investigated in preliminary studies. The compiled results showed that our PLLA membranes were not degraded up to 7 days of soaking in aqueous solution of PBS 1X at pH 7.4 and 37°C. This behavior was expected since PLLA is a material highly resistant to aqueous hydrolysis at neutral pH. Longer degradation times and membrane degradation under acidic conditions are planned to be done.

In vitro cytotoxicity studies were performed in L929 fibroblast cells and none of the systems resulted to be cytotoxic at the concentrations tested after 48 hours of treatment. Finally, studies of cell adhesion and morphology were performed in the same cell line. Analysis of cellular density and morphology by immunofluorescence cells showed that morphology of composite material by itself did not have an additional effect on the rate of proliferation of cells. However, it was clear that ES systems loaded with MPs with curcumin, conjugated or not in PACur were having an additional effect on cell proliferation. These results

were corroborated by the analysis of cell proliferation and distribution by Immunofluorescence and Scanning Electron Microscopy which demonstrated that cells owned a significant higher proliferation in drug loaded simple as well as composite materials. In fact, cells were able to adopt their typical fibroblast morphology. Besides, seeded cells were able to completely cover the surface material, a desirable feature in a system designed for wound healing.

Further *in vitro* as well as *in vivo* biological studies are planned to be done in order to unravel the entire biologic and biomechanics potential of these materials in the biological settings.

9. FINAL CONCLUSIONS

<u>Synthesis and Characterization of Polymer-Protein conjugated systems by two approaches: PEGylation and Protein-Polyacetal Conjugates</u>

1.   Polymer-Protein Conjugates have been effectively synthesized and characterized by applying two different approaches: i) Protein PEGylation, as example of system with non-biodegradable polymer carriers and ii) Protein conjugation with polyacetals (PA), as example of system with a biodegradable polymeric carrier under acidic conditions aiming to obtain a PUMPT system.

2.   PEGylation of Trypsin with MeO-PEG-COOH of 2000 g/mol resulted in a partial reduction of Trypsin activity, and an increase in its stability, what encouraged us in its use as models to be encapsulated in HA microparticles.

3.   Functionalized PA backbones have been synthesized and physico-chemically characterized for the conjugation of Trypsin to generate an acid sensitive PUMPT system. Influence of the presence of a linker (succinoylated PA) and the effect of the proportion of polymer to protein in the masking/unmasking capability of the PA has been studied. The protein conjugate was stable and protein activity was hidden at neutral pH (7.4). However, the ability of the protein to recover its full initial activity after the PUMPT process under acidic pH has been demonstrated.

Synthesis and Characterization of Curcumin Polyacetals, PACur

4.   Within this thesis, Polymer Therapeutics for the conjugates based on the biodegradable polyacetals and the antioxidant curcumin have been effectively synthesized (PACur), with high yields and the expected desired drug loadings.

5.   Controlled drug release of the free drug curcumin from PACur was achieved under acidic conditions (such as those found in endosomes, lysosomes or the extracellular fluid of some inflamed areas). Additionally, they were found to be stable over prolonged periods of time at pH 7.4 mimicking blood plasma.

6.   Cytotoxicity assays performed as a proof of safety ensured that PACur conjugates are not toxic within the therapeutic window for curcumin applications in wound healing, what validates its use in this disease target.

Hyaluronic acid microparticles, MPs HA

7.   HA microparticles have been effectively synthesized and characterized with good encapsulation efficiencies. From the systems built, it could be concluded that that the stirring rated, the organic solvent used for final emulsion, as well as chemical nature and hydrophilicity of the loaded compound do affect the morphology of resulting microparticles.

8.   Release kinetics of all systems encapsulated from MPs HA was highly dependent on the pH what could be attributed to the swelling properties of HA and interaction of loaded compounds with MPs HA

matrix. Nevertheless, For MPs HA- PACur, controlled release of PACur was achieved under acidic pH as expected. In the case of MPs HA- PEG-Trypsin, sustained release was achieved at neutral pH.

Polymeric composite system designed to promote a long lasting, stable, localized and controlled drug release

9.   Composite systems based on PLLA fibers and loaded MPs HA with dual mechanism of controlled release have been synthesized and characterized.

10.   For that, several methodologies for the fabrication of electrospinning-based systems have been explored. For the development of composite systems based of combination of microparticles with electrospinning membranes, the one-step method has been demonstrated to be the most efficient.

11.   This technique allowed us to obtain relatively homogenous systems with adequate thermal and mechanical properties in parallel with solution stability for materials to be used in bioapplications.

12.   As expected, the composite material provides an additional point of control on the release kinetic of loaded molecules in comparison with the release from parent microparticles, but only with the non-conjugated drug.

13.   Biological *in vitro* studies demonstrated that composite system is non-cytotoxic, and promotes fibroblast proliferation with cell morphology similar to normal tissue. However, cell proliferation was higher in those systems with Cur, conjugated or not. Furthermore,

morphological differences were observed between the fibroblast cultured on "composite membranes" and those cultured on "simple membranes" reflecting the influence of mechanical properties of the surface material over the interaction with cells.

14.   Composite systems proposed in this research are considered promising candidates to by evaluated *in vivo* models for promoting wound healing.

REFERENCES

(1)   Place, E. S.; Evans, N. D.; Stevens, M. M. Complexity in biomaterials for tissue engineering. *Nat. Mater.* **2009**, *8* (6), 457–470 DOI: 10.1038/nmat2441.

(2)   Vicent, M. J.; Duncan, R. Polymer conjugates: nanosized medicines for treating cancer. *Trends Biotechnol.* **2006**, *24* (1), 39–47 DOI: 10.1016/j.tibtech.2005.11.006.

(3)   Duncan, R.; Vicent, M. J. Polymer therapeutics-prospects for 21st century: the end of the beginning. *Adv. Drug Deliv. Rev.* **2013**, *65* (1), 60–70 DOI: 10.1016/j.addr.2012.08.012.

(4)   Vicent, M. J.; Ringsdorf, H.; Duncan, R. Polymer therapeutics: clinical applications and challenges for development. *Adv. Drug Deliv. Rev.* **2009**, *61* (13), 1117–1120 DOI: 10.1016/j.addr.2009.08.001.

(5)   Greco, F.; Vicent, M. J. Combination therapy: Opportunities and challenges for polymer–drug conjugates as anticancer nanomedicines. *Adv. Drug Deliv. Rev.* **2009**, *61* (13), 1203–1213 DOI: 10.1016/j.addr.2009.05.006.

(6)   Duncan, R. Polymer therapeutics: Top 10 selling pharmaceuticals - what next? *J. Control. Release* **2014**, *190*, 371–380 DOI: 10.1016/j.jconrel.2014.05.001.

(7)   Gaspar, R.; Duncan, R. Polymeric carriers: preclinical safety and the regulatory implications for design and development of

polymer therapeutics. *Adv. Drug Deliv. Rev.* **2009**, *61* (13), 1220–1231 DOI: 10.1016/j.addr.2009.06.003.

(8)   Canal, F.; Sanchis, J.; Vicent, M. J. Polymer--drug conjugates as nano-sized medicines. *Curr. Opin. Biotechnol.* **2011**, *22* (6), 894– 900 DOI: 10.1016/j.copbio.2011.06.003.

(9)   Duncan, R. The dawning era of polymer therapeutics. *Nat. Rev. Drug Discov.* **2003**, *2* (5), 347–360 DOI: 10.1038/nrd1088.

(10)   Duncan, R.; Vicent, M. J. Polymer therapeutics-prospects for 21st century: The end of the beginning. *Adv. Drug Deliv. Rev.* **2013**, *65* (1), 60–70 DOI: 10.1016/j.addr.2012.08.012.

(11)   Giménez, V.; James, C.; Armiñán, A.; Schweins, R.; Paul, A.; Vicent, M. J. Demonstrating the importance of polymer-conjugate conformation in solution on its therapeutic output: Diethylstilbestrol (DES)-polyacetals as prostate cancer treatment. *J. Control. Release* **2012**, *159* (2), 290–301 DOI: 10.1016/j.jconrel.2011.12.035.

(12)   England, R. M.; Masiá, E.; Giménez, V.; Lucas, R.; Vicent, M. J. Polyacetal-stilbene conjugates - The first examples of polymer therapeutics for the inhibition of HIF-1 in the treatment of solid tumours. *J. Control. Release* **2012**, *164* (3), 314–322 DOI: 10.1016/j.jconrel.2012.08.017.

(13)   Conejos-Sánchez, I.; Cardoso, I.; Oteo-Vives, M.; Romero-Sanz, E.; Paul, A.; Sauri, A. R.; Morcillo, M. A.; Saraiva, M. J.; Vicent,

M. J. Polymer-doxycycline conjugates as fibril disrupters: an approach towards the treatment of a rare amyloidotic disease. *J. Control. Release* **2015**, *198*, 80–90 DOI: 10.1016/j.jconrel.2014.12.003.

(14)   Barz, M.; Armiñán, A.; Canal, F.; Wolf, F.; Koynov, K.; Frey, H.; Zentel, R.; Vicent, M. J. P(HPMA)-block-P(LA) copolymers in paclitaxel formulations: polylactide stereochemistry controls micellization, cellular uptake kinetics, intracellular localization and drug efficiency. *J. Control. Release* **2012**, *163* (1), 63–74 DOI: 10.1016/j.jconrel.2012.05.024.

(15)   Agarwal, S.; Wendorff, J. H.; Greiner, A. Progress in the Field of Electrospinning for Tissue Engineering Applications. *Adv. Mater.* **2009**, *21* (32-33), 3343–3351 DOI: 10.1002/adma.200803092.

(16)   Agarwal, S.; Wendorff, J. H.; Greiner, A. Use of electrospinning technique for biomedical applications. *Polymer (Guildf).* **2008**, *49* (26), 5603–5621 DOI: 10.1016/j.polymer.2008.09.014.

(17)   Bellan, L. M.; Craighead, H. G. Applications of controlled electrospinning systems. *Polym. Adv. Technol.* **2011**, *22* (3), 304–309 DOI: 10.1002/pat.1790.

(18)   Guorui, J.; Prabhakaran, M. P.; Ramakrishna, S. Stem cell differentiation to epidermal lineages on electrospun nanofibrous substrates for skin tissue engineering. *Acta Biomater.* **2011**, *7* (8), 3113–3122 DOI:

10.1016/j.actbio.2011.04.017.

(19) Jiang, T.; Carbone, E. J.; Lo, K. W.-H.; Laurencin, C. T. *Electrospinning of polymer nanofibers for tissue regeneration*; Elsevier Ltd, 2015; Vol. 46.

(20) Min, B.-M.; Lee, G.; Kim, S. H.; Nam, Y. S.; Lee, T. S.; Park, W. H. Electrospinning of silk fibroin nanofibers and its effect on the adhesion and spreading of normal human keratinocytes and fibroblasts in vitro. *Biomaterials* **2004**, *25* (7-8), 1289–1297 DOI: 10.1016/j.biomaterials.2003.08.045.

(21) Liu, S.; Qin, M.; Hu, C.; Wu, F.; Cui, W.; Jin, T.; Fan, C. Tendon healing and anti-adhesion properties of electrospun fibrous membranes containing bFGF loaded nanoparticles. *Biomaterials* **2013**, *34* (19), 4690–4701 DOI: 10.1016/j.biomaterials.2013.03.026.

(22) Dhurai, B.; Saraswathy, N.; Maheswaran, R.; Sethupathi, P.; Vanitha, P.; Vigneshwaran, S.; Rameshbabu, V. Electrospinning of curcumin loaded chitosan/poly (lactic acid) nanofilm and evaluation of its medicinal characteristics. *Front. Mater. Sci.* **2013**, *7* (4), 350–361 DOI: 10.1007/s11706-013-0222-8.

(23) Sanchis, J.; Canal, F.; Lucas, R. Polymer-drug conjugates for novel molecular targets. *Nanomedicine* **2010**, *5* (6), 915–935.

(24) Duro-Castano, A.; Conejos-Sánchez, I.; Vicent, M. Peptide-Based Polymer Therapeutics. *Polymers (Basel).* **2014**, *6* (2),

515–551 DOI: 10.3390/polym6020515.

(25)   Talelli, M.; Duro-Castaño, A.; Rodríguez-Escalona, G.; Vicent, M. J. *Smart Polymers and their Applications*; Elsevier, 2014.

(26)   Qi, Z.; Yu, H.; Chen, Y.; Zhu, M. Highly porous fibers prepared by electrospinning a ternary system of nonsolvent/solvent/poly(l-lactic acid). *Mater. Lett.* **2009**, *63* (3-4), 415–418 DOI: 10.1016/j.matlet.2008.10.059.

(27)   Xu, J.; Jiao, Y.; Shao, X.; Zhou, C. Controlled dual release of hydrophobic and hydrophilic drugs from electrospun poly(l-lactic acid) fiber mats loaded with chitosan microspheres. *Mater. Lett.* **2011**, *65* (17-18), 2800–2803 DOI: 10.1016/j.matlet.2011.06.018.

(28)   Betbeder, D.; Lipka, E.; Howsan, M.; Carpentier, R. Evaluation of curcumin nanoparticles as a potential therapeutic for wounds. *Int. J. Nanomedicine* **2015**, *10*, 5355–5366 DOI: 10.1016/j.jaad.2014.01.130.

(29)   Krausz, A. E.; Adler, B. L.; Cabral, V.; Navati, M.; Doerner, J.; Charafeddine, R. a.; Chandra, D.; Liang, H.; Gunther, L.; Clendaniel, A.; et al. Curcumin-encapsulated nanoparticles as innovative antimicrobial and wound healing agent. *Nanomedicine Nanotechnology, Biol. Med.* **2015**, *11* (1), 195–206 DOI: 10.1016/j.nano.2014.09.004.

(30)   Kant, V.; Gopal, A.; Kumar, D.; Pathak, N. N.; Ram, M.; Jangir, B.

L.; Tandan, S. K.; Kumar, D. Curcumin-induced angiogenesis hastens wound healing in diabetic rats. *J. Surg. Res.* **2015**, *193* (2), 978–988 DOI: 10.1016/j.jss.2014.10.019.

(31)   Panchatcharam, M.; Miriyala, S.; Gayathri, V. S.; Suguna, L. Curcumin improves wound healing by modulating collagen and decreasing reactive oxygen species. *Mol. Cell. Biochem.* **2006**, *290* (1-2), 87–96 DOI: 10.1007/s11010-006-9170-2.

(32)   Treetharnmathurot, B.; Ovartlarnporn, C.; Wungsintaweekul, J.; Duncan, R.; Wiwattanapatapee, R. Effect of PEG molecular weight and linking chemistry on the biological activity and thermal stability of PEGylated trypsin. *Int. J. Pharm.* **2008**, *357* (1-2), 252–259 DOI: 10.1016/j.ijpharm.2008.01.016.

(33)   Treetharnmathurot, B.; Dieudonné, L.; Ferguson, E. L.; Schmaljohann, D.; Duncan, R.; Wiwattanapatapee, R. Dextrin-trypsin and ST-HPMA-trypsin conjugates: Enzyme activity, autolysis and thermal stability. *Int. J. Pharm.* **2009**, *373* (1-2), 68–76 DOI: 10.1016/j.ijpharm.2009.02.008.

(34)   Stupishina, E. a.; Faizullin, D. a.; Zakharchenko, N. L.; Fedotov, V. D.; Zuev, Y. F. Catalytic activity, structure and stability of trypsin in an AOT-stabilised water-in-decane microemulsion. *Mendeleev Commun.* **2001**, *11* (6), 237–239 DOI: 10.1070/MC2001v011n06ABEH001483.

(35)   Huebsch, N.; Mooney, D. J. Inspiration and application in the evolution of biomaterials. *Nature* **2009**, *462* (7272), 426–432

DOI: 10.1038/nature08601.

(36)   U.S. Departament of health and Human Services.
         RegenerativeMedicine(NIBIB).pdf
         http://report.nih.gov/nihfactsheets/Pdfs/RegenerativeMedicin
         e(NIBIB).pdf (accessed Sep 17, 2015).

(37)   Kleinheinz, S. J. and J. *Regenerative Medicine and Tissue
         Engineering*; Andrades, J. A., Ed.; InTech, 2013.

(38)   Jiang, T.; Carbone, E. J.; Lo, K. W.-H.; Laurencin, C. T.
         Electrospinning of Polymer Nanofibers for Tissue Regeneration.
         Prog. Polym. Sci. **2014**, *46*, 1–24 DOI:
         10.1016/j.progpolymsci.2014.12.001.

(39)   Groeber, F.; Holeiter, M.; Hampel, M.; Hinderer, S.; Schenke-
         Layland, K. Skin tissue engineering - In vivo and in vitro
         applications. *Adv. Drug Deliv. Rev.* **2011**, *63* (4), 352–366 DOI:
         10.1016/j.addr.2011.01.005.

(40)   Caramella, C.; Conti, B.; Modena, T.; Ferrari, F.; Bonferoni, M.
         C.; Genta, I.; Rossi, S.; Torre, M. L.; Sandri, G.; Sorrenti, M.; et
         al. Controlled delivery systems for tissue repair and
         regeneration. *J. Drug Deliv. Sci. Technol.* **2015** DOI:
         10.1016/j.jddst.2015.05.015.

(41)   Custódio, C. A.; Reis, R. L.; Mano, J. F.; Del Campo, A. Smart
         instructive polymer substrates for tissue engineering. In *Smart
         Polymers and their Applications*; Elsevier, 2014; pp 301–326.

(42) Rabkin, E.; Schoen, F. Cardiovascular Tissue Engineering Cardiovascular Tissue Engineering. *Canrdiovascular Pathol.* **2002**, *11*, 305–317 DOI: 10.1016/B978-0-08-055294-1.00177-X.

(43) Chaudhury, K.; Kumar, V.; Kandasamy, J.; RoyChoudhury, S. Regenerative nanomedicine: current perspectives and future directions. *Int. J. Nanomedicine* **2014**, *9* (1), 4153–4167 DOI: 10.2147/IJN.S45332.

(44) DEGIM, Z. G. Use of microparticulate systems to accelerate skin wound healing. *J. Drug Target.* **2008**, *16* (6), 437–448.

(45) Eming, S. A.; Martin, P.; Tomic-canic, M. STATE OF THE ART REVIEW Wound repair and regeneration : Mechanisms , signaling , and translation. *Sci. Transl. Med.* **2014**, *6* (265), 265sr6 DOI: 10.1126/scitranslmed.3009337.

(46) Sun, B. K.; Siprashvili, Z.; Khavari, P. a. Advances in skin grafting and treatment of cutaneous wounds. *Science* **2014**, *941* DOI: 10.1126/science.1253836.

(47) Sen, C. K.; Gordillo, G. M.; Roy, S.; Kirsner, R.; Lambert, L.; Hunt, T. K.; Gottrup, F.; Gurtner, G. C.; Longaker, M. T. Human skin wounds: a major and snowballing threat to public health and the economy. *Wound Repair Regen.* **2009**, *17* (6), 763–771 DOI: 10.1111/j.1524-475X.2009.00543.x.

(48) Peck, M. D. Epidemiology of burns throughout the world. Part I: Distribution and risk factors. *Burns* **2011**, *37* (7), 1087–1100

DOI: 10.1016/j.burns.2011.06.005.

(49)   Daniel S. Kohane. Microparticles and Nanoparticles for Drug
        Delivery. *Biotechnol. Bioeng.* **2007**, *96* (2), 203–209 DOI:
        10.1002/bit.21301.

(50)   Sokolsky-Papkov, M.; Agashi, K.; Olaye, A.; Shakesheff, K.;
        Domb, A. J. Polymer carriers for drug delivery in tissue
        engineering. *Adv. Drug Deliv. Rev.* **2007**, *59* (4-5), 187–206 DOI:
        10.1016/j.addr.2007.04.001.

(51)   Lee, J.-E.; Park, J.-C.; Lee, K. H.; Oh, S. H.; Suh, H. Laminin
        Modified Infection-Preventing Collagen Membrane Containing
        Silver Sulfadiazine-Hyaluronan Microparticles. *Artif. Organs*
        2002, *26* (6), 521–528 DOI: 10.1046/j.1525-1594.2002.06890.x.

(52)   Yue, H. G. and Z. *Basic Principles of Peripheral Nerve Disorders*;
        Rayegani, S. M., Ed.; InTech, 2012.

(53)   Feng, S.; Nie, L.; Zou, P.; Suo, J. Drug-loaded PLGA-mPEG
        microparticles as treatment for atopic dermatitis-like skin
        lesions in BALB/c mice model. *J. Microencapsul.* **2015**, *32* (2),
        201–209 DOI: 10.3109/02652048.2014.995727.

(54)   Wang, X.; Sng, M. K.; Foo, S.; Chong, H. C.; Lee, W. L.; Tang, M.
        B. Y.; Ng, K. W.; Luo, B.; Choong, C.; Wong, M. T. C.; et al. Early
        controlled   release   of   peroxisome   proliferator-activated
        receptor β/δ agonist GW501516 improves diabetic wound
        healing   through   redox   modulation   of   wound

microenvironment. *J. Control. Release* **2015**, *197*, 138–147 DOI: 10.1016/j.jconrel.2014.11.001.

(55) Rambhia, K. J.; Ma, P. X. Controlled drug release for tissue engineering. *J. Control. Release* **2015** DOI: 10.1016/j.jconrel.2015.08.049.

(56) Braghirolli, D. I.; Steffens, D.; Pranke, P. Electrospinning for regenerative medicine: A review of the main topics. *Drug Discov. Today* **2014**, *19* (6), 743–753 DOI: 10.1016/j.drudis.2014.03.024.

(57) Wendorff, J. H.; Agarwa, S.; Greiner, A. *Electrospinning: Materials, Processing, and Applications*; Wiley-VCH Verlag GmbH & Co. KCaA: Weinheim, Germany, 2012.

(58) Jin, G.; Prabhakaran, M. P.; Kai, D.; Ramakrishna, S. Controlled release of multiple epidermal induction factors through core-shell nanofibers for skin regeneration. *Eur. J. Pharm. Biopharm.* **2013**, *85* (3 PART A), 689–698 DOI: 10.1016/j.ejpb.2013.06.002.

(59) Vatankhah, E.; Prabhakaran, M. P.; Jin, G.; Mobarakeh, L. G.; Ramakrishna, S. Development of nanofibrous cellulose acetate/gelatin skin substitutes for variety wound treatment applications. *J. Biomater. Appl.* **2014**, *28* (6), 909–921 DOI: 10.1177/0885328213486527.

(60) Brahatheeswaran, D.; Mathew, A.; Aswathy, R. G.; Nagaoka, Y.; Venugopal, K.; Yoshida, Y.; Maekawa, T.; Sakthikumar, D.

Hybrid fluorescent curcumin loaded zein electrospun nanofibrous scaffold for biomedical applications. *Biomed. Mater.* **2012**, *7* (4), 045001 DOI: 10.1088/1748-6041/7/4/045001.

(61)   Trang Mai, T. T.; Thuy Nguyen, T. T.; Duong Le, Q.; Ngoan Nguyen, T.; Cham Ba, T.; Binh Nguyen, H.; Hoa Phan, T. B.; Lam Tran, D.; Nguyen, X. P.; Seo Park, J. A novel nanofiber Cur-loaded polylactic acid constructed by electrospinning. *Adv. Nat. Sci. Nanosci. Nanotechnol.* **2012**, *3* (2), 025014 DOI: 10.1088/2043-6262/3/2/025014.

(62)   Yakub, G.; Toncheva, a.; Manolova, N.; Rashkov, I.; Kussovski, V.; Danchev, D. Curcumin-loaded poly(l-lactide-co-D,l-lactide) electrospun fibers: Preparation and antioxidant, anticoagulant, and antibacterial properties. *J. Bioact. Compat. Polym.* **2014**, *29* (6), 607–627 DOI: 10.1177/0883911514553508.

(63)   Gandhimathi, C.; Venugopal, J. R.; Bhaarathy, V.; Ramakrishna, S.; Kumar, S. D. Biocomposite nanofibrous strategies for the controlled release of biomolecules for skin tissue regeneration. *Int. J. Nanomedicine* **2014**, *9*, 4709–4722 DOI: 10.2147/IJN.S65335.

(64)   Arnal-Pastor, M.; Martínez Ramos, C.; Pérez Garnés, M.; Monleón Pradas, M.; Vallés Lluch, A. Electrospun adherent-antiadherent bilayered membranes based on cross-linked hyaluronic acid for advanced tissue engineering applications. *Mater. Sci. Eng. C. Mater. Biol. Appl.* **2013**, *33* (7), 4086–4093

DOI: 10.1016/j.msec.2013.05.058.

(65) Xie, Z.; Paras, C. B.; Weng, H.; Punnakitikashem, P.; Su, L. C.; Vu, K.; Tang, L.; Yang, J.; Nguyen, K. T. *Dual growth factor releasing multi-functional nanofibers for wound healing*; Acta Materialia Inc., 2013; Vol. 9.

(66) Xie, Z.; Paras, C. B.; Weng, H.; Punnakitikashem, P.; Su, L.-C.; Vu, K.; Tang, L.; Yang, J.; Nguyen, K. T. *Dual growth factor releasing multi-functional nanofibers for wound healing*; Acta Materialia Inc., 2013; Vol. 9.

(67) Cacciotti, I.; Fortunati, E.; Puglia, D.; Kenny, J. M.; Nanni, F. Effect of silver nanoparticles and cellulose nanocrystals on electrospun poly(lactic) acid mats: morphology, thermal properties and mechanical behavior. *Carbohydr. Polym.* **2014**, *103*, 22–31 DOI: 10.1016/j.carbpol.2013.11.052.

(68) Rogina, A. Electrospinning process: Versatile preparation method for biodegradable and natural polymers and biocomposite systems applied in tissue engineering and drug delivery. *Appl. Surf. Sci.* **2014**, *296*, 221–230 DOI: 10.1016/j.apsusc.2014.01.098.

(69) Gandhimathi, C.; Venugopal, J. R.; Bhaarathy, V.; Ramakrishna, S.; Kumar, S. D. Biocomposite nanofibrous strategies for the controlled release of biomolecules for skin tissue regeneration. *Int. J. Nanomedicine* **2014**, *9*, 4709–4722 DOI: 10.2147/IJN.S65335.

(70)   Aduba, D. C.; Overlin, J. W.; Frierson, C. D.; Bowlin, G. L.; Yang, H. Electrospinning of PEGylated polyamidoamine dendrimer fibers. *Mater. Sci. Eng. C* **2015**, *56*, 189–194 DOI: 10.1016/j.msec.2015.06.025.

(71)   Hongxu, Q.; Hu, P.; Xu, J.; Wang, A. Encapsulation of drug reservoirs in fibers by emulsion electrospinning: morphology characterization and preliminary release assessment. *Biomacromolecules* **2006**, *7* (8), 2327–2330 DOI: 10.1021/bm060264z.

(72)   McCullen, S. D.; Stevens, D. R.; Roberts, W. A.; Clarke, L. I.; Bernacki, S. H.; Gorga, R. E.; Loboa, E. G. Characterization of electrospun nanocomposite scaffolds and biocompatibility with adipose-derived human mesenchymal stem cells. *Int. J. Nanomedicine* **2007** DOI: 10.1007/s10439-012-0728-8.

(73)   Ionescu, L. C.; Lee, G. C.; Sennett, B. J.; Burdick, J. a; Mauck, R. L. An anisotropic nanofiber/microsphere composite with controlled release of biomolecules for fibrous tissue engineering. *Biomaterials* **2010**, *31* (14), 4113–4120 DOI: 10.1016/j.biomaterials.2010.01.098.

(74)   Dhurai, B.; Saraswathy, N.; Maheswaran, R.; Sethupathi, P.; Vanitha, P.; Vigneshwaran, S.; Rameshbabu, V. Electrospinning of curcumin loaded chitosan/poly (lactic acid) nanofilm and evaluation of its medicinal characteristics. *Front. Mater. Sci.* **2013**, *7* (4), 350–361 DOI: 10.1007/s11706-013-0222-8.

(75) Greco, F.; Vicent, M. J.; Gee, S.; Jones, A. T.; Gee, J.; Nicholson, R. I.; Duncan, R. Investigating the mechanism of enhanced cytotoxicity of HPMA copolymer-Dox-AGM in breast cancer cells. *J. Control. Release* **2007**, *117* (1), 28–39 DOI: 10.1016/j.jconrel.2006.10.012.

(76) Ulbrich, K.; Etrych, T.; Chytil, P.; Pechar, M.; Jelinkova, M.; Rihova, B. Polymeric anticancer drugs with pH-controlled activation. *International Journal of Pharmaceutics*. 2004, pp 63–72.

(77) Heller, J., Penhale, D. W. H. and Helwing, R. F. Preparation of Polyacetals By the Reaction of Divinyl Ethers and Polyols. *J. Polym. Sci. B Polym. Lett. Ed* **1980**, *18* (4), 293–297 DOI: 10.1002/pol.1980.130180410.

(78) Tomlinson, R.; Klee, M.; Garrett, S.; Heller, J.; Duncan, R.; Brocchini, S. Pendent chain functionalized polyacetals that display pH-dependent degradation: A platform for the development of novel polymer therapeutics. *Macromolecules* **2002**, *35* (2), 473–480 DOI: 10.1021/ma0108867.

(79) Tomlinson, R.; Heller, J.; Brocchini, S.; Duncan, R. Polyacetal-Doxorubicin Conjugates Designed for pH-Dependent Degradation. *Bioconjug. Chem.* **2003**, *14* (6), 1096–1106 DOI: 10.1021/bc030028a.

(80) Vicent, M. J.; Tomlinson, R.; Brocchini, S.; Duncan, R. Polyacetal-diethylstilboestrol: a polymeric drug designed for

pH-triggered activation. *J. Drug Target.* **2004**, *12* (8), 491–501 DOI: 10.1080/10611860400011885.

(81)   Giménez, V.; James, C.; Armiñán, A.; Schweins, R.; Paul, A.; Vicent, M. J. Demonstrating the importance of polymer-conjugate conformation in solution on its therapeutic output: Diethylstilbestrol (DES)-polyacetals as prostate cancer treatment. *J. Control. Release* **2012**, *159* (2), 290–301 DOI: 10.1016/j.jconrel.2011.12.035.

(82)   Tang, H.; Murphy, C. J.; Zhang, B.; Shen, Y.; Van Kirk, E. A.; Murdoch, W. J.; Radosz, M. Curcumin polymers as anticancer conjugates. *Biomaterials* **2010**, *31* (27), 7139–7149 DOI: 10.1016/j.biomaterials.2010.06.007.

(83)   Chytil, P.; Etrych, T.; Kříž, J.; Šubr, V.; Ulbrich, K. N-(2-Hydroxypropyl)methacrylamide-based polymer conjugates with pH-controlled activation of doxorubicin for cell-specific or passive tumour targeting. Synthesis by RAFT polymerisation and physicochemical characterisation. *Eur. J. Pharm. Sci.* **2010**, *41* (3-4), 473–482 DOI: 10.1016/j.ejps.2010.08.003.

(84)   Sirova, M.; Mrkvan, T.; Etrych, T.; Chytil, P.; Rossmann, P.; Ibrahimova, M.; Kovar, L.; Ulbrich, K.; Rihova, B. Preclinical evaluation of linear HPMA-doxorubicin conjugates with pH-sensitive drug release: efficacy, safety, and immunomodulating activity in murine model. *Pharm. Res.* **2010**, *27* (1), 200–208 DOI: doi: 10.1007/s11095-009-9999-7.

(85) Chytil, P.; Etrych, T.; Konák, C.; Sírová, M.; Mrkvan, T.; Ríhová, B.; Ulbrich, K. Properties of HPMA copolymer-doxorubicin conjugates with pH-controlled activation: effect of polymer chain modification. *J. Control. Release* **2006**, *115* (1), 26–36.

(86) Abuchowski, A.; McCoy, J. R.; Palczuk, N. C.; Van Es, T.; Davis, F. F. Effect of Covalent Attachment of Polyethylene Glycol on Immunogenicity and Circulating Life of Bovine Liver Catalase. *J. Biol. Chem.* **1977**, *252*, 2582–3586.

(87) Hardwicke, J.; Ferguson, E. L.; Moseley, R.; Stephens, P.; Thomas, D. W.; Duncan, R. Dextrin-rhEGF conjugates as bioresponsive nanomedicines for wound repair. *J. Control. Release* **2008**, *130* (3), 275–283 DOI: 10.1016/j.jconrel.2008.07.023.

(88) Conejos-Sánchez, I.; Cardoso, I.; Saraiva, M. J.; Vicent, M. J. Targeting a rare amyloidotic disease through rationally designed polymer conjugates. *J. Control. Release* **2014**, *178*, 95–100 DOI: 10.1016/j.jconrel.2014.01.019.

(89) Smolinske, S. C. *Handbook of Food, Drug, and Cosmetic Excipients*; Boca Raton: CRC Press, 1992.

(90) Dorgan, J. R.; Lehermeier, H.; Mang, M. Thermal and Rheological Properties of Commercial-Grade Poly (Lactic Acid) s. **2000**, *8* (1), 1–9.

(91) Jamshidian, M.; Tehrany, E. A.; Imran, M.; Jacquot, M.;

Desobry, S. Poly-Lactic Acid: Production, applications, nanocomposites, and release studies. *Compr. Rev. Food Sci. Food Saf.* **2010**, *9* (5), 552–571 DOI: 10.1111/j.1541-4337.2010.00126.x.

(92) Fraser, J. R.; Laurent, T. C.; Laurent, U. B. Hyaluronan: its nature, distribution, functions and turnover. *J. Intern. Med.* **1997**, *242* (1), 27–33.

(93) Lei, Y.; Gojgini, S.; Lam, J.; Segura, T. The spreading, migration and proliferation of mouse mesenchymal stem cells cultured inside hyaluronic acid hydrogels. *Biomaterials* **2011**, *32* (1), 39–47 DOI: 10.1016/j.biomaterials.2010.08.103.

(94) Hornak, J. (Professor of C. at R. *The Basics of NMR - A non-technical overview of NMR theory, equipment, and techniques*; 2014.

(95) Billingham, N. C. .; Jenkins, A. D. *The Chemical Structure of Polymers*; American Elsevier Publishing Company: New York: Amsterdam and London, 1972.

(96) Painter, P. C. .; Coleman, M. M. *Molecular Weight and Branching*; CRC Press LLC: Boca Raton, 1997.

(97) Banerjee, S. S.; Aher, N.; Patil, R.; Khandare, J. Poly(ethylene glycol)-Prodrug Conjugates: Concept, Design, and Applications. *J. Drug Deliv.* **2012**, *2012*, 1–17 DOI: 10.1155/2012/103973.

(98) Jung, B.; Theato, P. Chemical Strategies for the Synthesis of

Protein – Polymer Conjugates. *Adv. Polym. Sci.* **2012**, No. May 2012, 1–34 DOI: 10.1007/12.

(99) Duncan, R.; Gilbert, H. R. P.; Carbajo, R. J.; Vicent, M. J. Polymer Masked # Unmasked Protein Therapy . 1 . Bioresponsive Dextrin # Trypsin and # Melanocyte Stimulating Hormone Conjugates Designed for # -Amylase Activation Polymer Masked - Unmasked Protein Therapy . 1 . Bioresponsive Dextrin - Trypsin and - Melano. **2008**, 1146–1154 DOI: 10.1021/bm701073n.

(100) Shakya, A. K.; Sami, H.; Srivastava, A.; Kumar, A. Stability of responsive polymer-protein bioconjugates. *Prog. Polym. Sci.* **2010**, *35* (4), 459–486 DOI: 10.1016/j.progpolymsci.2010.01.003.

(101) Ferguson, E. L.; Duncan, R. Dextrin # Phospholipase A : Synthesis and Evaluation as a Bioresponsive Anticancer Conjugate Dextrin-Phospholipase A 2 : Synthesis and Evaluation as a Bioresponsive Anticancer Conjugate. *Biomacromolecules* **2009**, 1358–1364 DOI: 10.1021/bm8013022.

(102) Ferguson, E. L.; Richardson, S. C. W.; Duncan, R. articles Studies on the Mechanism of Action of Dextrin-Phospholipase A 2 and Its Suitability for Use in Combination Therapy. **2010**, No. 4, 161–171.

(103) Ferguson, E. L.; Alshame, A. M. J.; Thomas, D. W. Evaluation of hyaluronic acid-protein conjugates for polymer masked-

unmasked protein therapy. *Int. J. Pharm.* **2010**, *402* (1-2), 95–102 DOI: 10.1016/j.ijpharm.2010.09.029.

(104) Talelli, M.; Vicent, M. J. Reduction Sensitive Poly(l-glutamic acid) (PGA)-Protein Conjugates Designed for Polymer Masked-Unmasked Protein Therapy. *Biomacromolecules* **2014**, 2–11 DOI: 10.1021/bm5011883.

(105) Buescher, J. M.; Margaritis, A. Microbial Biosynthesis of Polyglutamic Acid Biopolymer and Applications in the Biopharmaceutical, Biomedical and Food Industries. *Crit. Rev. Biotechnol.* **2007**, *27* (1), 1–19 DOI: 10.1080/07388550601166458.

(106) Maeda, H. Macromolecular therapeutics in cancer treatment: the EPR effect and beyond. *J. Control. Release* **2012**, *164* (2), 138–144 DOI: 10.1016/j.jconrel.2012.04.038.

(107) Winchester, B.; Vellodi, A.; Young, E. The molecular basis of lysosomal storage diseases and their treatment. *Biochem. Soc. Trans.* **2000**, *28* (2), 150–154.

(108) Platt, F. M.; Boland, B.; van der Spoel, A. C. The cell biology of disease: lysosomal storage disorders: the cellular impact of lysosomal dysfunction. *J. Cell Biol.* **2012**, *199* (5), 723–734 DOI: 10.1083/jcb.201208152.

(109) Bruni, S.; Loschi, L.; Incerti, C.; Gabrielli, O.; Coppa, G. V. Update on treatment of lysosomal storage diseases. *Acta Myol.* **2007**,

26 (1), 87–92.

(110) England, R. M.; Masiá, E.; Giménez, V.; Lucas, R.; Vicent, M. J. Polyacetal-stilbene conjugates - The first examples of polymer therapeutics for the inhibition of HIF-1 in the treatment of solid tumours. *J. Control. Release* **2012**, *164* (3), 314–322 DOI: 10.1016/j.jconrel.2012.08.017.

(111) Fields, R. The measurement of amino groups in proteins and peptides. *Biochem. J.* **1971**, *124* (3), 581–590.

(112) Zarafshani, Z.; Obata, T.; Lutz, J. F. Smart PEGylation of trypsin. *Biomacromolecules* **2010**, *11* (8), 2130–2135 DOI: 10.1021/bm1005036.

(113) Duncan, R.; Gaspar, R. Nanomedicine (s) under the Microscope. *Mol. Pharm.* **2011**, *8*, 2101–2141.

(114) http://www.etp-nanomedicine.eu/public/press-documents/publications/etpn-publications/etpn-white-paper-H2020. Accesed October 2015.

(115) Kaihara Nitta, S.; Numata, K. Biopolymer-Based Nanoparticles for Drug/Gene Delivery and Tissue Engineering. *Int. J. Mol. Sci.* **2013**, *14*, 1629–1654.

(116) Seymour, L. W.; Duncan, R.; Strohalm, J.; Kopeček, J. Effect of molecular weight (Mw) of N-(2-hydroxypropyl)methacrylamide copolymers on body distribution and rate of excretion after subcutaneous, intraperitoneal, and intravenous administration

to rats. *J. Biomed. Mater. Res.* **1987**, *21* (11), 1341–1358.

(117)   Schaffer, M.; Schaffer, P. M.; Zidan, J.; Bar Sela, G. Curcuma as a functional food in the control of cancer and inflammation. *Curr. Opin. Clin. Nutr. Metab. Care* **2011**, *14* (6), 588–597 DOI: 10.1097/MCO.0b013e32834bfe94.

(118)   Shen, Y.; Han, C.; Chen, X.; Hou, X.; Long, Z. Simultaneous determination of three Curcuminoids in Curcuma wenyujin Y.H.chen et C.Ling. by liquid chromatography-tandem mass spectrometry combined with pressurized liquid extraction. *J. Pharm. Biomed. Anal.* **2013**, *81-82*, 146–150 DOI: 10.1016/j.jpba.2013.03.027.

(119)   Pendurthi, U. R.; Williams, J. T.; Rao, L. V. Inhibition of tissue factor gene activation in cultured endothelial cells by curcumin. Suppression of activation of transcription factors Egr-1, AP-1, and NF-kappa B. *Arterioscler. Thromb. Vasc. Biol.* **1997**, *17* (12), 3406–3413.

(120)   Weber, W. M.; Hunsaker, L. A.; Gonzales, A. M.; Heynekamp, J. J.; Orlando, R. A.; Deck, L. M.; Vander Jagt, D. L. TPA-induced up-regulation of activator protein-1 can be inhibited or enhanced by analogs of the natural product curcumin. *Biochem. Pharmacol.* **2006**, *72* (8), 928–940 DOI: 10.1016/j.bcp.2006.07.007.

(121)   Chen, Y. R.; Tan, T. H. Inhibition of the c-Jun N-terminal kinase (JNK) signaling pathway by curcumin. *Oncogene* **1998**, *17* (2),

173–178 DOI: 10.1038/sj.onc.1201941.

(122) M. M. Y. Chan, H. I. Huang, M. R. Fenton, and D. F. In vivo inhibition of nitric oxide synthase gene expression by curcumin, a cancer preventive natural product with anti-inflammatory properties. *Biochem. Pharmacol.* **1998**, *55* (12), 1955–1962.

(123) SEYMOUR, L.; SCHACHT, E.; DUNCAN, R. The effect of size of polystyrene particles on their retention within the rat peritoneal compartment, and on their interaction with rat peritoneal macrophages. *Cell Biol. Int. Rep.* **1991**, *15* (4), 277–286 DOI: 10.1016/0309-1651(91)90166-G.

(124) Akbik, D.; Ghadiri, M.; Chrzanowski, W.; Rohanizadeh, R. Curcumin as a wound healing agent. *Life Sci.* **2014**, *116* (1), 1–7 DOI: 10.1016/j.lfs.2014.08.016.

(125) Wade, L. . J. *Qumica Orgánica*, segunda.; Prentice-Hall Hispanoamerica S.A.: Mexico, 1993.

(126) Akbik, D.; Ghadiri, M.; Chrzanowski, W.; Rohanizadeh, R. Curcumin as a wound healing agent. *Life Sci.* **2014**, *116* (1), 1–7 DOI: 10.1016/j.lfs.2014.08.016.

(127) Bae, M.-K.; Kim, S.-H.; Jeong, J.-W.; Lee, Y. M.; Kim, H.-S.; Kim, S.-R.; Yun, I.; Bae, S.-K.; Kim, K.-W. Curcumin inhibits hypoxia-induced angiogenesis via down-regulation of HIF-1. *Oncol. Rep.* **2006**, *15* (6), 1557–1562.

(128) Aggarwal, S.; Ichikawa, H.; Takada, Y.; Sandur, S. K.; Shishodia,

S.; Aggarwal, B. B. Curcumin (diferuloylmethane) down-regulates expression of cell proliferation and antiapoptotic and metastatic gene products through suppression of IkappaBalpha kinase and Akt activation. *Mol. Pharmacol.* **2006**, *69* (1), 195–206 DOI: 10.1124/mol.105.017400.

(129)   Betbeder, D.; Lipka, E.; Carpentier, R. Evolution of availability of curcumin inside poly-lactic-co-glycolic acid nanoparticles : impact on antioxidant and antinitrosant properties. **2015**, 5355–5366.

(130)   Sahiner, N.; Jia, X. One-step synthesis of hyaluronic acid-based (sub)micron hydrogel particles: Process optimization and preliminary characterization. *Turkish J. Chem.* **2008**, *32* (4), 397–409.

(131)   Laurent, T. C.; Laurent, U. B.; Fraser, J. R. The structure and function of hyaluronan: An overview. *Immunol. Cell Biol.* **1996**, *74* (2), A1–A7 DOI: 10.1038/icb.1996.32.

(132)   Collins, M. N.; Birkinshaw, C. Hyaluronic acid based scaffolds for tissue engineering - A review. *Carbohydr. Polym.* **2013**, *92* (2), 1262–1279 DOI: 10.1016/j.carbpol.2012.10.028.

(133)   Fakhari, a.; Berkland, C. Applications and emerging trends of hyaluronic acid in tissue engineering, as a dermal filler and in osteoarthritis treatment. *Acta Biomater.* **2013**, *9* (7), 7081–7092 DOI: 10.1016/j.actbio.2013.03.005.

(134) Simon, L. D.; Stella, V. J.; Charman, W. N.; Charman, S. a. Mechanisms controlling diffusion and release of model proteins through and from partially esterified hyaluronic acid membranes. *J. Control. Release* **1999**, *61* (3), 267–279 DOI: 10.1016/S0168-3659(99)00123-6.

(135) Luo, Y.; Kirker, K. R.; Prestwich, G. D. Cross-linked hyaluronic acid hydrogel films: New biomaterials for drug delivery. *J. Control. Release* **2000**, *69* (1), 169–184 DOI: 10.1016/S0168-3659(00)00300-X.

(136) Segura, T.; Anderson, B. C.; Chung, P. H.; Webber, R. E.; Shull, K. R.; Shea, L. D. Crosslinked hyaluronic acid hydrogels: A strategy to functionalize and pattern. *Biomaterials* **2005**, *26* (4), 359–371 DOI: 10.1016/j.biomaterials.2004.02.067.

(137) Hahn, S. K.; Oh, E. J.; Miyamoto, H.; Shimobouji, T. Sustained release formulation of erythropoietin using hyaluronic acid hydrogels crosslinked by Michael addition. *Int. J. Pharm.* **2006**, *322* (1-2), 44–51 DOI: 10.1016/j.ijpharm.2006.05.024.

(138) Lee, F.; Chung, J. E.; Kurisawa, M. An injectable hyaluronic acid-tyramine hydrogel system for protein delivery. *J. Control. Release* **2009**, *134* (3), 186–193 DOI: 10.1016/j.jconrel.2008.11.028.

(139) Prestwich, G. D. Hyaluronic acid-based clinical biomaterials derived for cell and molecule delivery in regenerative medicine. *J. Control. Release* **2011**, *155* (2), 193–199 DOI:

10.1016/j.jconrel.2011.04.007.

(140) Schanté, C. E.; Zuber, G.; Herlin, C.; Vandamme, T. F. Chemical modifications of hyaluronic acid for the synthesis of derivatives for a broad range of biomedical applications. *Carbohydr. Polym.* **2011**, *85* (3), 469–489 DOI: 10.1016/j.carbpol.2011.03.019.

(141) Uppal, R.; Ramaswamy, G. N.; Arnold, C.; Goodband, R.; Wang, Y. Hyaluronic acid nanofiber wound dressing-production, characterization, and in vivo behavior. *J. Biomed. Mater. Res. - Part B Appl. Biomater.* **2011**, *97 B* (1), 20–29 DOI: 10.1002/jbm.b.31776.

(142) Xiong, W.; Gao, X.; Zhao, Y.; Xu, H.; Yang, X. The dual temperature/pH-sensitive multiphase behavior of poly(N-isopropylacrylamide-co-acrylic acid) microgels for potential application in in situ gelling system. *Colloids Surfaces B Biointerfaces* **2011**, *84* (1), 103–110 DOI: 10.1016/j.colsurfb.2010.12.017.

(143) Iannitti, T.; Bingöl, A. Ö.; Rottigni, V.; Palmieri, B. A new highly viscoelastic hyaluronic acid gel: rheological properties, biocompatibility and clinical investigation in esthetic and restorative surgery. *Int. J. Pharm.* **2013**, *456* (2), 583–592 DOI: 10.1016/j.ijpharm.2013.06.066.

(144) Cui, N.; Qian, J.; Liu, T.; Zhao, N.; Wang, H. Hyaluronic acid hydrogel scaffolds with a triple degradation behavior for bone tissue engineering. *Carbohydr. Polym.* **2015**, *126*, 192–198 DOI:

10.1016/j.carbpol.2015.03.013.

(145) Fan, M.; Ma, Y.; Zhang, Z.; Mao, J.; Tan, H.; Hu, X. Biodegradable hyaluronic acid hydrogels to control release of dexamethasone through aqueous Diels-Alder chemistry for adipose tissue engineering. *Mater. Sci. Eng. C. Mater. Biol. Appl.* **2015**, *56*, 311–317 DOI: 10.1016/j.msec.2015.04.004.

(146) Kim, T. H.; Jiang, H. H.; Park, C. W.; Youn, Y. S.; Lee, S.; Chen, X.; Lee, K. C. PEGylated TNF-related apoptosis-inducing ligand (TRAIL)-loaded sustained release PLGA microspheres for enhanced stability and antitumor activity. *J. Control. Release* **2011**, *150* (1), 63–69 DOI: 10.1016/j.jconrel.2010.10.037.

(147) Habiboallah, G.; Nasroallah, S.; Mahdi, Z.; Nasser, M. S.; Massoud, Z.; Ehsan, B. N.; Mina, Z. J.; Heidar, P. Histological evaluation of Curcuma longa-ghee formulation and hyaluronic acid on gingival healing in dog. *J. Ethnopharmacol.* **2008**, *120* (3), 335–341 DOI: 10.1016/j.jep.2008.09.011.

(148) El-Refaie, W. M.; Elnaggar, Y. S. R.; El-Massik, M. a.; Abdallah, O. Y. Novel curcumin-loaded gel-core hyaluosomes with promising burn-wound healing potential: Development, in-vitro appraisal and in-vivo studies. *Int. J. Pharm.* **2015**, *486* (1-2), 88–98 DOI: 10.1016/j.ijpharm.2015.03.052.

(149) Collins, M. N.; Birkinshaw, C. Physical properties of crosslinked hyaluronic acid hydrogels. *J. Mater. Sci. Mater. Med.* **2008**, *19* (11), 3335–3343 DOI: 10.1007/s10856-008-3476-4.

(150) Pires, A. M. B.; Lichy, R.; Santana, M. H. A. The Performance of Crosslinking with Divinyl Sulfone as Controlled by the Interplay Between the Chemical Modification and Conformation of Hyaluronic Acid. *J. Braz. Chem. Soc* **2015**, *26* (3), 506–512.

(151) Kwon, S. S.; Kong, B. J.; Park, S. N. Physicochemical properties of pH-sensitive hydrogels based on hydroxyethyl cellulose–hyaluronic acid and for applications as transdermal delivery systems for skin lesions. *Eur. J. Pharm. Biopharm.* **2015**, *92*, 146–154 DOI: 10.1016/j.ejpb.2015.02.025.

(152) Ritger, P. L.; Peppas, N. a. A simple equation for description of solute release II. Fickian and anomalous release from swellable devices. *J. Control. Release* **1987**, *5* (1), 37–42 DOI: 10.1016/0168-3659(87)90035-6.

(153) Sampath, M.; Lakra, R.; Korrapati, P.; Sengottuvelan, B. Curcumin loaded poly (lactic-co-glycolic) acid nanofiber for the treatment of carcinoma. *Colloids Surfaces B Biointerfaces* **2014**, *117*, 128–134 DOI: 10.1016/j.colsurfb.2014.02.020.

(154) Pawlaczyk, M.; Lelonkiewicz, M.; Wieczorowski, M. Age-dependent biomechanical properties of the skin. *Postępy dermatologii i Alergol.* **2013**, *30* (5), 302–306 DOI: 10.5114/pdia.2013.38359.

(155) Ferguson, E. L.; De Luca, E.; Heenan, R. K.; King, S. M.; Griffiths, P. C. Time-resolved small-angle neutron scattering as a tool for studying controlled release from liposomes using polymer-

enzyme conjugates. *Macromol. Rapid Commun.* **2010**, *31* (19), 1685–1690 DOI: 10.1002/marc.201000241.

(156) Hardwicke, J. T.; Hart, J.; Bell, A.; Duncan, R.; Thomas, D. W.; Moseley, R. The effect of dextrin-rhEGF on the healing of full-thickness, excisional wounds in the (db/db) diabetic mouse. *J. Control. Release* **2011**, *152* (3), 411–417 DOI: 10.1016/j.jconrel.2011.03.016.

(157) Fontana, A.; Spolaore, B.; Mero, A.; Veronese, F. M. Site-specific modification and PEGylation of pharmaceutical proteins mediated by transglutaminase. *Adv. Drug Deliv. Rev.* **2008**, *60* (1), 13–28 DOI: 10.1016/j.addr.2007.06.015.

(158) Prestwich, G. D.; Marecak, D. M.; Marecek, J. F.; Vercruysse, K. P.; Ziebell, M. R. Controlled chemical modification of hyaluronic acid: Synthesis, applications, and biodegradation of hydrazide derivatives. *J. Control. Release* **1998**, *53* (1-3), 93–103 DOI: 10.1016/S0168-3659(97)00242-3.

(159) Manca, M. L.; Castangia, I.; Zaru, M.; Nacher, A.; Valenti, D.; Fernandez-Busquets, X.; Fadda, A. M.; Manconi, M. Development of curcumin loaded sodium hyaluronate immobilized vesicles (hyalurosomes) and their application on prevention and rapid restoring of mouse skin wound. *Biomaterials* **2015**, *71*, 100–109 DOI: 10.1016/j.biomaterials.2015.08.034.

(160) Sakai, S.; Ueda, K.; Taya, M. Peritoneal adhesion prevention by

a biodegradable hyaluronic acid-based hydrogel formed in situ through a cascade enzyme reaction initiated by contact with body fluid on tissue surfaces. *Acta Biomater.* **2015**, *24*, 152–158 DOI: 10.1016/j.actbio.2015.06.023.

(161) Qi, X.; Fan, Y.; He, H.; Wu, Z. Hyaluronic acid-grafted polyamidoamine dendrimers enable long circulation and active tumor targeting simultaneously. *Carbohydr. Polym.* **2015**, *126*, 231–239 DOI: 10.1016/j.carbpol.2015.03.019.

(162) Zhou, Z.; He, S.; Huang, T.; Peng, C.; Zhou, H.; Liu, Q.; Zeng, W.; Liu, L.; Huang, H.; Xiang, L.; et al. Preparation of gelatin/hyaluronic acid microspheres with different morphologies for drug delivery. *Polym. Bull.* **2015**, *72* (4), 713–723 DOI: 10.1007/s00289-015-1300-0.

ABBREVIATION LIST

AD	Alzheimer's disease
1-HP	1-heptanol
3x	triplicate
A.A.	Acrylamide, 2-Propenamide, Acrylic acid amide
AcOH	Acetic acid
ADSCs	Adipose-Derived Stem Cells
AgSD	Silver Sulfadiazine
Ala	Alanine
ALL	Acute lymphoblastic leukemia
AMD	Age-related Macular Degeneration
AOT	sodium bis(2-ethylhexyl)sulfosuccinate
APAF-1	Apoptotic Protease Activating Factor 1
APS	Ammonium peroxodisulfate, Ammonium peroxydisulfate
BBB	Blood-Brain-Barrier
BCA	Bicinchoninic Acid solution
BHMPA	2,2-tris (hydroxymethyl) propionic acid
BM	Bone Marrow
BSA	Bovine Serum Albumin
BuOH	n-Butanol, Butyl alcohol
CD	Cyclodextrin
CD	circular dicroism
CDCl$_3$	deuterated chloroform
CHCL3	Chloroform
CKD	Chronic Kidney Disease
CMFDA	5-chloromethylfluoresein diacetate
Cur	curcumin
d	doublet
DACH	1,2-diaminocyclohexane
DCM	Dichloromethane
dd	double doublet
ddH$_2$O	double distiled water

DEGDVE	Tri(ethylene glycol) divinyl ether
DMF	*N,N*-Dimethylformamide, Dimethylformamide
DMPA	N,N-Dimethylpyridin-4-amine, DMAP
DMSO	dimethyl sulfoxide
DMSO-6d	dimethyl sulfoxide deuterated
DOSY-NMR	Diffusion-ordered spectroscopy
DOX	Doxorubicin
DOXY	Doxyclycline
DTT	threo-1,4-Dimercapto-2,3-butanediol, DL-Dithiothreitol, Cleland's reagent, DTT
DVS	Divinyl sulfone
E.E.	encapsulation efficiency
ECM	Extracellular Matrix
EDAC	N-Ethyl-N'-(3-dimethylaminopropyl)carbodiimide hydrochloride
EIF	Epidermal Induction Factors
EPO	Epoetin beta
EPR	Enhanced Permeability and Retention
ES	Electrospinning
ES PLLA	electrospinning of PLLA
ES01	simple membrane constituted by PLLA fibers
ES02	composite membrane constituted by PLLA fibers and Microparticles of hyaluronic acid
ES03	composite membrane constituted by PLLA fibers and Microparticles of hyaluronic acid loaded with PACur
ES04	simple membrane constituted by PLLA fibers loaded with PACur
ES05	simple membrane constituted by PLLA fibers loaded with Cur
ES06	composite membrane constituted by PLLA fibers and Microparticles of hyaluronic acid loaded with Cur
Et$_3$N	Triethylamine, N,N-Diethylethanamine
EtOH	ethanol
Fab	Fragment antigen-binding
FAP	Familial Amyloidotic Polyneuropathy
FDA	US Food and Drug Administration

FMOC	9-Fluorenylmethoxycarbonyl chloride, 9-Fluorenylmethyl chloroformate, Fmoc-Cl
FPLC	Fast Protein liquid chromatography
GI	Gastro-Intestinal
GPC	Gel permeation chromatography
HA	hyaluronic acid
HCl	Hydrochloric acid
HGH	Human Growth Hormone
HPMA	N-(2-hydroxypropylmetacrylamide)
HrGCSF	human recombinant Granulocyte-Colony Stimulating Factor
HYD	Hydrazone
i.m.	Intramuscular
i.v.	Intravenous
IgE	Immunoglobulin E
KOH	potassium hydroxide
L-BAPNA	Nα-Benzoyl-L-arginine 4-nitroanilide hydrochloride
m	multiplet
MeOH	methanol
MeO-PEG-COOH	alpha-Methoxy-omega-carboxylic acid poly(ethylene glycol)
MeO-PEG-OH	alpha-Methoxy-omega-hydroxy poly(ethylene glycol)
MPs	Micro-particles
MPs	microparticles
MPs HA	microparticles of hyaluronic acid
MSC	Mesenchymal Stem Cells
MW	molecular weight
MWCN	Multi-Walled Carbon Nanotubes
MWCO	molecular weight cut-off
Na$_2$CO$_3$	sodium carbonate
NaHCO$_3$	sodium bicarbonate
NaOH	Sodium hydroxide solution
NCS	Neocarzinostatin
NGF	Nerve Growth Factor

NMR	nuclear magnetic resonance
NSCLC	Non-Small Cell Lung Cancer
NTFs	Neurothrophic Factors
O/W	Oil/Water
PACOOH	carboxylate pendant group polyacetal
PACOOH-T	carboxylate pendant group polyacetal-conjugated with trypsin
PACur	Polyacetal conjugated with curcumin
PAFS	FMOC protected amino-pendant polyacetal
PAMAM	Polyamidoamine
PANH$_2$	deprotected amino-pendant polyacetal
PASUcc	Succinoylated Polyacetal
PASUcc-T	Succinoylated Polyacetal conjugated with trypsin
PA-T	polyacetal conjugated with trypsin
PBS	Phosphate Buffer Saline
PC	Polymer Conjugates
PDGF	Platelet Derived Growth Factor
PEG	Poly(ethylene glycol)
PEG	polyethyleneglicol
PET	Positron Emission Tomography
PGA	Poly(glutamic acid)
PLA	Poly(lactic acid)
PLACL	poly(L-lactic acid)–co-poly(3-caprolactone)
PLGA	Poly(lactic glycolic acid)
PLLA	Poly(l-lactic acid)
PLLA	Poly-L-lactic acid
pNA	p-Nitroanilide
PPAR	Peroxisome Proliferation Activated Receptor
PT	Polymer Therapeutics
PT	polymer therapeutics
pTSA	para-toluene sulfonic acid
PUMPT	polymer-masking-unmasking-protein therapy
PVA	Poly(vinyl alcohol)
PVP	Poly(vinylpirrolidone)
qt	quadruplet

RES	Reticuloendothelial system
ROS	Reactive Oxygen Species
s	singlet
s.c.	Subcutaneous
SDS	Sodium dodecyl sulfate, Dodecyl sodium sulfate, Dodecyl sulfate sodium salt, Lauryl sulfate sodium salt, SDS, Sodium lauryl sulfate
SDS-PAGE	The method is called sodium dodecyl sulfate polyacrylamide gel electrophoresis
SF	Silk Fibroin
SMA	Styrene-co-maleic Anhydride
SMANCS	Styrene-co-maleic Anhydride- Neocarzinostatin
sulfo-NHS	N-Hydroxysulfosuccinimide sodium salt, Hydroxy-2,5-dioxopyrrolidine-3-sulfonicacid sodium salt, Sulfo-NHS
T	trypsin
t	triplet
td	triplet of doublet
TDL	Total drug loading
TE	Tissue Engineering
TEGDVE	Di(ethylene glycol) divinyl ether
TEMED	N,N,N',N'-Tetramethylethylenediamine, 1,2-Bis(dimethylamino)ethane, TEMED, TMEDA
THF	Tetrahydrofuran
TLC	Thin layer chromatography
TNBSA	2,4,6-Trinitrobenzenesulfonic acid solution, Picrylsulfonic acid solution
TNF	Tumor Necrosis Factor
TRIS	2-Amino-2-(hydroxymethyl)-1,3-propanediol, THAM, Tris base, Tris(hydroxymethyl)aminomethane, Trizma® base, Trometamol
TRIZMA base	2-Amino-2-(hydroxymethyl)-1,3-propanediol, THAM, Tris base, Tris(hydroxymethyl)aminomethane, Trometamol
Tyr	Tyrosine
VE	Vitamin E
VEGF	Vascular Endothelial Growth Factor
W/O	Water/Oil
wt%	Percentage in weight

TABLE LIST

FIGURE LIST